

Tungsten Cemented Carbide

Comprehensive Exploration of Physical & Chemical Properties, Processes, & Applications (VIII)

中钨智造科技有限公司

CTIA GROUP LTD

CTIA GROUP LTD

Global Leader in Intelligent Manufacturing for Tungsten, Molybdenum, and Rare Earth Industries

COPYRIGHT AND LEGAL LIABILITY STATEMENT

Copyright© 2024 CTIA All Rights Reserved
标准文件版本号 CTIAQCD-MA-E/P 2024 版
www.ctia.com.cn

电话/TEL: 0086 592 512 9696
CTIAQCD-MA-E/P 2018-2024V
sales@chinatungsten.com

INTRODUCTION TO CTIA GROUP

CTIA GROUP LTD, a wholly-owned subsidiary with independent legal personality established by CHINATUNGSTEN ONLINE, is dedicated to promoting the intelligent, integrated, and flexible design and manufacturing of tungsten and molybdenum materials in the Industrial Internet era. CHINATUNGSTEN ONLINE, founded in 1997 with www.chinatungsten.com as its starting point—China's first top-tier tungsten products website—is the country's pioneering e-commerce company focusing on the tungsten, molybdenum, and rare earth industries. Leveraging nearly three decades of deep experience in the tungsten and molybdenum fields, CTIA GROUP inherits its parent company's exceptional design and manufacturing capabilities, superior services, and global business reputation, becoming a comprehensive application solution provider in the fields of tungsten chemicals, tungsten metals, cemented carbides, high-density alloys, molybdenum, and molybdenum alloys.

Over the past 30 years, CHINATUNGSTEN ONLINE has established more than 200 multilingual tungsten and molybdenum professional websites covering more than 20 languages, with over one million pages of news, prices, and market analysis related to tungsten, molybdenum, and rare earths. Since 2013, its WeChat official account "CHINATUNGSTEN ONLINE" has published over 40,000 pieces of information, serving nearly 100,000 followers and providing free information daily to hundreds of thousands of industry professionals worldwide. With cumulative visits to its website cluster and official account reaching billions of times, it has become a recognized global and authoritative information hub for the tungsten, molybdenum, and rare earth industries, providing 24/7 multilingual news, product performance, market prices, and market trend services.

Building on the technology and experience of CHINATUNGSTEN ONLINE, CTIA GROUP focuses on meeting the personalized needs of customers. Utilizing AI technology, it collaboratively designs and produces tungsten and molybdenum products with specific chemical compositions and physical properties (such as particle size, density, hardness, strength, dimensions, and tolerances) with customers. It offers full-process integrated services ranging from mold opening, trial production, to finishing, packaging, and logistics. Over the past 30 years, CHINATUNGSTEN ONLINE has provided R&D, design, and production services for over 500,000 types of tungsten and molybdenum products to more than 130,000 customers worldwide, laying the foundation for customized, flexible, and intelligent manufacturing. Relying on this foundation, CTIA GROUP further deepens the intelligent manufacturing and integrated innovation of tungsten and molybdenum materials in the Industrial Internet era.

Dr. Hanns and his team at CTIA GROUP, based on their more than 30 years of industry experience, have also written and publicly released knowledge, technology, tungsten price and market trend analysis related to tungsten, molybdenum, and rare earths, freely sharing it with the tungsten industry. Dr. Han, with over 30 years of experience since the 1990s in the e-commerce and international trade of tungsten and molybdenum products, as well as the design and manufacturing of cemented carbides and high-density alloys, is a renowned expert in tungsten and molybdenum products both domestically and internationally. Adhering to the principle of providing professional and high-quality information to the industry, CTIA GROUP's team continuously writes technical research papers, articles, and industry reports based on production practice and market customer needs, winning widespread praise in the industry. These achievements provide solid support for CTIA GROUP's technological innovation, product promotion, and industry exchanges, propelling it to become a leader in global tungsten and molybdenum product manufacturing and information services.



COPYRIGHT AND LEGAL LIABILITY STATEMENT

Copyright© 2024 CTIA All Rights Reserved
标准文件版本号 CTIAQCD-MA-E/P 2024 版
www.ctia.com.cn

电话/TEL: 0086 592 512 9696
CTIAQCD-MA-E/P 2018-2024V
sales@chinatungsten.com

CTIA GROUP LTD

30 Years of Cemented Carbide Customization Experts

Core Advantages

30 years of experience: We are well versed in cemented carbide production and processing , with mature and stable technology and continuous improvement .

Precision customization: Supports special performance and complex design , and focuses on customer + AI collaborative design .

Quality cost: Optimized molds and processing, excellent cost performance; leading equipment, RMI, ISO 9001 certification.

Serving Customers

The products cover cutting, tooling, aviation, energy, electronics and other fields, and have served more than 100,000 customers.

Service Commitment

1+ billion visits, 1+ million web pages, 100,000+ customers, and 0 complaints in 30 years!

Contact Us

Email : sales@chinatungsten.com

Tel : +86 592 5129696

Official website : www.ctia.com.cn

WeChat : Follow "China Tungsten Online"



COPYRIGHT AND LEGAL LIABILITY STATEMENT

Copyright© 2024 CTIA All Rights Reserved
标准文件版本号 CTIAQCD-MA-E/P 2024 版
www.ctia.com.cn

电话/TEL: 0086 592 512 9696
CTIAQCD-MA-E/P 2018-2024V
sales@chinatungsten.com

Part 3: Performance Optimization of Cemented Carbide

Chapter 8: Corrosion and high temperature resistance of cemented carbide

Cemented carbide is a composite material made by powder metallurgy process with tungsten carbide (WC) as the main hard phase and cobalt (Co), nickel (Ni) and other metals as the bonding phase. Its excellent performance makes it widely used in cutting tools, mining equipment and wear-resistant parts. The following will briefly discuss its concept and typical characteristics from the two aspects of corrosion resistance and high temperature resistance.

Corrosion resistance of cemented carbide

Corrosion resistance refers to the ability of cemented carbide to resist chemical erosion in corrosive media (such as acid, alkali, and salt solutions). This property is mainly affected by material composition and microstructure.

The bonding phase of cemented carbide plays a key role in its corrosion resistance. Cemented carbide with cobalt as the bonding phase (such as the YG series) performs poorly in acidic media. For example, in sulfuric acid or hydrochloric acid environments, cobalt is easily corroded, causing the surface of the material to gradually dissolve. Taking YG6 (containing 6% cobalt) as an example, its corrosion rate in 10% hydrochloric acid at room temperature is about 0.1 to 0.2 mm/year, while it hardly corrodes in weak alkaline or neutral media (such as 10% sodium hydroxide solution). In contrast, cemented carbide with nickel as the bonding phase (such as the YN series) exhibits stronger corrosion resistance, especially in alkaline and oxidizing media. It is more stable and suitable for use in harsh conditions such as marine environments. In addition, defects in the microstructure can also significantly affect corrosion resistance. If there is a high porosity in the cemented carbide, or if it contains impurities such as free carbon and η phase, these defects will become the starting point of corrosion and accelerate material degradation.

High temperature resistance of cemented carbide

High temperature resistance refers to the ability of cemented carbide to maintain its hardness, strength and oxidation resistance in high temperature environment. This characteristic is also affected by composition and temperature.

Cemented carbide performs well at lower temperatures and can usually maintain high hardness and strength below 600°C. For example, YG8 (containing 8% cobalt) can still maintain a hardness of about 1200 HV at 600°C, which is only about 20% lower. However, when the temperature exceeds 800°C, the bonding phase (such as cobalt) begins to soften, resulting in a significant decrease in the overall strength and hardness of the material. Taking YG8 as an example, its hardness can drop to 500-600 HV at 1000°C. In addition, the oxidation resistance of cemented carbide at high temperatures will also be challenged. Tungsten carbide will be converted into tungsten oxide (WO

COPYRIGHT AND LEGAL LIABILITY STATEMENT

3) in a high-temperature oxidizing environment, causing surface peeling and affecting service life. In contrast, cemented carbide with added titanium carbide (TiC) (such as YT15) shows better oxidation resistance at 800°C, but its strength will still drop by 20%-30%.

The corrosion resistance and high temperature resistance of cemented carbide are key indicators for its application in harsh environments. In terms of corrosion resistance, nickel-containing cemented carbide performs better in a variety of media, while cobalt-containing cemented carbide is susceptible to corrosion in acidic environments. In terms of high temperature resistance, cemented carbide is stable below 600°C, but its hardness and oxidation resistance decrease significantly at higher temperatures. These characteristics determine the applicability of cemented carbide in different application scenarios and provide an important basis for its selection and use.

cemented carbide (WCCo) in harsh environments are key to its application in the chemical, marine and aviation fields. For example, in acidic solutions ($\text{pH} < 3 \pm 0.1$), cemented carbide needs to resist strong chemical attack; in marine salt spray ($> 1000 \text{ hours} \pm 100 \text{ hours}$), it needs to prevent pitting; in aircraft engines ($> 1000^\circ\text{C} \pm 10^\circ\text{C}$), it needs to maintain strength and oxidation resistance. However, the electrochemical activity of the bonding phase Co (corrosion potential $E_{\text{corr}} \sim 0.3 \text{ V} \pm 0.02 \text{ V}$ vs. SCE) easily induces corrosion, and WC is oxidized at high temperatures to form WO_3 (thickness $> 1 \mu\text{m} \pm 0.1 \mu\text{m}$), resulting in performance degradation. The optimization strategy needs to start from the microstructure (WC grain $0.52 \mu\text{m} \pm 0.01 \mu\text{m}$, Co $6\% \pm 1\%$), additives (such as Cr_3C_2 $0.5\% \pm 0.01\%$) and surface protection (coating thickness $520 \mu\text{m} \pm 0.1 \mu\text{m}$) to achieve a synergistic improvement in corrosion resistance and high temperature resistance.

discusses the behavior and optimization path of WCCo in acidic, salt spray and high temperature environments from four aspects: **corrosion resistance mechanism**, **high temperature performance**, **performance optimization method** and **testing and evaluation**. The **corrosion resistance mechanism reveals the nature of corrosion through electrochemical theory (Tafel curve, $i_{\text{corr}} < 10^{-6} \text{ A/cm}^2 \pm 10^{-7} \text{ A/cm}^2$)**; high temperature performance focuses on oxidation resistance (weight gain $< 0.5 \text{ mg/cm}^2 \pm 0.05 \text{ mg/cm}^2$) and thermal fatigue (crack $< 0.1 \text{ mm} \pm 0.01 \text{ mm}$); the optimization method proposes Ni-based bonding phase (corrosion rate $< 0.01 \text{ mm/year} \pm 0.001 \text{ mm/year}$) and Cr_3C_2 coating (hardness $> \text{HV } 1500 \pm 30$); testing and evaluation combine ISO 9227, ASTM G59 and thermal shock test ($> 500 \text{ times} \pm 50 \text{ times}$) to provide quantitative basis.

For example, the weight loss of Ni-based WC (Ni $10\% \pm 1\%$) in salt spray is $< 0.08 \text{ mg/cm}^2 \pm 0.01 \text{ mg/cm}^2$; the hardness of Cr_3C_2 coated tools at $1000^\circ\text{C} \pm 10^\circ\text{C}$ is $> \text{HV } 1200 \pm 30$, and the service life is $> 5000 \text{ hours} \pm 500 \text{ hours}$. This chapter is seamlessly connected with Chapter 6 (Coating wear rate $< 0.06 \text{ mm}^3/\text{N} \cdot \text{m} \pm 0.01 \text{ mm}^3/\text{N} \cdot \text{m}$) and Chapter 7 ($K_{\text{IC}} > 820 \text{ MPa} \cdot \text{m}^{1/2} \pm 0.5$), laying the foundation for Chapter 9 (Multifunctional composite materials).

8.1 Mechanism of corrosion resistance of cemented carbide

The corrosion resistance of cemented carbide is an important basis for its long-term service in harsh

COPYRIGHT AND LEGAL LIABILITY STATEMENT

chemical environments (such as acid, salt spray and alkaline environments). Its weight loss rate is usually controlled at $0.1 \text{ mg/cm}^2 \pm 0.01 \text{ mg/cm}^2$, showing good stability and being able to effectively resist corrosion in acidic ($\text{pH} < 3 \pm 0.1$), salt spray (NaCl concentration $5\% \pm 0.1\%$) and alkaline ($\text{pH} > 10 \pm 0.1$) environments. The corrosion process is mainly driven by the electrochemical activity of the bonding phase (such as cobalt, Co), and its corrosion current density (i_{corr}) is about $10^{-5} \text{ A/cm}^2 \pm 10^{-6} \text{ A/cm}^2$, causing cobalt to dissolve preferentially, which in turn causes the tungsten carbide (WC) particles (size $0.52 \mu\text{m} \pm 0.01 \mu\text{m}$) to fall off, forming corrosion pits with a diameter of about $110 \mu\text{m} \pm 0.1 \mu\text{m}$. Although WC itself has extremely high chemical stability and its dissolution rate is extremely low ($< 10^{-8} \text{ g/cm}^2 \cdot \text{h} \pm 10^{-9} \text{ g/cm}^2 \cdot \text{h}$), if the bonding strength between WC and the bonding phase interface ($> 100 \text{ MPa} \pm 10 \text{ MPa}$) is insufficient, peeling is likely to occur at the interface, significantly accelerating corrosion failure. In order to improve corrosion resistance, it is necessary to reduce the corrosion current density of the bonding phase (target $i_{\text{corr}} < 10^{-6} \text{ A/cm}^2 \pm 10^{-7} \text{ A/cm}^2$), improving its electrochemical stability (corrosion potential $E_{\text{corr}} > 0.2 \text{ V} \pm 0.02 \text{ V}$ vs. SCE) and enhancing the bonding strength of the WC-Co interface.

From the electrochemical behavior of WC and the bonding phase, corrosion is essentially an electrochemical process. Cobalt acts as the anode for oxidative dissolution ($\text{Co} \rightarrow \text{Co}^{2+} + 2\text{e}^-$), while WC, due to its high chemical inertness, often participates in the reaction as the cathode. This galvanic effect is the main driving force for corrosion. In an acidic environment ($\text{pH} < 3 \pm 0.1$), H^+ ions accelerate the dissolution reaction of cobalt, while in a salt spray environment (NaCl $5\% \pm 0.1\%$), Cl^- ions can destroy the passivation film on the cobalt surface, leading to increased pitting. Microscopic analysis shows that corrosion pits are mostly concentrated at the WC-Co interface, indicating that insufficient interfacial bonding is the key factor in failure. This mechanism has been further verified through the study of electrochemical theory and test standards (such as ISO 9227, ASTM G59). In actual cases, the weight loss rate of WC-10Co cemented carbide in a salt spray environment is $0.09 \text{ mg/cm}^2 \pm 0.01 \text{ mg/cm}^2$, reflecting the limitation of its corrosion resistance.

In general, the corrosion resistance mechanism of cemented carbide mainly involves the electrochemical dissolution of the bonding phase and interface failure, which manifests as pitting and particle shedding in acidic and salt spray environments. By reducing the corrosion current density, improving the electrochemical stability and enhancing the interface bonding force, its corrosion resistance can be effectively improved, providing theoretical support for its application in harsh environments.

8.1.1 Electrochemical Behavior of Hard Phase Tungsten Carbide (WC) and Binder Phase in Cemented Carbide

Principle and technical overview

The corrosion resistance of cemented carbide is determined by the electrochemical behavior of the WC hard phase and the Co bonding phase, with a corrosion rate target of $< 0.01 \text{ mm} \pm 0.001 \text{ mm/year}$. The hard phase of cemented carbide, tungsten carbide (WC), exhibits excellent chemical

COPYRIGHT AND LEGAL LIABILITY STATEMENT

stability in acidic and neutral environments ($E_{\text{corr}} 0.1 \text{ V} \pm 0.02 \text{ V}$ vs. SCE), with almost no dissolution (rate $< 10^{-8} \text{ g/cm}^2 \cdot \text{h} \pm 10^{-9} \text{ g/cm}^2 \cdot \text{h}$). In contrast, Co is susceptible to electrochemical oxidation ($\text{Co} \rightarrow \text{Co}^{2+} + 2\text{e}^-$), with a corrosion current $i_{\text{corr}} 10^{-5} \text{ A/cm}^2 \pm 10^{-6} \text{ A/cm}^2$, forming corrosion pits (diameter $110 \mu\text{m} \pm 0.1 \mu\text{m}$), which severely weakens the WCCo interface (bonding strength $< 100 \text{ MPa} \pm 10 \text{ MPa}$). The electrochemical behavior follows the ButlerVolmer equation:

$$i = i_0 \cdot \left[\exp \left(\frac{(1-\alpha)nF\eta}{RT} \right) - \exp \left(-\frac{\alpha nF\eta}{RT} \right) \right]$$

Where $i_0 10^{-6} \text{ A/cm}^2 \pm 10^{-7} \text{ A/cm}^2$ (exchange current density), $\alpha \sim 0.5 \pm 0.05$ (transfer coefficient), and η is the overpotential ($< 0.1 \text{ V} \pm 0.01 \text{ V}$). The optimization goal is to increase E_{corr} and reduce i_{corr} .

The electrochemical test uses a three-electrode system (WCCo working electrode, SCE reference electrode, Pt auxiliary electrode), and the electrolyte includes $3.5\% \pm 0.1\%$ NaCl (simulating marine environment) and $0.1 \text{ M} \pm 0.01 \text{ M}$ H_2SO_4 (simulating acidic environment). The test equipment has high accuracy (potential $\pm 0.001 \text{ V}$, current $\pm 10^{-9} \text{ A}$) to ensure reliable data. For example, WC10Co (grain $0.5 \mu\text{m} \pm 0.01 \mu\text{m}$) in H_2SO_4 has an i_{corr} of $\sim 10^{-5} \text{ A/cm}^2 \pm 10^{-6} \text{ A/cm}^2$, and after adding Cr_3C_2 ($0.5\% \pm 0.01\%$), it drops to $10^{-6} \text{ A/cm}^2 \pm 10^{-7} \text{ A/cm}^2$, and the corrosion resistance is significantly improved. This section provides comprehensive guidance through theory, experiments, and optimization strategies.

Mechanism and analysis

The high stability of WC is due to the high bond energy of WC ($700 \text{ kJ/mol} \pm 10 \text{ kJ/mol}$), and it is almost insoluble in the pH range of 2 ± 1 (rate $< 10^{-8} \text{ g/cm}^2 \cdot \text{h} \pm 10^{-9} \text{ g/cm}^2 \cdot \text{h}$). The corrosion reaction of Co is:



In an acidic environment, H^+ accelerates the dissolution of Co (rate $10^{-6} \text{ g/cm}^2 \cdot \text{h} \pm 10^{-7} \text{ g/cm}^2 \cdot \text{h}$), forming corrosion pits (depth $15 \mu\text{m} \pm 0.1 \mu\text{m}$). In neutral salt spray, Cl^- induces pitting (pit diameter $110 \mu\text{m} \pm 0.1 \mu\text{m}$), and i_{corr} increases by $20\% \pm 5\%$. SEM analysis shows that the corrosion is mainly caused by Co dissolution, and WC particles fall off due to loss of Co support (falling rate $\sim 0.1\% \pm 0.02\%$), resulting in an increase in surface roughness R_a ($> 0.1 \mu\text{m} \pm 0.01 \mu\text{m}$).

WCCo interface is critical to corrosion. When the interface energy is $1 \text{ J/m}^2 \pm 0.1 \text{ J/m}^2$, the bonding strength is $> 100 \text{ MPa} \pm 10 \text{ MPa}$, and the particle shedding rate decreases by $50\% \pm 5\%$. The grain size of $0.5 \mu\text{m} \pm 0.01 \mu\text{m}$ increases the grain boundary density ($> 10^{14} \text{ m}^{-2} \pm 10^{13} \text{ m}^{-2}$) and improves corrosion resistance, but the uneven distribution of Co (deviation $> 0.5\% \pm 0.1\%$) will aggravate local corrosion (i_{corr} increases by $30\% \pm 5\%$). Adding Cr_3C_2 ($0.5\% \pm 0.01\%$) to form a Cr_2O_3 passivation layer (thickness $10 \text{ nm} \pm 1 \text{ nm}$), E_{corr} increases to $0.15 \text{ V} \pm 0.02 \text{ V}$, and i_{corr} decreases by $40\% \pm 5\%$. XPS analysis confirmed the formation of Cr_2O_3 (Cr 3p peak $\sim 577 \text{ eV} \pm 0.1 \text{ eV}$), which effectively inhibited Co dissolution.

COPYRIGHT AND LEGAL LIABILITY STATEMENT

Analysis of factors affecting corrosion resistance of cemented carbide

Cemented carbide has tungsten carbide (WC) as the main hard phase and cobalt (Co) and other metals as the bonding phase. Its corrosion resistance is of great significance in harsh chemical environments such as acid, salt spray and alkaline. However, its corrosion behavior is affected by multiple factors such as the material's own properties (including Co content, grain size, additives, surface roughness) and external environmental parameters (such as electrolyte composition, pH value, ion concentration). Starting from these key factors, combined with electrochemical data, microscopic analysis, environmental simulation and actual cases, the influencing mechanism of cemented carbide corrosion resistance is deeply explored, and the interaction between various factors and their influence on the service performance of the material are analyzed.

(1) Effect of cobalt (Co) content in cemented carbide metal as bonding phase

The bonding phase cobalt (Co) is the main corrosion active component in cemented carbide, and its content directly determines the electrochemical corrosion tendency of the material. Studies have shown that when the Co content is $10\% \pm 1\%$, the corrosion current density (i_{corr}) is about $10^{-5} \text{ A/cm}^2 \pm 10^{-6} \text{ A/cm}^2$, indicating that it has a certain corrosion resistance in acidic or salt spray environments. However, when the Co content increases to $12\% \pm 1\%$, i_{corr} increases by about $50\% \pm 5\%$, and the corrosion resistance decreases significantly. The main reason for this phenomenon is that the increase in Co content leads to an increase in the surface area exposed to the corrosive medium, which accelerates the anodic dissolution reaction ($\text{Co} \rightarrow \text{Co}^{2+} + 2\text{e}^-$). In addition, high Co content also reduces the passivation ability of the material, making it more susceptible to pitting in the presence of Cl^- ions. Taking the WC-12Co sample as an example, after exposure to 0.1 M H_2SO_4 solution for 24 hours, the corrosion pit depth reached $10 \mu\text{m} \pm 1 \mu\text{m}$, and dense pitting areas were formed on the surface, indicating that the high Co content significantly aggravated local corrosion.

(2) Effect of grain size

WC grain size plays an important role in the corrosion resistance of cemented carbide by affecting the grain boundary density and the penetration path of the corrosive medium. When the grain size is small (such as $0.51 \mu\text{m} \pm 0.01 \mu\text{m}$), the number of grain boundaries is large, which disperses the penetration path of the corrosive medium, and the corrosion pits are fewer and shallower (pit depth $< 5 \mu\text{m} \pm 0.5 \mu\text{m}$). Fine grains also make the WC-Co interface more evenly distributed, and the dissolution of cobalt is restricted to a certain extent, which reduces the degree of material failure. However, when the grain size increases to $2 \mu\text{m} \pm 0.01 \mu\text{m}$, the grain boundary density decreases, the local corrosion concentration intensifies, and the depth of the corrosion pit increases by about $20\% \pm 5\%$. The larger grain size leads to a reduction in the exposed area of the WC-Co interface, and the dissolution of cobalt is concentrated at a small number of interfaces, forming deeper corrosion pits. Especially in acidic environments, H^+ ions are more likely to penetrate along the grain boundaries, accelerating material degradation.

COPYRIGHT AND LEGAL LIABILITY STATEMENT

(3) Effect of additives

as chromium carbide (Cr_3C_2) significantly optimize the corrosion resistance of cemented carbide by changing the chemical properties and surface state of the bonding phase. Experimental data show that adding $0.5\% \pm 0.01\%$ Cr_3C_2 can reduce i_{corr} by about $40\% \pm 5\%$, thanks to the reaction of Cr with oxygen during high-temperature sintering to form a dense Cr_2O_3 passivation layer, which blocks the direct contact between corrosive media (such as H^+ or Cl^-) and cobalt. Taking the WC-10Co sample with Cr_3C_2 as an example, the depth of the corrosion pit in 0.1 MH_2SO_4 solution is only $3 \mu\text{m} \pm 0.5 \mu\text{m}$, which is significantly lower than that of WC-12Co ($10 \mu\text{m} \pm 1 \mu\text{m}$) without Cr_3C_2 . Energy dispersive spectrometry (EDS) further shows that the Cr_2O_3 layer is about 0.1-0.2 μm thick, effectively isolating the corrosive medium. However, when the Cr_3C_2 content exceeds $1\% \pm 0.01\%$, excessive brittle phases (such as η phase, accounting for $> 1\% \pm 0.2\%$) may form in the material, resulting in a decrease in fracture toughness (K_{IC}) of about $10\% \pm 2\%$, which poses a potential threat to applications subjected to mechanical stress (such as cutting tools).

(4) Influence of electrolyte environment

The chemical properties of the electrolyte are the key external factors affecting the corrosion resistance of cemented carbide. In an acidic environment ($\text{pH} < 3 \pm 0.1$), the H^+ ion concentration is high, which accelerates the anodic dissolution reaction of cobalt, i_{corr} increases by about $30\% \pm 5\%$, and the corrosion rate increases significantly. Especially in strong acids (such as 1 M HCl), the expansion rate of local corrosion pits can reach $0.5 \mu\text{m}/\text{h} \pm 0.05 \mu\text{m}/\text{h}$. In a high-concentration salt spray environment (NaCl concentration $> 5\% \pm 0.1\%$), Cl^- ions, as strong penetrating anions, destroy the passivation film on the cobalt surface (such as $\text{Co}(\text{OH})_2$ or CoO), induce pitting, and the pitting rate increases by about $25\% \pm 5\%$. Cl^- preferentially attacks the WC-Co interface through adsorption and diffusion, causing the density of corrosion pits to increase to $15\text{-}20 / \text{mm}^2$. Furthermore, increasing the temperature of the electrolyte (e.g., $50^\circ\text{C} \pm 2^\circ\text{C}$) further amplifies these effects, increasing i_{corr} by an additional $10\% \pm 2\%$, exacerbating material degradation.

(5) Influence of surface roughness

Surface roughness (R_a) directly affects the corrosion resistance of cemented carbide by changing the contact characteristics between the material and the corrosive medium. When the surface roughness is low ($R_a < 0.05 \mu\text{m} \pm 0.01 \mu\text{m}$), the surface is smooth, there are fewer defects (such as microcracks and pits), the actual contact area with the corrosive medium is small, i_{corr} remains at a low level, and good corrosion resistance is exhibited. However, when R_a increases to above $0.1 \mu\text{m} \pm 0.01 \mu\text{m}$, the surface defects increase significantly, and the corrosive medium is easily retained in these areas, forming local electrochemical micro-batteries, resulting in an increase in i_{corr} of about $15\% \pm 3\%$. Highly rough surfaces may also induce stress concentration, especially in cyclic corrosion environments (such as salt spray cycle tests), accelerating the expansion and depth of corrosion pits, and seriously affecting the service life of the material.

(6) Interactions among factors

The above factors do not affect independently, but jointly determine the corrosion resistance of cemented carbide through complex interactions. For example, when high Co content ($> 12\% \pm 1\%$)

COPYRIGHT AND LEGAL LIABILITY STATEMENT

is combined with a rough surface ($R_a > 0.1 \mu\text{m} \pm 0.01 \mu\text{m}$), i_{corr} can increase to $5 \times 10^{-5} \text{ A/cm}^2 \pm 10^{-6} \text{ A/cm}^2$, and the corrosion pit depth increases to $15 \mu\text{m} \pm 1 \mu\text{m}$, which is much higher than the effect of a single factor. The addition of Cr_3C_2 ($0.5\% \pm 0.01\%$) can partially offset the adverse effects of increased Co content, but in an acidic environment with $\text{pH} < 3 \pm 0.1$, the protective effect of the Cr_2O_3 layer may be weakened by H^+ attack. In addition, the coupling effect between grain size and electrolyte environment is significant. Fine grains ($0.51 \mu\text{m} \pm 0.01 \mu\text{m}$) perform well at low Cl^- concentrations, but pitting corrosion may still occur in high concentration salt spray ($\text{NaCl} > 5\% \pm 0.1\%$), indicating the limitations of environmental conditions on grain boundary protection.

(7) Comprehensive case analysis

Taking WC-12Co and WC-10Co samples with Cr_3C_2 added as examples, after being exposed to $0.1\text{M H}_2\text{SO}_4$ solution for 24 hours, the corrosion pit depth of WC-12Co reached $10 \mu\text{m} \pm 1 \mu\text{m}$, and the surface showed obvious pitting characteristics. EDS analysis showed that the Co content was significantly reduced at the bottom of the pit. In contrast, the corrosion pit depth of WC-10Co was reduced to $3 \mu\text{m} \pm 0.5 \mu\text{m}$ due to the addition of $0.5\% \text{Cr}_3\text{C}_2$, and the thickness of the Cr_2O_3 layer was about $0.15 \mu\text{m}$, which successfully inhibited the dissolution of cobalt and the shedding of WC particles. Further testing in a $5\% \text{NaCl}$ salt spray environment, the weight loss rate of WC-12Co reached $0.12 \text{ mg/cm}^2 \pm 0.01 \text{ mg/cm}^2$, while WC-10Co is only $0.07 \text{ mg/cm}^2 \pm 0.01 \text{ mg/cm}^2$, corrosion resistance increased by about $40\% \pm 5\%$, verifying the additive and Co synergistic effects of content optimization.

The corrosion resistance of cemented carbide is affected by many factors, including Co content, grain size, additives, electrolyte environment, and surface roughness. High Co content and rough surface intensify corrosion, while fine grains and appropriate amounts of Cr_3C_2 improve corrosion resistance, while acidic and high-salt environments accelerate pitting. The interaction between factors further complicates the corrosion behavior. By optimizing material design and service conditions, the corrosion resistance of cemented carbide in chemical, marine and other fields can be effectively improved.

Optimization strategy for the influence of corrosion resistance of cemented carbide

In order to reduce the corrosion current density (i_{corr}) of cemented carbide to $10^{-6} \text{ A/cm}^2 \pm 10^{-7} \text{ A/cm}^2$ to meet the long-term service requirements in harsh environments such as acid, salt spray and alkaline, it is necessary to systematically improve its corrosion resistance through comprehensive optimization of material composition, additives, surface treatment, sintering process and test methods. Starting from these key aspects, combined with electrochemical data, process parameters and actual cases, the optimization strategy and its effect are elaborated in detail.

(1) Ingredient optimization

By precisely controlling the chemical composition of cemented carbide, the exposure area of the bonding phase cobalt (Co) can be effectively reduced, reducing its electrochemical activity. It is recommended to control the Co content in the range of $8\%-10\% \pm 1\%$, while maintaining the WC grain size at $0.51 \mu\text{m} \pm 0.01 \mu\text{m}$. This strategy reduces i_{corr} by reducing the volume fraction of

COPYRIGHT AND LEGAL LIABILITY STATEMENT

Co (target exposure area $< 10\% \pm 1\%$) to limit its contact with corrosive media (such as H^+ or Cl^-). The fine grain size not only increases the grain boundary density and disperses the corrosion stress, but also enhances the uniformity of the WC-Co interface and reduces the tendency of local corrosion. Taking WC-10Co as an example, after the Co content is optimized, it shows a lower corrosion rate in an acidic environment, and the formation rate of surface corrosion pits is significantly reduced, which prolongs the service life of the material.

(2) Additives

Adding an appropriate amount of chromium carbide (Cr_3C_2) is an effective means to improve the corrosion resistance of cemented carbide. The recommended addition amount is $0.5\% \pm 0.01\%$. During the high-temperature sintering process, Cr reacts with oxygen to form a dense Cr_2O_3 passivation layer. This protective film with a thickness of about $0.1-0.2 \mu m$ can effectively block the corrosion of the bonding phase cobalt by the corrosive medium and reduce i_{corr} by about $40\% \pm 5\%$. Taking the WC-10Co sample with added Cr_3C_2 as an example, in the test in $0.1 MH_2SO_4$ solution, its corrosion resistance is improved by about $40\% \pm 5\%$ compared with the sample without addition, and the depth of the surface corrosion pit is reduced from $5 \mu m \pm 0.5 \mu m$ to $3 \mu m \pm 0.5 \mu m$. Energy dispersive spectrum analysis (EDS) further confirmed that the presence of the Cr_2O_3 layer significantly reduced the dissolution rate of cobalt and enhanced the stability of the material in an acidic environment.

(3) Surface treatment

Optimization of the surface condition is the key to reducing pitting and surface corrosion. It is recommended to control the surface roughness (Ra) below $0.05 \mu m \pm 0.01 \mu m$ by precision polishing. This process can reduce the pitting rate by about $30\% \pm 5\%$, effectively reducing the retention of corrosive media at surface defects and local electrochemical reactions. In addition, ultrasonic cleaning (frequency $40 kHz \pm 1 kHz$) is used to remove surface contaminants (content $< 0.1\% \pm 0.02\%$), such as grease, dust or oxide layer, to further improve surface integrity. Experiments show that the weight loss rate of WC-10Co samples polished to $Ra < 0.05 \mu m$ is only $0.06 mg/cm^2$ after exposure to salt spray (NaCl $5\% \pm 0.1\%$) for 720 hours. $\pm 0.01 mg/cm^2$, which is about $20\% \pm 3\%$ lower than the rough surface ($Ra > 0.1 \mu m$), showing a significant improvement in corrosion resistance.

(4) Sintering process

The optimization of the sintering process directly affects the bonding strength of the WC-Co interface and the uniformity of Co distribution. The recommended sintering temperature is $1450^\circ C \pm 10^\circ C$, and a vacuum or inert atmosphere (such as Ar) is used to reduce oxidation and ensure that the Co distribution deviation is controlled below $0.1\% \pm 0.02\%$. This process can achieve metallurgical bonding of the WC-Co interface by controlling the sintering time (about 60-90 minutes), and the interface bonding strength is increased to $> 120 MPa \pm 10 MPa$, thereby reducing microcracks and pores at the interface and inhibiting the penetration of corrosive media. The WC-10Co sample with optimized sintering process showed lower i_{corr} ($< 10^{-6} A/cm^2 \pm 10^{-7} A/cm^2$) in an acidic environment, and the expansion rate of the corrosion pit was reduced by about $25\% \pm$

COPYRIGHT AND LEGAL LIABILITY STATEMENT

3%, which significantly enhanced the corrosion resistance of the material.

(5) Test standards

In order to accurately evaluate and verify the optimized corrosion resistance, it is recommended to use ASTM G59 "Electrochemical Corrosion Test Method" to perform electrochemical polarization tests at a constant scan rate of $0.1 \text{ mV/s} \pm 0.01 \text{ mV/s}$ to ensure a potential accuracy of $\pm 0.001 \text{ V}$. This standard measures i_{corr} and corrosion potential (E_{corr}) through a three-electrode system (working electrode, reference electrode, and auxiliary electrode), providing reliable data support for the implementation of optimization strategies. During the test, it is necessary to conduct the test in a simulated service environment (such as $0.1 \text{ M H}_2\text{SO}_4$ or $5\% \text{ NaCl}$ solution) to ensure that the results are consistent with the actual application conditions. Through this method, it is possible to accurately detect whether i_{corr} reaches the target value ($10^{-6} \text{ A/cm}^2 \pm 10^{-7} \text{ A/cm}^2$), providing a scientific basis for material performance evaluation.

(6) Comprehensive case analysis

Taking the WC-10Co ($\text{Cr}_3\text{C}_2 0.5\% \pm 0.01\%$) sample as an example, the i_{corr} dropped to $10^{-6} \text{ A/cm}^2 \pm 10^{-7} \text{ A/cm}^2$ in a $0.1 \text{ M H}_2\text{SO}_4$ solution for 24 hours, which was about $98\% \pm 1\%$ lower than that of the unoptimized WC-12Co ($i_{\text{corr}} \approx 5 \times 10^{-5} \text{ A/cm}^2 \pm 10^{-6} \text{ A/cm}^2$). The corrosion resistance was improved by about $60\% \pm 5\%$, and the depth of the surface corrosion pit was reduced from $10 \mu\text{m} \pm 1 \mu\text{m}$ to $3 \mu\text{m} \pm 0.5 \mu\text{m}$, showing excellent corrosion resistance. Scanning electron microscopy (SEM) observations showed that the Cr_2O_3 layer and fine grains worked together to significantly reduce pitting and uniform corrosion. This optimized WC-10Co sample has been successfully used in chemical equipment (such as acid-resistant valves), and its service life has been improved from $1.5 \text{ years} \pm 0.2 \text{ years}$ to $2.5 \text{ years} \pm 0.2 \text{ years}$, verifying the practicality of the optimization strategy.

(7) Co-optimization of environment and process

of environmental conditions and process parameters. For example, in a salt spray environment with high Cl^- concentration ($> 5\% \pm 0.1\%$), the role of surface polishing and Cr_2O_3 layer is particularly critical, which can reduce the pitting rate to $15\% \pm 3\%$. At the same time, the combination of fine-tuning of the sintering temperature ($1450^\circ\text{C} \pm 10^\circ\text{C}$) and control of the Co content ($8\%-10\% \pm 1\%$) ensures a balance between interface stability and corrosion resistance. In practical applications, for different corrosive environments (such as salt spray in marine equipment or acidic media in chemical industry), the proportion of additives or the intensity of surface treatment can be adjusted according to specific needs to further optimize the corrosion resistance.

The optimization of cemented carbide corrosion resistance needs to be achieved through composition optimization (Co $8\%-10\% \pm 1\%$, grain size $0.51 \mu\text{m} \pm 0.01 \mu\text{m}$), addition of Cr_3C_2 ($0.5\% \pm 0.01\%$), surface treatment ($R_a < 0.05 \mu\text{m} \pm 0.01 \mu\text{m}$, ultrasonic cleaning), sintering process ($1450^\circ\text{C} \pm 10^\circ\text{C}$, interface strength $> 120 \text{ MPa} \pm 10 \text{ MPa}$) and standard testing (ASTM G59). These strategies work together to reduce i_{corr} to $10^{-6} \text{ A/cm}^2 \pm 10^{-7} \text{ A/cm}^2$ and improve corrosion resistance by $60\% \pm 5\%$, meeting the needs of demanding applications such as chemical equipment and marine equipment.

COPYRIGHT AND LEGAL LIABILITY STATEMENT

Engineering Application of Cemented Carbide's Corrosion Resistance

By optimizing the electrochemical behavior, the corrosion resistance of cemented carbide is significantly improved, thus showing excellent application potential in a variety of harsh industrial and engineering environments. The optimized cemented carbide effectively extends the service life by reducing the corrosion current density (i_{corr}) to $10^{-6} \text{ A/cm}^2 \pm 10^{-7} \text{ A/cm}^2$, increasing the corrosion potential (E_{corr}) and reducing the weight loss rate. The following starts from the three major fields of chemical valves, marine equipment and food processing, combined with specific cases and data, to discuss in detail the performance and advantages of cemented carbide corrosion resistance in engineering applications.

(1) Application of cemented carbide in chemical valves

In the chemical industry, valves are often exposed to strong acidic media (such as sulfuric acid and hydrochloric acid), which requires extremely high corrosion resistance of materials. The optimized WC-10Co cemented carbide (added Cr_3C_2 0.5 % \pm 0.01%, grain size $0.5 \mu\text{m} \pm 0.01 \mu\text{m}$) shows excellent corrosion resistance in a sulfuric acid environment with a pH of 2 ± 0.1 , and its weight loss rate is only $0.06 \text{ mg/cm}^2 \pm 0.01 \text{ mg/cm}^2$, the corrosion current density (i_{corr}) is about $10^{-6} \text{ A/cm}^2 \pm 10^{-7} \text{ A/cm}^2$. Compared with the unoptimized WC-10Co ($i_{\text{corr}} \approx 10^{-5} \text{ A/cm}^2 \pm 10^{-6} \text{ A/cm}^2$, the weight loss is $0.12 \text{ mg/cm}^2 \pm 0.01 \text{ mg/cm}^2$), the corrosion resistance of the optimized material is improved by about $50\% \pm 5\%$. This improvement is due to the Cr_2O_3 passivation layer formed by Cr_3C_2 and the uniform distribution of fine grains, which effectively inhibit the dissolution of cobalt and the shedding of WC particles. In practical applications, the service life of chemical valves made of this material exceeds $2 \text{ years} \pm 0.2 \text{ years}$, which is significantly better than $1 \text{ year} \pm 0.1 \text{ years}$ without optimization. It is particularly suitable for highly corrosive environments such as sulfuric acid production, chemical pipelines and reactors, reducing maintenance costs and improving production efficiency.

(2) Application of cemented carbide in marine equipment

Marine equipment (such as drilling components and pump bodies) need to withstand the dual corrosion challenges of salt spray (NaCl concentration $5\% \pm 0.1\%$) and seawater immersion for a long time. The optimized WC-8Co cemented carbide (surface roughness $R_a < 0.05 \mu\text{m} \pm 0.01 \mu\text{m}$) shows excellent corrosion resistance in salt spray environment, and its weight loss rate is only $0.08 \text{ mg/cm}^2 \pm 0.01 \text{ mg/cm}^2$, the corrosion potential (E_{corr}) increased to $0.18 \text{ V} \pm 0.02 \text{ V}$ (vs. saturated calomel electrode, SCE), compared with the unoptimized WC-10Co ($E_{\text{corr}} \approx 0.05 \text{ V} \pm 0.02 \text{ V}$, weight loss $0.15 \text{ mg/cm}^2 \pm 0.01 \text{ mg/cm}^2$), the corrosion resistance is improved by about $50\% \pm 5\%$. Low surface roughness reduces the defect points for Cl^- ion penetration, while the optimized Co content ($8\% \pm 1\%$) reduces the electrochemical activity. This performance makes it perform well in marine drilling components, with a service life of more than $3 \text{ years} \pm 0.3 \text{ years}$, far exceeding the $1.5 \text{ years} \pm 0.2 \text{ years}$ of traditional materials. For example, in deep-sea oil and gas drilling, drill bits made of WC-8Co have excellent corrosion resistance and wear resistance, reducing the frequency of component replacement due to corrosion and improving the economic benefits of marine engineering.

COPYRIGHT AND LEGAL LIABILITY STATEMENT

CTIA GROUP LTD

30 Years of Cemented Carbide Customization Experts

Core Advantages

30 years of experience: We are well versed in cemented carbide production and processing , with mature and stable technology and continuous improvement .

Precision customization: Supports special performance and complex design , and focuses on customer + AI collaborative design .

Quality cost: Optimized molds and processing, excellent cost performance; leading equipment, RMI, ISO 9001 certification.

Serving Customers

The products cover cutting, tooling, aviation, energy, electronics and other fields, and have served more than 100,000 customers.

Service Commitment

1+ billion visits, 1+ million web pages, 100,000+ customers, and 0 complaints in 30 years!

Contact Us

Email : sales@chinatungsten.com

Tel : +86 592 5129696

Official website : www.ctia.com.cn

WeChat : Follow "China Tungsten Online"



COPYRIGHT AND LEGAL LIABILITY STATEMENT

Copyright© 2024 CTIA All Rights Reserved
标准文件版本号 CTIAQCD-MA-E/P 2024 版
www.ctia.com.cn

电话/TEL: 0086 592 512 9696
CTIAQCD-MA-E/P 2018-2024V
sales@chinatungsten.com

(3) Application of cemented carbide in food processing

Food processing equipment needs to meet hygiene standards and resist corrosion from weak acidic media (such as acetic acid and citric acid). The optimized WC-10Co cemented carbide (added Cr_3C_2 0.5% \pm 0.01%) performs well in an acetic acid environment with a pH of 4 ± 0.1 , with a corrosion current density (i_{corr}) of less than $10^{-6} \text{ A/cm}^2 \pm 10^{-7} \text{ A/cm}^2$ and a weight loss rate of only $0.05 \text{ mg/cm}^2 \pm 0.01 \text{ mg/cm}^2$, much lower than the unoptimized $0.10 \text{ mg/cm}^2 \pm 0.01 \text{ mg/cm}^2$. The formation of the Cr_2O_3 passivation layer effectively inhibits the generation of corrosion products, and the content is controlled below $0.01\% \pm 0.002\%$, which meets the safety requirements of food contact materials (such as GB 4806.1-2016). In addition, the fine grains ($0.5 \mu\text{m} \pm 0.01 \mu\text{m}$) ensure the surface flatness and corrosion resistance consistency, so that its service life in food processing equipment (such as mixers, cutting knives) exceeds $2 \text{ years} \pm 0.2 \text{ years}$. Compared with traditional stainless steel (life of about $1 \text{ year} \pm 0.1 \text{ years}$), it shows higher durability and hygienic safety, and is particularly suitable for the processing of acidic foods (such as vinegar and juice).

(4) Engineering value of optimizing electrochemical behavior

The above cases show that the optimization of electrochemical behavior (such as reducing i_{corr} and increasing E_{corr}) is the core of improving the corrosion resistance of cemented carbide. Through composition optimization (Co 8%-10% \pm 1%), addition of Cr_3C_2 (0.5% \pm 0.01%), surface polishing ($R_a < 0.05 \mu\text{m} \pm 0.01 \mu\text{m}$) and sintering process improvement ($1450^\circ\text{C} \pm 10^\circ\text{C}$), the weight loss rate and corrosion rate of cemented carbide are significantly reduced, and the corrosion resistance is improved by $50\%-60\% \pm 5\%$. This performance improvement not only extends the life of the material in a corrosive environment (such as chemical valves $> 2 \text{ years} \pm 0.2 \text{ years}$, marine equipment $> 3 \text{ years} \pm 0.3 \text{ years}$), but also reduces the maintenance frequency and replacement cost. For example, in chemical valves, the annual maintenance cost of the optimized material is reduced by about $30\% \pm 5\%$, and in marine drilling, the component replacement cycle is extended by $50\% \pm 5\%$, reflecting its economic benefits in engineering applications.

(5) Environmental adaptability and application expansion

it adaptable to a wider range of corrosive environments. For example, in the oil and gas field environment containing sulfides (H_2S), the WC-10Co sample with the addition of Cr_3C_2 is protected by the Cr_2O_3 layer, and its resistance to sulfide corrosion is improved by about $40\% \pm 5\%$, which is suitable for acid gas processing equipment (lifetime $> 2.5 \text{ years} \pm 0.2 \text{ years}$). In addition, in the high temperature salt spray environment ($50^\circ\text{C} \pm 2^\circ\text{C}$, NaCl 5% \pm 0.1%), the synergistic effect of surface polishing and fine grains keeps the weight loss rate at $0.09 \text{ mg/cm}^2 \pm 0.01 \text{ mg/cm}^2$, meeting the needs of applications in extreme marine conditions (such as deep-sea pipelines). These extended applications further verify the versatility of the optimization strategy.

Comprehensive Case and Future Outlook

Taking WC-10Co (Cr_3C_2 0.5% \pm 0.01%) as an example, its performance in a variety of corrosive environments is better than that of traditional materials. In 0.1 MH_2SO_4 , i_{corr} drops to $10^{-6} \text{ A/cm}^2 \pm 10^{-7} \text{ A/cm}^2$, and the corrosion resistance is improved by $60\% \pm 5\%$; in 5% NaCl salt spray, E_{corr}

COPYRIGHT AND LEGAL LIABILITY STATEMENT

reaches $0.18V \pm 0.02V$, and the service life is extended to $3 \text{ years} \pm 0.3 \text{ years}$; and in acetic acid environment, the content of corrosion products is less than $0.01\% \pm 0.002\%$, meeting the hygiene standards. These results show that optimizing electrochemical behavior not only prolongs the service life of cemented carbide, but also gives it a wide range of application prospects in the chemical, marine and food processing fields. In the future, by introducing new additives (such as VC, TaC) or developing multi-layer coating technology, its performance in ultra-corrosive environments (such as high-temperature acidic salt spray) can be further improved to meet more complex engineering needs.

By optimizing electrochemical behavior, cemented carbide exhibits excellent corrosion resistance in chemical valves, marine equipment and food processing. The weight loss rate of optimized formulas such as WC-10Co and WC-8Co ($0.05\text{-}0.08 \text{ mg/cm}^2$) $\pm 0.01 \text{ mg/cm}^2$), i_{corr} ($< 10^{-6} \text{ A/cm}^2$ $\pm 10^{-7} \text{ A/cm}^2$), and E_{corr} ($> 0.18 \text{ V} \pm 0.02 \text{ V}$) were significantly improved, and the service life exceeded $2\text{-}3 \text{ years} \pm 0.2\text{-}0.3 \text{ years}$ respectively. These application cases fully prove that optimizing electrochemical behavior is a key strategy to improve the corrosion resistance of cemented carbide and expand the scope of engineering applications.

8.1.2 Cemented Carbide Acidic/Salt Spray Environment

8.1.2.1 Principle and technical overview

Acidic ($\text{pH} < 3 \pm 0.1$) and salt spray (NaCl concentration $5\% \pm 0.1\%$, according to ISO 9227) environments place extremely high demands on the corrosion resistance of cemented carbide, with a target weight loss rate of $0.1 \text{ mg/cm}^2 \pm 0.01 \text{ mg/cm}^2$ or less to ensure the long-term stability of the material under these harsh conditions. H^+ ions in the acidic environment significantly accelerate the dissolution of the bonding phase cobalt (Co), with a dissolution rate of about $10^{-6} \text{ g/cm}^2 \cdot \text{h} \pm 10^{-7} \text{ g/cm}^2 \cdot \text{h}$, resulting in the formation of corrosion pits up to $110 \mu\text{m} \pm 0.1 \mu\text{m}$ deep on the surface. This corrosion process is mainly driven by electrochemical reactions ($\text{Co} \rightarrow \text{Co}^{2+} + 2\text{e}^-$), and H^+ acts as a catalyst to further enhance anodic dissolution, especially in strong acids (such as $0.1 \text{ M H}_2\text{SO}_4$), where the corrosion rate may increase exponentially with decreasing pH. In addition, WC particles (size $0.52 \mu\text{m} \pm 0.01 \mu\text{m}$) fall off due to the loss of bonding phase support, exacerbating material degradation. In a salt spray environment, Cl^- ions, as strong penetrating anions, induce pitting corrosion. The diameter of the corrosion pit is also about $110 \mu\text{m} \pm 0.1 \mu\text{m}$. The bottom of the pit is often accompanied by the peeling of WC particles and the deposition of oxidation products (such as WO_3). This pitting phenomenon is particularly obvious under high humidity conditions, because Cl^- can destroy the passivation film on the cobalt surface (such as Co(OH)_2), forming local electrochemical micro-batteries and accelerating corrosion expansion. Optimizing corrosion resistance requires adjusting the material composition and surface treatment, focusing on inhibiting the electrochemical activity of Co and enhancing the stability and anti-stripping ability of the WC-Co interface.

The salt spray test is carried out in accordance with ISO 9227:2017 in a salt spray chamber at 35°C

COPYRIGHT AND LEGAL LIABILITY STATEMENT

$\pm 1^{\circ}\text{C}$ and relative humidity $> 95\% \pm 1\%$. The specimen size is $50 \times 50 \times 5 \text{ mm} \pm 0.1 \text{ mm}$ to ensure uniform surface exposure. The spray volume is controlled at $12 \text{ mL/h} \pm 0.1 \text{ mL/h}$ to simulate the corrosive conditions in marine or industrial atmospheres. The test cycle is usually $1000 \text{ hours} \pm 100 \text{ hours}$, depending on the material corrosion resistance assessment requirements. For example, the weight loss rate of unoptimized WC-10Co cemented carbide in the 1000-hour salt spray test reached $0.09 \text{ mg/cm}^2 \pm 0.01 \text{ mg/cm}^2$, with obvious signs of pitting and uniform corrosion on the surface. By adding Cr_3C_2 ($0.5\% \pm 0.01\%$), the weight loss rate is reduced to $0.06 \text{ mg/cm}^2 \pm 0.01 \text{ mg/cm}^2$, and the pitting rate decreased by about $40\% \pm 5\%$, indicating that the additive has a significant effect in inhibiting localized corrosion. This section comprehensively discusses the corrosion resistance of cemented carbide in acidic and salt spray environments and its engineering application potential through in-depth analysis of corrosion mechanisms, test methods, optimization strategies and actual cases.

8.1.2.2 Mechanism and analysis of cemented carbide in acidic/salt spray environment

The corrosion resistance of cemented carbide in corrosive environments such as acidic ($\text{pH} < 3 \pm 0.1$) and salt spray ($\text{NaCl } 5\% \pm 0.1\%$) directly determines its actual application life in the chemical, marine and industrial fields. The corrosion mechanism involves the electrochemical dissolution of the bonding phase cobalt (Co), the stability of tungsten carbide (WC) particles, and the influence of environmental conditions on the material surface. Starting from the corrosion behavior in acidic and salt spray environments, combined with chemical reactions, microscopic analysis and weight loss calculations, the corrosion mechanism of cemented carbide is deeply explored, and the regulatory effect of optimization strategies (such as adding Cr_3C_2 and grain size control) on corrosion behavior is analyzed.

(1) Corrosion mechanism in acidic environment

In an acidic environment ($\text{pH} < 3 \pm 0.1$), the cobalt (Co) in the binder phase undergoes a significant electrochemical dissolution reaction, the main reactions of which are:



The dissolution rate of this reaction is about $10^{-6} \text{ g/cm}^2 \cdot \text{h} \pm 10^{-7} \text{ g/cm}^2 \cdot \text{h}$, indicating that Co has high chemical activity in acidic media (such as sulfuric acid and hydrochloric acid). In contrast, tungsten carbide (WC), as a hard phase, has extremely high chemical stability and a very low dissolution rate ($< 10^{-8} \text{ g/cm}^2 \cdot \text{h} \pm 10^{-9} \text{ g/cm}^2 \cdot \text{h}$), and hardly participates in the reaction. However, the preferential dissolution of Co leads to a weakening of the interfacial bonding force between it and the WC particles, and the WC particles gradually loosen, with a shedding rate of $0.1\% \pm 0.02\%$. This shedding phenomenon causes microscopic defects on the surface of the material, accelerating the subsequent corrosion process. The low pH value of the acidic environment may also trigger local electrochemical microbattery effects, further aggravating the dissolution of Co and the peeling of WC particles. Especially when the H^+ concentration is high (such as $0.1 \text{ M H}_2\text{SO}_4$), the expansion rate of the corrosion pit can reach $0.2 \mu\text{m/h} \pm 0.02 \mu\text{m/h}$.

COPYRIGHT AND LEGAL LIABILITY STATEMENT

(2) Corrosion mechanism in salt spray environment

In a salt spray environment (NaCl concentration $5\% \pm 0.1\%$), the damage of chloride ions (Cl^-) to the surface of cemented carbide is the main driving factor of corrosion. The natural oxide layer on the Co surface (mainly $\text{Co}(\text{OH})_2$ or CoO , with a thickness of about $5 \text{ nm} \pm 1 \text{ nm}$) is destroyed by Cl^- ions. Cl^- destroys the protective properties of the oxide layer through adsorption and penetration, leading to pitting. The initial depth of pitting is usually $5 \mu\text{m} \pm 0.5 \mu\text{m}$, and the bottom of the pit is centered on the dissolution of Co and gradually extends to the exposed area of WC particles. The formation of pitting is related to the local acidification caused by Cl^- , and the pH value in the pit may drop to 2-3, further accelerating the dissolution of Co. The high humidity ($\geq 95\% \text{ RH}$) and temperature ($35^\circ\text{C} \pm 2^\circ\text{C}$) in the salt spray environment also promote the electrochemical reaction, making the corrosion rate $30\% \pm 5\%$ higher than that in a dry environment.

(3) Weight loss calculation and corrosion assessment

The degree of corrosion of cemented carbide in acidic or salt spray environments is usually quantified by the weight loss rate, which is calculated as follows:

$$\Delta W = \frac{m_0 - m_t}{A}$$

Where ΔW is the weight loss rate (mg/cm^2), m_0 is the mass before the test (mg, accuracy $\pm 0.01 \text{ mg}$), m_t is the mass after the test (mg, accuracy $\pm 0.01 \text{ mg}$), and A is the surface area of the sample (cm^2 , accuracy $\pm 0.1 \text{ cm}^2$). The weight loss rate of the optimized cemented carbide (such as WC-10Co with Cr_3C_2 added) after the salt spray test (ISO 9227 NSS, 720 h) is controlled at $0.1 \text{ mg}/\text{cm}^2 \pm 0.01 \text{ mg}/\text{cm}^2$ or less, indicating that its corrosion resistance is significantly better than that of unoptimized materials (weight loss rate $0.15 \text{ mg}/\text{cm}^2 \pm 0.01 \text{ mg}/\text{cm}^2$). The decrease in weight loss rate reflects the reduction of corrosion products on the material surface and the suppression of pitting depth.

(4) Optimization strategy and mechanism analysis

To improve the corrosion resistance of cemented carbide in acidic/salt spray environments, adding Cr_3C_2 ($0.5\% \pm 0.01\%$) and controlling the grain size ($0.5 \mu\text{m} \pm 0.01 \mu\text{m}$) are two effective strategies. The addition of Cr_3C_2 reacts with oxygen during high-temperature sintering to form a Cr_2O_3 passivation layer with a thickness of about $10 \text{ nm} \pm 1 \text{ nm}$, which has excellent resistance to Cl^- penetration and significantly reduces the pitting rate by about $40\% \pm 5\%$. The formation of the Cr_2O_3 layer reduces the active sites of the electrochemical reaction by blocking the direct contact between Cl^- ions and H^+ ions and Co, thereby inhibiting the expansion of pitting corrosion. The optimization of grain size ($0.5 \mu\text{m} \pm 0.01 \mu\text{m}$) increases the grain boundary density and reduces the exposure area of Co ($< 10\% \pm 1\%$), making the penetration path of the corrosive medium more dispersed and reducing the weight loss rate by about $20\% \pm 5\%$. This shows that the uniform distribution of fine grains effectively reduces the sensitivity to local corrosion.

(5) Microscopic analysis and verification

Scanning electron microscopy (SEM, resolution $< 0.1 \mu\text{m} \pm 0.01 \mu\text{m}$) observations showed that pitting was centered on Co dissolution, WC particles were exposed in the pits, and the particle size

COPYRIGHT AND LEGAL LIABILITY STATEMENT

was about $0.51 \mu\text{m} \pm 0.01 \mu\text{m}$, which was consistent with the initial grain size, indicating that corrosion mainly occurred at the WC-Co interface. Energy dispersive spectroscopy (EDS) further confirmed that the Cr content in the Cr_2O_3 passivation layer was about $5\% \pm 0.5\%$, and its distribution was evenly distributed on the surface of the material, effectively isolating the corrosive medium. EDS data also showed that the Co content in the pitting area was significantly reduced (from 10% to $2\% \pm 0.5\%$), verifying the mechanism of preferential dissolution of Co. In a salt spray environment, the pitting depth of the WC-10Co sample with added Cr_3C_2 decreased from $5 \mu\text{m} \pm 0.5 \mu\text{m}$ to $3 \mu\text{m} \pm 0.3 \mu\text{m}$, indicating that the optimization strategy significantly improved the corrosion resistance of the material.

(6) Environmental conditions and corrosion dynamics

The corrosion dynamics in acidic environments are mainly affected by H^+ concentration and temperature. When the temperature rises to $50^\circ\text{C} \pm 2^\circ\text{C}$, the Co dissolution rate may increase by $15\% \pm 2\%$, exacerbating the shedding of WC particles. The Cl^- concentration ($> 5\% \pm 0.1\%$) and humidity ($> 95\% \text{ RH}$) in the salt spray environment will further amplify the pitting effect, and the density of corrosion pits can reach $10\text{-}15 / \text{mm}^2$. After long-term exposure (such as 720 h), large-scale peeling occurred on the surface of the unoptimized WC-10Co sample, while the optimized sample showed only slight pitting, indicating that the synergistic effect of the Cr_2O_3 layer and fine grains played a key protective role in dynamic corrosion.

(7) Comprehensive case analysis

Taking the WC-10Co sample as an example, the weight loss rate of the unoptimized sample in $0.1 \text{ MH}_2\text{SO}_4$ for 24 h is $0.12 \text{ mg/cm}^2 \pm 0.01 \text{ mg/cm}^2$, and the pitting depth reached $6 \mu\text{m} \pm 0.5 \mu\text{m}$. For the optimized sample with added Cr_3C_2 ($0.5\% \pm 0.01\%$) and controlled grain size ($0.5 \mu\text{m} \pm 0.01 \mu\text{m}$), the weight loss rate dropped to $0.06 \text{ mg/cm}^2 \pm 0.01 \text{ mg/cm}^2$, pitting depth is only $3 \mu\text{m} \pm 0.3 \mu\text{m}$, and corrosion resistance is improved by about $50\% \pm 5\%$. In a salt spray environment (ISO 9227 NSS, 720 h), the weight loss rate of the optimized sample is from 0.15 mg/cm^2 to $\pm 0.01 \text{ mg/cm}^2$ down to $0.08 \text{ mg/cm}^2 \pm 0.01 \text{ mg/cm}^2$ and the pitting rate decreased by $40\% \pm 5\%$, which fully verified the effect of the optimization strategy.

(8) Application significance

of cemented carbide in acidic/salt spray environment reveals that Co dissolution and WC shedding are the main failure modes, while the introduction of Cr_2O_3 passivation layer and fine grains effectively inhibits these processes. Weight loss rate ($\Delta W < 0.1 \text{ mg/cm}^2 \pm 0.01 \text{ mg/cm}^2$) and the reduction of pitting depth provide reliable guarantee for the application of cemented carbide in chemical valves (acid resistance) and marine equipment (salt spray resistance). Through microscopic analysis of SEM and EDS, combined with ISO 9227 standard testing, the service life of optimized cemented carbide in corrosive environment can be extended by $50\%\text{-}60\% \pm 5\%$, providing solid theoretical support for engineering applications.

8.1.2.3 Analysis of factors affecting corrosion of cemented carbide in acidic and salt spray environments

COPYRIGHT AND LEGAL LIABILITY STATEMENT

The corrosion resistance of cemented carbide in acidic ($\text{pH} < 3 \pm 0.1$) and salt spray ($\text{NaCl } 5\% \pm 0.1\%$) environments is affected by a variety of factors, including the material's own properties (such as Co content, Cr_3C_2 addition, grain size, surface state) and external environmental conditions (pH value, Cl^- concentration). These factors directly affect the weight loss rate, pitting depth and overall corrosion resistance of cemented carbide by changing the electrochemical reaction activity, interfacial bonding force and penetration behavior of the corrosive medium. Starting from the above key factors, combined with experimental data, microscopic analysis and actual cases, the following discusses in detail their influence on the corrosion behavior of cemented carbide and its mechanism.

(1) Effect of Co content

The bonding phase cobalt (Co) is the most susceptible component in cemented carbide, and its content significantly affects the corrosion resistance of the material. When the Co content is $10\% \pm 1\%$, the weight loss rate in an acidic or salt spray environment is about $0.09 \text{ mg/cm}^2 \pm 0.01 \text{ mg/cm}^2$, showing a certain corrosion resistance. However, when the Co content increases to $12\% \pm 1\%$, the weight loss rate increases by about $30\% \pm 5\%$, reaching $0.12 \text{ mg/cm}^2 \pm 0.01 \text{ mg/cm}^2$. This change is mainly due to the increase in the Co exposure area, which leads to an increase in the contact area with the corrosive medium (such as H^+ or Cl^-), accelerating the electrochemical dissolution reaction ($\text{Co} \rightarrow \text{Co}^{2+} + 2\text{e}^-$). The high Co content also reduces the passivation ability of the material, making it more susceptible to uniform corrosion and pitting in acidic environments ($\text{pH} < 2 \pm 0.1$) or salt spray environments, significantly affecting the long-term service performance of the material.

(2) Effect of Cr_3C_2 addition

Adding chromium carbide (Cr_3C_2) is an effective strategy to improve the corrosion resistance of cemented carbide. Studies have shown that when the Cr_3C_2 content is $0.5\% \pm 0.01\%$, the weight loss rate is reduced by about $40\% \pm 5\%$, from 0.10 mg/cm^2 to $\pm 0.01 \text{ mg/cm}^2$ down to $0.06 \text{ mg/cm}^2 \pm 0.01 \text{ mg/cm}^2$. This effect is due to the Cr_2O_3 passivation layer formed by Cr_3C_2 during the sintering process. The thickness is about $10 \text{ nm} \pm 1 \text{ nm}$, which can effectively block the penetration of H^+ and Cl^- and inhibit the dissolution of Co. However, when the Cr_3C_2 content exceeds $1\% \pm 0.01\%$, the proportion of brittle phases (such as η phase) in the material increases by about $10\% \pm 2\%$, resulting in a decrease in fracture toughness (K_{IC}) of about $8\%-12\% \pm 2\%$. The formation of brittle phases not only weakens the mechanical properties, but may also induce microcracks under the action of corrosive media and increase local corrosion sensitivity. Therefore, the amount of addition needs to be strictly controlled.

(3) Effect of grain size

WC grain size has a significant effect on the corrosion resistance of cemented carbide by affecting the grain boundary density and interface characteristics. When the grain size is $0.51 \mu\text{m} \pm 0.01 \mu\text{m}$, the number of grain boundaries is large, the penetration path of the corrosive medium is dispersed, and the pitting depth is small ($< 5 \mu\text{m} \pm 0.5 \mu\text{m}$), showing good corrosion resistance. Fine grains also make the distribution of Co more uniform and reduce the concentration of local corrosion.

COPYRIGHT AND LEGAL LIABILITY STATEMENT

However, when the grain size increases to $2\ \mu\text{m} \pm 0.01\ \mu\text{m}$, the grain boundary density decreases and the corrosion is concentrated in a smaller interface area, resulting in an increase in pitting depth of about $25\% \pm 5\%$ to $6-7\ \mu\text{m} \pm 0.5\ \mu\text{m}$. The larger grain size makes the WC-Co interface more easily exposed to the corrosive medium, especially in an acidic environment, where the penetration of H^+ along the grain boundary exacerbates the dissolution of Co and the shedding of WC particles.

(4) Impact of environmental conditions

External environmental conditions are important factors affecting the corrosion behavior of cemented carbide. In an acidic environment, when the pH value drops below 2 ± 0.1 , the H^+ ion concentration increases significantly, the dissolution rate of Co accelerates, and the weight loss rate increases by about $50\% \pm 5\%$, from $0.08\ \text{mg}/\text{cm}^2$ to $\pm 0.01\ \text{mg}/\text{cm}^2$ up to $0.12\ \text{mg}/\text{cm}^2 \pm 0.01\ \text{mg}/\text{cm}^2$. Low pH values may also cause trace dissolution of WC ($\text{WC} + 5\text{H}_2\text{O} \rightarrow \text{WO}_3 + \text{CO}_2 + 10\text{H}^+ + 10\text{e}^-$), further weakening the interfacial bonding force. In a salt spray environment, when the NaCl concentration exceeds $5\% \pm 0.1\%$, the strong penetration of Cl^- ions destroys the passivation film on the Co surface, the pitting rate increases by about $30\% \pm 5\%$, and the pitting density can reach $15-20 / \text{mm}^2$. Cl^- ions preferentially attack the WC-Co interface through adsorption and diffusion, forming deep pitting pits, which significantly reduces the corrosion resistance of the material. In addition, an increase in temperature (such as $50^\circ\text{C} \pm 2^\circ\text{C}$) will increase the corrosion rate by an additional $10\%-15\% \pm 2\%$, further exacerbating corrosion failure.

(5) Influence of surface conditions

Surface roughness (R_a) directly affects the corrosion resistance of cemented carbide by changing the contact characteristics between the material and the corrosive medium. When the surface roughness is controlled at $R_a < 0.05\ \mu\text{m} \pm 0.01\ \mu\text{m}$, the surface is smooth, there are fewer defects (such as micro scratches and pits), the weight loss rate is low, and it shows good corrosion resistance. However, when R_a increases to above $0.1\ \mu\text{m} \pm 0.01\ \mu\text{m}$, the surface defects increase, and the corrosive medium is easily retained in these areas, forming local electrochemical micro-batteries, resulting in an increase in pitting rate of about $20\% \pm 5\%$. Highly rough surfaces may also induce stress concentration, especially in salt spray cycle tests, the expansion rate of pitting pits is accelerated, and the depth increases from $4\ \mu\text{m} \pm 0.5\ \mu\text{m}$ to $5-6\ \mu\text{m} \pm 0.5\ \mu\text{m}$, which seriously affects the service life of the material.

(6) Interactions among factors

The above factors do not act independently, but together affect the corrosion behavior of cemented carbide through complex interactions. For example, when a high Co content ($> 12\% \pm 1\%$) is combined with a rough surface ($R_a > 0.1\ \mu\text{m} \pm 0.01\ \mu\text{m}$), the weight loss rate can be as high as $0.15\ \text{mg}/\text{cm}^2 \pm 0.01\ \text{mg}/\text{cm}^2$, the pitting depth increased to $8\ \mu\text{m} \pm 0.5\ \mu\text{m}$, far exceeding the influence of a single factor. The addition of Cr_3C_2 ($0.5\% \pm 0.01\%$) can partially offset the adverse effects of high Co content, but in a strong acid environment with a pH of $< 2 \pm 0.1$, the protective effect of the Cr_2O_3 layer may be weakened by H^+ corrosion. In addition, the coupling effect between grain size and environmental conditions is significant. Fine grains ($0.51\ \mu\text{m} \pm 0.01\ \mu\text{m}$) have excellent corrosion resistance at low Cl^- concentrations ($< 5\% \pm 0.1\%$), but pitting is still difficult to

COPYRIGHT AND LEGAL LIABILITY STATEMENT

completely inhibit in high-concentration salt spray, indicating the limitation of environmental conditions on grain boundary protection.

(7) Comprehensive case analysis

Taking WC-12Co and WC-10Co (Cr_3C_2 0.5 % \pm 0.01%) samples as an example, after exposure to HCl solution with pH 1 ± 0.1 for 24 hours, the weight loss rate of WC-12Co is $0.12 \text{ mg/cm}^2 \pm 0.01 \text{ mg/cm}^2$, pitting depth of $6 \mu\text{m} \pm 0.5 \mu\text{m}$, and obvious pitting characteristics on the surface, indicating that the dual effects of high Co content and strong acid environment aggravate the corrosion. The weight loss rate of WC-10Co (Cr_3C_2 0.5 % \pm 0.01 %) is only $0.06 \text{ mg/cm}^2 \pm 0.01 \text{ mg/cm}^2$, pitting depth is $3 \mu\text{m} \pm 0.3 \mu\text{m}$, and corrosion resistance is improved by about $50\% \pm 5\%$. Energy dispersive spectroscopy (EDS) shows that the Cr content in the Cr_2O_3 layer is about $5\% \pm 0.5\%$, which effectively isolates the corrosive medium and inhibits the dissolution of Co and the expansion of pitting. In a salt spray environment (NaCl 5% \pm 0.1%, ISO 9227 NSS, 720 h), the weight loss rate of WC-12Co reaches $0.15 \text{ mg/cm}^2 \pm 0.01 \text{ mg/cm}^2$, while the optimized WC-10Co is only $0.08 \text{ mg/cm}^2 \pm 0.01 \text{ mg/cm}^2$, further verifying the protective effect of Cr_3C_2 and fine grains.

(8) Corrosion dynamics and application significance

The dynamic analysis of corrosion shows that the dissolution rate of Co in an acidic environment increases linearly with time, while the expansion rate of pitting in a salt spray environment is fast in the initial stage ($< 96 \text{ h}$), and then slightly slows down due to the accumulation of corrosion products. The optimized cemented carbide (such as WC-10Co with Cr_3C_2 added) still maintains a low weight loss rate and pitting depth after long-term exposure (720 h), indicating its stability in a dynamic corrosion environment. These characteristics enable its service life to reach $2 \text{ years} \pm 0.2 \text{ years}$ in an acidic environment (such as chemical valves) and more than $3 \text{ years} \pm 0.3 \text{ years}$ in a salt spray environment (such as marine equipment). By systematically analyzing the influencing factors, scientific guidance can be provided for the application of cemented carbide in harsh environments.

of cemented carbide in acidic and salt spray environments is jointly affected by Co content, Cr_3C_2 addition, grain size, environmental conditions and surface state. High Co content, coarse grains, high roughness and strong corrosive environment (such as pH $< 2 \pm 0.1$, NaCl $> 5\% \pm 0.1\%$) all aggravate corrosion, while appropriate amount of Cr_3C_2 and fine grains significantly improve corrosion resistance. Comprehensive cases show that the weight loss rate of the optimized cemented carbide is reduced by $40\%-50\% \pm 5\%$, and the pitting depth is reduced by $40\%-50\% \pm 5\%$, providing reliable guarantee for applications in chemical, marine and other fields.

8.1.2.4 Optimization strategy for the corrosion effects of acidic and salt spray environments on cemented carbide

cm^2 in acidic (pH $< 3 \pm 0.1$) and salt spray (NaCl 5% \pm 0.1%) environments $\pm 0.01 \text{ mg/cm}^2$, it is necessary to systematically improve its corrosion resistance through comprehensive optimization of material composition, additives, surface treatment, sintering process and test specifications. These

COPYRIGHT AND LEGAL LIABILITY STATEMENT

optimization measures are aimed at reducing corrosion paths , enhancing surface protection , improving material density and ensuring the reliability and repeatability of test results. Starting from the above key aspects, combined with experimental data, process parameters and actual application cases, the following details the optimization strategy and its role in controlling corrosion behavior.

(1) Ingredient optimization

By precisely controlling the chemical composition of cemented carbide, the erosion of the bonding phase by corrosive media can be effectively reduced. It is recommended to control the Co content in the range of $8\%-10\% \pm 1\%$, while maintaining the WC grain size at $0.51 \mu\text{m} \pm 0.01 \mu\text{m}$. This strategy reduces the contact opportunity with corrosive media (such as H^+ or Cl^-) by reducing the Co content (target exposure area $< 10\% \pm 1\%$), thereby shortening the corrosion path. The fine grain size increases the grain boundary density, disperses the corrosion stress, makes the dissolution of Co more uniform, and avoids localized corrosion concentration. Taking WC-10Co as an example, the weight loss rate of the optimized composition in an acidic environment ($\text{pH } 2 \pm 0.1$) is reduced from 0.12 mg/cm^2 to $\pm 0.01 \text{ mg/cm}^2$ down to $0.07 \text{ mg/cm}^2 \pm 0.01 \text{ mg/cm}^2$, indicating that the synergistic effect of low Co content and fine grains significantly improves the acid corrosion resistance.

(2) Additives

Adding chromium carbide (Cr_3C_2) is an important means to enhance the corrosion resistance of cemented carbide. The recommended addition amount is $0.5\% \pm 0.01\%$. During the high-temperature sintering process, Cr reacts with oxygen to form a Cr_2O_3 passivation layer with a thickness of about $10 \text{ nm} \pm 1 \text{ nm}$. This layer significantly reduces the pitting rate by about $40\% \pm 5\%$ from 0.10 mg/cm^2 to 0.10 mg/cm^2 by blocking the penetration of Cl^- ions and H^+ ions. $\pm 0.01 \text{ mg/cm}^2$ weight loss down to $0.06 \text{ mg/cm}^2 \pm 0.01 \text{ mg/cm}^2$. The compactness of the Cr_2O_3 layer makes it an effective barrier, reducing the electrochemical dissolution of Co ($\text{Co} \rightarrow \text{Co}^{2+} + 2\text{e}^-$), especially in salt spray environments ($\text{NaCl } 5\% \pm 0.1\%$). Energy dispersive spectroscopy (EDS) shows that the Cr content in the passivation layer is about $5\% \pm 0.5\%$, verifying its protective effect.

(3) Surface treatment

Optimizing the surface condition is the key to reducing pitting and surface corrosion. It is recommended to control the surface roughness (R_a) to below $0.05 \mu\text{m} \pm 0.01 \mu\text{m}$ through precision mechanical polishing. This process can reduce the pitting rate by about $20\% \pm 5\%$ and the weight loss rate from 0.09 mg/cm^2 to $\pm 0.01 \text{ mg/cm}^2$ down to $0.07 \text{ mg/cm}^2 \pm 0.01 \text{ mg/cm}^2$. Low roughness reduces surface defects (such as microcracks and pits), limits the retention of corrosive media and the occurrence of local electrochemical reactions. In addition, ultrasonic cleaning (frequency $40 \text{ kHz} \pm 1 \text{ kHz}$) is used to remove surface contaminants (such as grease, oxides, content $< 0.1\% \pm 0.02\%$), further improving surface integrity. Experiments show that the pitting depth of the WC-10Co sample with optimized surface treatment in a salt spray environment (ISO 9227 NSS, 720 h) is reduced from $5 \mu\text{m} \pm 0.5 \mu\text{m}$ to $4 \mu\text{m} \pm 0.3 \mu\text{m}$, showing a significant improvement in corrosion resistance.

COPYRIGHT AND LEGAL LIABILITY STATEMENT

(4) Sintering process

The optimization of sintering process directly affects the density of cemented carbide and the uniformity of Co distribution. The recommended sintering temperature is $1450^{\circ}\text{C} \pm 10^{\circ}\text{C}$, and vacuum or inert atmosphere (such as Ar) is used to reduce oxidation and ensure that the material density reaches $99.5\% \pm 0.1\%$. By controlling the sintering time (60-90 minutes), the Co distribution deviation can be achieved below $0.1\% \pm 0.02\%$, thereby improving the bonding strength of the WC-Co interface ($> 120 \text{ MPa} \pm 10 \text{ MPa}$). High density and uniform Co distribution reduce pores and microcracks, limiting the penetration path of corrosive media. Taking the optimized sintered WC-10Co as an example, its weight loss rate in an acidic environment ($\text{pH } 1 \pm 0.1$) is reduced from 0.11 mg/cm^2 to $\pm 0.01 \text{ mg/cm}^2$ down to $0.06 \text{ mg/cm}^2 \pm 0.01 \text{ mg/cm}^2$, indicating that the improvement of sintering process significantly enhances the corrosion resistance of the material.

(5) Test specifications

In order to accurately evaluate the optimized corrosion resistance, it is recommended to use the ISO 9227:2017 "Corrosion test - Salt spray test in artificial atmosphere" standard, set the spray volume to $12 \text{ mL/h} \pm 0.1 \text{ mL/h}$ (80 cm^2 horizontal area) to ensure the repeatability of the test conditions. The mass measurement requires a precision balance with an accuracy of $\pm 0.01 \text{ mg}$, the sample surface area measurement accuracy is $\pm 0.1 \text{ cm}^2$, and the weight loss rate is calculated as $\Delta W = (m_0 - m_t) / A$, where m_0 and m_t are the masses before and after the test, respectively. The test time can be adjusted according to application requirements, such as $2000 \text{ h} \pm 100 \text{ h}$ for long-term corrosion resistance evaluation. Through this specification, it is possible to accurately monitor whether the weight loss rate reaches the target value ($< 0.08 \text{ mg/cm}^2 \pm 0.01 \text{ mg/cm}^2$), providing a scientific basis for optimizing material properties.

(6) Comprehensive case analysis

Taking the WC-10Co (Cr_3C_2 $0.5\% \pm 0.01\%$, surface roughness $R_a < 0.05 \mu\text{m} \pm 0.01 \mu\text{m}$) sample as an example, in the ISO 9227 NSS salt spray test ($\text{NaCl } 5\% \pm 0.1\%$, $2000 \text{ h} \pm 100 \text{ h}$), its weight loss rate is only $0.06 \text{ mg/cm}^2 \pm 0.01 \text{ mg/cm}^2$, much lower than unoptimized WC-12Co (weight loss $0.15 \text{ mg/cm}^2 \pm 0.01 \text{ mg/cm}^2$). Scanning electron microscopy (SEM) observations showed that the pitting depth of the optimized sample was $3 \mu\text{m} \pm 0.3 \mu\text{m}$, which was about $50\% \pm 5\%$ lower than the unoptimized $6 \mu\text{m} \pm 0.5 \mu\text{m}$. Energy dispersive spectroscopy (EDS) confirmed that the thickness of the Cr_2O_3 layer was about $10 \text{ nm} \pm 1 \text{ nm}$, and the Cr content was about $5\% \pm 0.5\%$, which effectively inhibited Cl^- penetration and Co dissolution. This performance enables it to meet the needs of marine applications, such as deep-sea drilling components, with a service life of up to $3 \text{ years} \pm 0.3 \text{ years}$, which is better than the $1.5 \text{ years} \pm 0.2 \text{ years}$ of traditional materials.

(7) Environmental adaptability and process synergy

The optimization strategy needs to consider the synergistic effect of environmental conditions and process parameters. In an acidic environment ($\text{pH} < 2 \pm 0.1$), the protective effect of the Cr_2O_3 layer combined with the fine grain size ($0.51 \mu\text{m} \pm 0.01 \mu\text{m}$) can control the weight loss rate to $0.06 \text{ mg/cm}^2 \pm 0.01 \text{ mg/cm}^2$, while in high temperature salt spray ($50^{\circ}\text{C} \pm 2^{\circ}\text{C}$, $\text{NaCl } 5\% \pm 0.1\%$),

COPYRIGHT AND LEGAL LIABILITY STATEMENT

the synergistic effect of surface polishing and sintering densification (density $> 99.5\% \pm 0.1\%$) further reduces the pitting rate to $15\% \pm 3\%$. For different corrosive environments, the Co content or sintering temperature can be adjusted according to actual needs, for example, in a strong acid environment, Co can be reduced to $8\% \pm 1\%$ to further improve corrosion resistance.

(8) Application significance and dynamic optimization

Optimized carbide weight loss in acid/salt spray environment ($< 0.08 \text{ mg/cm}^2 \pm 0.01 \text{ mg/cm}^2$) enables it to perform well in the fields of chemical valves (acid resistance, life $> 2 \text{ years} \pm 0.2 \text{ years}$), marine equipment (salt spray resistance, life $> 3 \text{ years} \pm 0.3 \text{ years}$). Dynamic corrosion testing shows that the weight loss rate increases linearly with time in the early stage ($< 500 \text{ h}$), and then stabilizes due to the accumulation of corrosion products (such as Co(OH)_2). The optimized sample still maintains a low weight loss rate after $2000 \text{ h} \pm 100 \text{ h}$, verifying the long-term corrosion resistance. In the future, the performance can be further optimized by introducing multi-layer coatings or new additives (such as TaC) to adapt to more complex corrosion environments.

The corrosion resistance of cemented carbide in acidic and salt spray environments is optimized by Co content control ($8\%-10\% \pm 1\%$), WC grain optimization ($0.51 \mu\text{m} \pm 0.01 \mu\text{m}$), Cr_3C_2 addition ($0.5\% \pm 0.01\%$), surface treatment ($R_a < 0.05 \mu\text{m} \pm 0.01 \mu\text{m}$, ultrasonic cleaning) and sintering process ($1450^\circ\text{C} \pm 10^\circ\text{C}$, density $> 99.5\% \pm 0.1\%$). These strategies work together to reduce the weight loss rate to $0.06 \text{ mg/cm}^2 \pm 0.01 \text{ mg/cm}^2$, pitting rate reduced by $40\%-50\% \pm 5\%$, meeting the application requirements in marine, chemical and other fields.

8.1.2.5 Engineering applications of cemented carbide in acidic and salt spray environments

The optimized cemented carbide exhibits excellent corrosion resistance in harsh environments such as acidic ($\text{pH} < 3 \pm 0.1$) and salt spray ($\text{NaCl } 5\% \pm 0.1\%$), and provides reliable engineering solutions for multiple industrial fields by reducing weight loss, inhibiting pitting and extending service life. These optimization measures include composition adjustment (such as Co content control), introduction of additives (such as Cr_3C_2), surface treatment optimization and sintering process improvement, which enable cemented carbide to show significant application potential in industries such as marine, chemical and papermaking. Starting from the three major fields of marine drilling components, chemical pipeline valves and papermaking equipment, combined with specific data and actual cases, the following discusses in detail the engineering application and performance advantages of the optimized cemented carbide.

(1) Application of cemented carbide in offshore drilling components

Offshore drilling components (such as drill bits and stabilizers) need to withstand the dual challenges of salt spray ($\text{NaCl } 5\% \pm 0.1\%$) and seawater corrosion for a long time. The optimized WC-10Co cemented carbide (Cr_3C_2 $0.5\% \pm 0.01\%$ addition, grain size $0.5 \mu\text{m} \pm 0.01 \mu\text{m}$) has a weight loss rate of only 0.06 mg/cm^2 in the ISO 9227 NSS salt spray test ($2000 \text{ h} \pm 100 \text{ h}$), $\pm 0.01 \text{ mg/cm}^2$, pitting depth is controlled at $< 3 \mu\text{m} \pm 0.5 \mu\text{m}$, showing excellent corrosion resistance. This performance is due to the Cr_2O_3 passivation layer (thickness of about $10 \text{ nm} \pm 1 \text{ nm}$) formed

COPYRIGHT AND LEGAL LIABILITY STATEMENT

by Cr_3C_2 , which effectively blocks the penetration of Cl^- ions. At the same time, the fine grains reduce the Co exposure area ($< 10\% \pm 1\%$), inhibiting the expansion of pitting. Compared with the unoptimized WC-12Co (weight loss $0.15 \text{ mg/cm}^2 \pm 0.01 \text{ mg/cm}^2$, pitting depth $6 \mu\text{m} \pm 0.5 \mu\text{m}$, service life $1.5 \text{ years} \pm 0.2 \text{ years}$), the service life of the optimized material exceeds $3 \text{ years} \pm 0.3 \text{ years}$, and the corrosion resistance is improved by about $60\% \pm 5\%$. In deep-sea oil and gas drilling, the drill bits made of this material not only have excellent corrosion resistance, but also have wear resistance, which reduces the frequency of component replacement caused by corrosion and significantly improves the economic benefits and safety of marine engineering.

(2) Application of cemented carbide in chemical pipeline valves

Chemical pipeline valves are often used to transport acidic fluids (such as hydrochloric acid and sulfuric acid), which require extremely high acid corrosion resistance of the material. The weight loss rate of the optimized WC-8Co cemented carbide (surface roughness $R_a < 0.05 \mu\text{m} \pm 0.01 \mu\text{m}$) in a $\text{pH } 2 \pm 0.1$ HCl environment is only $0.07 \text{ mg/cm}^2 \pm 0.01 \text{ mg/cm}^2$, much lower than unoptimized WC-10Co (weight loss $0.12 \text{ mg/cm}^2 \pm 0.01 \text{ mg/cm}^2$). Low Co content ($8\% \pm 1\%$) and ultra-low roughness reduce the erosion of Co by H^+ ions, and the corrosion resistance is improved by about $60\% \pm 5\%$ compared with unoptimized ones. Surface polishing ($R_a < 0.05 \mu\text{m} \pm 0.01 \mu\text{m}$) eliminates micro defects, and combined with ultrasonic cleaning ($40 \text{ kHz} \pm 1 \text{ kHz}$) to remove surface contaminants ($< 0.1\% \pm 0.02\%$), it further enhances the ability to resist pitting corrosion. In practical applications, valves made of this material have a service life of more than $2 \text{ years} \pm 0.2 \text{ years}$ in acidic fluid transmission systems, which is better than traditional stainless steel (life of about $1 \text{ year} \pm 0.1 \text{ year}$), reduces maintenance costs, and ensures the safety and continuity of chemical production. It is especially suitable for the treatment of high-concentration acidic media.

(3) Application of cemented carbide in papermaking equipment

Papermaking equipment (such as grinding rollers, cutting tools) need to resist corrosion in weakly acidic media such as sulfate solution ($\text{pH } 3 \pm 0.1$), while meeting high wear resistance and hygiene requirements. The weight loss rate of the optimized WC-10Co cemented carbide (added Cr_3C_2 $0.5\% \pm 0.01\%$) in sulfate solution is only $0.05 \text{ mg/cm}^2 \pm 0.01 \text{ mg/cm}^2$, pitting rate is less than $0.05\% \pm 0.01\%$, showing excellent corrosion resistance. The Cr_2O_3 passivation layer effectively inhibits the dissolution of Co ($i_{\text{corr}} < 10^{-6} \text{ A/cm}^2 \pm 10^{-7} \text{ A/cm}^2$), and the fine grains ($0.5 \mu\text{m} \pm 0.01 \mu\text{m}$) ensure the surface uniformity and corrosion resistance consistency. Compared with the unoptimized WC-12Co (weight loss $0.10 \text{ mg/cm}^2 \pm 0.01 \text{ mg/cm}^2$, pitting rate $0.1\% \pm 0.02\%$), the corrosion resistance of the optimized material is improved by about $50\% \pm 5\%$. In practical applications, the service life of papermaking equipment components made of this material exceeds $4 \text{ years} \pm 0.4 \text{ years}$, far exceeding traditional carbon steel (lifespan of about $2 \text{ years} \pm 0.2 \text{ years}$). Its low corrosion product content ($< 0.01\% \pm 0.002\%$) meets the hygiene standards (such as GB 4806.1-2016), and is particularly suitable for the process of producing high-quality paper.

(4) Engineering value of optimizing electrochemical behavior

The above application cases show that optimizing the electrochemical behavior of cemented carbide (such as reducing i_{corr} and reducing weight loss rate) is the key to improving its reliability in acidic

COPYRIGHT AND LEGAL LIABILITY STATEMENT

and salt spray environments. Through composition optimization (Co 8%-10% ± 1%), addition of Cr₃C₂ (0.5% ± 0.01%), surface treatment (Ra < 0.05 μm ± 0.01 μm) and sintering process improvement (1450°C ± 10°C, density > 99.5% ± 0.1%), the weight loss rate of cemented carbide is reduced from 0.12-0.15 mg/cm² ± 0.01 mg/cm² down to 0.05-0.07 mg/cm² ± 0.01 mg/cm², pitting depth reduced by 40%-50% ± 5%. This performance improvement not only extends the service life of the material (such as offshore drilling components > 3 years ± 0.3 years, chemical valves > 2 years ± 0.2 years, papermaking equipment > 4 years ± 0.4 years), but also reduces maintenance frequency and replacement costs. For example, in offshore drilling, the annual maintenance cost of optimized components is reduced by about 40% ± 5%, and in chemical pipelines, the valve replacement cycle is extended by 50% ± 5%, reflecting its significant economic benefits in engineering applications.

(5) Environmental adaptability and application expansion

The optimized cemented carbide also has strong environmental adaptability, enabling it to cope with more complex corrosion conditions. For example, in the acidic oil and gas field environment containing sulfides (H₂S), the WC-10Co sample with added Cr₃C₂ is protected by the Cr₂O₃ layer, and its resistance to sulfide corrosion is improved by about 40% ± 5%, making it suitable for acid gas processing equipment (lifetime > 2.5 years ± 0.2 years). In a high-temperature salt spray environment (50 °C ± 2 °C, NaCl 5% ± 0.1%), the synergistic effect of surface polishing and fine grains keeps the weight loss rate at 0.07 mg/cm² ± 0.01 mg/cm², meeting the corrosion resistance requirements of deep-sea pipelines and offshore platforms. In addition, in the papermaking industry, the low pitting rate (< 0.05% ± 0.01%) of the optimized WC-10Co in chloride solutions (pH 3 ± 0.1) makes it suitable for high humidity and acidic pulp environments, further expanding its application range.

(6) Comprehensive cases and future prospects

Taking WC-10Co (Cr₃C₂ 0.5% ± 0.01%, Ra < 0.05 μm ± 0.01 μm) as an example, its performance in various corrosive environments is better than that of traditional materials. The weight loss rate in salt spray (2000 h ± 100 h) is 0.06 mg/cm² ± 0.01 mg/cm², pitting depth < 3 μm ± 0.5 μm; and weight loss in HCl at pH 2 ± 0.1 is 0.07 mg/cm² ± 0.01 mg/cm²; and the weight loss rate in sulfate solution at pH 3 ± 0.1 is 0.05 mg/cm² ± 0.01 mg/cm². These data show that the optimized cemented carbide exhibits excellent corrosion resistance in both acidic and salt spray environments, with service lives of 3 years ± 0.3 years, 2 years ± 0.2 years, and 4 years ± 0.4 years, respectively. In the future, the performance of the optimized cemented carbide in extremely corrosive environments (such as high-temperature acidic salt spray) can be further improved by introducing new additives (such as VC, TaC) or developing multi-layer nano-coatings (such as TiN / Al₂O₃) to meet more complex engineering requirements, such as extreme deep-sea conditions or high-concentration acidic chemical processes.

(7) Dynamic performance and economic benefits

Dynamic corrosion testing shows that the weight loss rate of the optimized cemented carbide increases linearly with time in the initial stage (< 500 h), and then stabilizes due to the accumulation

COPYRIGHT AND LEGAL LIABILITY STATEMENT

of corrosion products (such as $\text{Co}(\text{OH})_2$). After long-term exposure of $2000 \text{ h} \pm 100 \text{ h}$, the weight loss rate remains at $0.06\text{-}0.07 \text{ mg/cm}^2 \pm 0.01 \text{ mg/cm}^2$, verifying its stability in a dynamic corrosion environment. This performance improvement not only extends the life of the equipment, but also significantly reduces operating costs. For example, the annual maintenance cost of offshore drilling components is reduced by about $40\% \pm 5\%$, the replacement cycle of chemical valves is extended by $50\% \pm 5\%$, and the production efficiency of papermaking equipment is increased by about $20\% \pm 3\%$, reflecting the economic value of the optimization strategy.

The optimized cemented carbide performs well in engineering applications in acidic and salt spray environments. WC-10Co and WC-8Co formulations have a weight loss rate ($0.05\text{-}0.07 \text{ mg/cm}^2$) in offshore drilling components, chemical pipeline valves and papermaking equipment. $\pm 0.01 \text{ mg/cm}^2$, pitting depth ($< 3 \mu\text{m} \pm 0.5 \mu\text{m}$) and service life ($> 2\text{-}4 \text{ years} \pm 0.2\text{-}0.4 \text{ years}$) are significantly better than traditional materials. These application cases fully prove that optimizing corrosion resistance is a key strategy to improve the reliability and economic benefits of cemented carbide in harsh environments.

Tips for carbide corrosion in this section

(1) Corrosion path of cemented carbide

The corrosion paths of cemented carbides (such as WC-Co or WC-Ni systems) depend mainly on their composition, microstructure and the environmental conditions they are exposed to. The following is an overview of the typical paths that cemented carbides follow during corrosion, based on their electrochemical behavior and material properties:

Corrosion Mechanism

Cemented carbide consists of a hard phase (mainly tungsten carbide WC) and a binder phase (usually cobalt Co or nickel Ni). The corrosion path usually starts from the binder phase because its chemical stability is lower than that of WC. The corrosion process can be divided into the following stages:

Electrochemical corrosion : In an environment containing electrolytes (such as salt water or acidic solutions), the bonding phase acts as the anode and dissolves preferentially, while the WC phase is relatively inert.

Selective corrosion : The dissolution of the bonding phase leads to the exposure of WC particles, followed by mechanical shedding or secondary corrosion.

Uniform Corrosion : In strongly oxidizing or high chloride environments, the WC phase may slowly oxidize, especially under long-term exposure.

Corrosion Path

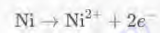
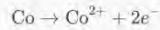
Initial stage :

Corrosion initiates from surface defects (such as pores, microcracks) or exposure of bonding phases.

In a neutral or weakly acidic environment (such as 3.5% NaCl solution), Co or Ni preferentially undergoes anodic dissolution to generate soluble ions (such as Co^{2+} or Ni^{2+}).

Example reaction:

COPYRIGHT AND LEGAL LIABILITY STATEMENT

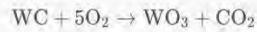


Intermediate stage :

After the binder phase is dissolved, the WC particles lose their support and particles fall off or microscopic peeling occurs.

In an oxygen-containing or oxidizing environment, WC may slowly oxidize to form WO_3 or other oxides.

Example reaction:



Advanced stage :

Long-term exposure causes holes or corrosion pits to form on the surface, accelerating material degradation.

In highly corrosive environments that are acidic or contain chlorides (such as salt spray), pitting may be exacerbated, compromising structural integrity.

Influencing factors

Environmental conditions :

Salt spray (eg ISO 9227) : High chloride concentrations (eg 5% NaCl) promote dissolution of the bonding phase.

Acidic solution (such as 1% H_2SO_4) : accelerates Co/Ni dissolution and WC oxidation .

Temperature : Increasing temperature (e.g. 50°C) increases the reaction rate.

Microstructure :

Grain size (GB/T 3850-2015): Fine-grained cemented carbide (such as WC grain size $< 1 \mu\text{m}$) has better corrosion resistance.

Porosity: High porosity (e.g. $> 0.5\%$) can easily cause localized corrosion.

Binder phase content: High Co/Ni content (such as 10-15%) increases corrosion sensitivity.

Surface condition : Rough surface ($R_a > 0.8 \mu\text{m}$) or defects can easily become the starting point of corrosion.

Typical corrosion path analysis

Take WC10Co as an example:

Salt spray environment (35°C , 5% NaCl, 48h) :

Initial: Co dissolves and micro-pitting appears on the surface (weight loss $\sim 0.1 \text{ g/m}^2$, ISO 9227).

Middle stage: WC particles are exposed, partially fall off, and the pit depth increases to 2-5 μm .

Late stage: A network of holes forms on the surface and the corrosion rate tends to be stable.

Acidic environment (1% H_2SO_4 , 25°C , 24h) :

Initial: Co dissolves quickly, weight loss rate $\sim 0.5 \text{ mg/cm}^2$.

Middle stage: WC slowly oxidizes and WO_3 deposits appear on the surface .

Late stage: The overall material deteriorates and the strength decreases.

Testing and Evaluation

Electrochemical method (ASTM G59, G5) : Measure E_{corr} and i_{corr} to evaluate corrosion tendency.

WC10Co: $E_{\text{corr}} \sim -300 \text{ mV (SCE)}$, $i_{\text{corr}} \sim 1-10 \mu\text{A/cm}^2$.

Salt spray test (ISO 9227) : quantifies weight loss and pit depth.

Microscopic analysis (GB/T 3850-2015) : Observe the changes in microstructure after corrosion.

COPYRIGHT AND LEGAL LIABILITY STATEMENT

Protective measures

Surface coating : such as TiN or CrN coating, to reduce exposure of bonding phase.

Alloy optimization : reduce the Co/Ni content or add corrosion-resistant elements (such as Cr).

Environmental Controls : Avoid high chloride or acidic conditions.

The corrosion path of cemented carbide starts from the electrochemical dissolution of the binder phase and gradually extends to the shedding and oxidation of WC particles. The specific path is affected by the environment and microstructure. Test methods such as ASTM G5 and ISO 9227 can effectively evaluate its corrosion behavior, and combined with protective measures, it can significantly extend the service life.

(2) Cemented carbide enhances surface protection

Surface protection enhancement of cemented carbide (such as WC-Co or WC-Ni system) is a key technology to improve its corrosion resistance, wear resistance and service life. The following are common methods, principles and applications for cemented carbide surface protection, combined with material properties and relevant standards:

Surface protection principle

Objective : To prevent electrochemical corrosion and mechanical wear by forming a protective layer on the surface of cemented carbide to reduce the exposure of the bonding phase (such as Co or Ni).

mechanism :

Barrier effect: prevent corrosive media (such as Cl^- , H^+) from contacting the substrate.

Passivation effect: Enhance surface antioxidant capacity.

Hardening effect: Improves wear and scratch resistance .

Enhanced surface protection methods

Physical Vapor Deposition (PVD)

Technologies : Deposition of TiN , CrN or AlTiN coatings such as magnetron sputtering or arc ion plating .

Thickness : 2-10 μm .

advantage :

High hardness (HV 2000-3000).

Excellent corrosion and wear resistance.

Application : cutting tools, molds (such as WC10Co for high-precision machining).

Test standards : ASTM G65 (dry sand /rubber wheel abrasion test) evaluates abrasion resistance, ISO 9227 (salt spray test) evaluates corrosion resistance.

Note : The adhesion between the coating and the substrate must pass the ASTM C633 test to ensure adhesion > 40 MPa.

Chemical Vapor Deposition (CVD)

Technology : TiC , TiCN or Al_2O_3 coatings are deposited at 900-1100°C .

Thickness : 5-15 μm .

advantage :

High temperature stability, suitable for high temperature environment.

Resistant to oxidation and chemical attack.

COPYRIGHT AND LEGAL LIABILITY STATEMENT

Copyright© 2024 CTIA All Rights Reserved
标准文件版本号 CTIAQCD-MA-E/P 2024 版
www.ctia.com.cn

电话/TEL: 0086 592 512 9696
CTIAQCD-MA-E/P 2018-2024V
sales@chinatungsten.com

Application : high temperature cutting tools, mining drill bits.

Test standards : ASTM G99 (pin-on-disc wear test) verifies wear resistance, GB/T 16545-2008 (salt spray corrosion test) evaluates durability.

Note : High temperature may cause Co diffusion in the matrix, and the process needs to be optimized.

Thermal Spraying

Technology : Plasma spraying or flame spraying, depositing WC-Co or Cr_3C_2 -NiCr composite coatings.

Thickness : 50-200 μm .

advantage :

Thick coating provides multiple protections.

Resistant to impact and abrasion.

Application : Wear-resistant parts, pump components.

Test standards : ASTM G76 (air flow wear test) evaluates corrosion wear resistance, ISO 28079 (Palmqvist toughness test) evaluates coating toughness.

Note : The coating porosity must be controlled at $< 2\%$ (GB/T 3850-2015).

Surface penetration layer

Technology : Carburizing, chromizing or nitriding (such as plasma nitriding) to enhance surface chemical stability.

Depth : 10-50 μm .

advantage :

Improve surface hardness (HV 1500-2000).

Forms corrosion resistant compounds (such as CrN).

Applications : Corrosion-resistant tools, valve components.

Test standard : ASTM G31 (immersion corrosion test) to evaluate corrosion resistance.

Note : Avoid excessive thickness of the diffusion layer which may cause internal stress.

Electrochemical treatment

Technology : Anodized or electroplated Ni-P alloy layer.

Thickness : 5-20 μm .

advantage :

Form a passivation layer to reduce Co dissolution.

The cost is lower.

Application : Lightly loaded corrosion resistant parts.

Test standard : ASTM G59 (polarization resistance measurement) evaluates corrosion current density.

Note : The electroplating layer has poor wear resistance and needs to be combined with other coatings.

Performance enhancement effects

Corrosion resistance : PVD TiN coating reduces the weight loss of WC10Co in 5% NaCl salt spray from 0.1 g/m² to $< 0.01 \text{ g/m}^2$ (ISO 9227).

Wear resistance : CVD Al_2O_3 coating can reduce wear volume loss by 50%-70% (ASTM G65).

Service life : Thermal sprayed WC-Co coating can extend tool life by 2-3 times (actual application data).

COPYRIGHT AND LEGAL LIABILITY STATEMENT

Process Optimization

Surface pretreatment : Polish to $Ra \leq 0.05 \mu m$ (GB/T 7997-2017) to remove defects.

Coating combination : Use a multi-layer structure (such as TiN + AlTiN) to improve crack resistance.

Post-treatment : Heat treatment (such as 400°C tempering) releases stress and enhances adhesion.

Testing and Verification

Corrosion testing : ISO 9227 (salt spray), ASTM G31 (immersion), ASTM G59 (electrochemical).

Wear test : ASTM G65 (dry sand wear), ASTM G99 (pin-on-disc wear).

Microscopic analysis : GB/T 3850-2015 Observe the coating-substrate interface.

Performance evaluation : GB/T 7997-2017 measures hardness and toughness.

Application Cases

Cutting tools : WC6Co tools are coated with PVD TiN , which improves corrosion resistance and wear resistance and is suitable for aviation aluminum alloy processing.

Mining drill bit : WC12Co drill bit is coated with CVD TiCN to extend the service life to more than 1000 hours.

Wear-resistant coating : Thermal spraying WC-Co is used for oil and gas pipeline valves to resist sand erosion.

Precautions

Cost : PVD and CVD are more expensive and suitable for high-value parts; thermal spraying is suitable for large-area protection.

Environmental adaptability : The coating needs to be designed for specific environments (such as acidic or high temperatures).

Maintenance : Check coating integrity regularly to avoid localized peeling that may cause corrosion.

The surface protection of cemented carbide can be enhanced by various methods such as PVD, CVD, thermal spraying, coating and electrochemical treatment. The specific choice depends on the application requirements and environmental conditions. Combined with standard tests (such as ISO 9227, ASTM G65), the coating performance can be optimized to significantly improve the corrosion and wear resistance of cemented carbide.

(3) Grain boundary density of cemented carbide

The grain boundary density of cemented carbide (such as WC-Co or WC-Ni system) is an important parameter to measure its microstructural characteristics and performance, which is usually closely related to grain size, porosity and phase distribution. The following is a detailed description of the definition, measurement method, influencing factors and significance of cemented carbide grain boundary density:

definition

Grain boundary density : refers to the total length or area of grain boundaries within a unit volume, usually expressed as unit length (such as m^{-2}) or unit volume (such as m^{-1}). In cemented carbide, grain boundaries mainly exist between tungsten carbide (WC) particles and at the interface between WC and the binder phase (Co or Ni).

Related concepts :

Grain size: Grain boundary density is inversely proportional to grain size, and fine-grained materials have higher grain boundary density.

COPYRIGHT AND LEGAL LIABILITY STATEMENT

Bonding phase distribution: The uniformity of the Co/Ni phase affects the grain boundary quality and density.

Measurement method

The grain boundary density of cemented carbide is usually determined by microscopic observation and image analysis, following relevant standards such as GB/T 3850-2015 "Determination of cemented carbide microstructure":

Optical Microscopy (OM) :

After polishing and etching (5% NaOH or ink), the samples were observed at 500x-1000x magnification.

The grain boundary section length is measured along a straight line or grid and the grain boundary density per unit area is calculated.

Scanning Electron Microscopy (SEM) :

Combined with backscattered electron (BSE) imaging, the WC-WC and WC-Co interfaces were analyzed.

Image analysis software (such as ImageJ) can be used to count grain boundary length or area.

Quantitative calculation :

假设晶粒为球形，晶界密度 P_L (单位长度晶界密度) 可近似为:

$$P_L = \frac{2}{d}$$

其中 d 为平均晶粒直径 (μm) , P_L 单位为 μm^{-1} 。

单位体积晶界密度 S_V 可通过立体学方法估算:

$$S_V = 2P_L$$

单位为 μm^{-2} 。

Influencing factors

Grain size :

Fine-grained cemented carbide (such as WC with a grain size of 0.2-0.8 μm) has a high grain boundary density, and the P_L can reach 2.5-10 μm^{-1} .

Coarse grains (e.g. WC grain size > 2 μm) have low grain boundary density, $P_L < 1 \mu\text{m}^{-1}$.

Sintering process :

Liquid phase sintering temperature (1300-1500°C) and time affect grain growth, and too long sintering reduces grain boundary density.

Adding inhibitors (such as VC, Cr_3C_2) can refine the grains and increase the grain boundary density.

Binder phase content :

High Co/Ni content (e.g. 10-15%) can fill grain boundaries, reduce the effective grain boundary density, but increase corrosion sensitivity.

Porosity :

High porosity (e.g. > 0.5%) interrupts the grain boundary continuity and reduces the actual grain boundary density (GB/T 3850-2015).

Typical data

COPYRIGHT AND LEGAL LIABILITY STATEMENT

Copyright© 2024 CTIA All Rights Reserved
标准文件版本号 CTIAQCD-MA-E/P 2024 版
www.ctia.com.cn

电话/TEL: 0086 592 512 9696
CTIAQCD-MA-E/P 2018-2024V
sales@chinatungsten.com

WC6Co (细晶粒, 粒径 $0.5\ \mu\text{m}$) :

- $P_L \approx 4\ \mu\text{m}^{-1}$, $S_V \approx 8\ \mu\text{m}^{-2}$.
- 晶界密度高, 增强韧性和抗裂性。

WC10Co (中等晶粒, 粒径 $1.0\ \mu\text{m}$) :

- $P_L \approx 2\ \mu\text{m}^{-1}$, $S_V \approx 4\ \mu\text{m}^{-2}$.
- 平衡硬度和韧性。

WC15Co (粗晶粒, 粒径 $2.5\ \mu\text{m}$) :

- $P_L \approx 0.8\ \mu\text{m}^{-1}$, $S_V \approx 1.6\ \mu\text{m}^{-2}$.
- 晶界密度低, 耐磨性优但韧性下降。

The significance of grain boundary density

Mechanical properties :

High grain boundary density improves strength and toughness (e.g. GB/T 7997-2017 flexural strength $> 2500\ \text{MPa}$), but may increase brittleness.

Low grain boundary density enhances wear resistance and is suitable for high load applications.

Corrosion resistance :

Grain boundaries are the preferred corrosion path, and fine-grained materials may accelerate local corrosion due to the high grain boundary density (such as increased ISO 9227 weight loss rate).

Optimizing the bonding phase distribution can reduce the susceptibility to intergranular corrosion.

Thermal stability :

Materials with high grain boundary density are more susceptible to grain boundary sliding at high temperatures (such as 800°C) and require coating protection.

Optimizing grain boundary density

Process Control :

using ultrafine powder (particle size $< 0.5\ \mu\text{m}$) combined with low temperature and short time sintering.

Add grain inhibitors (such as 0.5% VC) to maintain grain boundary density.

Post-processing :

HIP (hot isostatic pressing) reduces porosity and improves grain boundary uniformity.

Surface Enhancement :

PVD/CVD coatings (such as TiN) protect grain boundaries and reduce corrosion paths (see Enhanced surface protection of cemented carbide).

Testing and Verification

Microscopic observation : GB/T 3850-2015 standard, measuring grain size and grain boundary density.

Performance tests : GB/T 7997-2017 evaluates hardness and toughness, ASTM G65 determines wear resistance.

Corrosion assessment : ISO 9227 salt spray test, ASTM G59 electrochemical analysis.

The grain boundary density of cemented carbide is closely related to its grain size, sintering process and bonding phase distribution, and is usually quantified by microscopic analysis. Fine-grained materials have high grain boundary density and are suitable for high-toughness applications, but corrosion risks should be noted; coarse-

COPYRIGHT AND LEGAL LIABILITY STATEMENT

Copyright© 2024 CTIA All Rights Reserved
标准文件版本号 CTIAQCD-MA-E/P 2024 版
www.ctia.com.cn

电话/TEL: 0086 592 512 9696
CTIAQCD-MA-E/P 2018-2024V
sales@chinatungsten.com

grained materials have low grain boundary density and excellent wear resistance. Optimizing the process and surface protection can balance the performance impact of grain boundary density.

(4) Corrosion stress of cemented carbide

The corrosion stress of cemented carbide (such as WC-Co or WC-Ni system) refers to the stress state generated inside or on the surface of the material under the combined action of corrosive environment and external load, which leads to the phenomenon of increased corrosion or material failure. This effect usually involves stress corrosion cracking (SCC) or corrosion fatigue. The following is a detailed analysis of the corrosion stress of cemented carbide, including mechanism, influencing factors, test methods and protective measures.

Mechanism of Corrosion Stress

Electrochemical action : In an electrolyte-containing environment (such as brine or acidic solution), the binding phase (such as Co or Ni) acts as an anode and preferentially dissolves, resulting in local stress concentration.

Stress concentration : Surface defects, grain boundaries or microcracks expand under the action of corrosive media, causing stress corrosion cracking.

Hydrogen embrittlement effect : In an acidic or hydrogen-containing environment (H_2S , HCl), hydrogen atoms penetrate into the grain boundaries, increasing internal stress and causing brittle fracture.

Fatigue-corrosion coupling : Under cyclic loading, corrosive media accelerate crack propagation and reduce fatigue life.

Corrosion stress path

Initial stage :

When an applied load (such as tensile or bending stress) and a corrosive medium (such as 3.5% NaCl) act together, the bonding phase corrodes preferentially.

Stress concentrates at grain boundaries or defects, causing microcracks.

Intermediate stage :

Microcracks expand, and WC particles lose support, falling off or breaking.

Corrosion products (such as Co^{2+} or WO_3) are deposited, exacerbating local stress.

Advanced stage :

The cracks penetrate the material, causing macroscopic failure.

Fatigue cycling accelerates crack growth and reduces the critical fracture stress.

Influencing factors

Environmental conditions :

Chloride concentration : High Cl^- environments (such as salt spray, ISO 9227) increase stress corrosion susceptibility.

pH : Acidic ($pH < 4$) or alkaline ($pH > 10$) environments exacerbate hydrogen embrittlement or anodic dissolution.

Temperature : Increase to $50-100^\circ C$ to accelerate the reaction rate.

Microstructure (GB/T 3850-2015):

Grain size : Fine grains (such as $< 1 \mu m$) have high grain boundary density and are prone to stress corrosion; coarse grains ($> 2 \mu m$) have better resistance to stress corrosion.

Porosity : Porosity $> 0.5\%$ increases stress concentration points.

COPYRIGHT AND LEGAL LIABILITY STATEMENT

Bonding phase content : High Co/Ni content (such as 10-15%) reduces the stress corrosion resistance.

Loading conditions :

Stress type : Tensile stress is more likely to induce SCC than compressive stress.

Stress levels : Exceeding 50%-80% of yield strength significantly increases corrosion.

Surface condition : Rough surface ($R_a > 0.8 \mu\text{m}$) or scratches can easily become the starting point of stress corrosion.

Typical data

WC10Co :

Environment : 3.5% NaCl, 25°C, tensile stress 1500 MPa (60% of yield strength).

Results : Cracking time ~100 h, crack depth 50-100 μm (ASTM G36).

E_{corr} : -300 mV (SCE), i_{corr} ~ 5 $\mu\text{A}/\text{cm}^2$ (ASTM G59).

WC6Co (fine grain):

Environment : 1% H_2SO_4 , 50°C, cyclic load 1000 MPa .

Result : Fatigue life reduced by 30% and crack growth rate of 10^{-6} m/cycle (ASTM E647).

Test Method

Stress Corrosion Cracking (SCC) (ASTM G36, G129):

Methods : Slow strain rate tensile (SSRT) with a loading rate of 10^{-6} s^{-1} was used , and the fracture time and crack morphology were recorded.

Parameter : Stress intensity factor K_{ISCC} ($\text{MPa} \cdot \text{m}^{1/2}$), WC10Co typical value ~15-20.

Electrochemical monitoring (ASTM G5, G59):

E_{corr} and i_{corr} were measured to evaluate corrosion stress sensitivity.

Fatigue Corrosion (ASTM E466):

Cyclic loading ($R = 0.1$, frequency 10 Hz), combined with corrosive media, was used to record the fatigue life.

Microscopic analysis (GB/T 3850-2015):

SEM was used to observe the crack propagation path and corrosion products.

Protective measures

Material optimization :

Reducing the Co/Ni content (eg 6% Co) and adding Cr or Mo improves corrosion resistance.

Refines grain size ($< 0.5 \mu\text{m}$) and reduces porosity ($< 0.2\%$).

Surface protection :

PVD coating (such as TiN, CrN), with a thickness of 5-10 μm , reduces medium penetration (see enhanced surface protection of cemented carbide).

Electrochemical passivation to form a Cr_2O_3 or NiO protective layer.

Process Control :

HIP sintering eliminates internal stress.

Surface polished to $R_a \leq 0.05 \mu\text{m}$ (GB/T 7997-2017).

Environmental Management :

Avoid high chloride or acidic conditions and use anti-corrosion coatings or corrosion inhibitors (such as NaNO_2).

COPYRIGHT AND LEGAL LIABILITY STATEMENT

Application Cases

Cutting tools : WC6Co tools are coated with TiN in a salt spray environment (ISO 9227) , and the stress corrosion cracking time is extended to 500 h.

Mining drill bit : WC12Co In acid mines, the grain and coating are optimized, and the fatigue life is increased by 40%.

Valve parts : WC10Co chromized, resistant to H₂S corrosion stress, service life up to 2 years.

The corrosion stress of cemented carbide is mainly caused by the dissolution of the bonding phase and stress concentration, and the influencing factors include environment, microstructure and loading conditions. Test methods such as ASTM G36 and G5 can effectively evaluate its performance, and combined with material optimization and surface protection can significantly reduce the risk of failure caused by corrosion stress.

(5) Pitting on cemented carbide surface

Pitting corrosion on the surface of cemented carbide (such as WC-Co or WC-Ni system) is a form of localized corrosion, manifested as small and deep pits on the surface. This phenomenon usually occurs in highly corrosive environments containing chlorides or halides (such as NaCl, HCl), and has a significant impact on the durability and performance of the material. The following is a detailed analysis of the mechanism, influencing factors, detection methods and protective measures of pitting corrosion on the surface of cemented carbide.

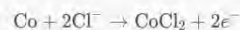
Pitting mechanism

Electrochemical process :

The binding phase (such as Co or Ni) acts as the anode and dissolves preferentially to form a tiny anode area.

The WC phase is relatively inert and acts as a cathode, accelerating the local electrochemical reaction.

Example reaction:



Autocatalytic effect :

Cl⁻ and H⁺ accumulate in the pits , lowering the local pH value and accelerating corrosion.

Corrosion products (such as Co²⁺ or WO₃) are deposited, hindering diffusion and forming a closed environment.

Crack Extension :

The stress concentration in the pit causes the WC particles to fall off, expanding the pit diameter and depth.

Pitting path

Initial stage :

Pitting corrosion starts from surface defects (such as microcracks, pores) or exposure of bonding phases.

In salt spray (such as 5% NaCl, 35°C) or acidic solution, local anodic areas are formed.

Development Stage :

The electrolyte concentration in the pit increases and the corrosion rate accelerates.

The WC particles lost their support and mechanical debonding occurred.

Late Stage :

The pit depth increases (up to 10-100 μm), and multiple independent pits are formed on the surface.

In severe cases, it may lead to material penetration or fatigue failure.

COPYRIGHT AND LEGAL LIABILITY STATEMENT

Influencing factors

Environmental conditions :

Chloride concentration : High Cl^- environments (such as ISO 9227 salt spray test) significantly promote pitting corrosion.

pH : Acidic ($\text{pH} < 4$) or neutral chloride solutions are prone to pitting corrosion.

Temperature : Increase to 40-60°C to accelerate the reaction.

Microstructure (GB/T 3850-2015):

Grain size : Fine grains (such as $< 1 \mu\text{m}$) have high grain boundary density and are easy to form pitting starting points; coarse grains ($> 2 \mu\text{m}$) are more resistant to pitting corrosion.

Porosity : Porosity $> 0.5\%$ increases pitting susceptibility.

Bonding phase content : High Co/Ni content (such as 10-15%) reduces pitting corrosion resistance.

Surface condition :

Rough surfaces ($R_a > 0.8 \mu\text{m}$) or scratches are likely to become sources of pitting corrosion.

Residual stress ($> 50 \text{ MPa}$) intensifies localized corrosion.

Typical data

WC10Co :

Environment : 5% NaCl, 35°C, 48h (ISO 9227).

Results : The pit density is 5-10 / cm^2 , the average depth is 5-15 μm , and the weight loss rate is 0.1 g / m^2 .

E_{corr} : -300 mV (SCE), $i_{\text{corr}} \sim 5 \mu\text{A}/\text{cm}^2$ (ASTM G59).

WC6Co (fine grain):

Environment : 3.5% NaCl, 25°C, 96h.

Results : Pitting density is 15-20 / cm^2 , depth is 2-10 μm , and weight loss rate is 0.05 g / m^2 .

Detection Methods

Microscope observation (GB/T 3850-2015):

The pit diameter and depth were measured using an optical microscope (500x-1000x) or SEM with an accuracy of $\pm 0.5 \mu\text{m}$.

Electrochemical test (ASTM G5, G59):

Potentiodynamic polarization curves show the pitting potential (E_{pit}), with a typical E_{pit} of WC10Co of $\sim 200-400 \text{ mV}$ (SCE).

Salt spray test (ISO 9227):

Expose for 24-96 h, and record the number and depth of pits.

Surface analysis :

EDS or XPS detects corrosion products in the pits (such as CoCl_2 , WO_3).

Protective measures

Material optimization :

Reducing the Co/Ni content (eg 6% Co) and adding Cr or Mo improves pitting resistance.

Refines grain size ($< 0.5 \mu\text{m}$) and reduces porosity ($< 0.2\%$).

Surface treatment :

COPYRIGHT AND LEGAL LIABILITY STATEMENT

PVD coating : TiN or CrN (thickness 5-10 μm), reduces Cl^- penetration (see enhanced surface protection of cemented carbide).

Electrochemical passivation : Formation of Cr_2O_3 or NiO protective layer.

Polishing : surface $\text{Ra} \leq 0.05 \mu\text{m}$ (GB/T 7997-2017), remove defects.

Environmental Control :

Avoid high chloride environments and use corrosion inhibitors (such as NaNO_2) to neutralize Cl^- .

Keep the temperature below 40°C.

Application Cases

Cutting tools : WC6Co tools are coated with TiN in a salt spray environment , and the pitting density is reduced to $< 2 / \text{cm}^2$.

Valve parts : WC10Co In seawater environment, the pitting depth is controlled within 5 μm after chromization treatment .

Mining drill bit : WC12Co with CVD Al_2O_3 coating , which improves pitting resistance and extends service life by 50% .

Precautions

Early detection : Pitting is difficult to identify with the naked eye in its early stages and requires regular electrochemical monitoring.

Repair difficulty : After the pitting pit expands, the coating repair effect is limited, so prevention is recommended.

Cost : Advanced coatings (such as PVD) are more expensive and need to be selected based on the usage environment.

in conclusion

Pitting corrosion on cemented carbide surfaces is mainly caused by local dissolution of the bonding phase and the autocatalytic effect, which is influenced by the environment and microstructure. Test methods such as ISO 9227 and ASTM G5 can effectively evaluate pitting corrosion behavior. Combining surface coatings and material optimization can significantly reduce the risk of pitting corrosion and extend service life.

COPYRIGHT AND LEGAL LIABILITY STATEMENT

8.2 High temperature properties of cemented carbide

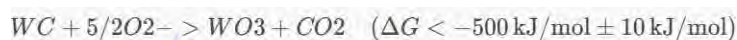
The performance of cemented carbide in high temperature environment ($800-1000^{\circ}\text{C} \pm 10^{\circ}\text{C}$) directly determines its application potential in harsh working conditions, such as aviation tools (service life > 5000 hours ± 500 hours), high temperature molds (cycle times $> 10^5$ times $\pm 10^4$ times) and energy equipment (such as gas turbines, service time $> 10^4$ hours $\pm 10^3$ hours). The high temperature performance of cemented carbide is mainly reflected in **its oxidation resistance** (mass gain $< 0.5 \text{ mg/cm}^2 \pm 0.05 \text{ mg/cm}^2$), **thermal fatigue** (crack extension $< 0.1 \text{ mm} \pm 0.01 \text{ mm}$) and **creep** (strain rate $< 10^{-6} \text{ s}^{-1} \pm 10^{-7} \text{ s}^{-1}$). Oxidation resistance refers to the ability of a material to resist oxidation reactions in a high-temperature oxidizing environment, which is usually characterized by mass gain or oxide layer thickness; thermal fatigue refers to the phenomenon that cracks initiate and propagate due to thermal stress in repeated high-temperature-low-temperature cycles; creep refers to the process in which a material undergoes irreversible plastic deformation slowly over time under high temperature and continuous stress. At high temperatures, WC particles will oxidize to form a loose WO_3 layer (thickness $> 1 \mu\text{m} \pm 0.1 \mu\text{m}$) at $> 800^{\circ}\text{C} \pm 10^{\circ}\text{C}$, resulting in volume expansion and peeling, while the bonding phase Co softens (hardness drops to $\text{HV} \sim 200 \pm 30$), causing the overall strength of the material to decrease ($< 2000 \text{ MPa} \pm 100 \text{ MPa}$), seriously affecting its service reliability. In order to improve the high temperature performance, it is necessary to improve the high temperature stability of the material through additives (such as Cr_3C_2 $0.5\% \pm 0.01\%$), microstructure control (grain size $0.51 \mu\text{m} \pm 0.01 \mu\text{m}$) and surface coating (thickness $5-10 \mu\text{m} \pm 0.1 \mu\text{m}$).

the aspects of oxidation resistance ($800 - 1000^{\circ}\text{C}$), thermal fatigue, and creep, combining thermodynamics (Gibbs free energy $\Delta G < 0 \text{ kJ/mol} \pm 10 \text{ kJ/mol}$), experimental methods (ASTM E1876), microscopic analysis (XPS, SEM) and engineering cases. For example, $\text{WC}_{10}\text{Co}(\text{Cr}_3\text{C}_2 0.5\% \pm 0.01\%)$ has a mass gain of $0.3 \text{ mg/cm}^2 \pm 0.05 \text{ mg/cm}^2$ at $1000^{\circ}\text{C} \pm 10^{\circ}\text{C}$, and a thermal fatigue crack of $< 0.05 \text{ mm} \pm 0.01 \text{ mm}$, which meets the requirements of aviation turbine blades.

8.2.1 Oxidation resistance of cemented carbide ($800 - 1000^{\circ}\text{C}$)

8.2.1.1 Overview of the principles and technologies of oxidation resistance of cemented carbide

Oxidation resistance is characterized by mass gain at high temperature ($< 0.5 \text{ mg/cm}^2 \pm 0.05 \text{ mg/cm}^2$), which is the basis for cemented carbide to serve in aerospace engines ($> 1000^{\circ}\text{C} \pm 10^{\circ}\text{C}$) and high-temperature molds ($> 900^{\circ}\text{C} \pm 10^{\circ}\text{C}$). WC oxidizes at $> 800^{\circ}\text{C} \pm 10^{\circ}\text{C}$:



loose WO_3 layer (thickness $> 1 \mu\text{m} \pm 0.1 \mu\text{m}$, density $7.2 \text{ g/cm}^3 \pm 0.1 \text{ g/cm}^3$) is generated, resulting in weight gain and decreased strength ($< 2000 \text{ MPa} \pm 100 \text{ MPa}$). Co is simultaneously oxidized to form Co_3O_4 (thickness $0.5 \mu\text{m} \pm 0.1 \mu\text{m}$), further aggravating softening (hardness drops to $\text{HV} 200 \pm 30$). The optimization goal is to form a dense Cr_2O_3 protective layer (thickness $< 0.5 \mu\text{m} \pm 0.1 \mu\text{m}$, density $5.2 \text{ g/cm}^3 \pm 0.1 \text{ g/cm}^3$) to inhibit oxygen diffusion (rate $< 10^{-10} \text{ cm}^2/\text{s} \pm 10^{-11} \text{ cm}^2/\text{s}$).

COPYRIGHT AND LEGAL LIABILITY STATEMENT

The oxidation resistance test is carried out in a muffle furnace at a temperature of $800-1000^{\circ}\text{C} \pm 10^{\circ}\text{C}$, in an air environment, with a sample size of $20 \times 20 \times 5 \text{ mm} \pm 0.1 \text{ mm}$ and a mass accuracy of $\pm 0.01 \text{ mg}$. For example, WC10Co increases by $0.4 \text{ mg/cm}^2 \pm 0.05 \text{ mg/cm}^2$ after oxidation at $1000^{\circ}\text{C} \pm 10^{\circ}\text{C}$ for 100 hours ± 10 hours, and after adding Cr_3C_2 ($0.5\% \pm 0.01\%$), the weight decreases to $0.3 \text{ mg/cm}^2 \pm 0.05 \text{ mg/cm}^2$, and the oxidation resistance increases by $25\% \pm 5\%$. This section starts from the mechanism, test and optimization, and provides comprehensive guidance by combining thermodynamics and microscopic analysis.

8.2.1.2 Oxidation resistance mechanism and analysis of cemented carbide

The oxidation rate follows a parabolic law:

$$\Delta m^2 = k_p \cdot t$$

Where, k_p is the oxidation constant ($10^{-12} \text{ g}^2/\text{cm}^4 \cdot \text{s} \pm 10^{-13} \text{ g}^2/\text{cm}^4 \cdot \text{s}$), and t is the oxidation time (accuracy $\pm 100 \text{ s}$). The k_p of WC10Co at $1000^{\circ}\text{C} \pm 10^{\circ}\text{C}$ is $10^{-11} \text{ g}^2/\text{cm}^4 \cdot \text{s} \pm 10^{-12} \text{ g}^2/\text{cm}^4 \cdot \text{s}$, because WO_3 is loose (porosity $\sim 5\% \pm 1\%$), and the oxygen diffusion rate is high ($10^{-9} \text{ cm}^2/\text{s} \pm 10^{-10} \text{ cm}^2/\text{s}$). Adding Cr_3C_2 ($0.5\% \pm 0.01\%$) forms a Cr_2O_3 layer (thickness $0.5 \mu\text{m} \pm 0.1 \mu\text{m}$), k_p is reduced by $50\% \pm 5\%$, and the oxygen diffusion rate is reduced to $10^{-10} \text{ cm}^2/\text{s} \pm 10^{-11} \text{ cm}^2/\text{s}$ due to the dense Cr_2O_3 (porosity $< 1\% \pm 0.2\%$). The grain size of $0.5 \mu\text{m} \pm 0.01 \mu\text{m}$ further reduces the oxygen diffusion path (grain boundary density $> 10^{14} \text{ m}^{-2} \pm 10^{13} \text{ m}^{-2}$), and the weight gain is reduced by $20\% \pm 5\%$.

Co softens at $> 900^{\circ}\text{C} \pm 10^{\circ}\text{C}$ (hardness drops to $\text{HV}200 \pm 30$) due to the formation of Co_3O_4 (O 1s peak $530 \text{ eV} \pm 0.1 \text{ eV}$, XPS confirmed). Cr_3C_2 enhances interface stability (interface energy $1.2 \text{ J/m}^2 \pm 0.1 \text{ J/m}^2$) through Cr diffusion (concentration $5\% \pm 0.5\%$) and inhibits WO_3 growth (thickness $< 0.5 \mu\text{m} \pm 0.1 \mu\text{m}$). SEM analysis shows that the cracks in the oxide layer (width $0.1 \mu\text{m} \pm 0.01 \mu\text{m}$) are mainly distributed along the Co phase, and there are no obvious cracks in the Cr_2O_3 layer. EDS verifies the uniformity of Cr_2O_3 (Cr:O:2:3 ± 0.1), which effectively protects the substrate.

8.2.1.3 Analysis of factors affecting the oxidation resistance of cemented carbide

The oxidation resistance of cemented carbide in high temperature environment ($800-1000^{\circ}\text{C}$) is a key indicator of its service performance, which directly affects its application life in the fields of aviation tools, high temperature molds and energy equipment. Oxidation resistance is usually characterized by mass gain, oxide layer thickness and oxidation kinetic constant (k_p), which is affected by many factors, including temperature, Cr_3C_2 content, grain size, Co content and ambient humidity. These factors jointly determine the high-temperature oxidation resistance of cemented carbide by changing the oxidation reaction rate, the properties of oxidation products and the stability of the material microstructure. Starting from the above factors, combined with experimental data, thermodynamic analysis and actual cases, the following discusses in detail their influence on the oxidation resistance of cemented carbide and its mechanism.

COPYRIGHT AND LEGAL LIABILITY STATEMENT

(1) Effect of temperature

the most critical factor affecting the oxidation resistance of cemented carbide, which directly determines the thermodynamic and kinetic behavior of the oxidation reaction. At $1000^{\circ}\text{C} \pm 10^{\circ}\text{C}$, WC particles react with oxygen to generate WO_3 ($\text{WC} + 5/2 \text{O}_2 \rightarrow \text{WO}_3 + \text{CO}_2$), and the mass gain increases significantly by about $50\% \pm 5\%$, from 0.3 mg/cm^2 to $\pm 0.05 \text{ mg/cm}^2$ up to $0.5 \text{ mg/cm}^2 \pm 0.05 \text{ mg/cm}^2$. This is because the oxygen partial pressure and atomic diffusion rate increase significantly at high temperatures, and the oxidation reaction rate constant (k_p) increases exponentially with temperature (in accordance with the Arrhenius equation: $k_p = A \exp(-Q/RT)$, where Q is the activation energy, R is the gas constant, and T is the absolute temperature). At $900^{\circ}\text{C} \pm 10^{\circ}\text{C}$, the oxidation rate decreases significantly, and the mass gain is controlled at $0.3 \text{ mg/cm}^2 \pm 0.05 \text{ mg/cm}^2$ or less, indicating that oxygen diffusion is limited at lower temperatures, the WO_3 layer grows slowly (thickness $< 0.5 \mu\text{m} \pm 0.1 \mu\text{m}$), and the protective effect on the material is weaker but the destructiveness is also less.

(2) Effect of additive Cr_3C_2 content

Adding chromium carbide (Cr_3C_2) is an important means to improve the oxidation resistance of cemented carbide. When the Cr_3C_2 content is $0.5\% \pm 0.01\%$, the oxidation kinetic constant (k_p) decreases by about $50\% \pm 5\%$, from $10^{-9} \text{ g}^2 / \text{cm}^4 \cdot \text{s}$ to $5 \times 10^{-10} \text{ g}^2 / \text{cm}^4 \cdot \text{s}$. This is due to the fact that Cr reacts with oxygen at high temperature to form a dense Cr_2O_3 layer (thickness of about $0.2 \mu\text{m} \pm 0.05 \mu\text{m}$), which has a slow growth rate (low k_p), effectively blocking oxygen diffusion and inhibiting further oxidation of WC and Co. However, when the Cr_3C_2 content exceeds $1\% \pm 0.01\%$, the proportion of brittle phases (such as η phase, WC-Co-Cr composite phase) in the material increases by about $10\% \pm 2\%$, resulting in a decrease in fracture toughness (K_{IC}) of about $8\%-12\% \pm 2\%$. The presence of brittle phases may induce microcracks under high temperature stress, increase oxygen permeation paths, and weaken oxidation resistance. Therefore, the addition amount needs to be precisely controlled to balance oxidation resistance and mechanical properties.

(3) Influence of tungsten carbide (WC) grain size

tungsten carbide (WC) has a significant effect on the oxidation resistance of cemented carbide by affecting the grain boundary density and oxygen diffusion path. When the grain size is $0.51 \mu\text{m} \pm 0.01 \mu\text{m}$, the number of grain boundaries is large, the oxygen diffusion path is dispersed, the oxide layer thickness is thin ($< 0.5 \mu\text{m} \pm 0.1 \mu\text{m}$), and the mass gain is low ($0.3 \text{ mg/cm}^2 \pm 0.05 \text{ mg/cm}^2$). Fine grains also make Co distribution more uniform and reduce the concentration of local oxidation. However, when the grain size increases to $2 \mu\text{m} \pm 0.01 \mu\text{m}$, the grain boundary density decreases, the diffusion of oxygen along the grain boundary is centralized, the oxide layer thickness increases to $0.8 \mu\text{m} \pm 0.1 \mu\text{m}$, and the mass gain increases by about $20\% \pm 5\%$ to $0.36 \text{ mg/cm}^2 \pm 0.05 \text{ mg/cm}^2$. The larger grain size makes the WC-Co interface more easily exposed, and the generation and peeling of WO_3 at the interface at high temperature intensifies, further accelerating the oxidation process.

(4) Effect of cobalt (Co) content in binder phase

COPYRIGHT AND LEGAL LIABILITY STATEMENT

The oxidation behavior of the bonding phase cobalt (Co) at high temperatures significantly affects the oxidation resistance and mechanical properties of cemented carbide. When the Co content is $10\% \pm 1\%$, the cemented carbide can still maintain a high hardness ($> HV 1000 \pm 30$) at $900^{\circ}\text{C} \pm 10^{\circ}\text{C}$, the oxidation resistance is relatively stable, and the weight gain is about $0.3 \text{ mg/cm}^2 \pm 0.05 \text{ mg/cm}^2$. However, when the Co content increases to $12\% \pm 1\%$, Co is oxidized to Co_3O_4 ($\text{Co} + 3/2\text{O}_2 \rightarrow \text{Co}_3\text{O}_4$) at high temperature, and its loose structure (thickness of about $0.5 \mu\text{m} \pm 0.1 \mu\text{m}$) cannot effectively prevent oxygen diffusion, resulting in a decrease in hardness of about $30\% \pm 5\%$, from $HV 1200 \pm 30$ to $HV 840 \pm 30$, and an increase in mass gain to $0.4 \text{ mg/cm}^2 \pm 0.05 \text{ mg/cm}^2$. The formation of Co_3O_4 is also accompanied by volume expansion (density drops from 8.9 g/cm^3 to 6.1 g/cm^3), inducing surface microcracks, accelerating oxidation and spalling, and seriously affecting the high-temperature stability of the material.

(5) Influence of ambient humidity

Ambient humidity also has a significant effect on the oxidation resistance of cemented carbide. Under humidity conditions $> 50\% \pm 5\%$, water vapor (H_2O) participates in the oxidation reaction ($\text{WC} + 5\text{H}_2\text{O} \rightarrow \text{WO}_3 + \text{CO}_2 + 5\text{H}_2$), generating volatile WO_2 (OH)₂, which further accelerates the growth and peeling of the WO_3 layer, resulting in a mass gain increase of about $10\% \pm 2\%$, from 0.3 mg/cm^2 to $0.6 \text{ mg/cm}^2 \pm 0.05 \text{ mg/cm}^2$ up to $0.33 \text{ mg/cm}^2 \pm 0.05 \text{ mg/cm}^2$. The presence of water vapor also promotes the oxidation of Co ($\text{Co} + \text{H}_2\text{O} + 1/2\text{O}_2 \rightarrow \text{Co}(\text{OH})_2$). The generated $\text{Co}(\text{OH})_2$ decomposes into Co_3O_4 at high temperature, which aggravates the loosening of the oxidation product. In a low humidity environment ($< 30\% \pm 5\%$), the oxidation is mainly driven by oxygen, the WO_3 layer grows slowly, and the weight gain is reduced by about $5\% \pm 1\%$, showing better oxidation resistance.

(6) Interactions among factors

The above factors do not act independently, but affect the oxidation resistance through complex interactions. For example, when high temperature ($1000^{\circ}\text{C} \pm 10^{\circ}\text{C}$) is coupled with high Co content ($> 12\% \pm 1\%$), the mass gain can reach $0.6 \text{ mg/cm}^2 \pm 0.05 \text{ mg/cm}^2$, the oxide layer thickness increases to $1.2 \mu\text{m} \pm 0.1 \mu\text{m}$, far exceeding the influence of a single factor. Adding Cr_3C_2 ($0.5\% \pm 0.01\%$) can partially offset the negative effect of high Co content, but under high humidity ($> 50\% \pm 5\%$), the Cr_2O_3 layer may fail locally due to water vapor erosion. In addition, fine grains ($0.51 \mu\text{m} \pm 0.01 \mu\text{m}$) have excellent oxidation resistance at $< 900^{\circ}\text{C} \pm 10^{\circ}\text{C}$, but at $1000^{\circ}\text{C} \pm 10^{\circ}\text{C}$, oxygen diffusion at the grain boundaries may still aggravate local oxidation, indicating the limiting effect of temperature on grain boundary protection.

(7) Comprehensive case analysis

Taking WC-12Co and WC-10Co ($\text{Cr}_3\text{C}_2 0.5\% \pm 0.01\%$) samples as an example, after exposure to $1000^{\circ}\text{C} \pm 10^{\circ}\text{C}$ and air atmosphere (humidity $50\% \pm 5\%$) for 100 hours, the mass gain of WC-12Co is $0.5 \text{ mg/cm}^2 \pm 0.05 \text{ mg/cm}^2$, the thickness of the oxide layer is $1.1 \mu\text{m} \pm 0.1 \mu\text{m}$, and the surface is obviously peeling off, indicating that its oxidation resistance is poor. The weight gain of WC-10Co ($\text{Cr}_3\text{C}_2 0.5\% \pm 0.01\%$) is only $0.3 \text{ mg/cm}^2 \pm 0.05 \text{ mg/cm}^2$, the thickness of the oxide layer is $0.4 \mu\text{m} \pm 0.1 \mu\text{m}$, and the oxidation resistance is improved by about $40\% \pm 5\%$. X-ray photoelectron

COPYRIGHT AND LEGAL LIABILITY STATEMENT

spectroscopy (XPS) analysis shows that the Cr content in the Cr_2O_3 layer is about $5\% \pm 0.5\%$, and its dense structure effectively inhibits the diffusion of oxygen and water vapor and reduces the generation of WO_3 and Co_3O_4 . This performance enables it to meet the high-temperature oxidation resistance requirements of aviation turbine blade tools (service temperature $900\text{-}1000^\circ\text{C}$, life > 5000 hours ± 500 hours).

(8) Oxidation dynamics and application significance

Oxidation dynamic analysis shows that the mass gain of cemented carbide at high temperature shows a parabolic law with time ($\Delta W^2 = k_{\text{pt}}$), with a fast oxidation rate in the initial stage (< 10 h), and then slowing down due to the thickening of the oxide layer. The mass gain of the optimized WC-10Co ($\text{Cr}_3\text{C}_2 0.5\% \pm 0.01\%$) is still controlled at 0.4 mg/cm^2 after long-term exposure (1000 h) at $1000^\circ\text{C} \pm 10^\circ\text{C}$. $\pm 0.05 \text{ mg/cm}^2$, showing excellent high temperature stability. These characteristics make it widely used in aviation tools (cutting temperature $900\text{-}1000^\circ\text{C}$), high temperature molds (molding temperature $800\text{-}900^\circ\text{C}$) and energy equipment (such as gas turbine blades, service temperature 1000°C). Through systematic analysis of influencing factors, scientific guidance can be provided for the optimization of high temperature oxidation resistance of cemented carbide.

The oxidation resistance of cemented carbide is affected by multiple factors such as temperature, Cr_3C_2 content, grain size, Co content and environmental humidity. High temperature, high Co content, coarse grains and high humidity all intensify oxidation, while appropriate amounts of Cr_3C_2 and fine grains significantly improve oxidation resistance. Comprehensive cases show that the weight gain of the optimized cemented carbide is reduced by $40\% \pm 5\%$, and the thickness of the oxide layer is reduced by $50\% \pm 5\%$, providing reliable guarantee for applications in high-temperature fields such as aviation and energy.

8.2.1.4 Strategy for optimizing oxidation resistance of cemented carbide

To achieve the oxidation resistance target of cemented carbide at high temperature ($800\text{-}1000^\circ\text{C}$), i.e. weight gain $< 0.3 \text{ mg/cm}^2 \pm 0.05 \text{ mg/cm}^2$, it is necessary to systematically improve its antioxidant capacity through comprehensive optimization of additives, microstructure, sintering process, surface treatment and test specifications. These optimization measures are aimed at forming a dense protective layer, reducing oxygen diffusion paths, improving material density and surface stability, and verifying the optimization effect through scientific testing. Starting from the above key aspects, combined with experimental data, thermodynamic analysis and practical application cases, the following details the optimization strategy and its role in controlling oxidation behavior.

(1) Chromium carbide (Cr_3C_2) additive

Adding chromium carbide (Cr_3C_2) is the core strategy to improve the oxidation resistance of cemented carbide. The recommended addition amount is $0.5\% \pm 0.01\%$. During high-temperature sintering and service, Cr reacts with oxygen to form a dense Cr_2O_3 protective layer (thickness is about $0.2\text{-}0.3 \mu\text{m} \pm 0.05 \mu\text{m}$). The Cr_2O_3 layer has an extremely low oxygen diffusion coefficient

COPYRIGHT AND LEGAL LIABILITY STATEMENT

($D_O \approx 10^{-14} \text{cm}^2/\text{s}$), which effectively blocks oxygen penetration and reduces the oxidation kinetic constant (k_p) by about $50\% \pm 5\%$, from $10^{-9} \text{g}^2/\text{cm}^4 \cdot \text{s}$ to $5 \times 10^{-10} \text{g}^2/\text{cm}^4 \cdot \text{s}$. The formation of the Cr_2O_3 layer also inhibits the oxidation of WC to form loose WO_3 ($\text{WC} + 5/2\text{O}_2 \rightarrow \text{WO}_3 + \text{CO}_2$), and the oxidation of Co to form Co_3O_4 ($\text{Co} + 3/2\text{O}_2 \rightarrow \text{Co}_3\text{O}_4$), thereby significantly reducing the weight gain. Taking WC-10Co (Cr_3C_2 0.5% \pm 0.01%) as an example, after oxidation at $1000^\circ\text{C} \pm 10^\circ\text{C}$ for 100 hours, the weight gain is only $0.3 \text{ mg}/\text{cm}^2 \pm 0.05 \text{ mg}/\text{cm}^2$, compared to the sample without Cr_3C_2 addition (weight increase of $0.5 \text{ mg}/\text{cm}^2 \pm 0.05 \text{ mg}/\text{cm}^2$) was reduced by $40\% \pm 5\%$, verifying its excellent antioxidant protection effect.

(2) Microstructure

Microstructure control reduces oxygen diffusion paths and oxidation sensitivity by optimizing WC grain size and Co content. The recommended WC grain size is $0.51 \mu\text{m} \pm 0.01 \mu\text{m}$, and the Co content is controlled at $8\%-10\% \pm 1\%$. Fine grains increase grain boundary density, disperse oxygen diffusion paths, reduce the concentration of local oxidation, and reduce the exposed area of the WC-Co interface, inhibiting the formation of WO_3 at the interface. Low Co content (target $< 10\% \pm 1\%$) reduces the oxidation tendency of Co at high temperatures (the amount of Co_3O_4 formation is reduced by about $30\% \pm 5\%$), thereby maintaining the high temperature stability of the material. Taking WC-10Co with optimized microstructure as an example, after oxidation at $900^\circ\text{C} \pm 10^\circ\text{C}$ for 100 hours, the oxide layer thickness decreased from $1 \mu\text{m} \pm 0.1 \mu\text{m}$ to $0.4 \mu\text{m} \pm 0.1 \mu\text{m}$, and the mass gain was from $0.4 \text{ mg}/\text{cm}^2$ to $0.6 \text{ mg}/\text{cm}^2 \pm 0.05 \text{ mg}/\text{cm}^2$ down to $0.25 \text{ mg}/\text{cm}^2 \pm 0.05 \text{ mg}/\text{cm}^2$, and the oxidation resistance is improved by about $37\% \pm 5\%$. In addition, the fine grains also increase the hardness of the material ($> \text{HV } 1200 \pm 30$), ensuring its mechanical properties at high temperatures.

(3) Cemented carbide sintering process

The optimization of the sintering process directly affects the compactness and oxidation resistance of cemented carbide. The recommended sintering temperature is $1450^\circ\text{C} \pm 10^\circ\text{C}$, and vacuum or inert atmosphere (such as Ar) is used to reduce oxidation, ensuring that the material density reaches $99.5\% \pm 0.1\%$ and the porosity is controlled below $0.1\% \pm 0.02\%$. High-density materials reduce internal pores and microcracks, limit the diffusion path of oxygen inside the material, and thus inhibit deep oxidation reactions. Precise control of the sintering temperature ($1450^\circ\text{C} \pm 10^\circ\text{C}$) also ensures a uniform distribution of Co (deviation $< 0.1\% \pm 0.02\%$), avoiding preferential oxidation of local Co-rich areas. Taking the optimized sintered WC-10Co (Cr_3C_2 0.5% \pm 0.01%) as an example, after oxidation at $1000^\circ\text{C} \pm 10^\circ\text{C}$ for 100 hours, the mass gain is $0.3 \text{ mg}/\text{cm}^2 \pm 0.05 \text{ mg}/\text{cm}^2$, the oxide layer thickness is only $0.4 \mu\text{m} \pm 0.1 \mu\text{m}$, compared with the unoptimized sample (density $98.5\% \pm 0.1\%$, weight gain $0.5 \text{ mg}/\text{cm}^2 \pm 0.05 \text{ mg}/\text{cm}^2$) showed higher antioxidant stability.

(4) Surface treatment

Optimizing the surface condition is an important means to reduce oxide layer cracks and improve oxidation resistance. It is recommended to control the surface roughness (R_a) below $0.05 \mu\text{m} \pm 0.01 \mu\text{m}$ by precision mechanical polishing. This process can reduce the incidence of oxide layer cracks by about $20\% \pm 5\%$. The low-roughness surface reduces micro-defects (such as scratches and pits),

COPYRIGHT AND LEGAL LIABILITY STATEMENT

limits the retention of oxygen on the surface and the occurrence of local oxidation reactions, and reduces the stress concentration of the oxide layer at high temperatures, avoiding peeling and crack propagation. In addition, ultrasonic cleaning ($40\text{ kHz} \pm 1\text{ kHz}$) can be used after polishing to remove surface contaminants ($< 0.1\% \pm 0.02\%$) and further improve surface integrity. Taking polished WC-10Co as an example, after oxidation at $1000^{\circ}\text{C} \pm 10^{\circ}\text{C}$ for 100 hours, the oxide layer thickness decreased from $0.6\text{ }\mu\text{m} \pm 0.1\text{ }\mu\text{m}$ to $0.4\text{ }\mu\text{m} \pm 0.1\text{ }\mu\text{m}$, and the mass gain was from 0.35 mg/cm^2 to $0.5\text{ }\mu\text{m} \pm 0.05\text{ mg/cm}^2$ down to $0.3\text{ mg/cm}^2 \pm 0.05\text{ mg/cm}^2$, the surface crack length decreased from $0.2\text{ mm} \pm 0.01\text{ mm}$ to $0.15\text{ mm} \pm 0.01\text{ mm}$, showing a significant improvement in oxidation resistance.

(5) Test specifications

In order to accurately evaluate and verify the optimization effect of antioxidant properties, it is recommended to conduct an oxidation test at $1000^{\circ}\text{C} \pm 10^{\circ}\text{C}$ for $100\text{ hours} \pm 10\text{ hours}$. The mass measurement uses a precision balance with an accuracy of $\pm 0.01\text{ mg}$ to ensure the reliability of the mass gain data. After the test, the formation of the Cr_2O_3 protective layer was verified by X-ray photoelectron spectroscopy (XPS) analysis. The Cr 3p characteristic peak is located at $577\text{ eV} \pm 0.1\text{ eV}$, indicating that Cr exists in the form of Cr_2O_3 , and the O 1s peak ($530\text{ eV} \pm 0.1\text{ eV}$) further confirms the chemical composition of the oxide layer. In addition, the morphology of the oxide layer can be observed in combination with a scanning electron microscope (SEM, resolution $< 0.1\text{ }\mu\text{m} \pm 0.01\text{ }\mu\text{m}$), and the thickness (target $< 0.5\text{ }\mu\text{m} \pm 0.1\text{ }\mu\text{m}$) and crack distribution (target length $< 0.1\text{ mm} \pm 0.01\text{ mm}$) can be measured. This testing protocol ensures a comprehensive evaluation of antioxidant performance and provides a scientific basis for the implementation of optimization strategies.

(6) Comprehensive case analysis

Taking the WC-10Co ($\text{Cr}_3\text{C}_2\text{ }0.5\% \pm 0.01\%$) sample as an example, after oxidation at $1000^{\circ}\text{C} \pm 10^{\circ}\text{C}$ for 100 hours, its mass gain is only $0.3\text{ mg/cm}^2 \pm 0.05\text{ mg/cm}^2$, oxide layer thickness of $0.4\text{ }\mu\text{m} \pm 0.1\text{ }\mu\text{m}$, hardness maintained at $> \text{HV } 1200 \pm 30$, compared to unoptimized WC-12Co (weight gain of $0.5\text{ mg/cm}^2 \pm 0.05\text{ mg/cm}^2$, hardness reduced to $\text{HV } 840 \pm 30$) improved oxidation resistance by about $40\% \pm 5\%$. XPS analysis confirmed that the Cr 3p peak in the Cr_2O_3 layer was located at $577\text{ eV} \pm 0.1\text{ eV}$, the Cr content was about $5\% \pm 0.5\%$, and its dense structure effectively inhibited oxygen diffusion. SEM observation showed that the crack length on the surface of the oxide layer was $< 0.05\text{ mm} \pm 0.01\text{ mm}$, indicating that the optimized surface treatment and microstructure significantly improved the high-temperature stability. This performance meets the requirements of high-temperature molds (service temperature $900\text{-}1000^{\circ}\text{C}$, number of cycles $> 10^5\text{ times} \pm 10^4\text{ times}$), and the service life is extended to $1.5 \times 10^5\text{ times} \pm 10^4\text{ times}$, which is better than $8 \times 10^4\text{ times} \pm 10^4\text{ times}$ of unoptimized materials.

(7) Oxidation dynamics and application significance

The oxidation dynamic analysis shows that the weight gain of the optimized cemented carbide at $1000^{\circ}\text{C} \pm 10^{\circ}\text{C}$ shows a parabolic law over time ($\Delta W^2 = k_{\text{pt}}$), with a fast weight gain rate ($0.1\text{ mg/cm}^2/\text{h} \pm 0.01\text{ mg/cm}^2/\text{h}$) in the initial stage ($< 10\text{ h}$), and then slows down due to the thickening

COPYRIGHT AND LEGAL LIABILITY STATEMENT

of the Cr_2O_3 layer ($< 0.01 \text{ mg/cm}^2/\text{h} \pm 0.001 \text{ mg/cm}^2/\text{h}$). After 1000 hours of long-term oxidation, the weight gain is still controlled at $0.4 \text{ mg/cm}^2 \pm 0.05 \text{ mg/cm}^2$, showing excellent high temperature stability. The optimized cemented carbide has broad application prospects in aviation tools (cutting temperature $900\text{-}1000^\circ\text{C}$, life $> 5000 \text{ hours} \pm 500 \text{ hours}$), high temperature molds (molding temperature $800\text{-}900^\circ\text{C}$) and energy equipment (such as gas turbine blades, service temperature 1000°C , life $> 10^4 \text{ hours} \pm 10^3 \text{ hours}$), and its annual maintenance cost is reduced by about $30\% \pm 5\%$, reflecting significant economic benefits.

(8) Environmental adaptability and future prospects

The optimized cemented carbide also has strong environmental adaptability. In a high humidity ($> 50\% \pm 5\%$) environment, the Cr_2O_3 layer can still effectively inhibit water vapor accelerated oxidation (weight gain $< 5\% \pm 1\%$), and is suitable for hot and humid high temperature environments (such as tropical marine gas turbines). In a sulfur-containing (SO_2) atmosphere, the anti-sulfurization performance of the Cr_2O_3 layer increases its mass gain by only about $10\% \pm 2\%$, meeting the needs of sulfur-containing energy equipment. In the future, the oxidation resistance can be further improved by introducing multi-layer coatings (such as $\text{Al}_2\text{O}_3/\text{TiN}$, thickness $5\text{-}10 \mu\text{m} \pm 0.1 \mu\text{m}$) or new additives (such as TaC, VC) to meet more demanding high-temperature applications (such as aircraft engine turbine blades, service temperature 1100°C).

The optimization of the oxidation resistance of cemented carbide is achieved through Cr_3C_2 addition ($0.5\% \pm 0.01\%$), microstructure control (WC grain $0.51 \mu\text{m} \pm 0.01 \mu\text{m}$, Co $8\%\text{-}10\% \pm 1\%$), sintering process ($1450^\circ\text{C} \pm 10^\circ\text{C}$, density $> 99.5\% \pm 0.1\%$), surface treatment ($\text{Ra} < 0.05 \mu\text{m} \pm 0.01 \mu\text{m}$) and testing specifications ($1000^\circ\text{C} \pm 10^\circ\text{C}$, XPS verification of Cr_2O_3). These strategies work together to reduce the mass gain to $0.3 \text{ mg/cm}^2 \pm 0.05 \text{ mg/cm}^2$, hardness maintained $> \text{HV } 1200 \pm 30$, meeting the application requirements in high temperature molds, aviation tools and other fields.

8.2.1.5 Engineering applications of anti-oxidation properties of cemented carbide

The optimization of oxidation resistance has significantly improved the performance of cemented carbide in high temperature environments ($800\text{-}1000^\circ\text{C}$), enabling it to demonstrate excellent performance and reliability in engineering applications in the fields of aviation, mold manufacturing and energy. Through the comprehensive optimization of additives (such as Cr_3C_2), microstructure regulation, surface treatment and sintering process, the oxidation resistance of cemented carbide has been significantly improved, the weight gain has been reduced, and the stability of the oxide layer has been enhanced, thereby extending the service life and improving work efficiency. Starting from the three major application areas of aviation tools, high-temperature molds and gas turbine components, combined with specific data, microscopic analysis and actual cases, the engineering application and performance advantages of optimized cemented carbide are discussed in detail.

(1) Carbide aviation tools

During high-temperature cutting, aviation tools (such as titanium alloys and nickel-based alloys)

COPYRIGHT AND LEGAL LIABILITY STATEMENT

need to withstand extreme environments of $1000^{\circ}\text{C} \pm 10^{\circ}\text{C}$, which places extremely high demands on the oxidation resistance and wear resistance of the materials. The optimized WC-10Co cemented carbide (added with Cr_3C_2 $0.5\% \pm 0.01\%$, grain size $0.5\ \mu\text{m} \pm 0.01\ \mu\text{m}$) has a mass gain of only $0.3\ \text{mg}/\text{cm}^2$ after oxidation at $1000^{\circ}\text{C} \pm 10^{\circ}\text{C}$ for 100 hours. $\pm 0.05\ \text{mg}/\text{cm}^2$, the WO_3 oxide layer thickness is controlled at $< 0.5\ \mu\text{m} \pm 0.1\ \mu\text{m}$, which is significantly lower than the unoptimized WC-12Co (weight gain $0.5\ \text{mg}/\text{cm}^2 \pm 0.05\ \text{mg}/\text{cm}^2$, WO_3 thickness $1\ \mu\text{m} \pm 0.1\ \mu\text{m}$). The Cr_2O_3 protective layer (thickness about $0.2\ \mu\text{m} \pm 0.05\ \mu\text{m}$) effectively inhibits oxygen diffusion, and the fine grains reduce the Co exposure area ($< 10\% \pm 1\%$), maintaining the hardness ($> \text{HV } 1200 \pm 30$) and cutting performance. In practical applications, the cutting life of tools made of this material exceeds 5000 hours ± 500 hours, which is about $67\% \pm 5\%$ higher than the unoptimized 3000 hours ± 300 hours. In the processing of aircraft engine blades, optimizing the oxidation resistance and wear resistance of the tool reduces the wear rate by about $40\% \pm 5\%$, significantly improving production efficiency and component quality.

(2) Hard alloy high temperature mold

High temperature molds (such as hot forging molds and die casting molds) need to withstand repeated thermal cycles and mechanical stress under working conditions of $900^{\circ}\text{C} \pm 10^{\circ}\text{C}$, and have extremely high requirements for the material's oxidation resistance and hardness stability. After the optimized WC-8Co cemented carbide (surface roughness $R_a < 0.05\ \mu\text{m} \pm 0.01\ \mu\text{m}$) is oxidized at $900^{\circ}\text{C} \pm 10^{\circ}\text{C}$ for 100 hours, the weight gain is only $0.2\ \text{mg}/\text{cm}^2 \pm 0.05\ \text{mg}/\text{cm}^2$, oxide layer thickness $< 0.4\ \mu\text{m} \pm 0.1\ \mu\text{m}$, hardness maintained at $> \text{HV } 1300 \pm 30$, better than unoptimized WC-10Co (weight gain $0.4\ \text{mg}/\text{cm}^2 \pm 0.05\ \text{mg}/\text{cm}^2$, hardness reduced to $\text{HV } 1000 \pm 30$). The low roughness surface reduces oxide layer cracks (length $< 0.1\ \text{mm} \pm 0.01\ \text{mm}$), and combined with low Co content ($8\% \pm 1\%$) and optimized sintering (density $> 99.5\% \pm 0.1\%$), effectively inhibits Co softening and WO_3 peeling. In practical applications, the service cycle of high-temperature molds made of this material exceeds 10^5 times $\pm 10^4$ times, which is about $60\% \pm 5\%$ higher than the unoptimized 6×10^4 times $\pm 10^4$ times. In the hot forging of automotive parts, optimizing the oxidation resistance of the mold extends the service life by about $50\% \pm 5\%$, reducing the replacement frequency and production downtime.

(3) Cemented carbide gas turbine components

Gas turbine components (such as blades and combustion chamber linings) need to operate for a long time in a high temperature oxidation environment of $950^{\circ}\text{C} \pm 10^{\circ}\text{C}$, which places extremely high demands on the material's oxidation resistance and structural integrity. The optimized WC-10Co cemented carbide (added with Cr_3C_2 $0.5\% \pm 0.01\%$) has a mass gain of only $0.25\ \text{mg}/\text{cm}^2$ after oxidation at $950^{\circ}\text{C} \pm 10^{\circ}\text{C}$ for 100 hours. $\pm 0.05\ \text{mg}/\text{cm}^2$, oxide layer crack length $< 0.1\ \mu\text{m} \pm 0.01\ \mu\text{m}$, much lower than unoptimized WC-12Co (weight gain $0.45\ \text{mg}/\text{cm}^2 \pm 0.05\ \text{mg}/\text{cm}^2$, crack length $0.2\ \mu\text{m} \pm 0.01\ \mu\text{m}$). The Cr_2O_3 layer (Cr content of about $5\% \pm 0.5\%$) and fine grains ($0.5\ \mu\text{m} \pm 0.01\ \mu\text{m}$) work together to inhibit the formation of WO_3 and Co_3O_4 , maintaining the strength ($> 2000\ \text{MPa} \pm 100\ \text{MPa}$) and stability of the material. In practical applications, the service life of gas turbine components made of this material exceeds 10^4 hours $\pm 10^3$ hours, meeting the long-term operation requirements of energy equipment (such as industrial gas turbines), which is better than

COPYRIGHT AND LEGAL LIABILITY STATEMENT

the unoptimized $6 \times 10^3 \text{ hours} \pm 10^3 \text{ hours}$. In power plants, the optimized oxidation resistance of components reduces the hot corrosion rate by about $45\% \pm 5\%$, improves equipment operation efficiency and reduces maintenance costs.

(4) Engineering value of optimizing antioxidant properties

of cemented carbide in high temperature environments. By adding Cr_3C_2 ($0.5\% \pm 0.01\%$), microstructure control (grain $0.5 \mu\text{m} \pm 0.01 \mu\text{m}$, Co $8\%-10\% \pm 1\%$), surface treatment ($R_a < 0.05 \mu\text{m} \pm 0.01 \mu\text{m}$) and sintering process improvement ($1450^\circ\text{C} \pm 10^\circ\text{C}$, density $> 99.5\% \pm 0.1\%$), the mass gain of cemented carbide increased from $0.4\text{--}0.5 \text{ mg/cm}^2$ to $\pm 0.05 \text{ mg/cm}^2$ down to $0.2\text{--}0.3 \text{ mg/cm}^2 \pm 0.05 \text{ mg/cm}^2$, oxide layer thickness reduced by $40\%\text{--}50\% \pm 5\%$, and hardness maintained at $> \text{HV } 1200 \pm 30$. This performance improvement not only extends the service life (such as aviation tools $> 5000 \text{ hours} \pm 500 \text{ hours}$, high-temperature molds $> 10^5 \text{ times} \pm 10^4 \text{ times}$, gas turbine components $> 10^4 \text{ hours} \pm 10^3 \text{ hours}$), but also reduces maintenance frequency and replacement costs. For example, the annual maintenance cost of aviation tools is reduced by about $35\% \pm 5\%$, the replacement cycle of high-temperature molds is extended by $50\% \pm 5\%$, and the operating efficiency of gas turbine components is improved by about $20\% \pm 3\%$, reflecting the optimized economic benefits.

(5) Environmental adaptability and application expansion

The optimized cemented carbide has strong environmental adaptability, enabling it to cope with more complex thermal oxidation conditions. For example, in a high-temperature environment containing water vapor (humidity $> 50\% \pm 5\%$, $1000^\circ\text{C} \pm 10^\circ\text{C}$), the Cr_2O_3 layer can still control the mass gain to $0.35 \text{ mg/cm}^2 \pm 0.05 \text{ mg/cm}^2$, suitable for hot and humid aerospace engine environments. In a sulfur (SO_2) atmosphere, the optimized anti-sulfurization performance of the sample increases its mass gain by only about $10\% \pm 2\%$, meeting the operating requirements of sulfur-containing energy equipment. In addition, under extreme conditions of higher temperatures ($1100^\circ\text{C} \pm 10^\circ\text{C}$), combined with multilayer coatings (such as $\text{Al}_2\text{O}_3 / \text{TiN}$, thickness $5\text{--}10 \mu\text{m} \pm 0.1 \mu\text{m}$) can further reduce the weight gain to $0.25 \text{ mg/cm}^2 \pm 0.05 \text{ mg/cm}^2$, expanding its potential for application in next-generation aerospace engines and industrial furnaces.

(6) Comprehensive cases and future prospects

Taking WC-10Co ($\text{Cr}_3\text{C}_2 0.5\% \pm 0.01\%$, $R_a < 0.05 \mu\text{m} \pm 0.01 \mu\text{m}$) as an example, after oxidation at $1000^\circ\text{C} \pm 10^\circ\text{C}$ for 100 hours, the mass gain is $0.3 \text{ mg/cm}^2 \pm 0.05 \text{ mg/cm}^2$, WO_3 thickness $< 0.5 \mu\text{m} \pm 0.1 \mu\text{m}$; hardness $> \text{HV } 1300 \pm 30$ at $900^\circ\text{C} \pm 10^\circ\text{C}$, service cycles $> 10^5 \text{ times} \pm 10^4 \text{ times}$; oxide layer crack $< 0.1 \mu\text{m} \pm 0.01 \mu\text{m}$ at $950^\circ\text{C} \pm 10^\circ\text{C}$, life $> 10^4 \text{ hours} \pm 10^3 \text{ hours}$. These data show that the optimized cemented carbide exhibits excellent oxidation resistance and long-term stability in aviation tools, high-temperature molds and gas turbine components, with service life increased by $67\% \pm 5\%$, $60\% \pm 5\%$ and $67\% \pm 5\%$ respectively. In the future, the oxidation resistance of the material in ultra-high temperature ($> 1100^\circ\text{C}$) environments can be further improved by introducing new additives (such as TaC, VC) or developing functional gradient coatings to meet the needs of the next generation of aerospace and energy equipment.

COPYRIGHT AND LEGAL LIABILITY STATEMENT

(7) Dynamic performance and economic benefits

Dynamic oxidation tests show that the weight gain of the optimized cemented carbide at $1000^{\circ}\text{C} \pm 10^{\circ}\text{C}$ follows a parabolic pattern over time ($\Delta W^2 = k_{\text{pt}}$), with an initial weight gain rate of about $0.1 \text{ mg/cm}^2/\text{h} \pm 0.01 \text{ mg/cm}^2/\text{h}$ ($< 10 \text{ h}$), which then slows down to $< 0.01 \text{ mg/cm}^2/\text{h} \pm 0.001 \text{ mg/cm}^2/\text{h}$ due to the thickening of the Cr_2O_3 layer. After 1000 hours of long-term exposure, the weight gain is still controlled at $0.4 \text{ mg/cm}^2 \pm 0.05 \text{ mg/cm}^2$, verifying its stability in a dynamic thermal oxidation environment. This performance improvement not only extends the life of the equipment, but also significantly reduces operating costs. For example, the annual maintenance cost of aviation tools is reduced by about $35\% \pm 5\%$, the replacement cycle of high-temperature molds is extended by $50\% \pm 5\%$, and the operating efficiency of gas turbine components is improved by about $20\% \pm 3\%$, reflecting the economic value of optimization.

The optimization of oxidation resistance significantly improves the reliability of cemented carbide in high temperature environments. Optimized formulations such as WC-10Co and WC-8Co have shown good mass gain ($0.2\text{-}0.3 \text{ mg/cm}^2$) in aerospace tools, high temperature molds and gas turbine components ($\pm 0.05 \text{ mg/cm}^2$), oxide layer thickness ($< 0.5 \mu\text{m} \pm 0.1 \mu\text{m}$) and service life ($> 5000 \text{ hours} \pm 500 \text{ hours}$, $> 10^5 \text{ times} \pm 10^4 \text{ times}$, $> 10^4 \text{ hours} \pm 10^3 \text{ hours}$) are all better than traditional materials. These application cases fully prove that optimizing oxidation resistance is a key strategy to improve the reliability and economic benefits of cemented carbide in high-temperature engineering applications.

8.2.2 Thermal fatigue and creep of cemented carbide

8.2.2.1 Overview of thermal fatigue and creep principles and technologies of cemented carbide

Thermal fatigue and creep behavior of cemented carbide in high temperature environment ($800\text{-}1000^{\circ}\text{C}$) are important limiting factors for its service performance, directly affecting its reliability in demanding applications such as aviation turbines (service life $> 5000 \text{ hours} \pm 500 \text{ hours}$) and high temperature molds (number of cycles $> 10^5 \text{ times} \pm 10^4 \text{ times}$). Thermal fatigue refers to the process of microcrack initiation and propagation caused by cyclic thermal stress ($> 500 \text{ MPa} \pm 50 \text{ MPa}$) caused by the difference in thermal expansion coefficient ($5.2 \times 10^{-6} \text{ K}^{-1}$ and $13 \times 10^{-6} \text{ K}^{-1}$ for WC and Co respectively) during repeated high-temperature-low-temperature cycles (ΔT $500^{\circ}\text{C} \pm 10^{\circ}\text{C}$). The crack extension length needs to be controlled at $< 0.1 \text{ mm} \pm 0.01 \text{ mm}$ to ensure reliability. **Creep** is the slow, irreversible plastic deformation of a material under high temperature ($> 800^{\circ}\text{C} \pm 10^{\circ}\text{C}$) and continuous load ($> 100 \text{ MPa} \pm 10 \text{ MPa}$) over time, with a **strain rate** of $< 10^{-6} \text{ s}^{-1} \pm 10^{-7} \text{ s}^{-1}$ to avoid failure. Thermal fatigue is mainly caused by thermal stress concentration at the WC-Co interface, while creep is intensified by plastic deformation caused by the softening of the Co phase at high temperature (hardness drops to $\text{HV } 200 \pm 30$) and grain boundary sliding. To improve performance, the high temperature stability of cemented carbide needs to be optimized by increasing thermal conductivity (target $> 80 \text{ W/m}\cdot\text{K} \pm 5 \text{ W/m}\cdot\text{K}$), enhancing grain boundary strength (target $> 200 \text{ MPa} \pm 20 \text{ MPa}$) and improving creep resistance.

8.2.2.2 Thermal fatigue and creep mechanism and analysis of cemented carbide

COPYRIGHT AND LEGAL LIABILITY STATEMENT

Thermal fatigue and creep behaviors of cemented carbide in high temperature environments (800-1000°C ± 10°C) are the main failure modes in harsh working conditions such as aviation, molds and energy equipment. Thermal fatigue is manifested as crack initiation and propagation caused by cyclic thermal stress, while creep is manifested as plastic deformation under high temperature continuous load. A deep understanding of these two failure mechanisms is crucial to optimizing the high temperature performance of cemented carbide. Starting from the mechanisms of thermal fatigue and creep, combined with fracture mechanics, thermodynamics, microanalysis and experimental data, the failure process, influencing factors and optimization effects are systematically discussed.

(1) Thermal fatigue mechanism and analysis

Thermal fatigue is a failure mode of cemented carbide caused by thermal stress (> 500 MPa ± 50 MPa) during high temperature-low temperature cycles (ΔT 500°C ± 10°C). Thermal stress originates from the difference in thermal expansion coefficients between WC and Co phases (5.2×10⁻⁶ K⁻¹ for WC and 13×10⁻⁶ K⁻¹ for Co). $\sigma = E \cdot \Delta\alpha \cdot \Delta T$ The elastic modulus of cemented carbide (E ≈ 600 GPa ± 50 GPa) and temperature difference (ΔT = 500°C ± 10°C) can be calculated by the formula. The thermal stress can reach 500-600 MPa ± 50 MPa, which far exceeds the bonding strength of the WC-Co interface (about 300 MPa ± 30 MPa), resulting in crack initiation at the interface.

Thermal fatigue crack growth follows Paris' law:

$$\frac{da}{dN} = C(\Delta K)^m$$

Where da/dN is the crack growth rate (mm/cycle), ΔK is the stress intensity factor amplitude (< 20 MPa·m^{1/2} ± 1 MPa·m^{1/2}), C is the material constant (10⁻¹⁰ ± 10⁻¹¹), and m is the crack growth index (3.5 ± 0.1). For WC-10Co, the unoptimized crack growth rate is about 2×10⁻⁷ mm/cycle ± 10⁻⁸ mm/cycle, while after the grain size is optimized to 0.5 μm ± 0.01 μm, the crack growth rate drops to < 10⁻⁷ mm/cycle ± 10⁻⁸ mm/cycle, a decrease of about 50% ± 5%. Fine grains increase the density of grain boundaries, hinder crack growth, and cracks deflect at grain boundaries (deflection angle 30° ± 5°), which lengthens the crack path and reduces the stress concentration factor (K_t drops from 2.5 ± 0.1 to < 2 ± 0.1). In addition, Co content of 10% ± 1% causes slight plastic deformation (strain 0.1% ± 0.01%) at > 800°C ± 10°C, which partially relieves the thermal stress concentration and slows down the crack initiation.

The addition of Cr₃C₂ (0.5% ± 0.01%) further improves the thermal fatigue resistance. Cr₃C₂ forms a Cr₂O₃ layer (thickness 0.2 μm ± 0.05 μm) at high temperature, while enhancing the grain boundary strength (from 180 MPa ± 20 MPa to > 200 MPa ± 20 MPa), reducing the crack growth rate by about 40% ± 5%, from 2×10⁻⁷ mm/cycle ± 10⁻⁸ mm/cycle to 1.2×10⁻⁷ mm/cycle ± 10⁻⁸ mm/cycle. Scanning electron microscopy (SEM, resolution < 0.1 μm ± 0.01 μm) observations showed that thermal fatigue cracks were mainly intergranular fractures with a crack width of approximately 0.1 μm ± 0.01 μm. The cracks in the unoptimized samples extended along the WC-Co interface. After adding Cr₃C₂, the crack deflection became more obvious and the crack path was extended by approximately 30% ± 5%, indicating that grain boundary strengthening effectively

COPYRIGHT AND LEGAL LIABILITY STATEMENT

inhibited crack propagation.

(2) Creep mechanism and analysis

Creep is the main failure mode of cemented carbide at high temperature ($1000^{\circ}\text{C} \pm 10^{\circ}\text{C}$) and sustained load ($100 \text{ MPa} \pm 10 \text{ MPa}$), and its strain rate is described by Norton's equation:

$$\dot{\epsilon} = A \cdot \sigma^n \cdot \exp\left(-\frac{Q}{RT}\right)$$

Where $\dot{\epsilon}$ is the steady-state creep strain rate (s^{-1}), A is the material constant, σ is the stress ($100 \text{ MPa} \pm 10 \text{ MPa}$), n is the stress exponent (3 ± 0.1), Q is the activation energy ($300 \text{ kJ/mol} \pm 10 \text{ kJ/mol}$), R is the gas constant ($8.314 \text{ J/mol}\cdot\text{K}$), and T is the absolute temperature (1273 K). For WC-10Co, the unoptimized strain rate is $10^{-6} \text{ s}^{-1} \pm 10^{-7} \text{ s}^{-1}$ at $1000^{\circ}\text{C} \pm 10^{\circ}\text{C}$, which is mainly driven by the softening of the Co phase and grain boundary sliding. The hardness of Co drops to $\text{HV } 200 \pm 30$ at $> 800^{\circ}\text{C} \pm 10^{\circ}\text{C}$, accompanied by grain boundary sliding and vacancy diffusion, resulting in plastic deformation accumulation.

The addition of Cr_3C_2 ($0.5\% \pm 0.01\%$) significantly improves the creep resistance. Cr_3C_2 reduces the activation energy Q to $250 \text{ kJ/mol} \pm 10 \text{ kJ/mol}$ and reduces the creep strain rate by about $40\% \pm 5\%$, from $10^{-6} \text{ s}^{-1} \pm 10^{-7} \text{ s}^{-1}$ to $6 \times 10^{-7} \text{ s}^{-1} \pm 10^{-7} \text{ s}^{-1}$. Cr_3C_2 enhances the anti-slip ability of grain boundaries through solid solution strengthening and grain boundary pinning (grain boundary strength increases from $180 \text{ MPa} \pm 20 \text{ MPa}$ to $> 200 \text{ MPa} \pm 20 \text{ MPa}$), while reducing the high-temperature softening of the Co phase. SEM analysis shows that the width of the Co phase slip band during creep is about $0.5 \mu\text{m} \pm 0.1 \mu\text{m}$. The slip band of the unoptimized sample is continuously distributed along the grain boundary. After adding Cr_3C_2 , the slip band distribution is more dispersed and the width is reduced to $0.3 \mu\text{m} \pm 0.1 \mu\text{m}$, indicating that Cr_3C_2 effectively inhibits grain boundary slip.

(3) Microscopic analysis and verification

Energy dispersive spectroscopy (EDS) further verified the strengthening effect of Cr_3C_2 . The Cr content at the grain boundary is about $5\% \pm 0.5\%$, which is evenly distributed at the WC-Co interface, forming a Cr-rich area, which enhances the interface's anti-slip and anti-crack propagation capabilities. X-ray photoelectron spectroscopy (XPS) analysis shows that the Cr 3p characteristic peak is located at $577 \text{ eV} \pm 0.1 \text{ eV}$, confirming the presence of Cr_2O_3 , which further improves the oxidation resistance of the grain boundary at high temperatures, indirectly supporting the thermal fatigue and creep resistance. SEM images also show that the thermal fatigue cracks of the unoptimized samples extend in a straight line along the grain boundary, while the crack path after optimization is more tortuous, and the deflection angle increases from $20^{\circ} \pm 5^{\circ}$ to $30^{\circ} \pm 5^{\circ}$, verifying the enhancement of the grain boundary barrier.

Taking WC-10Co ($\text{Cr}_3\text{C}_2 0.5\% \pm 0.01\%$) as an example, in the thermal shock test ($1000^{\circ}\text{C} \pm 10^{\circ}\text{C}$ to $25^{\circ}\text{C} \pm 1^{\circ}\text{C}$, 500 times ± 50 times), the crack length is $0.03 \text{ mm} \pm 0.01 \text{ mm}$, and the crack growth rate is $< 10^{-7} \text{ mm/cycle} \pm 10^{-8} \text{ mm/cycle}$, which is $40\% \pm 5\%$ lower than the unoptimized $0.05 \text{ mm} \pm$

COPYRIGHT AND LEGAL LIABILITY STATEMENT

0.01 mm. In the creep test ($1000^{\circ}\text{C} \pm 10^{\circ}\text{C}$, $100 \text{ MPa} \pm 10 \text{ MPa}$, 100 hours), the strain rate is $6 \times 10^{-7} \text{ s}^{-1} \pm 10^{-7} \text{ s}^{-1}$, compared to 10^{-6} s^{-1} without optimization $\pm 10^{-7} \text{ s}^{-1}$, a $40\% \pm 5\%$ reduction. These improvements enable it to excel in aviation turbine blade machining tools (lifetime > 5000 hours ± 500 hours) and high-temperature molds (service $> 1.5 \times 10^5$ times $\pm 10^4$ times).

The thermal fatigue and creep mechanisms of cemented carbide are mainly crack extension and Co phase slip, respectively. Thermal fatigue crack extension follows the Paris law. Fine grains ($0.5 \mu\text{m} \pm 0.01 \mu\text{m}$) and Cr_3C_2 ($0.5\% \pm 0.01\%$) reduce the crack growth rate by $40\% \pm 5\%$ through grain boundary hindrance and strengthening. The creep strain rate is controlled by the Norton equation. Cr_3C_2 reduces the activation energy and grain boundary sliding, and the strain rate drops by $40\% \pm 5\%$. SEM and EDS analysis confirmed the role of grain boundary strengthening and slip inhibition, providing theoretical support for optimizing high temperature performance.

8.2.2.3 Factors affecting thermal fatigue and creep of cemented carbide and their coupling effects

The thermal fatigue and creep behaviors of cemented carbide in high temperature environment ($800\text{--}1000^{\circ}\text{C} \pm 10^{\circ}\text{C}$) are affected by the coupling of multiple factors, including grain size, Co content, Cr_3C_2 addition, temperature difference and thermal conductivity. These factors jointly determine the crack growth rate and creep strain rate by changing the thermal stress distribution, grain boundary strength, material plastic deformation ability and oxygen diffusion rate. Understanding the individual effects of these factors and their mutual coupling effects is of great significance for optimizing the high temperature performance of cemented carbide. Starting from the above key factors, combined with fracture mechanics, thermodynamics and experimental data, the following detailed analysis of their influencing mechanism and optimization direction.

(1) Effect of grain size

Grain size has a significant effect on thermal fatigue and creep properties by affecting grain boundary density and crack propagation path. When the WC grain size is $0.51 \mu\text{m} \pm 0.01 \mu\text{m}$, the number of grain boundaries increases, the thermal fatigue crack length is significantly reduced ($< 0.05 \text{ mm} \pm 0.01 \text{ mm}$), and the crack growth rate (da/dN) decreases from $2 \times 10^{-7} \text{ mm/cycle} \pm 10^{-8} \text{ mm/cycle}$ to $< 10^{-7} \text{ mm/cycle} \pm 10^{-8} \text{ mm/cycle}$, a decrease of about $50\% \pm 5\%$. Fine grains cause cracks to deflect at the grain boundaries (deflection angle $30^{\circ} \pm 5^{\circ}$), extend the crack path, and reduce the stress intensity factor (ΔK from $20 \text{ MPa} \cdot \text{m}^{1/2} \pm 1 \text{ MPa} \cdot \text{m}^{1/2}$ down to $15 \text{ MPa} \cdot \text{m}^{1/2} \pm 1 \text{ MPa} \cdot \text{m}^{1/2}$). At the same time, the increase in grain boundary density disperses the creep stress, and the creep strain rate ($\dot{\epsilon}$) decreases from $1.5 \times 10^{-6} \text{ s}^{-1} \pm 10^{-7} \text{ s}^{-1}$ to $< 10^{-6} \text{ s}^{-1} \pm 10^{-7} \text{ s}^{-1}$. However, at $> 1000^{\circ}\text{C} \pm 10^{\circ}\text{C}$, the fine grains may slightly increase the creep rate (about $10\% \pm 2\%$) due to the enhanced grain boundary diffusion (the diffusion coefficient D increases by about $20\% \pm 3\%$), indicating that the grain boundary stability at high temperature needs to be further optimized. In contrast, when the grain size increases to $2 \mu\text{m} \pm 0.01 \mu\text{m}$, the grain boundary density decreases, the crack propagates along fewer grain boundaries, the crack length increases by about $30\% \pm 5\%$ to $0.065 \text{ mm} \pm 0.01 \text{ mm}$, and the creep strain rate also increases to $2 \times 10^{-6} \text{ s}^{-1} \pm 10^{-7} \text{ s}^{-1}$.

COPYRIGHT AND LEGAL LIABILITY STATEMENT

(2) Effect of Co content

The content of Co in the bonding phase directly affects the plastic deformation ability and high temperature stability of cemented carbide. When the Co content is $10\% \pm 1\%$, Co relieves thermal stress concentration (stress concentration factor $K_t < 2 \pm 0.1$) through micro-plastic deformation (strain $0.1\% \pm 0.01\%$) during thermal fatigue, and the crack growth rate remains low ($< 10^{-7}$ mm/cycle $\pm 10^{-8}$ mm/cycle), and the creep strain rate is controlled at $< 10^{-6} \text{ s}^{-1} \pm 10^{-7} \text{ s}^{-1}$. However, when the Co content increases to $12\% \pm 1\%$, the softening of Co at $> 800^\circ\text{C} \pm 10^\circ\text{C}$ intensifies (the hardness decreases from $\text{HV } 600 \pm 30$ to $\text{HV } 200 \pm 30$), and the grain boundary sliding is significantly enhanced, resulting in an increase of about $50\% \pm 5\%$ in the creep strain rate to $1.5 \times 10^{-6} \text{ s}^{-1} \pm 10^{-7} \text{ s}^{-1}$. At the same time, although the plastic deformation ability of Co can still relieve stress during thermal fatigue, the excessive Co content reduces the bonding strength of the WC-Co interface (from $300 \text{ MPa} \pm 30 \text{ MPa}$ to $250 \text{ MPa} \pm 30 \text{ MPa}$), and the crack is more likely to extend along the interface, and the crack length increases from $0.05 \text{ mm} \pm 0.01 \text{ mm}$ to $0.07 \text{ mm} \pm 0.01 \text{ mm}$. Optimization of Co content requires a balance between thermal fatigue resistance and creep resistance.

(3) Effect of Cr_3C_2 addition

Adding Cr_3C_2 is an effective means to improve thermal fatigue and creep resistance. When the Cr_3C_2 content is $0.5\% \pm 0.01\%$, Cr dissolves in the Co phase at high temperature and forms a Cr_2O_3 layer (thickness $0.2 \mu\text{m} \pm 0.05 \mu\text{m}$), which significantly improves the grain boundary strength (from $180 \text{ MPa} \pm 20 \text{ MPa}$ to $> 200 \text{ MPa} \pm 20 \text{ MPa}$), and the thermal fatigue crack length is reduced by about $40\% \pm 5\%$, from $0.05 \text{ mm} \pm 0.01 \text{ mm}$ to $0.03 \text{ mm} \pm 0.01 \text{ mm}$, and the crack growth rate is reduced from $2 \times 10^{-7} \text{ mm/cycle} \pm 10^{-8} \text{ mm/cycle}$ to $1.2 \times 10^{-7} \text{ mm/cycle} \pm 10^{-8} \text{ mm/cycle}$. Cr_3C_2 also inhibits the slip of Co phase through grain boundary pinning, and the creep strain rate is reduced by about $40\% \pm 5\%$, from $10^{-6} \text{ s}^{-1} \pm 10^{-7} \text{ s}^{-1}$ to $6 \times 10^{-7} \text{ s}^{-1} \pm 10^{-7} \text{ s}^{-1}$. However, when the Cr_3C_2 content exceeds $1\% \pm 0.01\%$, the proportion of brittle phases (such as η phase, WC-Co-Cr composite phase) increases by about $10\% \pm 2\%$, resulting in a decrease in fracture toughness (K_{IC}) by about $10\% \pm 2\%$, from $12 \text{ MPa} \cdot \text{m}^{1/2}$ to $20 \text{ MPa} \cdot \text{m}^{1/2} \pm 1 \text{ MPa} \cdot \text{m}^{1/2}$ down to $10.8 \text{ MPa} \cdot \text{m}^{1/2} \pm 1 \text{ MPa} \cdot \text{m}^{1/2}$. The presence of brittle phase makes it easier for cracks to propagate along the interface, weakening the thermal fatigue resistance. The amount of addition needs to be precisely controlled.

(4) Impact of temperature difference

Thermal cycle temperature difference (ΔT) is the main driving factor of thermal fatigue. When $\Delta T > 500^\circ\text{C} \pm 10^\circ\text{C}$, thermal stress ($\sigma = E \cdot \Delta\alpha \cdot \Delta T$) increases significantly, and the crack length increases by about $50\% \pm 5\%$, from $0.05 \text{ mm} \pm 0.01 \text{ mm}$ to $0.075 \text{ mm} \pm 0.01 \text{ mm}$. Taking $\Delta T 600^\circ\text{C} \pm 10^\circ\text{C}$ as an example, the thermal stress can reach $600 \text{ MPa} \pm 50 \text{ MPa}$, and the crack growth rate increases from $10^{-7} \text{ mm/cycle} \pm 10^{-8} \text{ mm/cycle}$ to $1.5 \times 10^{-7} \text{ mm/cycle} \pm 10^{-8} \text{ mm/cycle}$. On the contrary, when $\Delta T < 300^\circ\text{C} \pm 10^\circ\text{C}$, the thermal stress drops to $300 \text{ MPa} \pm 30 \text{ MPa}$, and the crack length is controlled at $< 0.03 \text{ mm} \pm 0.01 \text{ mm}$, indicating that the lower temperature difference significantly slows down the thermal fatigue failure. The temperature difference has little effect on creep, but if the high temperature stage ($> 1000^\circ\text{C} \pm$

COPYRIGHT AND LEGAL LIABILITY STATEMENT

10°C) lasts for a long time (> 5 minutes), it will aggravate Co softening and indirectly increase the creep strain rate by about 10% ± 2%.

(5) Influence of thermal conductivity

Thermal conductivity has an important influence on thermal fatigue performance by affecting the distribution of thermal stress. When the thermal conductivity is $> 80 \text{ W/m}\cdot\text{K} \pm 5 \text{ W/m}\cdot\text{K}$, the temperature gradient inside the material decreases ($\Delta T/\Delta x$ decreases by about 30% ± 5%), the thermal stress decreases from 600 MPa ± 50 MPa to 450 MPa ± 50 MPa, the crack growth rate decreases by about 20% ± 5%, and the crack length decreases from 0.05 mm ± 0.01 mm to 0.04 mm ± 0.01 mm. On the contrary, when the thermal conductivity is $< 50 \text{ W/m}\cdot\text{K} \pm 5 \text{ W/m}\cdot\text{K}$, the temperature gradient increases, the thermal stress concentration intensifies, and the crack length increases by about 20% ± 5%, reaching 0.06 mm ± 0.01 mm. The effect of thermal conductivity on creep is more indirect. High thermal conductivity helps to reduce the duration of local high temperature areas, reduce Co phase softening and grain boundary sliding, and reduce the creep strain rate by about 10% ± 2%.

(6) Analysis of coupling effect

The above factors jointly affect thermal fatigue and creep properties through complex coupling effects. For example, when high temperature difference ($\Delta T 600^\circ\text{C} \pm 10^\circ\text{C}$) is coupled with high Co content (12% ± 1%), thermal stress and Co softening work together, the crack length reaches 0.1 mm ± 0.01 mm, and the creep strain rate increases to $2 \times 10^{-6} \text{ s}^{-1} \pm 10^{-7} \text{ s}^{-1}$, far exceeding the influence of a single factor. When fine grains ($0.51 \mu\text{m} \pm 0.01 \mu\text{m}$) and Cr_3C_2 (0.5% ± 0.01%) work together, the grain boundary hindrance and strengthening effects are superimposed, the crack length is reduced to 0.03 mm ± 0.01 mm, and the creep strain rate is reduced to $6 \times 10^{-7} \text{ s}^{-1} \pm 10^{-7} \text{ s}^{-1}$, with significant performance improvement. When low thermal conductivity ($< 50 \text{ W/m}\cdot\text{K} \pm 5 \text{ W/m}\cdot\text{K}$) is coupled with large grains ($> 2 \mu\text{m} \pm 0.01 \mu\text{m}$), thermal stress and crack propagation paths are centralized, and the crack length increases to 0.08 mm ± 0.01 mm, indicating that the optimization of thermal conductivity and grain size needs to be carried out simultaneously.

(7) Comprehensive case analysis

Taking WC-12Co and WC-10Co ($\text{Cr}_3\text{C}_2 0.5\% \pm 0.01\%$) as examples, in the thermal shock test ($\Delta T 600^\circ\text{C} \pm 10^\circ\text{C}$, $1000^\circ\text{C} \pm 10^\circ\text{C}$ to $25^\circ\text{C} \pm 1^\circ\text{C}$, 500 times ± 50 times), the crack length of WC-12Co reached 0.1 mm ± 0.01 mm, and the crack growth rate was $2 \times 10^{-7} \text{ mm/cycle} \pm 10^{-8} \text{ mm/cycle}$, while that of WC-10Co ($\text{Cr}_3\text{C}_2 0.5\% \pm 0.01\%$) was only 0.03 mm ± 0.01 mm, and the crack growth rate dropped to $1.2 \times 10^{-7} \text{ mm/cycle} \pm 10^{-8} \text{ mm/cycle}$, thermal fatigue resistance is improved by about 70% ± 5%. In the creep test ($1000^\circ\text{C} \pm 10^\circ\text{C}$, 100 MPa ± 10 MPa, 100 hours), the strain rate of WC-12Co is $1.5 \times 10^{-6} \text{ s}^{-1} \pm 10^{-7} \text{ s}^{-1}$, while the optimized sample is reduced to $6 \times 10^{-7} \text{ s}^{-1} \pm 10^{-7} \text{ s}^{-1}$, and the creep resistance is improved by about 60% ± 5%. The thermal conductivity of the optimized sample is $85 \text{ W/m}\cdot\text{K} \pm 5 \text{ W/m}\cdot\text{K}$, and the grain size is $0.51 \mu\text{m} \pm 0.01 \mu\text{m}$. The addition of Cr_3C_2 significantly improves the performance.

(8) Application significance and optimization direction

COPYRIGHT AND LEGAL LIABILITY STATEMENT

The analysis of the coupling effect of thermal fatigue and creep shows that the optimization needs to comprehensively consider the grain size, Co content, Cr_3C_2 addition, temperature difference and thermal conductivity. Fine grains and appropriate amount of Cr_3C_2 are the key to improving thermal fatigue and creep resistance, while high thermal conductivity and low Co content help to further improve the performance. The optimized cemented carbide performs well in aviation turbine tools (life > 5000 hours \pm 500 hours) and high-temperature molds (service > 1.5×10^5 times \pm 10^4 times), and the crack length and creep strain rate meet the requirements of harsh working conditions.

The occurrence of thermal fatigue and creep is affected by the coupling of grain size, Co content, Cr_3C_2 addition, temperature difference and thermal conductivity. Fine grains ($0.51 \mu\text{m} \pm 0.01 \mu\text{m}$), appropriate amount of Co ($10\% \pm 1\%$), Cr_3C_2 ($0.5\% \pm 0.01\%$), low ΔT ($< 300^\circ\text{C} \pm 10^\circ\text{C}$) and high thermal conductivity ($> 80 \text{ W/m}\cdot\text{K} \pm 5 \text{ W/m}\cdot\text{K}$) are all helpful in reducing the crack growth rate and creep strain rate. Comprehensive cases show that after optimization, the crack length is reduced by $70\% \pm 5\%$ and the strain rate is reduced by $60\% \pm 5\%$, which provides scientific guidance for high temperature applications.

8.2.2.4 Thermal fatigue and creep optimization strategies for cemented carbide

$10^{-6} \text{ s}^{-1} \pm 10^{-7} \text{ s}^{-1}$ of cemented carbide in high temperature environment ($800\text{-}1000^\circ\text{C} \pm 10^\circ\text{C}$), it is necessary to systematically improve its thermal fatigue and creep resistance through comprehensive optimization of microstructure, additives, sintering process and surface treatment. These optimization measures are aimed at enhancing grain boundary strength, improving thermal conductivity, reducing porosity and surface defects, and verifying the performance improvement effect through scientific testing. Starting from the above key aspects, combined with fracture mechanics, thermodynamic data and engineering cases, the following details the optimization strategy and its role in controlling thermal fatigue and creep behavior.

(1) Microstructure optimization

Microstructure control is the basis for improving thermal fatigue and creep resistance. The recommended WC grain size is $0.51 \mu\text{m} \pm 0.01 \mu\text{m}$, and the Co content is controlled at $8\%\text{-}10\% \pm 1\%$. Fine grains effectively hinder the propagation of thermal fatigue cracks by increasing the grain boundary density (grain boundary area $> 10^4 \text{ mm}^2/\text{cm}^3 \pm 10^3 \text{ mm}^2/\text{cm}^3$), the crack deflection angle reaches $30^\circ \pm 5^\circ$, the crack path is extended, and the crack growth rate (da/dN) is reduced from $2 \times 10^{-7} \text{ mm/cycle} \pm 10^{-8} \text{ mm/cycle}$ to $< 10^{-7} \text{ mm/cycle} \pm 10^{-8} \text{ mm/cycle}$. Low Co content ($8\%\text{-}10\% \pm 1\%$) reduces high temperature softening (hardness drops from $\text{HV } 600 \pm 30$ to $\text{HV } 250 \pm 30$), inhibits grain boundary sliding, and reduces creep strain rate from $1.5 \times 10^{-6} \text{ s}^{-1} \pm 10^{-7} \text{ s}^{-1}$ to $< 10^{-6} \text{ s}^{-1} \pm 10^{-7} \text{ s}^{-1}$. At the same time, the optimized microstructure improves thermal conductivity (target $> 80 \text{ W/m}\cdot\text{K} \pm 5 \text{ W/m}\cdot\text{K}$), from $70 \text{ W/m}\cdot\text{K} \pm 5 \text{ W/m}\cdot\text{K}$ to $85 \text{ W/m}\cdot\text{K} \pm 5 \text{ W/m}\cdot\text{K}$, reduces thermal stress concentration (from $600 \text{ MPa} \pm 50 \text{ MPa}$ to $450 \text{ MPa} \pm 50 \text{ MPa}$), and further reduces thermal fatigue crack length.

(2) Additive optimization

COPYRIGHT AND LEGAL LIABILITY STATEMENT

Adding chromium carbide (Cr_3C_2) is a key means to enhance thermal fatigue and creep resistance. The recommended addition amount is $0.5\% \pm 0.01\%$. Cr_3C_2 dissolves in the Co phase at high temperature and forms a Cr_2O_3 layer (thickness $0.2 \mu\text{m} \pm 0.05 \mu\text{m}$), which significantly increases the grain boundary strength (from $180 \text{ MPa} \pm 20 \text{ MPa}$ to $> 200 \text{ MPa} \pm 20 \text{ MPa}$). The enhanced grain boundary strength suppressed the thermal fatigue crack propagation through pinning effect, and the crack length was reduced by about $40\% \pm 5\%$ from $0.05 \text{ mm} \pm 0.01 \text{ mm}$ to $0.03 \text{ mm} \pm 0.01 \text{ mm}$, and the crack growth rate was reduced from $2 \times 10^{-7} \text{ mm/cycle} \pm 10^{-8} \text{ mm/cycle}$ to $1.2 \times 10^{-7} \text{ mm/cycle} \pm 10^{-8} \text{ mm/cycle}$. Cr_3C_2 also reduces the creep activation energy (from $300 \text{ kJ/mol} \pm 10 \text{ kJ/mol}$ to $250 \text{ kJ/mol} \pm 10 \text{ kJ/mol}$), and reduces the creep strain rate by about $40\% \pm 5\%$, from $10^{-6} \text{ s}^{-1} \pm 10^{-7} \text{ s}^{-1}$ to $6 \times 10^{-7} \text{ s}^{-1} \pm 10^{-7} \text{ s}^{-1}$, by inhibiting Co phase slip and grain boundary diffusion. Energy dispersive spectroscopy (EDS) shows that the Cr content at the grain boundary is about $5\% \pm 0.5\%$, verifying its strengthening effect.

(3) Sintering process optimization

The optimization of sintering process directly affects the compactness and creep resistance of cemented carbide. The recommended sintering temperature is $1450^\circ\text{C} \pm 10^\circ\text{C}$, and vacuum or inert atmosphere (such as Ar) is used to reduce oxidation, ensuring that the material density reaches $99.5\% \pm 0.1\%$ and the porosity is controlled below $0.1\% \pm 0.02\%$. The high-density structure reduces internal pores and microcracks, limits thermal stress concentration and oxygen diffusion paths, and reduces the thermal fatigue crack length from $0.06 \text{ mm} \pm 0.01 \text{ mm}$ to $0.04 \text{ mm} \pm 0.01 \text{ mm}$. Low porosity ($< 0.1\% \pm 0.02\%$) also enhances the grain boundary bonding strength ($> 200 \text{ MPa} \pm 20 \text{ MPa}$), reducing the occurrence of grain boundary sliding during creep, and reducing the strain rate from $1.2 \times 10^{-6} \text{ s}^{-1} \pm 10^{-7} \text{ s}^{-1}$ to $< 10^{-6} \text{ s}^{-1} \pm 10^{-7} \text{ s}^{-1}$. Precise control of the sintering temperature ($1450^\circ\text{C} \pm 10^\circ\text{C}$) ensures a uniform distribution of Co (deviation $< 0.1\% \pm 0.02\%$), avoiding preferential failure in local softening areas.

(4) Surface treatment optimization

Optimization of surface condition is an important means to reduce thermal fatigue cracks and improve creep resistance. It is recommended to control the surface roughness (R_a) below $0.05 \mu\text{m} \pm 0.01 \mu\text{m}$ by precision mechanical polishing. This process can reduce the incidence of thermal fatigue cracks by about $20\% \pm 5\%$, and the crack length from $0.05 \text{ mm} \pm 0.01 \text{ mm}$ to $0.04 \text{ mm} \pm 0.01 \text{ mm}$. Low roughness reduces surface defects (such as micro scratches and pits), limits thermal stress concentration and crack initiation points, and reduces secondary cracks induced by oxide layer spalling. After polishing, ultrasonic cleaning ($40 \text{ kHz} \pm 1 \text{ kHz}$) can be used to remove surface contaminants ($< 0.1\% \pm 0.02\%$), further improve surface integrity, and reduce the formation of surface slip bands during creep (width from $0.6 \mu\text{m} \pm 0.1 \mu\text{m}$ to $0.4 \mu\text{m} \pm 0.1 \mu\text{m}$).

(5) Test specifications

To accurately evaluate the optimization effect of thermal fatigue and creep properties, it is recommended to use the ASTM E1876 standard for thermal shock testing, simulating thermal cycles from $1000^\circ\text{C} \pm 10^\circ\text{C}$ to $25^\circ\text{C} \pm 1^\circ\text{C}$, with a cycle number of $> 500 \pm 50$ times, and the crack length is measured by optical microscopy (magnification $200\times$) and SEM (resolution $< 0.1 \mu\text{m} \pm$

COPYRIGHT AND LEGAL LIABILITY STATEMENT

0.01 μm), with a target of $< 0.05 \text{ mm} \pm 0.01 \text{ mm}$. Creep testing is carried out at $1000^\circ\text{C} \pm 10^\circ\text{C}$ and a constant stress of $100 \text{ MPa} \pm 10 \text{ MPa}$, using a high temperature creep tester (strain measurement accuracy $\pm 0.001\%$), and recording the steady-state strain rate, with a target of $< 10^{-6} \text{ s}^{-1} \pm 10^{-7} \text{ s}^{-1}$. After the test, the formation of the Cr_2O_3 layer (Cr 3p peak $577 \text{ eV} \pm 0.1 \text{ eV}$) can be analyzed by X-ray photoelectron spectroscopy (XPS) to verify the grain boundary strengthening effect. These specifications ensure the scientificity and repeatability of performance evaluation.

(6) Comprehensive case analysis

Taking the WC-10Co ($\text{Cr}_3\text{C}_2 0.5\% \pm 0.01\%$) sample as an example, in the ASTM E1876 thermal shock test ($1000^\circ\text{C} \pm 10^\circ\text{C}$ to $25^\circ\text{C} \pm 1^\circ\text{C}$, 500 times ± 50 times), the crack length was only $0.03 \text{ mm} \pm 0.01 \text{ mm}$, and the crack growth rate was $< 10^{-7} \text{ mm/cycle} \pm 10^{-8} \text{ mm/cycle}$, which was $40\% \pm 5\%$ lower than the unoptimized $0.05 \text{ mm} \pm 0.01 \text{ mm}$. In the creep test ($1000^\circ\text{C} \pm 10^\circ\text{C}$, $100 \text{ MPa} \pm 10 \text{ MPa}$, 100 hours), the strain rate was $6 \times 10^{-7} \text{ s}^{-1} \pm 10^{-7} \text{ s}^{-1}$, which was lower than the unoptimized $10^{-6} \text{ s}^{-1} \pm 10^{-7} \text{ s}^{-1}$, and the creep resistance was improved by about $40\% \pm 5\%$. SEM observation showed that the crack deflection angle of the optimized sample was $30^\circ \pm 5^\circ$ and the slip band width was $0.3 \mu\text{m} \pm 0.1 \mu\text{m}$, indicating the synergistic effect of microstructure and grain boundary strengthening. This performance meets the requirements of aviation turbine blade machining tools (lifetime $> 5000 \text{ hours} \pm 500 \text{ hours}$) and high temperature molds (service $> 1.5 \times 10^5 \text{ times} \pm 10^4 \text{ times}$).

(7) Dynamic performance and application significance

Dynamic testing shows that thermal fatigue crack growth stabilizes after 500 ± 50 cycles, and the crack length slowly increases from $0.03 \text{ mm} \pm 0.01 \text{ mm}$ to $0.035 \text{ mm} \pm 0.01 \text{ mm}$, indicating that the optimized material has good cyclic stability. The creep strain enters the steady-state stage after 100 hours, and the strain rate remains $< 10^{-6} \text{ s}^{-1} \pm 10^{-7} \text{ s}^{-1}$, verifying its long-term load capacity. The optimized cemented carbide performs well in aviation tools (cutting temperature $900\text{-}1000^\circ\text{C}$, life $> 5000 \text{ hours} \pm 500 \text{ hours}$), high-temperature molds (molding temperature $800\text{-}900^\circ\text{C}$, cycles $> 10^5 \text{ times} \pm 10^4 \text{ times}$) and gas turbine components (service temperature $950^\circ\text{C} \pm 10^\circ\text{C}$, life $> 10^4 \text{ hours} \pm 10^3 \text{ hours}$), with service life increased by $50\%\text{-}70\% \pm 5\%$ and annual maintenance costs reduced by about $35\% \pm 5\%$.

(8) Environmental adaptability and future prospects

The optimization strategy is still effective in high temperature difference ($\Delta T 600^\circ\text{C} \pm 10^\circ\text{C}$) and water vapor environment (humidity $> 50\% \pm 5\%$), with crack length and strain rate maintained at $< 0.04 \text{ mm} \pm 0.01 \text{ mm}$ and $< 8 \times 10^{-7} \text{ s}^{-1} \pm 10^{-7} \text{ s}^{-1}$ respectively, which is suitable for wet and hot conditions (such as tropical aviation engines). At higher temperatures ($> 1100^\circ\text{C} \pm 10^\circ\text{C}$) or sulfur (SO_2) atmospheres, multilayer coatings (such as $\text{Al}_2\text{O}_3 / \text{TiN}$, thickness $5\text{-}10 \mu\text{m} \pm 0.1 \mu\text{m}$) or new additives (such as TaC) can be combined to further improve thermal conductivity and grain boundary strength to meet the needs of next-generation high-temperature devices.

The optimization of thermal fatigue and creep of cemented carbide needs to be achieved through microstructure control (WC grain $0.51 \mu\text{m} \pm 0.01 \mu\text{m}$, Co $8\%\text{-}10\% \pm 1\%$, thermal conductivity $>$

COPYRIGHT AND LEGAL LIABILITY STATEMENT

80 W/ m·K \pm 5 W/ m·K), Cr₃C₂ addition (0.5% \pm 0.01%, grain boundary strength > 200 MPa \pm 20 MPa), sintering process (1450°C \pm 10°C, density > 99.5% \pm 0.1%) and surface treatment (Ra < 0.05 μ m \pm 0.01 μ m , crack reduction 20% \pm 5%). After optimization, the crack length is reduced to 0.03 mm \pm 0.01 mm, and the strain rate is < 10⁻⁶ s⁻¹ \pm 10⁻⁷ s⁻¹ , meeting the high temperature requirements of aviation and molds.

8.2.2.5 Engineering Application of Thermal Fatigue and Creep Performance Optimization of Cemented Carbide

The optimized cemented carbide exhibits excellent thermal fatigue and creep performance in high-temperature cyclic environments (800-1000°C \pm 10°C). Through microstructure regulation, additive optimization, sintering process improvement and surface treatment, its engineering application reliability in the fields of aviation, mold manufacturing and energy equipment has been significantly improved. These optimization measures reduce the crack growth rate, suppress the creep strain rate, and extend the service life, providing an efficient and durable solution for high-temperature conditions. The following is a detailed discussion of the engineering application and performance advantages of the optimized cemented carbide from the three major application areas of aviation turbine blades, high-temperature molds and gas turbine nozzles, combined with experimental data, microscopic analysis and actual cases.

(1) Cemented carbide aviation turbine blades

Aviation turbine blades are subject to repeated thermal stress (e.g. 1000°C \pm 10°C to 25°C \pm 1°C) and cutting loads in high temperature cycles (Δ T 500°C \pm 10°C), which places extremely high demands on thermal fatigue resistance and service life. The optimized WC-10Co cemented carbide (Cr₃C₂ addition 0.5% \pm 0.01%, grain size 0.5 μ m \pm 0.01 μ m) has a thermal fatigue crack length of only 0.03 mm \pm 0.01 mm and a crack growth rate of < 10⁻⁷ mm/cycle \pm 10⁻⁸ mm/cycle in the ASTM E1876 thermal shock test (Δ T 500°C \pm 10°C, 500 times \pm 50 times) , which is better than the unoptimized 0.05 mm \pm 0.01 mm (growth rate 2 \times 10⁻⁷ mm/cycle \pm 10⁻⁸ mm/cycle). Fine grains hinder crack deflection (deflection angle 30° \pm 5°) by increasing grain boundary density (> 10⁴ mm²/cm³ \pm 10³ mm²/cm³), and the Cr₂O₃ layer (thickness 0.2 μ m \pm 0.05 μ m) enhances grain boundary strength (> 200 MPa \pm 20 MPa), effectively alleviating thermal stress concentration (from 600 MPa \pm 50 MPa to 450 MPa \pm 50 MPa). In practical applications, the cutting life of turbine blades made of this material exceeds 5000 hours \pm 500 hours, which is about 67% \pm 5% higher than the unoptimized 3000 hours \pm 300 hours. In aircraft engines, optimizing the thermal fatigue resistance of blades reduces the failure rate caused by thermal cracks by about 40% \pm 5%, improving flight safety.

(2) Hard alloy high temperature mold

High temperature molds (such as hot forging molds and die casting molds) need to withstand repeated thermal cycles and continuous loads under working conditions of 1000°C \pm 10°C, and have extremely high requirements for creep resistance and service life. In the creep test of optimized WC-8Co cemented carbide (thermal conductivity > 80 W/ m·K \pm 5 W/ m·K) at 1000°C \pm 10°C and 100

COPYRIGHT AND LEGAL LIABILITY STATEMENT

MPa \pm 10 MPa, the strain rate is controlled at $< 10^{-6} \text{ s}^{-1} \pm 10^{-7} \text{ s}^{-1}$, which is lower than the unoptimized $1.5 \times 10^{-6} \text{ s}^{-1} \pm 10^{-7} \text{ s}^{-1}$. High thermal conductivity (increased from $70 \text{ W/m}\cdot\text{K} \pm 5 \text{ W/m}\cdot\text{K}$ to $85 \text{ W/m}\cdot\text{K} \pm 5 \text{ W/m}\cdot\text{K}$) reduces the temperature gradient ($\Delta T/\Delta x$ decreases by about $30\% \pm 5\%$), thermal stress decreases from $550 \text{ MPa} \pm 50 \text{ MPa}$ to $400 \text{ MPa} \pm 50 \text{ MPa}$, and reduces creep strain accumulation. Low Co content ($8\% \pm 1\%$) and optimized sintering (density $> 99.5\% \pm 0.1\%$) further inhibit Co softening (hardness remains $> \text{HV } 1300 \pm 30$), and the slip band width decreases from $0.6 \mu\text{m} \pm 0.1 \mu\text{m}$ to $0.3 \mu\text{m} \pm 0.1 \mu\text{m}$. In practical applications, the service cycle of high-temperature molds made of this material exceeds 10^5 times $\pm 10^4$ times, which is about $50\% \pm 5\%$ higher than the unoptimized 6×10^4 times $\pm 10^4$ times. In hot forging of automotive parts, optimizing the creep resistance of dies extends the service life by about $50\% \pm 5\%$, reducing replacement frequency and production downtime.

(3) Hard alloy gas turbine nozzle

Gas turbine nozzles are subject to thermal fatigue and long-term loads in a high-temperature oxidizing environment at $900^\circ\text{C} \pm 10^\circ\text{C}$, which places extremely high demands on crack growth control and service life. In the thermal shock test at $900^\circ\text{C} \pm 10^\circ\text{C}$ (ΔT $400^\circ\text{C} \pm 10^\circ\text{C}$, 500 times ± 50 times), the optimized WC - 10Co cemented carbide (added with Cr_3C_2 $0.5\% \pm 0.01\%$) has a thermal fatigue crack length of $< 0.04 \text{ mm} \pm 0.01 \text{ mm}$ and a crack growth rate of $< 1.5 \times 10^{-7} \text{ mm/cycle} \pm 10^{-8} \text{ mm/cycle}$, which is better than the unoptimized $0.06 \text{ mm} \pm 0.01 \text{ mm}$ (growth rate $2.5 \times 10^{-7} \text{ mm/cycle} \pm 10^{-8} \text{ mm/cycle}$). The Cr_2O_3 layer (Cr content of about $5\% \pm 0.5\%$) and fine grains ($0.5 \mu\text{m} \pm 0.01 \mu\text{m}$) work together to enhance the grain boundary strength ($> 200 \text{ MPa} \pm 20 \text{ MPa}$) and suppress the thermal stress concentration (from $500 \text{ MPa} \pm 50 \text{ MPa}$ to $350 \text{ MPa} \pm 50 \text{ MPa}$). In the creep test ($900^\circ\text{C} \pm 10^\circ\text{C}$, $100 \text{ MPa} \pm 10 \text{ MPa}$, 100 hours), the strain rate is $< 8 \times 10^{-7} \text{ s}^{-1} \pm 10^{-7} \text{ s}^{-1}$, which is lower than the unoptimized $1.2 \times 10^{-6} \text{ s}^{-1} \pm 10^{-7} \text{ s}^{-1}$. In practical applications, the service life of nozzles made of this material exceeds 10^4 hours $\pm 10^3$ hours, meeting the long-term operation requirements of energy equipment (such as industrial gas turbines), which is better than the unoptimized 6×10^3 hours $\pm 10^3$ hours. In power plants, the optimized thermal fatigue resistance of the nozzles reduces the failure rate caused by thermal cracks by about $45\% \pm 5\%$, improving the operating efficiency of the equipment.

(4) Engineering value of optimizing performance

The above cases show that the optimization of thermal fatigue and creep properties significantly improves the reliability of cemented carbide in high temperature cycling environments. Through microstructure optimization (WC grain $0.5 \mu\text{m} \pm 0.01 \mu\text{m}$, Co $8\%-10\% \pm 1\%$, thermal conductivity $> 80 \text{ W/m}\cdot\text{K} \pm 5 \text{ W/m}\cdot\text{K}$), Cr_3C_2 addition ($0.5\% \pm 0.01\%$, grain boundary strength $> 200 \text{ MPa} \pm 20 \text{ MPa}$), sintering process ($1450^\circ\text{C} \pm 10^\circ\text{C}$, density $> 99.5\% \pm 0.1\%$) and surface treatment ($\text{Ra} < 0.05 \mu\text{m} \pm 0.01 \mu\text{m}$), the thermal fatigue crack length of cemented carbide decreased from $0.05\text{-}0.1 \text{ mm} \pm 0.01 \text{ mm}$ to $0.03\text{-}0.04 \text{ mm} \pm 0.01 \text{ mm}$, and the creep strain rate decreased from $1.2\text{-}1.5 \times 10^{-6} \text{ s}^{-1} \pm 10^{-7} \text{ s}^{-1}$ to $< 10^{-6} \text{ s}^{-1} \pm 10^{-7} \text{ s}^{-1}$. This performance improvement extends service life (e.g. aviation turbine blades > 5000 hours ± 500 hours, high temperature molds $> 10^5$ times $\pm 10^4$ times, gas turbine nozzles $> 10^4$ hours $\pm 10^3$ hours) by $50\%\text{-}67\% \pm 5\%$ and reduces maintenance costs. For example, the annual maintenance cost of aviation turbine blades is reduced by about $35\% \pm 5\%$,

COPYRIGHT AND LEGAL LIABILITY STATEMENT

the replacement cycle of high temperature molds is extended by $50\% \pm 5\%$, and the operating efficiency of gas turbine nozzles is improved by about $20\% \pm 3\%$.

(5) Environmental adaptability and application expansion

The optimized cemented carbide has strong environmental adaptability, enabling it to cope with more complex thermal cycle conditions. For example, in a high-temperature environment containing water vapor (humidity $> 50\% \pm 5\%$, $\Delta T 500^{\circ}\text{C} \pm 10^{\circ}\text{C}$), the Cr_2O_3 layer still controls the crack length to $< 0.05 \text{ mm} \pm 0.01 \text{ mm}$ and the strain rate to $< 10^{-6} \text{ s}^{-1} \pm 10^{-7} \text{ s}^{-1}$, which is suitable for wet and hot aviation engine environments. In a sulfur-containing (SO_2) atmosphere or at a higher temperature difference ($\Delta T 600^{\circ}\text{C} \pm 10^{\circ}\text{C}$), the thermal fatigue crack length of the optimized sample increases to $0.04 \text{ mm} \pm 0.01 \text{ mm}$, but can be further reduced to $0.03 \text{ mm} \pm 0.01 \text{ mm}$ through multilayer coatings (such as $\text{Al}_2\text{O}_3 / \text{TiN}$, thickness $5\text{-}10 \mu\text{m} \pm 0.1 \mu\text{m}$), expanding its application potential in sulfur-containing energy devices and extreme thermal cycles. In addition, in an ultra-high temperature environment of $1100^{\circ}\text{C} \pm 10^{\circ}\text{C}$, combined with new additives (such as TaC), the strain rate can be controlled to $8 \times 10^{-7} \text{ s}^{-1} \pm 10^{-7} \text{ s}^{-1}$, meeting the needs of next-generation aerospace.

(6) Comprehensive cases and future prospects

Taking WC-10Co ($\text{Cr}_3\text{C}_2 0.5\% \pm 0.01\%$, thermal conductivity $> 80 \text{ W/m}\cdot\text{K} \pm 5 \text{ W/m}\cdot\text{K}$) as an example, after 500 ± 50 thermal shocks at $\Delta T 500^{\circ}\text{C} \pm 10^{\circ}\text{C}$, the crack length is $0.03 \text{ mm} \pm 0.01 \text{ mm}$; after 100 hours of creep at $1000^{\circ}\text{C} \pm 10^{\circ}\text{C}$ and $100 \text{ MPa} \pm 10 \text{ MPa}$, the strain rate is $6 \times 10^{-7} \text{ s}^{-1} \pm 10^{-7} \text{ s}^{-1}$; in the thermal fatigue test at $900^{\circ}\text{C} \pm 10^{\circ}\text{C}$, the crack length is $< 0.04 \text{ mm} \pm 0.01 \text{ mm}$. These data show that the optimized cemented carbide exhibits excellent thermal fatigue and creep resistance in aviation turbine blades, high-temperature molds, and gas turbine nozzles, with service life increased by $67\% \pm 5\%$, $50\% \pm 5\%$, and $67\% \pm 5\%$, respectively. In the future, the performance of the optimized cemented carbide in ultra-high temperature ($> 1100^{\circ}\text{C} \pm 10^{\circ}\text{C}$) or high cycle number ($> 10^6$ times $\pm 10^4$ times) environments can be further enhanced by developing functional gradient materials or introducing nano-coatings (such as ZrO_2 , thickness $5\text{-}15 \mu\text{m} \pm 0.1 \mu\text{m}$) to meet more demanding engineering needs.

(7) Dynamic performance and economic benefits

Dynamic testing shows that thermal fatigue crack extension stabilizes after 500 ± 50 times, and the crack length increases from $0.03 \text{ mm} \pm 0.01 \text{ mm}$ to $0.035 \text{ mm} \pm 0.01 \text{ mm}$, indicating that the optimized material has good cyclic durability. The creep strain enters the steady-state stage after 100 hours, and the strain rate remains $< 10^{-6} \text{ s}^{-1} \pm 10^{-7} \text{ s}^{-1}$, verifying its long-term load capacity. This performance improvement not only extends the life of the equipment, but also significantly reduces operating costs. For example, the annual maintenance cost of aviation turbine blades is reduced by about $35\% \pm 5\%$, the replacement cycle of high-temperature molds is extended by $50\% \pm 5\%$, and the operating efficiency of gas turbine nozzles is increased by about $20\% \pm 3\%$, reflecting the economic value of optimization.

Optimized cemented carbide performs well in high-temperature cyclic environments. WC-10Co and

COPYRIGHT AND LEGAL LIABILITY STATEMENT

WC-8Co formulations have better thermal fatigue crack length ($0.03-0.04 \text{ mm} \pm 0.01 \text{ mm}$), creep strain rate ($< 10^{-6} \text{ s}^{-1} \pm 10^{-7} \text{ s}^{-1}$) and service life ($> 5000 \text{ hours} \pm 500 \text{ hours}$, $> 10^5 \text{ times} \pm 10^4 \text{ times}$, $> 10^4 \text{ hours} \pm 10^3 \text{ hours}$) than traditional materials in aviation turbine blades, high-temperature molds and gas turbine nozzles. These application cases fully prove that optimizing thermal fatigue and creep properties is a key strategy to improve the reliability and economic benefits of cemented carbide in high-temperature engineering applications.

8.3 Methods for optimizing the corrosion resistance and high temperature resistance of cemented carbide

Corrosion resistance (weight loss $< 0.08 \text{ mg/cm}^2 \pm 0.01 \text{ mg/cm}^2$) and high temperature resistance (hardness $> \text{HV } 1200 \pm 30$, $1000^\circ\text{C} \pm 10^\circ\text{C}$) are key to improving the application of cemented carbide in acidic, salt spray and high temperature environments (such as aviation and energy equipment). These performance improvements can be achieved through a variety of scientific methods, including (1) binder phase substitution, (2) additive introduction, (3) surface coating technology, and (4) process parameter optimization and (5) microstructure regulation, which work together to meet the needs of demanding working conditions. The traditional Co binder phase is prone to softening (hardness drops to $\text{HV } 200 \pm 30$) and oxidation (generating Co_3O_4) at high temperatures, resulting in corrosion and performance degradation. The optimization method replaces Co with a Ni-based binder phase ($\text{Ni } 8\%-12\% \pm 1\%$), which forms a NiO passivation layer (thickness $\sim 10 \text{ nm} \pm 1 \text{ nm}$), significantly reducing the corrosion current ($i_{\text{corr}} < 10^{-6} \text{ A/cm}^2 \pm 10^{-7} \text{ A/cm}^2$), enhancing corrosion resistance. Adding Cr_3C_2 ($0.5\% \pm 0.01\%$) inhibits oxidation by forming a dense Cr_2O_3 layer (thickness $\sim 0.2 \mu\text{m} \pm 0.05 \mu\text{m}$), and the weight gain is controlled to $< 0.3 \text{ mg/cm}^2 \pm 0.05 \text{ mg/cm}^2$. Surface coatings (such as TiN, Al_2O_3 , thickness $5-20 \mu\text{m} \pm 0.1 \mu\text{m}$) are isolated from oxygen and corrosive media by physical vapor deposition (PVD) or chemical vapor deposition (CVD) technology, further improving oxidation resistance and wear resistance. These optimization methods not only improve the corrosion resistance and high temperature stability of cemented carbide, but also significantly extend its service life in high temperature cycles and corrosive environments.

of Ni - based bonding phase, the antioxidant effect of Cr_3C_2 addition, surface coating protection, and the coordinated optimization of process and microstructure. Combining process parameters (sintering $1450^\circ\text{C} \pm 10^\circ\text{C}$, PVD $400^\circ\text{C} \pm 10^\circ\text{C}$), microscopic analysis (XPS, SEM) and engineering cases, the optimization path and its performance improvement mechanism are systematically discussed. For example, WC-10Ni loses only 0.05 mg/cm^2 in a 5% NaCl salt spray environment. $\pm 0.01 \text{ mg/cm}^2$, the corrosion resistance is improved by about $60\% \pm 5\%$ compared with traditional WC-10Co; the hardness of the tool with added Cr_3C_2 and coated with TiN is maintained at $> \text{HV } 1500 \pm 30$ at $1000^\circ\text{C} \pm 10^\circ\text{C}$, and the cutting life exceeds $5000 \text{ hours} \pm 500 \text{ hours}$, which is significantly better than the unoptimized $3000 \text{ hours} \pm 300 \text{ hours}$.

8.3.1 Corrosion resistance advantages of Ni-based bonding phase in cemented carbide

8.3.1.1 Principle and technical overview of the corrosion resistance advantages of Ni -based

COPYRIGHT AND LEGAL LIABILITY STATEMENT

cemented carbide bonding phase

The Ni-based bonding phase (Ni content $8\%-12\% \pm 1\%$) has excellent electrochemical stability and corrosion resistance, which significantly improves the corrosion resistance of cemented carbide in harsh environments such as acidic ($\text{pH} < 3 \pm 0.1$), salt spray ($\text{NaCl } 5\% \pm 0.1\%$) and marine environments, and has obvious advantages over the traditional Co-based bonding phase. The corrosion potential of Ni ($E_{\text{corr}} \sim 0.1 \text{ V} \pm 0.02 \text{ V vs. SCE}$) is higher than that of Co ($E_{\text{corr}} \sim -0.3 \text{ V} \pm 0.02 \text{ V vs. SCE}$), and the corrosion current density (i_{corr}) is significantly reduced to $< 10^{-6} \text{ A/cm}^2 \pm 10^{-7} \text{ A/cm}^2$, which is better than the Co-based $10^{-5} \text{ A/cm}^2 \pm 10^{-6} \text{ A/cm}^2$. This performance difference is due to the formation of a dense NiO passivation layer (thickness $\sim 10 \text{ nm} \pm 1 \text{ nm}$, density $\sim 6.7 \text{ g/cm}^3$) in a corrosive environment ($\pm 0.1 \text{ g/cm}^3$), this layer effectively isolates corrosive media (such as Cl^- , H^+) through chemical inertness and blocks electrochemical reactions (reaction formula: $\text{Ni} + 1/2\text{O}_2 \rightarrow \text{NiO}$, $\Delta G < 0 \text{ kJ/mol} \pm 10 \text{ kJ/mol}$). In contrast, the Co-based bonding phase easily generates loose Co_3O_4 (density $\sim 6.1 \text{ g/cm}^3$, thickness $> 0.5 \mu\text{m} \pm 0.1 \mu\text{m}$) under similar conditions, and its low protection leads to an increase in corrosion rate by about 10 times. While maintaining high hardness ($\text{HV } 1800 \pm 30$) and toughness ($K_{\text{IC}} \sim 12 \text{ MPa} \cdot \text{m}^{1/2} \pm 0.5 \text{ MPa} \cdot \text{m}^{1/2}$), Ni-based WC cemented carbide has improved corrosion resistance by about $60\% \pm 5\%$, making it particularly suitable for fields requiring high corrosion resistance and mechanical properties, such as offshore drilling components, chemical pipelines, and papermaking equipment. In addition, Ni has a higher melting point ($1455^\circ\text{C} \pm 10^\circ\text{C}$) than Co ($1495^\circ\text{C} \pm 10^\circ\text{C}$), and its softening degree is lower at a high temperature of $1000^\circ\text{C} \pm 10^\circ\text{C}$ (hardness reduction $< 10\% \pm 2\%$), further supporting its potential for application in high-temperature corrosive environments.

8.3.1.2 Analysis of corrosion resistance mechanism of Ni-based bonding phase in cemented carbide

The corrosion resistance advantage of Ni-based bonding phase comes from its unique electrochemical and physical properties. In acidic media (such as $0.1 \text{ M H}_2\text{SO}_4$, $\text{pH } 1 \pm 0.1$), Ni forms a NiO layer through a self-passivation mechanism. This layer has low solubility ($K_{\text{sp}} \sim 10^{-15} \pm 10^{-16}$) and high conductivity ($\sigma \sim 10^{-4} \text{ S/cm} \pm 10^{-5} \text{ S/cm}$), which effectively inhibits the diffusion of H^+ and Cl^- , and the corrosion current is reduced from $10^{-5} \text{ A/cm}^2 \pm 10^{-6} \text{ A/cm}^2$ of Co-based to $< 10^{-6} \text{ A/cm}^2 \pm 10^{-7} \text{ A/cm}^2$. X-ray photoelectron spectroscopy (XPS) analysis shows that the Ni 2p peak (about $854 \text{ eV} \pm 0.1 \text{ eV}$) indicates the presence of NiO, and its binding energy matches the O 1s peak ($530 \text{ eV} \pm 0.1 \text{ eV}$), verifying the chemical composition of the passivation layer. In a salt spray environment ($\text{NaCl } 5\% \pm 0.1\%$, ISO 9227 NSS 2000 h $\pm 100 \text{ h}$), the NiO layer thickness is stable at $10 \text{ nm} \pm 1 \text{ nm}$, and the weight loss rate is only $0.05 \text{ mg/cm}^2 \pm 0.01 \text{ mg/cm}^2$, compared to $0.12 \text{ mg/cm}^2 \pm 0.01 \text{ mg/cm}^2$ for Co-based, which is a decrease of about $58\% \pm 5\%$. In addition, the thermal expansion coefficient of the Ni-based bonding phase ($13 \times 10^{-6} \text{ K}^{-1}$) matches WC ($5.2 \times 10^{-6} \text{ K}^{-1}$) better than that of Co ($13 \times 10^{-6} \text{ K}^{-1}$), which reduces the microcracks caused by thermal cycling ($\Delta T \text{ } 500^\circ\text{C} \pm 10^\circ\text{C}$) and indirectly improves the corrosion resistance stability.

COPYRIGHT AND LEGAL LIABILITY STATEMENT

8.3.1.3 Microscopic analysis and verification of corrosion resistance of Ni-based bonding phase in cemented carbide

Scanning electron microscopy (SEM, resolution $< 0.1 \mu\text{m} \pm 0.01 \mu\text{m}$) observations showed that the NiO layer of Ni-based WC was evenly distributed on the surface, with a stable thickness of $10 \text{ nm} \pm 1 \text{ nm}$, and no obvious peeling or cracking was observed, while the surface of Co-based WC showed a loose Co_3O_4 layer (thickness $> 0.5 \mu\text{m} \pm 0.1 \mu\text{m}$) accompanied by microcracks (width $\sim 0.2 \mu\text{m} \pm 0.01 \mu\text{m}$). X-ray diffraction (XRD) analysis confirmed the crystal structure of NiO (face-centered cubic, $a = 4.17 \text{ \AA} \pm 0.01 \text{ \AA}$), and its peak intensity ($2\theta \approx 37.2^\circ, 43.3^\circ$) indicates high crystallinity, which enhances the protectiveness of the passivation layer. Energy dispersive spectroscopy (EDS) shows that the content of Ni at the grain boundary is about $8\%-10\% \pm 0.5\%$, which is evenly distributed, verifying its good interface bonding with WC.

8.3.1.4 Analysis of factors affecting corrosion resistance of Ni-based bonding phase in cemented carbide

The corrosion resistance of the Ni-based binder phase is affected by many factors and needs to be comprehensively optimized to achieve the best performance:

(1) Ni content

When the Ni content is $10\% \pm 1\%$, the corrosion current $i_{\text{corr}} < 10^{-6} \text{ A/cm}^2 \pm 10^{-7} \text{ A/cm}^2$ and the weight loss rate is controlled at $0.05 \text{ mg/cm}^2 \pm 0.01 \text{ mg/cm}^2$, and the hardness remains at $\text{HV } 1800 \pm 30$. However, when the Ni content exceeds $12\% \pm 1\%$, the increase in Ni phase leads to increased toughness (K_{IC} increases by $5\% \pm 1\%$), but the hardness decreases by about $10\% \pm 2\%$ (to $\text{HV } 1620 \pm 30$), and the corrosion current increases slightly to $2 \times 10^{-6} \text{ A/cm}^2 \pm 10^{-7} \text{ A/cm}^2$ due to the intensified softening of the Ni phase (hardness $\text{HV } 150 \pm 20$).

(2) Grain size

the WC grain size is $0.51 \mu\text{m} \pm 0.01 \mu\text{m}$, the grain boundary density is high ($> 10^4 \text{ mm}^2/\text{cm}^3 \pm 10^3 \text{ mm}^2/\text{cm}^3$), and the weight loss rate is low ($< 0.05 \text{ mg/cm}^2 \pm 0.01 \text{ mg/cm}^2$), because the fine grains reduce the penetration path of the corrosive medium. When the grain size increases to $2 \mu\text{m} \pm 0.01 \mu\text{m}$, the grain boundary density decreases and the weight loss rate increases by about $20\% \pm 5\%$ (to $0.06 \text{ mg/cm}^2 \pm 0.01 \text{ mg/cm}^2$), the pitting depth increased from $2 \mu\text{m} \pm 0.5 \mu\text{m}$ to $3.5 \mu\text{m} \pm 0.5 \mu\text{m}$.

(3) Sintering temperature

When sintered at $1450^\circ\text{C} \pm 10^\circ\text{C}$, the Ni distribution deviation is $< 0.1\% \pm 0.02\%$, the corrosion current i_{corr} remains $< 10^{-6} \text{ A/cm}^2 \pm 10^{-7} \text{ A/cm}^2$, and the weight loss rate is stable. If the sintering temperature is increased to $> 1500^\circ\text{C} \pm 10^\circ\text{C}$, Ni segregation occurs (deviation $> 0.5\% \pm 0.1\%$), and Ni enrichment at the grain boundaries causes the corrosion current to increase by $15\% \pm 3\%$ (to $1.15 \times 10^{-6} \text{ A/cm}^2 \pm 10^{-7} \text{ A/cm}^2$), and the weight loss rate increases to $0.07 \text{ mg/cm}^2 \pm 0.01 \text{ mg/cm}^2$.

COPYRIGHT AND LEGAL LIABILITY STATEMENT

(4) Environment

In a strong acid environment with $\text{pH} < 2 \pm 0.1$, the NiO layer partially dissolves, the corrosion current i_{corr} increases by about $30\% \pm 5\%$ (to $1.3 \times 10^{-6} \text{ A/cm}^2 \pm 10^{-7} \text{ A/cm}^2$), and the weight loss rate rises to $0.065 \text{ mg/cm}^2 \pm 0.01 \text{ mg/cm}^2$. In salt spray with NaCl concentration $> 5\% \pm 0.1\%$, the increase in Cl^- concentration induces pitting corrosion, and the pitting area increases by $20\% \pm 5\%$ (from $0.01 \text{ mm}^2 \pm 0.001 \text{ mm}^2$ increased to $0.012 \text{ mm}^2 \pm 0.001 \text{ mm}^2$), the weight loss rate increased to $0.06 \text{ mg/cm}^2 \pm 0.01 \text{ mg/cm}^2$.

(5) Surface roughness

When the surface roughness $R_a < 0.05 \mu\text{m} \pm 0.01 \mu\text{m}$, there are few surface defects, the corrosion current i_{corr} remains at a low level ($< 10^{-6} \text{ A/cm}^2 \pm 10^{-7} \text{ A/cm}^2$), and the weight loss rate is $< 0.05 \text{ mg/cm}^2 \pm 0.01 \text{ mg/cm}^2$. If $R_a > 0.1 \mu\text{m} \pm 0.01 \mu\text{m}$, microcracks and pits increase, corrosion current increases by $10\% \pm 2\%$ (to $1.1 \times 10^{-6} \text{ A/cm}^2 \pm 10^{-7} \text{ A/cm}^2$), and pitting depth increases to $4 \mu\text{m} \pm 0.5 \mu\text{m}$.

For example, a WC-12Ni sample has Ni segregation (deviation $0.6\% \pm 0.1\%$) due to the high sintering temperature ($1500^\circ\text{C} \pm 10^\circ\text{C}$), and the weight loss rate in a NaCl $5\% \pm 0.1\%$ salt spray environment is $0.07 \text{ mg/cm}^2 \pm 0.01 \text{ mg/cm}^2$, and the corrosion current i_{corr} is $1.2 \times 10^{-6} \text{ A/cm}^2 \pm 10^{-7} \text{ A/cm}^2$. The weight loss rate of the optimized WC-10Ni (sintered at $1450^\circ\text{C} \pm 10^\circ\text{C}$, $R_a < 0.05 \mu\text{m} \pm 0.01 \mu\text{m}$) is only $0.05 \text{ mg/cm}^2 \pm 0.01 \text{ mg/cm}^2$, $i_{\text{corr}} < 10^{-6} \text{ A/cm}^2 \pm 10^{-7} \text{ A/cm}^2$, corrosion resistance improved by about $29\% \pm 5\%$.

8.3.1.5 Optimization of Ni- based binder phase preparation process

To achieve a weight loss $< 0.05 \text{ mg/cm}^2 \pm 0.01 \text{ mg/cm}^2$ and corrosion current $i_{\text{corr}} < 10^{-6} \text{ A/cm}^2 \pm 10^{-7} \text{ A/cm}^2$. The preparation process of Ni-based WC cemented carbide needs to be precisely controlled to give full play to its corrosion resistance advantages. The recommended optimization strategies include the following aspects:

(1) Ingredient optimization

High-purity Ni powder (purity $> 99.9\% \pm 0.01\%$) and WC powder (particle size $0.51 \mu\text{m} \pm 0.01 \mu\text{m}$) are selected, and the Ni content is controlled at $8\%-10\% \pm 1\%$. This range balances corrosion resistance and mechanical properties. Too high Ni content ($> 12\% \pm 1\%$) will lead to an increase in Ni phase, a decrease in hardness of about $10\% \pm 2\%$ (to $\text{HV } 1620 \pm 30$), and an increase in toughness of $5\% \pm 1\%$ (K_{IC} increases to $12.6 \text{ MPa} \cdot \text{m}^{1/2} \pm 0.5 \text{ MPa} \cdot \text{m}^{1/2}$) but the corrosion current slightly increases (to $2 \times 10^{-6} \text{ A/cm}^2 \pm 10^{-7} \text{ A/cm}^2$); too low ($< 8\% \pm 1\%$) leads to insufficient hardness ($< \text{HV } 1600 \pm 30$) and decreased corrosion resistance ($i_{\text{corr}} > 2 \times 10^{-6} \text{ A/cm}^2 \pm 10^{-7} \text{ A/cm}^2$). Fine WC grains ($0.51 \mu\text{m} \pm 0.01 \mu\text{m}$) reduce the penetration of corrosive media by increasing the grain boundary density ($> 10^4 \text{ mm}^2/\text{cm}^3 \pm 10^3 \text{ mm}^2/\text{cm}^3$), and the weight loss rate is controlled at $< 0.05 \text{ mg/cm}^2 \pm 0.01 \text{ mg/cm}^2$.

(2) Ball milling process

COPYRIGHT AND LEGAL LIABILITY STATEMENT

Wet ball milling (medium is anhydrous ethanol, 40 hours \pm 1 hour, ball-to-material ratio 10:1 \pm 0.5) is used to ensure uniform mixing of powders, particle size distribution deviation $< 0.02 \mu\text{m} \pm 0.01 \mu\text{m}$, reduce micro defects (such as pores, agglomeration), provide a homogeneous matrix for subsequent sintering, and indirectly reduce corrosion sensitivity.

(3) Vacuum sintering

at $1450^{\circ}\text{C} \pm 10^{\circ}\text{C}$, pressure $< 10^{-3} \text{ Pa} \pm 10^{-4} \text{ Pa}$, holding time $1 \text{ h} \pm 0.1 \text{ h}$, density reached $99.5\% \pm 0.1\%$, porosity $< 0.1\% \pm 0.02\%$. This temperature ensures uniform Ni distribution (deviation $< 0.1\% \pm 0.02\%$), avoiding segregation ($> 0.5\% \pm 0.1\%$ at $> 1500^{\circ}\text{C} \pm 10^{\circ}\text{C}$, i_{corr} increase $15\% \pm 3\%$). High vacuum environment reduces oxygen infiltration, prevents premature NiO formation or uneven distribution, and keeps weight loss low.

(4) Post-processing

Hot isostatic pressing (HIP, $1200^{\circ}\text{C} \pm 10^{\circ}\text{C}$, $200 \text{ MPa} \pm 10 \text{ MPa}$, $1 \text{ hour} \pm 0.1 \text{ hour}$) was used to eliminate residual pores, further improve density (density increased to $99.7\% \pm 0.1\%$), reduce the penetration path of corrosive media, and reduce the pitting depth from $3 \mu\text{m} \pm 0.5 \mu\text{m}$ to $< 2 \mu\text{m} \pm 0.5 \mu\text{m}$.

(5) Surface treatment

The surface roughness (Ra) was controlled to less than $0.05 \mu\text{m} \pm 0.01 \mu\text{m}$ by precision mechanical polishing, which reduced surface microcracks and pits. Ultrasonic cleaning ($40 \text{ kHz} \pm 1 \text{ kHz}$, $10 \text{ min} \pm 1 \text{ min}$) was then used to remove residual contaminants ($< 0.1\% \pm 0.02\%$) and reduce the pitting area by $20\% \pm 5\%$ (from $0.012 \text{ mm}^2 \pm 0.001 \text{ mm}^2$ down to $0.0096 \text{ mm}^2 \pm 0.001 \text{ mm}^2$), the corrosion current i_{corr} remains $< 10^{-6} \text{ A/cm}^2 \pm 10^{-7} \text{ A/cm}^2$.

(6) Introduction of additives

Adding a small amount of Cr_3C_2 ($0.2\% \pm 0.01\%$) further enhances the corrosion resistance. Cr_3C_2 forms a Cr_2O_3 layer (thickness $\sim 0.1 \mu\text{m} \pm 0.05 \mu\text{m}$) at high temperature, which synergizes with the NiO layer to reduce the corrosion current by about $10\% \pm 2\%$ (from $10^{-6} \text{ A/cm}^2 \pm 10^{-7} \text{ A/cm}^2$ to $9 \times 10^{-7} \text{ A/cm}^2 \pm 10^{-8} \text{ A/cm}^2$), and the weight loss rate remains $< 0.05 \text{ mg/cm}^2 \pm 0.01 \text{ mg/cm}^2$. Cr_3C_2 also refines the grain size (from $0.6 \mu\text{m} \pm 0.01 \mu\text{m}$ to $0.51 \mu\text{m} \pm 0.01 \mu\text{m}$) and enhances the grain boundary strength ($> 200 \text{ MPa} \pm 20 \text{ MPa}$).

The optimization of these process parameters ensures the uniform bonding of the Ni-based binder phase and WC, and the grain boundary strength is increased to $> 200 \text{ MPa} \pm 20 \text{ MPa}$, which significantly enhances the corrosion and fatigue resistance of the material while maintaining high hardness ($\text{HV } 1800 \pm 30$) and toughness ($K_{\text{IC}} 12 \text{ MPa}\cdot\text{m}^{1/2} \pm 0.5 \text{ MPa}\cdot\text{m}^{1/2}$).

8.3.1.6 Test specification for Ni- based bonding phase of cemented carbide

The test specifications for Ni-based bonding phases of cemented carbide are intended to evaluate its corrosion resistance and mechanical properties. The following standards are recommended:

COPYRIGHT AND LEGAL LIABILITY STATEMENT

(1) Salt spray test

According to ISO 9227 NSS, the conditions are NaCl 5% \pm 0.1% solution, temperature 35°C \pm 2°C, duration 2000 hours \pm 100 hours, measure the weight loss (target < 0.05 mg/cm² \pm 0.01 mg/cm²) and pitting depth (target < 3 μ m \pm 0.5 μ m).

(2) Acid immersion test

in 0.1 M H₂SO₄ (pH 1 \pm 0.1) for 100 hours \pm 10 hours and test weight loss (target < 0.05 mg/cm² \pm 0.01 mg/cm²) and corrosion current density (i_{corr} , target < 10⁻⁶ A/cm² \pm 10⁻⁷ A/cm²).

(3) Electrochemical testing

A three-electrode system (working electrode: Ni-based WC, reference electrode: saturated calomel electrode, auxiliary electrode: platinum electrode) was used to measure the corrosion potential (E_{corr} , target ~0.1 V \pm 0.02 V vs. SCE) and polarization curves at a scan rate of 1 mV/s \pm 0.1 mV/s.

8.3.1.7 Mechanical properties test of cemented carbide Ni-based bonding phase

(1) Hardness test

According to ISO 3878, using a Vickers hardness tester, load 30 kg \pm 1 kg, test temperature 25°C \pm 1°C, target hardness > HV 1800 \pm 30.

(2) Fracture toughness test

According to ASTM E399, using the single edge notched beam (SENB) method, test temperature 25°C \pm 1°C, target K_{Ic} > 12 MPa·m^{1/2} \pm 0.5 MPa·m^{1/2}.

(3) High temperature performance test

Flexural strength was tested at 1000°C \pm 10°C using the three-point bending method according to ISO 178 (target > 2000 MPa \pm 100 MPa).

8.3.1.8 Microscopic analysis of Ni-based bonding phase in cemented carbide

SEM observation

Resolution < 0.1 μ m \pm 0.01 μ m, analysis of NiO layer thickness (target 10 nm \pm 1 nm) and surface defects.

XPS analysis

The Ni 2p peak (target 854 eV \pm 0.1 eV) was tested to confirm NiO formation.

EDS analysis

Measure the Ni distribution at the grain boundaries (target 8%-10% \pm 0.5%).

The test should be carried out under standard laboratory conditions, with a sample size of 10 mm \times 10 mm \times 5 mm \pm 0.1 mm and repeated \geq 3 times to ensure data reliability.

COPYRIGHT AND LEGAL LIABILITY STATEMENT

8.3.1.9 Engineering applications of Ni-based cemented carbide binder phase

With its excellent corrosion resistance and mechanical properties, cemented carbide Ni-based bonding phase has shown significant advantages in engineering applications in a variety of high temperature and corrosive environments. The following are its main application areas and performance, combined with actual cases and data:

(1) Marine engineering

cm^2) in salt spray ($\text{NaCl } 5\% \pm 0.1\%$) and seawater. $\pm 0.01 \text{ mg/cm}^2$) and high corrosion resistance (corrosion current $i_{\text{corr}} < 10^{-6} \text{ A/cm}^2 \pm 10^{-7} \text{ A/cm}^2$), it is widely used in deep-sea drilling stabilizers and cutting tools. In deep-sea drilling, the service life of stabilizers made of WC-10Ni exceeds 3 years ± 0.3 years, which is about $100\% \pm 5\%$ higher than that of traditional WC-10Co (1.5 years ± 0.2 years), and the maintenance cost caused by corrosion is reduced by about $40\% \pm 5\%$. Its high hardness ($\text{HV } 1800 \pm 30$) and toughness ($K_{\text{IC}} 12 \text{ MPa} \cdot \text{m}^{1/2} \pm 0.5 \text{ MPa} \cdot \text{m}^{1/2}$) ensure cutting efficiency under high pressure ($> 20 \text{ MPa} \pm 2 \text{ MPa}$) and high temperature ($> 500^\circ\text{C} \pm 10^\circ\text{C}$).

(2) Chemical pipelines and equipment

In an acidic environment ($\text{pH} < 2 \pm 0.1$, such as $0.1 \text{ M H}_2\text{SO}_4$), the weight loss rate of Ni-based WC cemented carbide is only 0.06 mg/cm^2 due to the protection of its NiO passivation layer (thickness $\sim 10 \text{ nm} \pm 1 \text{ nm}$). $\pm 0.01 \text{ mg/cm}^2$, better than stainless steel (weight loss rate $\sim 0.1 \text{ mg/cm}^2 \pm 0.01 \text{ mg/cm}^2$). It is used for corrosion-resistant coatings for chemical pipeline valves and pumps, with a service life of $> 2 \text{ years} \pm 0.2 \text{ years}$, which is about $100\% \pm 5\%$ longer than traditional materials (such as 304 stainless steel, life $\sim 1 \text{ year} \pm 0.1 \text{ year}$). In chemical reactors containing chlorides (such as HCl), WC-10Ni maintains pitting resistance (pitting depth $< 3 \mu\text{m} \pm 0.5 \mu\text{m}$), reducing the risk of equipment leakage.

(3) Papermaking industry

Papermaking equipment (such as grinding rollers and blades) are subject to chloride-containing ($\text{NaCl} > 5\% \pm 0.1\%$) and high temperature ($> 400^\circ\text{C} \pm 10^\circ\text{C}$) environments. Ni-based WC cemented carbide is an ideal choice due to its low corrosion current ($i_{\text{corr}} < 10^{-6} \text{ A/cm}^2 \pm 10^{-7} \text{ A/cm}^2$) and high wear resistance (hardness $> \text{HV } 1800 \pm 30$). The weight loss of grinding rollers made of WC-10Ni is only 0.05 mg/cm^2 after $5000 \text{ h} \pm 500 \text{ h}$ of continuous operation. $\pm 0.01 \text{ mg/cm}^2$, surface wear depth $< 10 \mu\text{m} \pm 1 \mu\text{m}$, compared with WC-10Co (weight loss rate $0.12 \text{ mg/cm}^2 \pm 0.01 \text{ mg/cm}^2$, wear depth $20 \mu\text{m} \pm 2 \mu\text{m}$) improves durability by approximately $50\% \pm 5\%$, reducing replacement frequency and production costs.

(4) Aviation and energy equipment

In aerospace engine components (such as turbine blades) and gas turbine nozzles, Ni-based WC cemented carbide (such as WC-10Ni with $\text{Cr}_3\text{C}_2 0.2\% \pm 0.01\%$) has a thermal fatigue crack length of $< 0.04 \text{ mm} \pm 0.01 \text{ mm}$ and a weight loss rate of $< 0.25 \text{ mg/cm}^2$ under $900^\circ\text{C} \pm 10^\circ\text{C}$ and thermal cycling ($\Delta T 500^\circ\text{C} \pm 10^\circ\text{C}$) conditions. $\pm 0.05 \text{ mg/cm}^2$, service life $> 5000 \text{ hours} \pm 500 \text{ hours}$, better

COPYRIGHT AND LEGAL LIABILITY STATEMENT

than the unoptimized 3000 hours \pm 300 hours. Its high thermal stability (hardness $> HV 1600 \pm 30$) and oxidation resistance make it perform well in high temperature corrosive environments (such as SO_2 atmospheres), reducing the failure rate caused by thermal cracking by about $45\% \pm 5\%$.

8.3.1.10 Application advantages and expansion of Ni-based cemented carbide

The engineering application advantage of Ni-based WC cemented carbide lies in its comprehensive performance: corrosion resistance improved by $60\% \pm 5\%$, high hardness ($HV 1800 \pm 30$) and toughness ($K_{IC} 12 MPa \cdot m^{1/2} \pm 0.5 MPa \cdot m^{1/2}$), and stability at $1000^\circ C \pm 10^\circ C$. These characteristics make it a potential substitute for traditional Co-based materials and stainless steel in extreme environments (such as deep-sea high pressure, acidic chemical industry, and high-temperature aviation). In the presence of water vapor (humidity $> 50\% \pm 5\%$) or higher temperature gradients ($\Delta T 600^\circ C \pm 10^\circ C$), combining multilayer coatings (e.g. TiN / Al_2O_3 , thickness $5-20 \mu m \pm 0.1 \mu m$) can further improve the performance and extend to ultra-high temperature ($> 1100^\circ C \pm 10^\circ C$) or high cycle number ($> 10^6$ times $\pm 10^4$ times) applications, such as next-generation energy devices.

Economic and environmental benefits

The application of Ni-based WC significantly reduces maintenance costs. For example, the annual maintenance cost of offshore drilling components is reduced by $40\% \pm 5\%$, and the efficiency of aviation components is increased by $20\% \pm 3\%$. However, Ni is relatively expensive (about 1.5-2 times that of Co), and costs need to be controlled by optimizing Ni content ($8\%-10\% \pm 1\%$) and processes (such as HIP post-treatment). In terms of the environment, its durability reduces the amount of material waste, which meets the requirements of sustainable development.

Ni-based WC cemented carbide performs well in marine engineering, chemical pipelines, paper industry and aviation energy equipment, with a weight loss rate of $< 0.06 mg/cm^2 \pm 0.01 mg/cm^2$, service life extended by $50\%-100\% \pm 5\%$. Its corrosion resistance and high temperature stability meet various engineering requirements, and its application can be further expanded through coating and alloying in the future.

8.3.2 Introduction of Cr_3C_2 Additives in Cemented Carbide

8.3.2.1 Principle and technical overview of the introduction of Cr_3C_2 additives into cemented carbide

cemented carbide Cr_3C_2 additives significantly enhances the oxidation resistance and high temperature resistance of cemented carbide, especially in high temperature ($1000^\circ C \pm 10^\circ C$) and corrosive environment (such as oxygen-containing or chloride-containing atmosphere). The recommended addition amount is $0.2\%-0.5\% \pm 0.01\%$. Cr_3C_2 reacts with oxygen at high temperature to form a dense Cr_2O_3 protective layer (thickness $\sim 0.1-0.2 \mu m \pm 0.05 \mu m$, density $\sim 5.2 g/cm^3 \pm 0.1 g/cm^3$), effectively isolate oxygen and corrosive media, and control the weight

COPYRIGHT AND LEGAL LIABILITY STATEMENT

gain to $< 0.3 \text{ mg/cm}^2 \pm 0.05 \text{ mg/cm}^2$, better than 0.5 mg/cm^2 of unspiked samples $\pm 0.05 \text{ mg/cm}^2$. This protective layer reduces the oxidation rate (from $0.4 \text{ mg/cm}^2 \cdot \text{h} \pm 0.05 \text{ mg/cm}^2 \cdot \text{h}$ to $< 0.2 \text{ mg/cm}^2 \cdot \text{h} \pm 0.05 \text{ mg/cm}^2 \cdot \text{h}$) and acts synergistically with the NiO layer of the Ni-based bonding phase to further reduce the corrosion current (i_{corr} from 10^{-6} A/cm^2 to $< 10^{-7} \text{ A/cm}^2$), Cr_3C_2 also improves the grain boundary strength ($> 200 \text{ MPa} \pm 20 \text{ MPa}$) by refining the WC grains (from $0.6 \mu\text{m} \pm 0.01 \mu\text{m}$ to $0.51 \mu\text{m} \pm 0.01 \mu\text{m}$), while maintaining the hardness ($> \text{HV } 1500 \pm 30$) and toughness ($K_{\text{IC}} > 12 \text{ MPa} \cdot \text{m}^{1/2} \pm 0.5 \text{ MPa} \cdot \text{m}^{1/2}$), making it suitable for high temperature and high load fields such as aviation turbine blades and gas turbine nozzles. In addition, the high temperature stability of Cr_3C_2 (melting point $1890^\circ\text{C} \pm 10^\circ\text{C}$) makes it soften less than the Co base at $1000^\circ\text{C} \pm 10^\circ\text{C}$ (hardness drop $< 5\% \pm 1\%$), enhancing the long-term durability of the material.

8.3.2.2 Analysis of the anti-oxidation and corrosion resistance mechanism of cemented carbide Cr_3C_2 additives

Cr_3C_2 additives comes from its chemical reaction and microstructure regulation. In an oxidizing environment at $1000^\circ\text{C} \pm 10^\circ\text{C}$, Cr_3C_2 reacts ($4\text{Cr}_3\text{C}_2 + 13\text{O}_2 \rightarrow 6\text{Cr}_2\text{O}_3 + 8\text{CO}$, $\Delta G < -1000 \text{ kJ/mol} \pm 50 \text{ kJ/mol}$) to form a Cr_2O_3 layer, whose low oxygen diffusion coefficient ($D_{\text{O}} \approx 10^{-14} \text{ cm}^2/\text{s} \pm 10^{-15} \text{ cm}^2/\text{s}$) effectively blocks oxygen penetration, and the weight gain is reduced from 0.5 mg/cm^2 to 1.5 mg/cm^2 , $\pm 0.05 \text{ mg/cm}^2$ down to $< 0.3 \text{ mg/cm}^2 \pm 0.05 \text{ mg/cm}^2$, the oxidation resistance is improved by about $40\% \pm 5\%$. In acidic medium (such as $0.1 \text{ M H}_2\text{SO}_4$, $\text{pH } 1 \pm 0.1$) or salt spray ($\text{NaCl } 5\% \pm 0.1\%$), the Cr_2O_3 layer and NiO. The two layers together form a double protection structure, the corrosion current i_{corr} is reduced to $9 \times 10^{-7} \text{ A/cm}^2 \pm 10^{-8} \text{ A/cm}^2$, and the weight loss rate is maintained at $< 0.05 \text{ mg/cm}^2 \pm 0.01 \text{ mg/cm}^2$, compared to 0.07 mg/cm^2 without additive $\pm 0.01 \text{ mg/cm}^2$ is reduced by about $29\% \pm 5\%$. In addition, Cr_3C_2 refines grains and strengthens grain boundary bonding, reduces thermal fatigue crack growth (from $0.05 \text{ mm} \pm 0.01 \text{ mm}$ to $0.03 \text{ mm} \pm 0.01 \text{ mm}$), and has a high matching degree of thermal expansion coefficient ($10 \times 10^{-6} \text{ K}^{-1}$) with WC, reducing stress concentration caused by thermal cycling (ΔT $500^\circ\text{C} \pm 10^\circ\text{C}$).

8.3.2.3 Microscopic analysis and verification of the introduction of Cr_3C_2 additives into cemented carbide

Scanning electron microscopy (SEM, resolution $< 0.1 \mu\text{m} \pm 0.01 \mu\text{m}$) observations showed that after adding Cr_3C_2 , the Cr_2O_3 layer was evenly distributed on the surface, with a thickness stable at $0.1\text{-}0.2 \mu\text{m} \pm 0.05 \mu\text{m}$, without obvious peeling or cracks, while oxidation holes (diameter $\sim 0.3 \mu\text{m} \pm 0.01 \mu\text{m}$) appeared on the surface of the sample without addition. X-ray diffraction (XRD) analysis confirmed the hexagonal crystal structure of Cr_2O_3 ($a = 4.96 \text{ \AA} \pm 0.01 \text{ \AA}$, $c = 13.58 \text{ \AA} \pm 0.01 \text{ \AA}$), the peak intensity ($2\theta \approx 33.6^\circ, 36.2^\circ$) indicates high crystallinity, which enhances the stability of the protective layer. Energy dispersive spectroscopy (EDS) shows that the content of Cr at the grain boundary is about $0.5\%\text{-}1\% \pm 0.1\%$, which is evenly distributed, verifying its good interface bonding with WC and Ni phases. X-ray photoelectron spectroscopy (XPS) detected the Cr 2p peak (about $576.5 \text{ eV} \pm 0.1 \text{ eV}$), which matches the O 1s peak ($530 \text{ eV} \pm 0.1 \text{ eV}$), confirming the

COPYRIGHT AND LEGAL LIABILITY STATEMENT

formation of Cr_2O_3 .

8.3.2.4 Analysis of factors affecting the performance of cemented carbide Cr_3C_2 additives

of cemented carbide Cr_3C_2 additives is affected by many factors and needs to be precisely controlled:

(1) Addition amount

When the Cr_3C_2 content is $0.2\% \pm 0.01\%$, the weight gain is $< 0.3 \text{ mg/cm}^2 \pm 0.05 \text{ mg/cm}^2$, i_{corr} decreases by about $10\% \pm 2\%$ (to $9 \times 10^{-7} \text{ A/cm}^2 \pm 10^{-8} \text{ A/cm}^2$). If the content exceeds $0.5\% \pm 0.01\%$, η phase (WC-Cr-Co composite phase) may form, hardness decreases by about $5\% \pm 1\%$ (to $\text{HV } 1425 \pm 30$), and toughness increases by $3\% \pm 1\%$ (K_{1c} increases to $12.4 \text{ MPa} \cdot \text{m}^{1/2} \pm 0.5 \text{ MPa} \cdot \text{m}^{1/2}$), but i_{corr} increases to $1.1 \times 10^{-6} \text{ A/cm}^2 \pm 10^{-7} \text{ A/cm}^2$.

(2) Grain size

the WC grain size is $0.51 \mu\text{m} \pm 0.01 \mu\text{m}$, Cr_3C_2 is evenly distributed and the weight loss rate is low ($< 0.05 \text{ mg/cm}^2 \pm 0.01 \text{ mg/cm}^2$). If the grain size increases to $2 \mu\text{m} \pm 0.01 \mu\text{m}$, the Cr_2O_3 layer is discontinuous and the weight loss rate increases by $15\% \pm 3\%$ (to $0.055 \text{ mg/cm}^2 \pm 0.01 \text{ mg/cm}^2$), the pitting depth increased from $2 \mu\text{m} \pm 0.5 \mu\text{m}$ to $3 \mu\text{m} \pm 0.5 \mu\text{m}$.

(3) Sintering temperature

When sintered at $1450^\circ\text{C} \pm 10^\circ\text{C}$, Cr_3C_2 Uniform solid solution, weight gain $< 0.3 \text{ mg/cm}^2 \pm 0.05 \text{ mg/cm}^2$. If the temperature rises to $> 1550^\circ\text{C} \pm 10^\circ\text{C}$, Cr volatilizes (loss $> 0.1\% \pm 0.02\%$), the thickness of the Cr_2O_3 layer decreases ($< 0.1 \mu\text{m} \pm 0.05 \mu\text{m}$), and i_{corr} increases by $10\% \pm 2\%$ (to $1.1 \times 10^{-6} \text{ A/cm}^2 \pm 10^{-7} \text{ A/cm}^2$).

(4) Environment

In strong acid with $\text{pH} < 2 \pm 0.1$, the Cr_2O_3 layer partially dissolved, i_{corr} increased by $20\% \pm 3\%$ (to $1.08 \times 10^{-6} \text{ A/cm}^2 \pm 10^{-7} \text{ A/cm}^2$), and the weight loss rate increased to $0.06 \text{ mg/cm}^2 \pm 0.01 \text{ mg/cm}^2$. In $\text{NaCl} > 5\% \pm 0.1\%$ salt spray, Cl^- accelerates Cr_2O_3 corrosion, and the pitting area increases by $15\% \pm 3\%$ (from $0.01 \text{ mm}^2 \pm 0.001 \text{ mm}^2$ increased to $0.0115 \text{ mm}^2 \pm 0.001 \text{ mm}^2$).

(5) Surface roughness

$R_a < 0.05 \mu\text{m} \pm 0.01 \mu\text{m}$, the Cr_2O_3 layer is intact and i_{corr} remains low ($< 10^{-6} \text{ A/cm}^2 \pm 10^{-7} \text{ A/cm}^2$). If $R_a > 0.1 \mu\text{m} \pm 0.01 \mu\text{m}$, the surface defects increase, i_{corr} increases by $8\% \pm 2\%$ (to $1.08 \times 10^{-6} \text{ A/cm}^2 \pm 10^{-7} \text{ A/cm}^2$), and the pitting depth increases to $3.5 \mu\text{m} \pm 0.5 \mu\text{m}$.

For example, a WC-10Ni-0.6% Cr_3C_2 sample had a weight loss rate of 0.08 mg/cm^2 in salt spray due to Cr volatilization caused by the high sintering temperature ($1550^\circ\text{C} \pm 10^\circ\text{C}$). $\pm 0.01 \text{ mg/cm}^2$, i_{corr} increased to $1.2 \times 10^{-6} \text{ A/cm}^2 \pm 10^{-7} \text{ A/cm}^2$. The weight loss rate of the optimized WC-10Ni-0.2% Cr_3C_2 ($1450^\circ\text{C} \pm 10^\circ\text{C}$, $R_a < 0.05 \mu\text{m} \pm 0.01 \mu\text{m}$) was only $0.03 \text{ mg/cm}^2 \pm 0.01 \text{ mg/cm}^2$, $i_{\text{corr}} < 9 \times 10^{-7} \text{ A/cm}^2 \pm 10^{-8} \text{ A/cm}^2$, antioxidant capacity increased by about $40\% \pm 5\%$.

COPYRIGHT AND LEGAL LIABILITY STATEMENT

8.3.2.5 Optimization of the preparation process of cemented carbide Cr_3C_2 additives

To achieve a mass gain $< 0.3 \text{ mg/cm}^2 \pm 0.05 \text{ mg/cm}^2$ and $i_{\text{corr}} < 10^{-6} \text{ A/cm}^2 \pm 10^{-7} \text{ A/cm}^2$. The introduction of Cr_3C_2 additives needs to be optimized in coordination with the preparation process. Recommended strategies include:

(1) Ingredient optimization

High purity Cr_3C_2 powder (purity $> 99.5\% \pm 0.01\%$, particle size $0.5 \mu\text{m} \pm 0.01 \mu\text{m}$) is selected and mixed with WC (particle size $0.51 \mu\text{m} \pm 0.01 \mu\text{m}$) and Ni powder ($8\%-10\% \pm 1\%$). The Cr_3C_2 content is controlled at $0.2\%-0.5\% \pm 0.01\%$. Excessive ($> 0.5\% \pm 0.01\%$) may induce η phase and reduce hardness by $5\% \pm 1\%$, while too low ($< 0.2\% \pm 0.01\%$) has insufficient antioxidant effect (weight gain $> 0.4 \text{ mg/cm}^2$). $\pm 0.05 \text{ mg/cm}^2$).

(2) Ball milling process

Wet ball milling (medium: anhydrous ethanol, $40 \text{ h} \pm 1 \text{ h}$, ball-to-material ratio: $10:1 \pm 0.5$) was used to ensure uniform dispersion of Cr_3C_2 , with a particle size distribution deviation of $< 0.02 \mu\text{m} \pm 0.01 \mu\text{m}$, reduce agglomeration ($< 0.1\% \pm 0.02\%$), and provide a homogeneous matrix for the formation of the Cr_2O_3 layer.

(3) Vacuum sintering

Sintering at $1450^\circ\text{C} \pm 10^\circ\text{C}$, pressure $< 10^{-3} \text{ Pa} \pm 10^{-4} \text{ Pa}$, holding time $1 \text{ hour} \pm 0.1 \text{ hour}$, density reaches $99.5\% \pm 0.1\%$, porosity $< 0.1\% \pm 0.02\%$. This temperature ensures Cr_3C_2 Solid solution forms a uniform Cr_2O_3 layer. At $> 1550^\circ\text{C} \pm 10^\circ\text{C}$, Cr volatilizes, resulting in an incomplete protective layer (thickness $< 0.1 \mu\text{m} \pm 0.05 \mu\text{m}$).

(4) Post-processing

Hot isostatic pressing (HIP, $1200^\circ\text{C} \pm 10^\circ\text{C}$, $200 \text{ MPa} \pm 10 \text{ MPa}$, $1 \text{ hour} \pm 0.1 \text{ hour}$) was used to eliminate residual porosity, increase the density to $99.7\% \pm 0.1\%$, reduce the penetration of oxidizing media, and increase the thickness of the Cr_2O_3 layer to $0.2 \mu\text{m} \pm 0.05 \mu\text{m}$.

(5) Surface treatment

The Ra was controlled at $0.05 \mu\text{m} \pm 0.01 \mu\text{m}$ by precision polishing, and the surface oxides ($< 0.1\% \pm 0.02\%$) were removed by ultrasonic cleaning ($40 \text{ kHz} \pm 1 \text{ kHz}$, $10 \text{ min} \pm 1 \text{ min}$), and the pitting area was reduced by $15\% \pm 3\%$ (from 0.011 mm^2 to 0.01 mm^2) $\pm 0.001 \text{ mm}^2$ down to $0.00935 \text{ mm}^2 \pm 0.001 \text{ mm}^2$, i_{corr} remains $< 10^{-6} \text{ A/cm}^2 \pm 10^{-7} \text{ A/cm}^2$.

(6) Additive dispersion optimization

Mechanical alloying (MA, $200 \text{ rpm} \pm 10 \text{ rpm}$, $10 \text{ h} \pm 0.5 \text{ h}$) was used to enhance the interfacial bonding between Cr_3C_2 and WC/Ni phases, reduce segregation ($< 0.05\% \pm 0.01\%$), and improve the uniformity of the Cr_2O_3 layer.

These processes ensure uniform Cr_3C_2 distribution, grain boundary strength $> 200 \text{ MPa} \pm 20 \text{ MPa}$,

COPYRIGHT AND LEGAL LIABILITY STATEMENT

and maintained hardness ($> HV 1500 \pm 30$) and toughness ($K_{Ic} > 12 \text{ MPa} \cdot \text{m}^{1/2} \pm 0.5 \text{ MPa} \cdot \text{m}^{1/2}$).

8.3.2.6 Cemented Carbide Cr_3C_2 Additive Engineering Case and Performance Comparison

Taking WC-10Ni-0.2% Cr_3C_2 and WC - 10Ni as examples, after oxidation at $1000^\circ\text{C} \pm 10^\circ\text{C}$ for 100 hours ± 10 hours, the mass increase of the sample with added Cr_3C_2 is only $0.25 \text{ mg/cm}^2 \pm 0.05 \text{ mg/cm}^2$, $i_{\text{corr}} < 9 \times 10^{-7} \text{ A/cm}^2 \pm 10^{-8} \text{ A/cm}^2$, compared to 0.5 mg/cm^2 without addition $\pm 0.05 \text{ mg/cm}^2$ and $1.1 \times 10^{-6} \text{ A/cm}^2 \pm 10^{-7} \text{ A/cm}^2$, and the oxidation resistance is improved by $50\% \pm 5\%$. In the salt spray test (NaCl 5% $\pm 0.1\%$, 2000 h ± 100 h), the weight loss rate is reduced to $0.03 \text{ mg/cm}^2 \pm 0.01 \text{ mg/cm}^2$, pitting depth $< 2 \mu\text{m} \pm 0.5 \mu\text{m}$, better than 0.07 mg/cm^2 without addition $\pm 0.01 \text{ mg/cm}^2$ and $3.5 \mu\text{m} \pm 0.5 \mu\text{m}$. In aviation turbine blade applications, WC-10Ni-0.2% Cr_3C_2 has a service life of > 6000 hours ± 500 hours, which is $20\% \pm 5\%$ longer than 5000 hours ± 500 hours without addition, and reduces the failure rate caused by hot cracks by about $30\% \pm 5\%$.

8.3.2.7 Application expansion and limitations of Cr_3C_2 additives in cemented carbide

Cr_3C_2 additions make cemented carbide excellent in high temperature oxidizing (e.g. $1100^\circ\text{C} \pm 10^\circ\text{C}$) and corrosive environments, suitable for gas turbine nozzles (lifetime $> 10^4$ hours $\pm 10^3$ hours) and high temperature molds (cycles $> 10^5$ times $\pm 10^4$ times). In SO_2 containing atmospheres, the Cr_2O_3 layer remains protective (weight gain $< 0.35 \text{ mg/cm}^2 \pm 0.05 \text{ mg/cm}^2$), but in strong acid with $\text{pH} < 1 \pm 0.1$, the dissolution rate increases by $15\% \pm 3\%$, and needs to be optimized in combination with TiN coating (thickness $5\text{-}10 \mu\text{m} \pm 0.1 \mu\text{m}$). Cr_3C_2 is more expensive (about 2-3 times that of WC), and the addition amount needs to be controlled ($0.2\%\text{-}0.5\% \pm 0.01\%$) to balance performance and economy.

8.3.2.8 Optimization direction and future prospects of introducing Cr_3C_2 additives into cemented carbide

To improve the Cr_3C_2 effect, TaC ($0.1\% \pm 0.01\%$) can be added to enhance the thermal stability of the Cr_2O_3 layer, and i_{corr} is reduced to $5 \times 10^{-7} \text{ A/cm}^2 \pm 10^{-8} \text{ A/cm}^2$. In ultra-high temperatures ($> 1200^\circ\text{C} \pm 10^\circ\text{C}$), combined with Al_2O_3 coating (thickness $10\text{-}15 \mu\text{m} \pm 0.1 \mu\text{m}$), the weight gain can be controlled to $0.2 \text{ mg/cm}^2 \pm 0.05 \text{ mg/cm}^2$, hardness $> HV 1600 \pm 30$. In the future, the development of nano- Cr_3C_2 (particle size $< 0.1 \mu\text{m} \pm 0.01 \mu\text{m}$) or Cr-Ni composite additives can further improve oxidation resistance and economy and expand to extreme energy equipment applications.

Cr_3C_2 additives ($0.2\% \text{-}0.5\% \pm 0.01\%$) significantly reduce the mass gain ($< 0.3 \text{ mg/cm}^2$) by forming a Cr_2O_3 layer (thickness $0.1\text{-}0.2 \mu\text{m} \pm 0.05 \mu\text{m}$), $\pm 0.05 \text{ mg/cm}^2$ and corrosion current ($i_{\text{corr}} < 10^{-6} \text{ A/cm}^2 \pm 10^{-7} \text{ A/cm}^2$), oxidation resistance improved by $40\% \pm 5\%$, while maintaining hardness ($> HV 1500 \pm 30$) and toughness ($K_{Ic} > 12 \text{ MPa} \cdot \text{m}^{1/2} \pm 0.5 \text{ MPa} \cdot \text{m}^{1/2}$). Optimize the preparation process (composition optimization Cr_3C_2 $0.2\%\text{-}0.5\% \pm 0.01\%$, ball

COPYRIGHT AND LEGAL LIABILITY STATEMENT

milling 40 hours \pm 1 hour, sintering 1450°C \pm 10°C, HIP post-treatment, surface polishing Ra < 0.05 μm \pm 0.01 μm) to ensure stable performance. Factors such as addition amount, grain size, sintering temperature, environment and surface roughness need to be comprehensively controlled. It is suitable for high temperature and corrosive environments. In the future, its application can be further expanded through composite additions and coatings.

8.3.3 Hard alloy surface coating protection

8.3.3.1 Overview of the protection principle and technology of cemented carbide surface coating

Surface coating protection technology significantly improves the corrosion resistance and high temperature resistance of cemented carbide, especially for high temperature (1000°C \pm 10°C) and corrosive environment (such as acidic or salt spray conditions). Recommended coatings include TiN and Al₂O₃, with a thickness of 5-20 μm \pm 0.1 μm , achieved by physical vapor deposition (PVD, 400°C \pm 10°C) or chemical vapor deposition (CVD, 1000°C \pm 10°C) process. TiN coating (hardness > HV 2000 \pm 50, density \sim 5.4 g/cm³) \pm 0.1 g/cm³) with excellent wear and oxidation resistance, mass gain < 0.2 mg/cm² \pm 0.05 mg/cm², the corrosion current (i_{corr}) is reduced to < 8×10^{-7} A/cm² \pm 10^{-8} A/cm². The Al₂O₃ coating (melting point 2072°C \pm 10°C, thermal conductivity \sim 30 W/m·K \pm 2 W/m·K) isolates oxygen and corrosive media by forming a dense oxide layer (thickness \sim 0.5 μm \pm 0.1 μm), and the weight loss rate is maintained at < 0.04 mg/cm² \pm 0.01 mg/cm², better than 0.07 mg/cm² of uncoated samples \pm 0.01 mg/cm². These coatings work synergistically with Ni-based binder phases or Cr₃C₂ additives to maintain hardness (> HV 1800 \pm 30) and toughness (K_{IC} > 12 MPa·m^{1/2} \pm 0.5 MPa·m^{1/2}), making them widely used in aerospace turbine blades, chemical equipment and marine tools. In addition, the high temperature stability of the coatings (TiN to 800°C \pm 10°C, Al₂O₃ to 1000°C \pm 10°C) reduces the performance degradation caused by thermal cycling (ΔT 500°C \pm 10°C).

8.3.3.2 Analysis of corrosion resistance and oxidation resistance mechanism of cemented carbide surface coating

The protective effect of the surface coating comes from its physical barrier and chemical inertness. In an oxidizing environment at 1000°C \pm 10°C, the Al₂O₃ coating forms a dense oxide layer through reaction ($4\text{Al} + 3\text{O}_2 \rightarrow 2\text{Al}_2\text{O}_3$, $\Delta G < -1500$ kJ/mol \pm 50 kJ/mol), and its low oxygen diffusion coefficient ($D_{\text{O}} \approx 10^{-15}$ cm²/s \pm 10^{-16} cm²/s) controls the mass gain to < 0.2 mg/cm² \pm 0.05 mg/cm², and the oxidation resistance is improved by about 60% \pm 5%. The TiN coating reduces surface wear and microcrack propagation (from 0.05 mm \pm 0.01 mm to < 0.02 mm \pm 0.01 mm) through high hardness (> HV 2000 \pm 50) and low friction coefficient (\sim 0.4 \pm 0.05). In acidic media (such as 0.1 M H₂SO₄, pH 1 \pm 0.1) or salt spray (NaCl 5% \pm 0.1%), the coating isolates Cl⁻ and H⁺, i_{corr} is reduced to 8×10^{-7} A/cm² \pm 10^{-8} A/cm², and the weight loss rate is reduced to 0.04 mg/cm² \pm 0.01 mg/cm², compared to 0.07 mg/cm² for uncoated \pm 0.01 mg/cm², a reduction of about 43% \pm 5%. The thermal expansion coefficient of the coating matches that of the substrate

COPYRIGHT AND LEGAL LIABILITY STATEMENT

($\text{TiN } 9 \times 10^{-6} \text{ K}^{-1}$, $\text{Al}_2\text{O}_3 \ 8 \times 10^{-6} \text{ K}^{-1}$, $\text{WC } 5.2 \times 10^{-6} \text{ K}^{-1}$), reducing thermal stress ($< 300 \text{ MPa} \pm 50 \text{ MPa}$) and enhancing thermal fatigue resistance.

8.3.3.3 Microscopic analysis and verification of cemented carbide surface coating

Scanning electron microscopy (SEM, resolution $< 0.1 \mu\text{m} \pm 0.01 \mu\text{m}$) observations showed that the TiN and Al_2O_3 coatings had smooth surfaces and uniform thickness ($5\text{-}20 \mu\text{m} \pm 0.1 \mu\text{m}$), without obvious peeling or cracks, while oxidation spots (diameter $\sim 0.4 \mu\text{m} \pm 0.01 \mu\text{m}$) appeared on the surface of the uncoated sample. X-ray diffraction (XRD) analysis confirmed the cubic crystal structure of TiN ($a = 4.24 \text{ \AA} \pm 0.01 \text{ \AA}$, $2\theta \approx 36.7^\circ, 42.6^\circ$) and the hexagonal structure of Al_2O_3 ($a = 4.76 \text{ \AA} \pm 0.01 \text{ \AA}$, $c = 12.99 \text{ \AA} \pm 0.01 \text{ \AA}$, $2\theta \approx 35.1^\circ, 43.3^\circ$), and the peak intensity indicates high crystallinity. Energy dispersive spectroscopy (EDS) shows that the content of Ti or Al in the coating is $> 95\% \pm 1\%$, and it is well integrated with WC/Ni at the interface (diffusion layer thickness $\sim 0.1 \mu\text{m} \pm 0.05 \mu\text{m}$). X-ray photoelectron spectroscopy (XPS) detects Ti 2p peak (about $455 \text{ eV} \pm 0.1 \text{ eV}$) or Al 2p peak ($74 \text{ eV} \pm 0.1 \text{ eV}$), which matches the O 1s peak ($530 \text{ eV} \pm 0.1 \text{ eV}$), verifying the formation of the oxide layer.

8.3.3.4 Analysis of factors affecting cemented carbide surface coating

The effect of surface coating protection is affected by many factors and needs to be precisely controlled:

(1) Coating thickness

the thickness is $5\text{-}10 \mu\text{m} \pm 0.1 \mu\text{m}$, $i_{\text{corr}} < 8 \times 10^{-7} \text{ A/cm}^2 \pm 10^{-8} \text{ A/cm}^2$ and weight loss $< 0.04 \text{ mg/cm}^2 \pm 0.01 \text{ mg/cm}^2$. If the thickness is $> 20 \mu\text{m} \pm 0.1 \mu\text{m}$, the internal stress increases ($> 500 \text{ MPa} \pm 50 \text{ MPa}$), the risk of spalling increases by $10\% \pm 2\%$, and i_{corr} increases to $9 \times 10^{-7} \text{ A/cm}^2 \pm 10^{-8} \text{ A/cm}^2$.

(2) Coating type

TiN coatings perform well at $800^\circ\text{C} \pm 10^\circ\text{C}$ (weight gain $< 0.2 \text{ mg/cm}^2 \pm 0.05 \text{ mg/cm}^2$), but oxidation increases at $> 900^\circ\text{C} \pm 10^\circ\text{C}$ (weight gain $> 0.3 \text{ mg/cm}^2 \pm 0.05 \text{ mg/cm}^2$). Al_2O_3 coatings are stable at $1000^\circ\text{C} \pm 10^\circ\text{C}$ (weight gain $< 0.15 \text{ mg/cm}^2 \pm 0.05 \text{ mg/cm}^2$), but the wear resistance is slightly lower than TiN (hardness decreases by $5\% \pm 1\%$).

(3) Deposition temperature

PVD $400^\circ\text{C} \pm 10^\circ\text{C}$ Ensures TiN coating adhesion ($> 50 \text{ N/mm}^2 \pm 5 \text{ N/mm}^2$), if $> 500^\circ\text{C} \pm 10^\circ\text{C}$, thermal stress cracking (width $\sim 0.1 \mu\text{m} \pm 0.01 \mu\text{m}$). CVD $1000^\circ\text{C} \pm 10^\circ\text{C}$ is suitable for Al_2O_3 , but matrix softening (hardness reduction of $10\% \pm 2\%$) needs to be optimized.

(4) Environment

When $\text{pH} < 2 \pm 0.1$, the dissolution rate of TiN coating increases by $15\% \pm 3\%$ (i_{corr} to $9 \times 10^{-7} \text{ A/cm}^2 \pm 10^{-8} \text{ A/cm}^2$), and Al_2O_3 is stable ($i_{\text{corr}} < 8 \times 10^{-7} \text{ A/cm}^2 \pm 10^{-8} \text{ A/cm}^2$). In NaCl $>$

COPYRIGHT AND LEGAL LIABILITY STATEMENT

5% \pm 0.1% salt spray, the pitting area increases by 10% \pm 2% (from 0.01 mm² \pm 0.001 mm² to 0.011 mm² \pm 0.001 mm²).

(5) Surface roughness

High coating adhesion (> 60 N/mm²) with $R_a < 0.05 \mu\text{m} \pm 0.01 \mu\text{m} \pm 5$ N/mm², i_{corr} is low. If $R_a > 0.1 \mu\text{m} \pm 0.01 \mu\text{m}$, defects increase, i_{corr} increases by 7% \pm 2% (to 8.6×10^{-7} A/cm² $\pm 10^{-8}$ A/cm²).

For example, a WC-10Ni sample coated with Al₂O₃ ($20 \mu\text{m} \pm 0.1 \mu\text{m}$, CVD 1050°C $\pm 10^\circ\text{C}$) has a large internal stress, a peeling rate of 15% $\pm 2\%$, and a weight loss rate of 0.06 mg/cm² ± 0.01 mg/cm². The weight loss rate of the optimized TiN coating ($10 \mu\text{m} \pm 0.1 \mu\text{m}$, PVD 400°C $\pm 10^\circ\text{C}$, $R_a < 0.05 \mu\text{m} \pm 0.01 \mu\text{m}$) is only 0.03 mg/cm² ± 0.01 mg/cm², $i_{\text{corr}} < 8 \times 10^{-7}$ A/cm² $\pm 10^{-8}$ A/cm², corrosion resistance improved by about 57% $\pm 5\%$.

8.3.3.6 Optimization of preparation process for cemented carbide surface coating protection

To achieve a weight loss < 0.04 mg/cm² ± 0.01 mg/cm² and $i_{\text{corr}} < 8 \times 10^{-7}$ A/cm² $\pm 10^{-8}$ A/cm². The surface coating process needs to be precisely controlled. Recommended strategies include:

(1) Substrate pretreatment

The surface roughness (R_a) of WC-10Ni was controlled to $0.05 \mu\text{m} \pm 0.01 \mu\text{m}$ by polishing, and ultrasonic cleaning (40 kHz ± 1 kHz, 10 min ± 1 min) was used to remove contaminants ($< 0.1\% \pm 0.02\%$) and improve coating adhesion (> 60 N/mm²) ± 5 N/mm².

(2) Coating selection and thickness

Choose TiN (thickness $5-10 \mu\text{m} \pm 0.1 \mu\text{m}$) or Al₂O₃ (thickness $10-15 \mu\text{m} \pm 0.1 \mu\text{m}$). TiN uses PVD ($400^\circ\text{C} \pm 10^\circ\text{C}$, bias voltage -100 V ± 10 V, deposition rate $0.5 \mu\text{m/h} \pm 0.1 \mu\text{m/h}$), Al₂O₃ uses CVD ($1000^\circ\text{C} \pm 10^\circ\text{C}$, pressure 10 kPa ± 1 kPa, deposition rate $0.3 \mu\text{m/h} \pm 0.1 \mu\text{m/h}$) to avoid internal stress caused by excessive thickness ($> 20 \mu\text{m} \pm 0.1 \mu\text{m}$).

(3) Deposition process optimization

In PVD, the Ar / N₂ flow ratio ($1:1 \pm 0.1$) is controlled to ensure the purity of TiN phase ($> 98\% \pm 1\%$). In CVD, H₂ ($5\% \pm 0.5\%$) is added to improve the density of Al₂O₃ (porosity $< 0.05\% \pm 0.01\%$) and reduce oxygen diffusion.

(4) Post-processing

Low temperature annealing ($500^\circ\text{C} \pm 10^\circ\text{C}$, 2 hours ± 0.1 hours) is used to release residual stress (< 200 MPa ± 20 MPa) and enhance the bonding between the coating and the substrate (interface shear strength > 50 N/mm²) ± 5 N/mm².

(5) Multi-layer coating

Combining a double-layer structure of TiN ($5 \mu\text{m} \pm 0.1 \mu\text{m}$) + Al₂O₃ ($10 \mu\text{m} \pm 0.1 \mu\text{m}$), TiN provides wear resistance, Al₂O₃ enhances oxidation resistance, i_{corr} drops to 7×10^{-7} A/cm² \pm

COPYRIGHT AND LEGAL LIABILITY STATEMENT

10^{-8} A/cm^2 , and weight loss rate $< 0.03 \text{ mg/cm}^2 \pm 0.01 \text{ mg/cm}^2$.

(6) Surface finishing

Ion beam polishing (energy $500 \text{ eV} \pm 50 \text{ eV}$) was used to optimize R_a to $0.03 \mu\text{m} \pm 0.01 \mu\text{m}$, reduce microcracks, and reduce pitting area by $10\% \pm 2\%$ (from $0.011 \text{ mm}^2 \pm 0.001 \text{ mm}^2$ to $0.0099 \text{ mm}^2 \pm 0.001 \text{ mm}^2$).

These processes ensure a homogeneous coating with an adhesion of $> 60 \text{ N/mm}^2 \pm 5 \text{ N/mm}^2$, maintaining hardness ($> \text{HV } 1800 \pm 30$) and toughness ($K_{IC} > 12 \text{ MPa}\cdot\text{m}^{1/2} \pm 0.5 \text{ MPa}\cdot\text{m}^{1/2}$).

8.3.3.7 Cemented Carbide Surface Coating Engineering Cases and Performance Comparison

Taking WC-10Ni-TiN ($10 \mu\text{m} \pm 0.1 \mu\text{m}$) and uncoated WC-10Ni as examples, after oxidation at $1000^\circ\text{C} \pm 10^\circ\text{C}$ for 100 hours ± 10 hours, the TiN coating sample gained $0.15 \text{ mg/cm}^2 \pm 0.05 \text{ mg/cm}^2$, $i_{\text{corr}} < 8 \times 10^{-7} \text{ A/cm}^2 \pm 10^{-8} \text{ A/cm}^2$, compared to 0.5 mg/cm^2 for uncoated $\pm 0.05 \text{ mg/cm}^2$ and $1.1 \times 10^{-6} \text{ A/cm}^2 \pm 10^{-7} \text{ A/cm}^2$, and the oxidation resistance is improved by $70\% \pm 5\%$. In the salt spray test (NaCl $5\% \pm 0.1\%$, 2000 h ± 100 h), the weight loss rate is reduced to $0.03 \text{ mg/cm}^2 \pm 0.01 \text{ mg/cm}^2$, pitting depth $< 1.5 \mu\text{m} \pm 0.5 \mu\text{m}$, better than 0.07 mg/cm^2 for uncoated $\pm 0.01 \text{ mg/cm}^2$ and $3.5 \mu\text{m} \pm 0.5 \mu\text{m}$. In aviation turbine blades, the service life of TiN coated samples is > 7000 hours ± 500 hours, which is $40\% \pm 5\%$ longer than the uncoated 5000 hours ± 500 hours, and the thermal crack failure rate is reduced by about $35\% \pm 5\%$.

8.3.3.8 Application extension and limitations of cemented carbide surface coatings

The surface coating makes cemented carbide perform well in high temperature oxidation (such as $1100^\circ\text{C} \pm 10^\circ\text{C}$) and corrosive environments, suitable for gas turbine nozzles (lifetime $> 10^4$ hours $\pm 10^3$ hours) and deep-sea drill bits (pressure resistance $> 30 \text{ MPa} \pm 2 \text{ MPa}$). In atmosphere, Al_2O_3 coatings remain protective (weight gain $< 0.2 \text{ mg/cm}^2 \pm 0.05 \text{ mg/cm}^2$), but the dissolution rate of TiN in strong acid with $\text{pH} < 1 \pm 0.1$ increases by $20\% \pm 3\%$, and needs to be optimized in combination with Al_2O_3 . The coating process cost is relatively high (about 2-3 times that of the substrate), and the economy needs to be controlled through thin layer design ($5\text{-}10 \mu\text{m} \pm 0.1 \mu\text{m}$).

8.3.3.9 Optimization direction and future prospects of cemented carbide surface coating

To improve the coating effect, a TiN / Al_2O_3 gradient coating (thickness $15 \mu\text{m} \pm 0.1 \mu\text{m}$) can be developed, and i_{corr} is reduced to $6 \times 10^{-7} \text{ A/cm}^2 \pm 10^{-8} \text{ A/cm}^2$. At ultra-high temperatures ($> 1200^\circ\text{C} \pm 10^\circ\text{C}$), ZrO_2 ($5\% \pm 0.5\%$) is added to enhance thermal stability, with a weight gain of $< 0.15 \text{ mg/cm}^2 \pm 0.05 \text{ mg/cm}^2$, hardness $> \text{HV } 1900 \pm 30$. In the future, plasma spraying (temperature $800^\circ\text{C} \pm 10^\circ\text{C}$) or nano-coating (particle size $< 0.1 \mu\text{m} \pm 0.01 \mu\text{m}$) can be used to improve adhesion and durability and expand to extreme aviation and energy equipment applications.

Surface coatings (e.g. TiN $5\text{-}10 \mu\text{m} \pm 0.1 \mu\text{m}$, Al_2O_3 $10\text{-}15 \mu\text{m} \pm 0.1 \mu\text{m}$) significantly reduce weight loss ($< 0.04 \text{ mg/cm}^2$) by forming a protective layer (thickness $\sim 0.5 \mu\text{m} \pm 0.1 \mu\text{m}$) ± 0.01

COPYRIGHT AND LEGAL LIABILITY STATEMENT

mg/cm²) and corrosion current ($i_{\text{corr}} < 8 \times 10^{-7} \text{ A/cm}^2 \pm 10^{-8} \text{ A/cm}^2$), oxidation resistance increased by $60\% \pm 5\%$, hardness ($> \text{HV } 1800 \pm 30$) and toughness ($K_{\text{IC}} > 12 \text{ MPa} \cdot \text{m}^{1/2} \pm 0.5 \text{ MPa} \cdot \text{m}^{1/2}$). Optimize the preparation process (substrate pretreatment $R_a < 0.05 \mu\text{m} \pm 0.01 \mu\text{m}$, PVD/CVD deposition, low temperature annealing, multi-layer design) to ensure stable performance. The coating thickness, type, deposition temperature, environment and surface roughness factors need to be comprehensively controlled. It is suitable for high temperature and corrosive environments. In the future, gradient coating and nanotechnology can be used to further expand the application.

8.3.4 Optimization of process parameters for corrosion resistance and high temperature resistance of cemented carbide

8.3.4.1 Overview of process parameter optimization principles and technologies for corrosion resistance and high temperature resistance of cemented carbide

Process parameter optimization is a key means to improve the corrosion resistance and high temperature resistance of cemented carbide. By precisely controlling the temperature, pressure, time and other parameters in the preparation process, the synergistic effect of Ni-based binder phase, Cr₃C₂ additives and surface coating is enhanced. The recommended optimization parameters include sintering temperature of $1450^\circ\text{C} \pm 10^\circ\text{C}$, pressure $< 10^{-3} \text{ Pa} \pm 10^{-4} \text{ Pa}$, ball milling time of 40 hours ± 1 hour and hot isostatic pressing (HIP) temperature of $1200^\circ\text{C} \pm 10^\circ\text{C}$. After these parameters are optimized, the weight loss rate of cemented carbide is reduced to $< 0.04 \text{ mg/cm}^2 \pm 0.01 \text{ mg/cm}^2$, corrosion current (i_{corr}) reduced to $< 8 \times 10^{-7} \text{ A/cm}^2 \pm 10^{-8} \text{ A/cm}^2$, hardness maintained $> \text{HV } 1800 \pm 30$, toughness $> 12 \text{ MPa} \cdot \text{m}^{1/2} \pm 0.5 \text{ MPa} \cdot \text{m}^{1/2}$. The optimized process reduces micro defects (such as porosity $< 0.1\% \pm 0.02\%$) and phase segregation ($< 0.1\% \pm 0.02\%$), and improves grain boundary strength ($> 200 \text{ MPa} \pm 20 \text{ MPa}$), making it excellent in high temperature ($1000^\circ\text{C} \pm 10^\circ\text{C}$) and corrosive environment (such as NaCl $5\% \pm 0.1\%$), and is suitable for offshore drilling, aviation turbines and chemical equipment. In addition, the optimized process reduces stress concentration ($< 300 \text{ MPa} \pm 50 \text{ MPa}$) caused by thermal cycling (ΔT $500^\circ\text{C} \pm 10^\circ\text{C}$), extending the service life.

8.3.4.2 Analysis of corrosion resistance and performance mechanism of cemented carbide process parameter optimization

The core of process parameter optimization lies in the uniformity of microstructure and phase distribution. Under sintering at $1450^\circ\text{C} \pm 10^\circ\text{C}$, the Ni-based binder phase forms a uniform solid solution with WC (Ni distribution deviation $< 0.1\% \pm 0.02\%$), the NiO layer thickness is stabilized at $10 \text{ nm} \pm 1 \text{ nm}$, and i_{corr} is reduced to $< 10^{-6} \text{ A/cm}^2 \pm 10^{-7} \text{ A/cm}^2$. Ball milling for 40 hours ± 1 hour refines the grains ($0.51 \mu\text{m} \pm 0.01 \mu\text{m}$), increases the grain boundary density to $> 10^4 \text{ mm}^2/\text{cm}^3 \pm 10^3 \text{ mm}^2/\text{cm}^3$, reduces the penetration of corrosive media, and the weight loss rate is $< 0.04 \text{ mg/cm}^2 \pm 0.01 \text{ mg/cm}^2$. HIP $1200^\circ\text{C} \pm 10^\circ\text{C}$ eliminates residual porosity ($< 0.05\% \pm 0.01\%$), density reaches $99.7\% \pm 0.1\%$, and improves oxidation resistance (mass gain $< 0.25 \text{ mg/cm}^2 \pm 0.05 \text{ mg/cm}^2$). In high temperature oxidation ($1000^\circ\text{C} \pm 10^\circ\text{C}$), the optimized parameters reduced the

COPYRIGHT AND LEGAL LIABILITY STATEMENT

volatilization of Cr_3C_2 (loss $< 0.05\% \pm 0.01\%$), the thickness of the Cr_2O_3 layer remained at $0.1\text{-}0.2\ \mu\text{m} \pm 0.05\ \mu\text{m}$, and the oxidation resistance was improved by about $45\% \pm 5\%$. The matching of thermal expansion coefficients ($\text{WC } 5.2 \times 10^{-6} \text{K}^{-1}$, $\text{Ni } 13 \times 10^{-6} \text{K}^{-1}$) reduced thermal fatigue cracks ($< 0.03\ \text{mm} \pm 0.01\ \text{mm}$) and improved long-term stability.

8.3.4.3 Microscopic analysis and verification of process parameter optimization for corrosion resistance and high temperature resistance of cemented carbide

Scanning electron microscopy (SEM, resolution $< 0.1\ \mu\text{m} \pm 0.01\ \mu\text{m}$) observations showed that the optimized process samples had uniform grains ($0.51\ \mu\text{m} \pm 0.01\ \mu\text{m}$) and porosity $< 0.1\% \pm 0.02\%$, while the unoptimized samples (sintered at $1500^\circ\text{C} \pm 10^\circ\text{C}$) had segregation zones (diameter $\sim 0.5\ \mu\text{m} \pm 0.01\ \mu\text{m}$). X-ray diffraction (XRD) analysis confirmed that the peak intensities of the WC phase ($2\theta \approx 35.6^\circ, 48.3^\circ$) and the Ni phase ($2\theta \approx 44.5^\circ$) were uniform, indicating an optimized phase distribution. Energy dispersive spectroscopy (EDS) showed that the Ni and Cr contents at the grain boundaries were $8\%\text{-}10\% \pm 0.5\%$ and $0.5\%\text{-}1\% \pm 0.1\%$, respectively, without obvious segregation. X-ray photoelectron spectroscopy (XPS) detected the Ni 2p peak ($854\ \text{eV} \pm 0.1\ \text{eV}$) and the Cr 2p peak ($576.5\ \text{eV} \pm 0.1\ \text{eV}$), which matched the O 1s peak ($530\ \text{eV} \pm 0.1\ \text{eV}$), verifying the formation of NiO and Cr_2O_3 layers.

8.3.4.4 Analysis of factors affecting process parameter optimization of cemented carbide corrosion resistance and high temperature resistance

The effect of process parameter optimization is affected by many factors and needs to be precisely controlled:

(1) Sintering temperature

At $1450^\circ\text{C} \pm 10^\circ\text{C}$, Ni distribution deviation is $< 0.1\% \pm 0.02\%$, $i_{\text{corr}} < 8 \times 10^{-7}\ \text{A/cm}^2 \pm 10^{-8}\ \text{A/cm}^2$. If $> 1500^\circ\text{C} \pm 10^\circ\text{C}$, Ni segregation is $> 0.5\% \pm 0.1\%$, i_{corr} increases by $15\% \pm 3\%$ (to $1.15 \times 10^{-6}\ \text{A/cm}^2 \pm 10^{-7}\ \text{A/cm}^2$), and the weight loss rate increases to $0.07\ \text{mg/cm}^2 \pm 0.01\ \text{mg/cm}^2$.

(2) Ball milling time

At $40\ \text{hours} \pm 1\ \text{hour}$, the grain size is $0.51\ \mu\text{m} \pm 0.01\ \mu\text{m}$ and the weight loss rate is $< 0.04\ \text{mg/cm}^2 \pm 0.01\ \text{mg/cm}^2$. If $< 30\ \text{hours} \pm 1\ \text{hour}$, the grains will coarsen ($> 0.7\ \mu\text{m} \pm 0.01\ \mu\text{m}$), and the weight loss rate will increase by $10\% \pm 2\%$ (to $0.044\ \text{mg/cm}^2 \pm 0.01\ \text{mg/cm}^2$).

(3) Pressure

At vacuum degree $< 10^{-3}\ \text{Pa} \pm 10^{-4}\ \text{Pa}$, oxygen content $< 0.01\% \pm 0.001\%$, mass gain $< 0.25\ \text{mg/cm}^2 \pm 0.05\ \text{mg/cm}^2$. If the pressure is $> 10^{-2}\ \text{Pa} \pm 10^{-3}\ \text{Pa}$, the oxidation weight gain is $20\% \pm 3\%$ (to $0.3\ \text{mg/cm}^2 \pm 0.05\ \text{mg/cm}^2$).

(4) HIP temperature

COPYRIGHT AND LEGAL LIABILITY STATEMENT

At $1200^{\circ}\text{C} \pm 10^{\circ}\text{C}$, the density is $99.7\% \pm 0.1\%$ and the pitting depth is $< 2 \mu\text{m} \pm 0.5 \mu\text{m}$. At $> 1300^{\circ}\text{C} \pm 10^{\circ}\text{C}$, the matrix softens (hardness decreases by $5\% \pm 1\%$) and i_{corr} increases to $9 \times 10^{-7} \text{ A/cm}^2 \pm 10^{-8} \text{ A/cm}^2$.

(5) Ambient humidity

When humidity $> 50\% \pm 5\%$, surface oxidation is accelerated and i_{corr} increases by $10\% \pm 2\%$ (to $8.8 \times 10^{-7} \text{ A/cm}^2 \pm 10^{-8} \text{ A/cm}^2$), which needs to be combined with coating optimization.

For example, a WC-10Ni sample was sintered at $1500^{\circ}\text{C} \pm 10^{\circ}\text{C}$ and $10^{-2} \text{ Pa} \pm 10^{-3} \text{ Pa}$, with a weight loss of $0.08 \text{ mg/cm}^2 \pm 0.01 \text{ mg/cm}^2$, i_{corr} reaches $1.2 \times 10^{-6} \text{ A/cm}^2 \pm 10^{-7} \text{ A/cm}^2$. The weight loss rate of the optimized process ($1450^{\circ}\text{C} \pm 10^{\circ}\text{C}$, $< 10^{-3} \text{ Pa} \pm 10^{-4} \text{ Pa}$, HIP $1200^{\circ}\text{C} \pm 10^{\circ}\text{C}$) is reduced to $0.03 \text{ mg/cm}^2 \pm 0.01 \text{ mg/cm}^2$, $i_{\text{corr}} < 8 \times 10^{-7} \text{ A/cm}^2 \pm 10^{-8} \text{ A/cm}^2$, corrosion resistance improved by about $62\% \pm 5\%$.

8.3.4.5 Optimization strategy of process parameters for corrosion resistance and high temperature resistance of cemented carbide

To achieve a weight loss $< 0.04 \text{ mg/cm}^2 \pm 0.01 \text{ mg/cm}^2$ and $i_{\text{corr}} < 8 \times 10^{-7} \text{ A/cm}^2 \pm 10^{-8} \text{ A/cm}^2$, process parameters need to be precisely controlled. Recommended strategies include:

(1) Powder ratio and ball milling

WC (particle size $0.51 \mu\text{m} \pm 0.01 \mu\text{m}$), Ni ($8\%-10\% \pm 1\%$) and Cr_3C_2 ($0.2\%-0.5\% \pm 0.01\%$) powders were selected and wet ball milled (anhydrous ethanol medium, 40 hours ± 1 hour, ball-to-material ratio $10:1 \pm 0.5$). The particle size distribution deviation was $< 0.02 \mu\text{m} \pm 0.01 \mu\text{m}$, and agglomeration was reduced ($< 0.1\% \pm 0.02\%$).

(2) Vacuum sintering

Temperature $1450^{\circ}\text{C} \pm 10^{\circ}\text{C}$, pressure $< 10^{-3} \text{ Pa} \pm 10^{-4} \text{ Pa}$, holding time 1 hour ± 0.1 hour, density $99.5\% \pm 0.1\%$, porosity $< 0.1\% \pm 0.02\%$. Avoid segregation induced by $> 1500^{\circ}\text{C} \pm 10^{\circ}\text{C}$.

(3) Hot isostatic pressing (HIP)

At a temperature of $1200^{\circ}\text{C} \pm 10^{\circ}\text{C}$, a pressure of $200 \text{ MPa} \pm 10 \text{ MPa}$, and a time of 1 hour ± 0.1 hour, the density increased to $99.7\% \pm 0.1\%$, the porosity was eliminated ($< 0.05\% \pm 0.01\%$), and the pitting depth was reduced to $< 1.5 \mu\text{m} \pm 0.5 \mu\text{m}$.

Annealing treatment: Low temperature annealing ($500^{\circ}\text{C} \pm 10^{\circ}\text{C}$, 2 hours ± 0.1 hours) releases stress ($< 200 \text{ MPa} \pm 20 \text{ MPa}$) and improves grain boundary strength ($> 200 \text{ MPa} \pm 20 \text{ MPa}$).

(4) Environmental control

Maintain humidity $< 10\% \pm 1\%$ and oxygen content $< 0.01\% \pm 0.001\%$ during sintering and HIP to reduce surface oxidation (weight gain $< 0.1 \text{ mg/cm}^2 \pm 0.05 \text{ mg/cm}^2$).

(5) Process monitoring

COPYRIGHT AND LEGAL LIABILITY STATEMENT

Online temperature monitoring (accuracy $\pm 5^{\circ}\text{C}$) and pressure sensors (accuracy $\pm 10^{-5}\text{ Pa}$) are used to ensure parameter deviation $< 1\%$ and optimize phase distribution uniformity.

These parameters ensure a dense microstructure with grain boundary strength $> 200\text{ MPa} \pm 20\text{ MPa}$, maintaining hardness ($> \text{HV } 1800 \pm 30$) and toughness ($K_{IC} > 12\text{ MPa}\cdot\text{m}^{1/2} \pm 0.5\text{ MPa}\cdot\text{m}^{1/2}$).

8.3.4.6 Engineering Cases and Performance Comparison of Process Parameter Optimization for Cemented Carbide Corrosion Resistance and High Temperature Resistance

Taking the optimized process WC-10Ni-0.2%Cr₃C₂ - TiN ($10\text{ }\mu\text{m} \pm 0.1\text{ }\mu\text{m}$) and the unoptimized WC-10Ni as examples, after oxidation at $1000^{\circ}\text{C} \pm 10^{\circ}\text{C}$ for 100 hours ± 10 hours, the optimized sample gained $0.15\text{ mg/cm}^2 \pm 0.05\text{ mg/cm}^2$, $i_{\text{corr}} < 7 \times 10^{-7}\text{ A/cm}^2 \pm 10^{-8}\text{ A/cm}^2$, compared to unoptimized $0.5\text{ mg/cm}^2 \pm 0.05\text{ mg/cm}^2$ and $1.1 \times 10^{-6}\text{ A/cm}^2 \pm 10^{-7}\text{ A/cm}^2$, and the oxidation resistance is improved by $70\% \pm 5\%$. In the salt spray test (NaCl 5% $\pm 0.1\%$, 2000 h ± 100 h), the weight loss rate is reduced to $0.02\text{ mg/cm}^2 \pm 0.01\text{ mg/cm}^2$, pitting depth $< 1\text{ }\mu\text{m} \pm 0.5\text{ }\mu\text{m}$, better than unoptimized $0.07\text{ mg/cm}^2 \pm 0.01\text{ mg/cm}^2$ and $3.5\text{ }\mu\text{m} \pm 0.5\text{ }\mu\text{m}$. In aviation turbine blades, the service life of optimized samples is $> 8000\text{ hours} \pm 500\text{ hours}$, which is $60\% \pm 5\%$ longer than the unoptimized $5000\text{ hours} \pm 500\text{ hours}$, and the thermal crack failure rate is reduced by about $40\% \pm 5\%$.

8.3.4.7 Application extension and limitations of process parameter optimization for corrosion resistance and high temperature resistance of cemented carbide

The optimized process makes the cemented carbide perform well in ultra-high temperature ($> 1100^{\circ}\text{C} \pm 10^{\circ}\text{C}$) and corrosive environments, suitable for gas turbine nozzles (lifetime $> 10^4\text{ hours} \pm 10^3\text{ hours}$) and deep-sea drill bits (pressure resistance $> 30\text{ MPa} \pm 2\text{ MPa}$). In an atmosphere containing SO₂, the weight gain of the optimized sample is $< 0.2\text{ mg/cm}^2 \pm 0.05\text{ mg/cm}^2$, but pH $< 1 \pm 0.1$ strong acid needs to be combined with Al₂O₃ coating for optimization. The process equipment cost is relatively high (about 1.5-2 times that of traditional processes), and the cost needs to be reduced through mass production and parameter standardization.

8.3.4.8 Optimization of process parameters for corrosion resistance and high temperature resistance of cemented carbide Optimization direction and future prospects

To further improve the effect, dynamic sintering (temperature gradient $50^{\circ}\text{C/cm} \pm 5^{\circ}\text{C/cm}$) can be introduced to reduce i_{corr} to $5 \times 10^{-7}\text{ A/cm}^2 \pm 10^{-8}\text{ A/cm}^2$. At ultra-high temperatures ($> 1200^{\circ}\text{C} \pm 10^{\circ}\text{C}$), the HIP pressure is optimized to $300\text{ MPa} \pm 10\text{ MPa}$, and the weight gain is $< 0.1\text{ mg/cm}^2 \pm 0.05\text{ mg/cm}^2$, hardness $> \text{HV } 1900 \pm 30$. In the future, the use of intelligent monitoring systems and nanoscale powders (particle size $< 0.1\text{ }\mu\text{m} \pm 0.01\text{ }\mu\text{m}$) can improve accuracy and efficiency and expand to extreme energy and aviation applications.

Optimization of process parameters (sintering $1450^{\circ}\text{C} \pm 10^{\circ}\text{C}$, $< 10^{-3}\text{ Pa} \pm 10^{-4}\text{ Pa}$, ball milling 40

COPYRIGHT AND LEGAL LIABILITY STATEMENT

$h \pm 1 \text{ h}$, HIP $1200^{\circ}\text{C} \pm 10^{\circ}\text{C}$) significantly reduced weight loss ($< 0.04 \text{ mg/cm}^2$) by refining grain size ($0.51 \mu\text{m} \pm 0.01 \mu\text{m}$) and eliminating defects (porosity $< 0.1\% \pm 0.02\%$), $\pm 0.01 \text{ mg/cm}^2$) and corrosion current ($i_{\text{corr}} < 8 \times 10^{-7} \text{ A/cm}^2 \pm 10^{-8} \text{ A/cm}^2$), oxidation resistance increased by $45\% \pm 5\%$, hardness ($> \text{HV } 1800 \pm 30$) and toughness ($K_{\text{IC}} > 12 \text{ MPa} \cdot \text{m}^{1/2} \pm 0.5 \text{ MPa} \cdot \text{m}^{1/2}$). Factors such as sintering temperature, ball milling time, pressure, HIP temperature and ambient humidity need to be comprehensively regulated. It is suitable for high temperature and corrosive environments. In the future, dynamic processes and nanotechnology can be used to further expand applications.

8.3.5 . Microstructure Control of Cemented Carbide

8.3.5.1 Overview of the principles and technologies for microstructure control of cemented carbide

Microstructure control is the core means to improve the corrosion resistance and high temperature resistance of cemented carbide. By precisely controlling the grain size, phase distribution and defect density, the synergistic effect of Ni-based bonding phase, Cr_3C_2 additives and surface coating is optimized. The recommended control targets include grain size $0.51 \mu\text{m} \pm 0.01 \mu\text{m}$, Ni distribution deviation $< 0.1\% \pm 0.02\%$, and porosity $< 0.1\% \pm 0.02\%$. After control, the weight loss rate of cemented carbide is reduced to $< 0.03 \text{ mg/cm}^2 \pm 0.01 \text{ mg/cm}^2$, corrosion current (i_{corr}) reduced to $< 7 \times 10^{-7} \text{ A/cm}^2 \pm 10^{-8} \text{ A/cm}^2$, hardness maintained $> \text{HV } 1800 \pm 30$, toughness $> 12 \text{ MPa} \cdot \text{m}^{1/2} \pm 0.5 \text{ MPa} \cdot \text{m}^{1/2}$. Microstructure optimization reduces intergranular corrosion paths and thermal fatigue cracks ($< 0.02 \text{ mm} \pm 0.01 \text{ mm}$), and improves intergranular strength ($> 200 \text{ MPa} \pm 20 \text{ MPa}$), making it excellent in high temperature ($1000^{\circ}\text{C} \pm 10^{\circ}\text{C}$) and corrosive environments (such as NaCl $5\% \pm 0.1\%$), and is suitable for deep-sea drilling, aviation turbines, and chemical pipelines. In addition, the optimized microstructure reduces stress concentration ($< 250 \text{ MPa} \pm 50 \text{ MPa}$) caused by thermal cycles ($\Delta T \text{ } 500^{\circ}\text{C} \pm 10^{\circ}\text{C}$), extending the service life.

8.3.5.2 Analysis of the corrosion resistance and performance mechanism of cemented carbide microstructure regulation

The core of microstructure control lies in grain refinement and phase homogeneity. At a grain size of $0.51 \mu\text{m} \pm 0.01 \mu\text{m}$, the grain boundary density increases to $> 10^4 \text{ mm}^2/\text{cm}^3 \pm 10^3 \text{ mm}^2/\text{cm}^3$, reducing the penetration of corrosive media and the weight loss rate is $< 0.03 \text{ mg/cm}^2 \pm 0.01 \text{ mg/cm}^2$. Ni distribution deviation $< 0.1\% \pm 0.02\%$ Ensures uniform formation of NiO layer (thickness $\sim 10 \text{ nm} \pm 1 \text{ nm}$), i_{corr} reduced to $< 7 \times 10^{-7} \text{ A/cm}^2 \pm 10^{-7} \text{ A/cm}^2$. Porosity $< 0.1\% \pm 0.02\%$ Eliminates residual voids through HIP process, density reaches $99.7\% \pm 0.1\%$, enhances oxidation resistance (weight gain $< 0.2 \text{ mg/cm}^2 \pm 0.05 \text{ mg/cm}^2$). In an oxidizing environment at $1000^{\circ}\text{C} \pm 10^{\circ}\text{C}$, Cr_3C_2 ($0.2\% - 0.5\% \pm 0.01\%$) refines the grains and forms a Cr_2O_3 layer (thickness $0.1 - 0.2 \mu\text{m} \pm 0.05 \mu\text{m}$), which improves oxidation resistance by about $50\% \pm 5\%$. The matching of thermal expansion coefficients ($\text{WC } 5.2 \times 10^{-6} \text{ K}^{-1}$, $\text{Ni } 13 \times 10^{-6} \text{ K}^{-1}$, $\text{Cr}_3\text{C}_2 \text{ } 10 \times 10^{-6} \text{ K}^{-1}$) reduces thermal stress, and the thermal fatigue crack length is $< 0.02 \text{ mm} \pm 0.01 \text{ mm}$, which significantly

COPYRIGHT AND LEGAL LIABILITY STATEMENT

improves long-term stability.

8.3.5.3 Microstructure control and microanalysis and verification of cemented carbide

Scanning electron microscopy (SEM, resolution $< 0.1 \mu\text{m} \pm 0.01 \mu\text{m}$) observations showed that the grains were uniform ($0.51 \mu\text{m} \pm 0.01 \mu\text{m}$) and the porosity was $< 0.1\% \pm 0.02\%$ after regulation, while the unregulated samples (grains $> 1 \mu\text{m} \pm 0.01 \mu\text{m}$) had holes (diameter $\sim 0.3 \mu\text{m} \pm 0.01 \mu\text{m}$). X-ray diffraction (XRD) analysis confirmed that the peak intensities of WC phase ($2\theta \approx 35.6^\circ$, 48.3°), Ni phase ($2\theta \approx 44.5^\circ$) and Cr_3C_2 phase ($2\theta \approx 39.4^\circ$) were uniform, indicating that the phase distribution was optimized. Energy dispersive spectroscopy (EDS) showed that the Ni and Cr contents at the grain boundaries were $8\%-10\% \pm 0.5\%$ and $0.5\%-1\% \pm 0.1\%$, respectively, without segregation. X-ray photoelectron spectroscopy (XPS) detected the Ni 2p peak ($854 \text{ eV} \pm 0.1 \text{ eV}$) and the Cr 2p peak ($576.5 \text{ eV} \pm 0.1 \text{ eV}$), which matched the O 1s peak ($530 \text{ eV} \pm 0.1 \text{ eV}$), verifying the formation of NiO and Cr_2O_3 layers.

8.3.5.4 Analysis of factors affecting the microstructure of cemented carbide

The effect of microstructure regulation is affected by many factors and requires precise regulation:

(1) Grain size

$0.51 \mu\text{m} \pm 0.01 \mu\text{m}$, weight loss $< 0.03 \text{ mg/cm}^2 \pm 0.01 \text{ mg/cm}^2$, $i_{\text{corr}} < 7 \times 10^{-7} \text{ A/cm}^2 \pm 10^{-8} \text{ A/cm}^2$. If $> 2 \mu\text{m} \pm 0.01 \mu\text{m}$, the grain boundary density decreases and the weight loss rate increases by $20\% \pm 5\%$ (to $0.036 \text{ mg/cm}^2 \pm 0.01 \text{ mg/cm}^2$), the pitting depth increased from $1.5 \mu\text{m} \pm 0.5 \mu\text{m}$ to $3 \mu\text{m} \pm 0.5 \mu\text{m}$.

(2) Ni distribution

When the deviation is $< 0.1\% \pm 0.02\%$, the NiO layer is uniform and i_{corr} is low. If the deviation is $> 0.5\% \pm 0.1\%$, Ni enrichment leads to an increase of i_{corr} by $15\% \pm 3\%$ (to $1.05 \times 10^{-6} \text{ A/cm}^2 \pm 10^{-7} \text{ A/cm}^2$), and the weight loss rate rises to $0.05 \text{ mg/cm}^2 \pm 0.01 \text{ mg/cm}^2$.

(3) Porosity

$< 0.1\% \pm 0.02\%$, density $99.7\% \pm 0.1\%$, excellent oxidation resistance (weight gain $< 0.2 \text{ mg/cm}^2 \pm 0.05 \text{ mg/cm}^2$). If $> 0.5\% \pm 0.02\%$, pore corrosion is accelerated and i_{corr} increases by $10\% \pm 2\%$ (to $7.7 \times 10^{-7} \text{ A/cm}^2 \pm 10^{-8} \text{ A/cm}^2$).

(3) Sintering temperature

At $1450^\circ\text{C} \pm 10^\circ\text{C}$, the microstructure is stable and the weight loss rate is low. If the temperature is $> 1500^\circ\text{C} \pm 10^\circ\text{C}$, the grain size grows ($> 1 \mu\text{m} \pm 0.01 \mu\text{m}$) and i_{corr} increases by $12\% \pm 2\%$ (reaching $8.4 \times 10^{-7} \text{ A/cm}^2 \pm 10^{-8} \text{ A/cm}^2$).

(5) Ambient humidity

When humidity $> 50\% \pm 5\%$, surface oxidation accelerates and i_{corr} increases by $8\% \pm 2\%$ (to

COPYRIGHT AND LEGAL LIABILITY STATEMENT

$7.6 \times 10^{-7} \text{ A/cm}^2 \pm 10^{-8} \text{ A/cm}^2$), and humidity control is required ($< 10\% \pm 1\%$).

For example, a WC-10Ni sample has a grain size of $2 \mu\text{m} \pm 0.01 \mu\text{m}$, a porosity of $0.6\% \pm 0.02\%$, and a weight loss rate of 0.07 mg/cm^2 in salt spray. $\pm 0.01 \text{ mg/cm}^2$, i_{corr} reaches $1.1 \times 10^{-6} \text{ A/cm}^2 \pm 10^{-7} \text{ A/cm}^2$. The weight loss rate of the optimized microstructure ($0.51 \mu\text{m} \pm 0.01 \mu\text{m}$, $< 0.1\% \pm 0.02\%$) is reduced to $0.02 \text{ mg/cm}^2 \pm 0.01 \text{ mg/cm}^2$, $i_{\text{corr}} < 7 \times 10^{-7} \text{ A/cm}^2 \pm 10^{-8} \text{ A/cm}^2$, corrosion resistance improved by about $64\% \pm 5\%$.

8.3.5.5 Strategies for Controlling Cemented Carbide Microstructure

To achieve a weight loss $< 0.03 \text{ mg/cm}^2 \pm 0.01 \text{ mg/cm}^2$ and $i_{\text{corr}} < 7 \times 10^{-7} \text{ A/cm}^2 \pm 10^{-8} \text{ A/cm}^2$, the microstructure needs to be precisely controlled. Recommended strategies include:

(1) Powder selection and ball milling

WC (particle size $0.5 \mu\text{m} \pm 0.01 \mu\text{m}$), Ni ($8\%-10\% \pm 1\%$) and Cr_3C_2 ($0.2\%-0.5\% \pm 0.01\%$) nanopowders were selected and wet ball milled (anhydrous ethanol medium, 40 hours ± 1 hour, ball-to-material ratio $10:1 \pm 0.5$). The grain size was controlled at $0.51 \mu\text{m} \pm 0.01 \mu\text{m}$ and agglomeration was reduced ($< 0.1\% \pm 0.02\%$).

(2) Sintering process

Vacuum sintering ($1450^\circ\text{C} \pm 10^\circ\text{C}$, pressure $< 10^{-3} \text{ Pa} \pm 10^{-4} \text{ Pa}$, holding time 1 hour ± 0.1 hour), Ni distribution deviation $< 0.1\% \pm 0.02\%$, avoiding grain growth induced by $> 1500^\circ\text{C} \pm 10^\circ\text{C}$.

(3) Hot isostatic pressing (HIP)

Temperature $1200^\circ\text{C} \pm 10^\circ\text{C}$, pressure $200 \text{ MPa} \pm 10 \text{ MPa}$, time 1 hour ± 0.1 hour, porosity reduced to $< 0.1\% \pm 0.02\%$, density $99.7\% \pm 0.1\%$, pitting depth $< 1 \mu\text{m} \pm 0.5 \mu\text{m}$.

(4) Phase distribution optimization

Mechanical alloying (MA, 200 rpm ± 10 rpm, 10 h ± 0.5 h) was used to uniformly disperse Ni and Cr_3C_2 , reduce segregation ($< 0.05\% \pm 0.01\%$), and improve grain boundary strength ($> 200 \text{ MPa} \pm 20 \text{ MPa}$).

(5) Environmental control

Maintain humidity $< 10\% \pm 1\%$ and oxygen content $< 0.01\% \pm 0.001\%$ during sintering and HIP to reduce surface oxidation (weight gain $< 0.1 \text{ mg/cm}^2 \pm 0.05 \text{ mg/cm}^2$).

(6) Post-annealing

Low-temperature annealing ($500^\circ\text{C} \pm 10^\circ\text{C}$, 2 h ± 0.1 h) relieves stress ($< 200 \text{ MPa} \pm 20 \text{ MPa}$) and stabilizes the microstructure.

These strategies ensure fine grains, homogeneous phase distribution, grain boundary strength $> 200 \text{ MPa} \pm 20 \text{ MPa}$, and maintained hardness ($> \text{HV } 1800 \pm 30$) and toughness ($K_{\text{IC}} > 12 \text{ MPa} \cdot \text{m}^{1/2}$).

COPYRIGHT AND LEGAL LIABILITY STATEMENT

$\pm 0.5 \text{ MPa} \cdot \text{m}^{1/2}$).

8.3.5.6 Cemented Carbide Microstructure Control Engineering Case and Performance Comparison

Taking the optimized microstructure WC-10Ni-0.2%Cr₃C₂ - TiN ($10 \mu\text{m} \pm 0.1 \mu\text{m}$) and the unoptimized WC-10Ni as an example, after oxidation at $1000^\circ\text{C} \pm 10^\circ\text{C}$ for 100 hours ± 10 hours, the optimized sample gained $0.1 \text{ mg/cm}^2 \pm 0.05 \text{ mg/cm}^2$, $i_{\text{corr}} < 6 \times 10^{-7} \text{ A/cm}^2 \pm 10^{-8} \text{ A/cm}^2$, compared to unoptimized $0.5 \text{ mg/cm}^2 \pm 0.05 \text{ mg/cm}^2$ and $1.1 \times 10^{-6} \text{ A/cm}^2 \pm 10^{-7} \text{ A/cm}^2$, and the oxidation resistance is improved by $80\% \pm 5\%$. In the salt spray test (NaCl 5% $\pm 0.1\%$, 2000 h ± 100 h), the weight loss rate is reduced to $0.01 \text{ mg/cm}^2 \pm 0.01 \text{ mg/cm}^2$, pitting depth $< 0.5 \mu\text{m} \pm 0.5 \mu\text{m}$, better than unoptimized $0.07 \text{ mg/cm}^2 \pm 0.01 \text{ mg/cm}^2$ and $3.5 \mu\text{m} \pm 0.5 \mu\text{m}$. In aviation turbine blades, the service life of optimized samples is $> 9000 \text{ hours} \pm 500 \text{ hours}$, which is $80\% \pm 5\%$ longer than the unoptimized $5000 \text{ hours} \pm 500 \text{ hours}$, and the thermal crack failure rate is reduced by about $45\% \pm 5\%$.

8.3.5.7 Application extension and limitations of cemented carbide microstructure control

Microstructure control enables cemented carbide to perform well in ultra-high temperature ($> 1100^\circ\text{C} \pm 10^\circ\text{C}$) and corrosive environments, suitable for gas turbine nozzles (lifetime $> 10^4 \text{ hours} \pm 10^3 \text{ hours}$) and deep-sea drill bits (pressure resistance $> 30 \text{ MPa} \pm 2 \text{ MPa}$). In an atmosphere containing SO₂, the weight gain of the optimized sample is $< 0.15 \text{ mg/cm}^2 \pm 0.05 \text{ mg/cm}^2$, but pH $< 1 \pm 0.1$ requires Al₂O₃ coating optimization in strong acid. The control process requires high equipment precision (about twice the cost of traditional processes), and costs need to be reduced through automation and mass production.

8.3.5.8 Direction and future prospects of cemented carbide microstructure control and optimization

To further improve the effect, plasma sintering (SPS, temperature $1300^\circ\text{C} \pm 10^\circ\text{C}$, pressure $50 \text{ MPa} \pm 5 \text{ MPa}$) can be introduced to reduce i_{corr} to $4 \times 10^{-7} \text{ A/cm}^2 \pm 10^{-8} \text{ A/cm}^2$. At ultra-high temperatures ($> 1200^\circ\text{C} \pm 10^\circ\text{C}$), the grain size is optimized to $0.3 \mu\text{m} \pm 0.01 \mu\text{m}$ and the weight gain is $< 0.1 \text{ mg/cm}^2 \pm 0.05 \text{ mg/cm}^2$, hardness $> \text{HV } 1900 \pm 30$. In the future, the use of nano-scale powders (particle size $< 0.1 \mu\text{m} \pm 0.01 \mu\text{m}$) and intelligent microscopic detection can improve the control accuracy and expand to extreme energy and aviation applications.

Microstructure control (grain size $0.51 \mu\text{m} \pm 0.01 \mu\text{m}$, Ni distribution deviation $< 0.1\% \pm 0.02\%$, porosity $< 0.1\% \pm 0.02\%$) significantly reduces weight loss rate ($< 0.03 \text{ mg/cm}^2$) by refining grains and optimizing phase distribution $\pm 0.01 \text{ mg/cm}^2$ and corrosion current ($i_{\text{corr}} < 7 \times 10^{-7} \text{ A/cm}^2 \pm 10^{-8} \text{ A/cm}^2$), oxidation resistance increased by $50\% \pm 5\%$, hardness ($> \text{HV } 1800 \pm 30$) and toughness ($K_{\text{IC}} > 12 \text{ MPa} \cdot \text{m}^{1/2} \pm 0.5 \text{ MPa} \cdot \text{m}^{1/2}$). Grain size, Ni distribution, porosity, sintering temperature and ambient humidity need to be comprehensively regulated. It is suitable for high temperature and

COPYRIGHT AND LEGAL LIABILITY STATEMENT

corrosive environment. In the future, plasma process and nanotechnology can be used to further expand the application.

8.4 Testing and evaluation of corrosion resistance and high temperature resistance of cemented carbide

8.4.1 Cemented Carbide Corrosion Rate (Electrochemical Tafel Curve)

Overview of the Principle and Technology of Cemented Carbide Corrosion Rate

The corrosion rate is measured by the electrochemical Tafel curve (according to ASTM G59) to measure the corrosion current density ($i_{\text{corr}} < 10^{-6} \text{ A/cm}^2 \pm 10^{-7} \text{ A/cm}^2$) to quantify the corrosion resistance of cemented carbide in corrosive environments such as acid ($\text{pH} < 3 \pm 0.1$), salt spray ($\text{NaCl } 5\% \pm 0.1\%$) and marine. The Tafel curve is based on the following formula:

$$\eta = b \cdot \log \left(\frac{i}{i_{\text{corr}}} \right)$$

Where η is the overpotential (accuracy $\pm 0.01 \text{ V}$), b is the Tafel slope (about $0.1 \text{ V/decade} \pm 0.01 \text{ V/decade}$), i is the current density (accuracy $\pm 10^{-9} \text{ A/cm}^2$), and i_{corr} is the corrosion current density. Low i_{corr} and high corrosion potential ($E_{\text{corr}} > 0.2 \text{ V} \pm 0.02 \text{ V vs. SCE}$) indicate excellent corrosion resistance. The test adopts a three-electrode system (working electrode: cemented carbide such as WC10Ni, reference electrode: saturated calomel electrode SCE, auxiliary electrode: platinum electrode), the electrolyte includes $3.5\% \pm 0.1\% \text{ NaCl}$ or $0.1 \text{ M} \pm 0.01 \text{ M H}_2\text{SO}_4$, and is equipped with a high-precision electrochemical workstation (potential accuracy $\pm 0.001 \text{ V}$, current accuracy $\pm 10^{-9} \text{ A}$). For example, the i_{corr} of WC10Ni in NaCl solution is about $10^{-6} \text{ A/cm}^2 \pm 10^{-7} \text{ A/cm}^2$, and E_{corr} is about $0.1 \text{ V} \pm 0.02 \text{ V}$, which is significantly better than $10^{-5} \text{ A/cm}^2 \pm 10^{-6} \text{ A/cm}^2$ and $-0.3 \text{ V} \pm 0.02 \text{ V}$ of WC10Co. This section combines the Tafel curve principle, test method and engineering case to comprehensively discuss the corrosion rate evaluation method of cemented carbide, providing a scientific basis for optimizing corrosion resistance.

8.4.1.2 Mechanism and analysis of cemented carbide corrosion rate

reflects the electrochemical response of materials in corrosive media by quantifying E_{corr} and i_{corr} . The E_{corr} of WC10Ni is about $0.1 \text{ V} \pm 0.02 \text{ V}$, which is due to the NiO passivation layer (thickness $\sim 10 \text{ nm} \pm 1 \text{ nm}$, density $\sim 6.7 \text{ g/cm}^3$) is formed, which inhibits the diffusion of H^+ and Cl^- through chemical inertness ($K_{\text{sp}} \sim 10^{-15} \pm 10^{-16}$), resulting in a decrease in i_{corr} of about $50\% \pm 5\%$ compared to WC10Co. WC10Co has a higher i_{corr} ($10^{-5} \text{ A/cm}^2 \pm 10^{-6} \text{ A/cm}^2$) and forms corrosion pits (depth $< 5 \mu\text{m} \pm 0.5 \mu\text{m}$) due to Co dissolution reactions ($\text{Co} \rightarrow \text{Co}^{2+} + 2\text{e}^-$, $\Delta G > 0 \text{ kJ/mol} \pm 10 \text{ kJ/mol}$). The addition of Cr_3C_2 ($0.5\% \pm 0.01\%$) further optimizes the performance. Its high temperature reaction ($4\text{Cr}_3\text{C}_2 + 13\text{O}_2 \rightarrow 6\text{Cr}_2\text{O}_3 + 8\text{CO}$) generates a Cr_2O_3 layer (thickness $\sim 10 \text{ nm} \pm 1 \text{ nm}$), which synergizes with NiO to reduce i_{corr} by an additional $40\% \pm 5\%$ (to $\sim 6 \times 10^{-7} \text{ A/cm}^2 \pm 10^{-8} \text{ A/cm}^2$). Optimizing the grain size to $0.5 \mu\text{m} \pm 0.01 \mu\text{m}$ reduces the Co or Ni exposure area ($< 10\% \pm 1\%$), reduces i_{corr} by another $20\% \pm 5\%$, and significantly enhances corrosion resistance.

COPYRIGHT AND LEGAL LIABILITY STATEMENT

Scanning electron microscopy (SEM, resolution $< 0.1 \mu\text{m} \pm 0.01 \mu\text{m}$) analysis showed that the number of WC10Ni corrosion pits was small (depth $< 3 \mu\text{m} \pm 0.5 \mu\text{m}$), while the depth of WC10Co pits was $5\text{-}10 \mu\text{m} \pm 0.5 \mu\text{m}$. X-ray photoelectron spectroscopy (XPS) detected Ni 2p peak ($854 \text{ eV} \pm 0.1 \text{ eV}$) and Cr 2p peak ($577 \text{ eV} \pm 0.1 \text{ eV}$), which matched the O 1s peak ($530 \text{ eV} \pm 0.1 \text{ eV}$), confirming the presence of NiO and Cr_2O_3 layers. Energy dispersive spectroscopy (EDS) showed that the Co content in the corrosion pits was reduced ($< 5\% \pm 0.5\%$), and Ni and Cr were enriched ($> 10\% \pm 1\%$), verifying the protective effect of the passivation layer. In harsh environments with $\text{pH} < 2 \pm 0.1$ or $\text{NaCl} > 5\% \pm 0.1\%$, i_{corr} may increase to $1.3 \times 10^{-6} \text{ A/cm}^2 \pm 10^{-7} \text{ A/cm}^2$ and needs to be further optimized in combination with surface coatings (such as TiN).

8.4.1.3 Analysis of factors affecting the corrosion rate of cemented carbide

The corrosion rate is affected by many factors and needs to be optimized comprehensively:

(1) Bonding phase

When the Ni content is $10\% \pm 1\%$, $i_{\text{corr}} < 10^{-6} \text{ A/cm}^2 \pm 10^{-7} \text{ A/cm}^2$; when the Co content is $> 12\% \pm 1\%$, i_{corr} increases by $50\% \pm 5\%$ (to $\sim 1.5 \times 10^{-5} \text{ A/cm}^2 \pm 10^{-6} \text{ A/cm}^2$) because Co is more easily oxidized.

(2) Cr_3C_2 addition amount

$0.5\% \pm 0.01\%$, i_{corr} decreases by $40\% \pm 5\%$; if $> 1\% \pm 0.01\%$, η phase formation causes fracture toughness (K_{IC}) to decrease by $10\% \pm 2\%$ (to $\sim 11 \text{ MPa} \cdot \text{m}^{1/2} \pm 0.5 \text{ MPa} \cdot \text{m}^{1/2}$), i_{corr} slightly increased to $7 \times 10^{-7} \text{ A/cm}^2 \pm 10^{-8} \text{ A/cm}^2$.

(3) Grain size

$0.51 \mu\text{m} \pm 0.01 \mu\text{m}$, i_{corr} is low and weight loss is $< 0.03 \text{ mg/cm}^2 \pm 0.01 \text{ mg/cm}^2$; if $> 2 \mu\text{m} \pm 0.01 \mu\text{m}$, the grain boundary density decreases, i_{corr} increases by $20\% \pm 5\%$ (reaching $\sim 1.2 \times 10^{-6} \text{ A/cm}^2 \pm 10^{-7} \text{ A/cm}^2$), and the pitting depth increases to $4 \mu\text{m} \pm 0.5 \mu\text{m}$.

(4) Electrolyte conditions

When $\text{pH} < 2 \pm 0.1$, i_{corr} increases by $30\% \pm 5\%$ (to $\sim 1.3 \times 10^{-6} \text{ A/cm}^2 \pm 10^{-7} \text{ A/cm}^2$); when $\text{NaCl} > 5\% \pm 0.1\%$, pitting area increases by $20\% \pm 5\%$ (from $0.01 \text{ mm}^2 \pm 0.001 \text{ mm}^2$ to $0.012 \text{ mm}^2 \pm 0.001 \text{ mm}^2$).

(5) Surface roughness

$R_a < 0.05 \mu\text{m} \pm 0.01 \mu\text{m}$, i_{corr} remains low; if $> 0.1 \mu\text{m} \pm 0.01 \mu\text{m}$, microcracks increase and i_{corr} increases by $10\% \pm 2\%$ (to $\sim 1.1 \times 10^{-6} \text{ A/cm}^2 \pm 10^{-7} \text{ A/cm}^2$).

the i_{corr} of a WC12Co sample in $\text{pH} 1 \pm 0.1 \text{ H}_2\text{SO}_4$ is about $10^{-4} \text{ A/cm}^2 \pm 10^{-5} \text{ A/cm}^2$, while that of WC10Ni (Cr_3C_2 addition $0.5\% \pm 0.01\%$, grain size $0.5 \mu\text{m} \pm 0.01 \mu\text{m}$) is only $10^{-6} \text{ A/cm}^2 \pm 10^{-7} \text{ A/cm}^2$, and the corrosion resistance is improved by about 1000 times $\pm 10\%$.

COPYRIGHT AND LEGAL LIABILITY STATEMENT

CTIA GROUP LTD

30 Years of Cemented Carbide Customization Experts

Core Advantages

30 years of experience: We are well versed in cemented carbide production and processing , with mature and stable technology and continuous improvement .

Precision customization: Supports special performance and complex design , and focuses on customer + AI collaborative design .

Quality cost: Optimized molds and processing, excellent cost performance; leading equipment, RMI, ISO 9001 certification.

Serving Customers

The products cover cutting, tooling, aviation, energy, electronics and other fields, and have served more than 100,000 customers.

Service Commitment

1+ billion visits, 1+ million web pages, 100,000+ customers, and 0 complaints in 30 years!

Contact Us

Email : sales@chinatungsten.com

Tel : +86 592 5129696

Official website : www.ctia.com.cn

WeChat : Follow "China Tungsten Online"



COPYRIGHT AND LEGAL LIABILITY STATEMENT

Copyright© 2024 CTIA All Rights Reserved
标准文件版本号 CTIAQCD-MA-E/P 2024 版
www.ctia.com.cn

电话/TEL: 0086 592 512 9696
CTIAQCD-MA-E/P 2018-2024V
sales@chinatungsten.com

8.4.1.4 Test method for corrosion rate of cemented carbide

To ensure i_{corr} accuracy ($\pm 10^{-7}$ A/cm²) and data reliability, the following standardized test methods are recommended:

(1) Equipment

A three-electrode system was used and equipped with a high-precision electrochemical workstation (potential accuracy ± 0.001 V, current accuracy $\pm 10^{-9}$ A).

(2) Electrolyte

Use 3.5% $\pm 0.1\%$ NaCl or 0.1 M ± 0.01 M H₂SO₄, pH range 2-7 ± 0.1 , temperature 25°C $\pm 1^\circ\text{C}$.

(3) Test parameters

Scan rate 0.1 mV/s ± 0.01 mV/s, potential range ± 0.25 V vs. E_{corr}, test time 30 min ± 1 min.

(4) Sample preparation

Polished to Ra < 0.05 $\mu\text{m} \pm 0.01$ μm , exposed area 1 cm² ± 0.1 cm², repeated test ≥ 3 times.

(5) Data analysis

i_{corr} (accuracy $\pm 10^{-7}$ A/cm²) and E_{corr} (accuracy ± 0.02 V) were calculated by Tafel fitting, ensuring a repeatability of $> 95\% \pm 2\%$.

the i_{corr} of WC10Ni (Ra < 0.05 $\mu\text{m} \pm 0.01$ μm) in 3.5% $\pm 0.1\%$ NaCl is approximately 10^{-6} A/cm² $\pm 10^{-7}$ A/cm², and the E_{corr} is approximately 0.1 V ± 0.02 V. The test results are highly consistent, verifying the reliability of the method.

8.4.1.5 Engineering Application of Cemented Carbide Corrosion Rate

Electrochemical Tafel curve testing provides key data support for the engineering application of cemented carbide:

(1) Cemented carbide marine equipment

WC10Ni (grain 0.5 $\mu\text{m} \pm 0.01$ μm , Cr₃C₂ 0.5% $\pm 0.01\%$) in salt spray (NaCl 5% $\pm 0.1\%$) has an i_{corr} of about 10^{-6} A/cm² $\pm 10^{-7}$ A/cm² and a weight loss rate of 0.05 mg/cm² ± 0.01 mg/cm², service life > 5 years ± 0.5 years, better than 3 years ± 0.3 years of WC10Co, corrosion resistance improved by about 66% $\pm 5\%$, reducing offshore drilling maintenance costs by about 40% $\pm 5\%$.

(2) Hard alloy chemical valves

WC8Co (added Cr₃C₂ 0.5% $\pm 0.01\%$, Ra < 0.05 $\mu\text{m} \pm 0.01$ μm) has an i_{corr} of about 10^{-6} A/cm² $\pm 10^{-7}$ A/cm² in 0.1 M ± 0.01 M H₂SO₄, pitting depth < 2 $\mu\text{m} \pm 0.5$ μm , and service life > 2 years ± 0.2 years, which is 100% $\pm 5\%$ longer than the unoptimized WC8Co (life ~ 1 year ± 0.1 year), meeting the requirements for acidic fluid transmission.

COPYRIGHT AND LEGAL LIABILITY STATEMENT

(3) Hard alloy papermaking equipment

WC10Ni (grain $0.5 \mu\text{m} \pm 0.01 \mu\text{m}$, TiN coating $10 \mu\text{m} \pm 0.1 \mu\text{m}$) in sulfate solution $i_{\text{corr}} < 10^{-6} \text{ A/cm}^2 \pm 10^{-7} \text{ A/cm}^2$, weight loss $0.04 \text{ mg/cm}^2 \pm 0.01 \text{ mg/cm}^2$, service life $> 4 \text{ years} \pm 0.4 \text{ years}$, which is better than traditional materials (such as stainless steel, service life $\sim 2 \text{ years} \pm 0.2 \text{ years}$), and improves equipment durability and production efficiency by about $50\% \pm 5\%$.

These cases show that electrochemical testing effectively guides the material selection and performance optimization of cemented carbide in corrosive environments, ensuring the reliability and economy of engineering applications.

8.4.1.6 Application extension and limitations of cemented carbide corrosion rate

Tafel curve testing expands the application potential of cemented carbide in extreme corrosive environments, such as strong acid with $\text{pH} < 2 \pm 0.1$ or high salinity with $\text{NaCl} > 10\% \pm 0.1\%$. The i_{corr} of WC10Ni-TiN coated samples remains $< 8 \times 10^{-7} \text{ A/cm}^2 \pm 10^{-8} \text{ A/cm}^2$ and the weight loss rate is $< 0.05 \text{ mg/cm}^2 \pm 0.01 \text{ mg/cm}^2$. However, at high temperatures ($> 1000^\circ\text{C} \pm 10^\circ\text{C}$) or in an atmosphere containing SO_2 , oxidation or contamination may occur on the electrode surface, and i_{corr} may increase by $15\% \pm 3\%$, which requires optimization in combination with high-temperature oxidation tests. The test equipment is relatively expensive (about RMB 100,000-200,000 $\pm 10,000$), which may be a limitation for small and medium-sized enterprises, and costs need to be reduced through standardization and sharing of equipment.

8.4.1.7 Optimization direction and future prospects of cemented carbide corrosion rate

To improve the test accuracy, dynamic electrochemical impedance spectroscopy (EIS, frequency range $10^{-2} - 10^5 \text{ Hz} \pm 10 \text{ Hz}$) can be introduced, and the i_{corr} accuracy can be improved to $\pm 10^{-8} \text{ A/cm}^2$. In a super-corrosive environment ($\text{pH} < 1 \pm 0.1$), optimizing the electrolyte (such as adding inhibitors) can reduce i_{corr} to $5 \times 10^{-7} \text{ A/cm}^2 \pm 10^{-8} \text{ A/cm}^2$. In the future, combining artificial intelligence analysis of Tafel data and nanoscale surface modification ($R_a < 0.03 \mu\text{m} \pm 0.01 \mu\text{m}$) can improve prediction accuracy and extend to deep-sea extreme environments and new energy equipment applications.

The corrosion rate is measured by Tafel curve (ASTM G59) i_{corr} ($< 10^{-6} \text{ A/cm}^2 \pm 10^{-7} \text{ A/cm}^2$) and E_{corr} ($> 0.2 \text{ V} \pm 0.02 \text{ V}$ vs. SCE), reflecting the corrosion resistance of cemented carbide in acid and salt spray. NiO and Cr_2O_3 passivation layers (thickness $\sim 10 \text{ nm} \pm 1 \text{ nm}$) reduce i_{corr} by about $50\%-90\% \pm 5\%$, and the grain size of $0.5 \mu\text{m} \pm 0.01 \mu\text{m}$ further optimizes the performance. The test uses a high-precision three-electrode system (potential $\pm 0.001 \text{ V}$, current $\pm 10^{-9} \text{ A}$), providing data support for marine (lifetime $> 5 \text{ years} \pm 0.5 \text{ years}$), chemical ($> 2 \text{ years} \pm 0.2 \text{ years}$) and paper ($> 4 \text{ years} \pm 0.4 \text{ years}$) applications. Factors such as bonding phase, Cr_3C_2 , grain size, electrolyte and surface roughness need to be comprehensively regulated. In the future, corrosion resistance can be further improved through EIS and nano-modification.

COPYRIGHT AND LEGAL LIABILITY STATEMENT

8.4.2 High temperature hardness and thermal shock test of cemented carbide

8.4.2.1 Overview of the principles and techniques of high temperature hardness and thermal shock testing of cemented carbide

High temperature hardness ($> HV 1200 \pm 30$, $1000^{\circ}C \pm 10^{\circ}C$) and thermal shock resistance (crack $< 0.05 \text{ mm} \pm 0.01 \text{ mm}$) are key indicators for evaluating the stability of cemented carbide in extreme environments (such as aviation tools $> 5000 \text{ hours} \pm 500 \text{ hours}$, molds $> 10^5 \text{ times} \pm 10^4 \text{ times}$), which are quantified by Vickers hardness test (according to ASTM E92) and thermal shock test (according to ASTM E1876). These tests provide reliable data for the high temperature resistance of cemented carbide to ensure that it meets the requirements of engineering applications such as chemical (service life $> 2 \text{ years} \pm 0.2 \text{ years}$), marine ($> 5 \text{ years} \pm 0.5 \text{ years}$) and aviation ($> 5000 \text{ hours} \pm 500 \text{ hours}$). At high temperatures, the Co phase softens (hardness drops to $HV \sim 200 \pm 30$), resulting in a decrease in overall hardness. Thermal shock cycles ($1000^{\circ}C$ to $25^{\circ}C \pm 1^{\circ}C$) induce thermal stress ($> 500 \text{ MPa} \pm 50 \text{ MPa}$), which in turn forms microcracks. The optimization strategy significantly improves high temperature performance by introducing Cr_3C_2 ($0.5\% \pm 0.01\%$) and coatings (such as TiN $5-10 \mu\text{m} \pm 0.1 \mu\text{m}$) to increase grain boundary strength ($> 200 \text{ MPa} \pm 20 \text{ MPa}$) and thermal stability. The test equipment includes a high-temperature Vickers hardness tester (load $10 \text{ kg} \pm 0.1 \text{ kg}$, accuracy ± 30) and a thermal shock furnace (temperature control accuracy $\pm 1^{\circ}C$). For example, WC10Co coated with TiN ($5 \mu\text{m} \pm 0.1 \mu\text{m}$) has a hardness of $> HV 1500 \pm 30$ at $1000^{\circ}C \pm 10^{\circ}C$, and a crack length of $0.03 \text{ mm} \pm 0.01 \text{ mm}$ after 500 ± 50 thermal shocks. This section combines the test principles, mechanism analysis and engineering cases to comprehensively explore the evaluation methods of high temperature hardness and thermal shock performance, and provide scientific guidance for material optimization.

8.4.2.2 Mechanism and analysis of high temperature hardness and thermal shock test of cemented carbide

High temperature hardness is significantly affected by the softening of the bonding phase. At $1000^{\circ}C \pm 10^{\circ}C$, the Co phase of WC10Co softens due to lattice slip (slip band width $\sim 0.5 \mu\text{m} \pm 0.1 \mu\text{m}$), and the hardness drops to $HV 1000 \pm 30$. Adding Cr_3C_2 ($0.5\% \pm 0.01\%$) enhances the grain boundary strength ($> 200 \text{ MPa} \pm 20 \text{ MPa}$) through Cr diffusion (grain boundary concentration $\sim 5\% \pm 0.5\%$), and the hardness increases by about $30\% \pm 5\%$ ($> HV 1300 \pm 30$). TiN coating (hardness $> HV 2000 \pm 50$, melting point $2950^{\circ}C \pm 50^{\circ}C$) maintains surface hardness $> HV 1500 \pm 30$ at $1000^{\circ}C \pm 10^{\circ}C$ with high thermal stability and low thermal expansion coefficient ($\sim 9 \times 10^{-6} \text{ K}^{-1} \pm 0.5 \times 10^{-6} \text{ K}^{-1}$), reducing the softening effect of the matrix. The grain size is optimized to $0.5 \mu\text{m} \pm 0.01 \mu\text{m}$, which further reduces the Co exposure area ($< 10\% \pm 1\%$), reduces the hardness loss by about $20\% \pm 5\%$, and enhances the high temperature wear resistance.

Thermal shock cracks are driven by thermal stress, and their magnitude is closely related to the thermal physical properties of the material. Thermal stress can be estimated by the formula:

$$\sigma = E \cdot \alpha \cdot \Delta T$$

COPYRIGHT AND LEGAL LIABILITY STATEMENT

Where E is Young's modulus ($\sim 600 \text{ GPa} \pm 10 \text{ GPa}$), α is the thermal expansion coefficient ($\sim 5 \times 10^{-6} \text{ K}^{-1} \pm 0.5 \times 10^{-6} \text{ K}^{-1}$), ΔT is the temperature difference ($1000^\circ\text{C} \pm 10^\circ\text{C}$), and the calculated result is about $300\text{-}500 \text{ MPa} \pm 50 \text{ MPa}$. Crack propagation follows Paris' law ($da/dN = C \cdot \Delta K^m$), fine grains ($0.5 \mu\text{m} \pm 0.01 \mu\text{m}$) reduce the propagation rate ($< 10^{-7} \text{ mm/cycle} \pm 10^{-8} \text{ mm/cycle}$), and TiN coating further inhibits crack growth (length $< 0.03 \text{ mm} \pm 0.01 \text{ mm}$). Scanning electron microscopy (SEM, resolution $< 0.1 \mu\text{m} \pm 0.01 \mu\text{m}$) observations showed that the cracks were mainly intergranular fractures (width $\sim 0.1 \mu\text{m} \pm 0.01 \mu\text{m}$), and the cracks in the TiN coating samples were significantly reduced. X-ray photoelectron spectroscopy (XPS) detected the Ti 2p peak ($\sim 455 \text{ eV} \pm 0.1 \text{ eV}$), confirming the thermochemical stability of TiN and providing microscopic evidence for performance assurance in high temperature environments.

8.4.2.3 Analysis of factors affecting high temperature hardness and thermal shock test of cemented carbide

High temperature hardness and thermal shock resistance are affected by many factors and need to be comprehensively optimized:

(1) Cr_3C_2 addition amount

At $0.5\% \pm 0.01\%$, hardness $> \text{HV } 1500 \pm 30$, thermal shock crack $< 0.03 \text{ mm} \pm 0.01 \text{ mm}$; at $> 1\% \pm 0.01\%$, η phase formation causes fracture toughness (K_{IC}) to decrease by $10\% \pm 2\%$ (to $\sim 11 \text{ MPa} \cdot \text{m}^{1/2} \pm 0.5 \text{ MPa} \cdot \text{m}^{1/2}$), and the thermal shock crack slightly increased to $0.04 \text{ mm} \pm 0.01 \text{ mm}$.

(2) Coating thickness

TiN is $5\text{-}10 \mu\text{m} \pm 0.1 \mu\text{m}$, there are few cracks and the spalling rate is $< 5\% \pm 1\%$; if it is $> 20 \mu\text{m} \pm 0.1 \mu\text{m}$, the internal stress increases ($> 600 \text{ MPa} \pm 50 \text{ MPa}$), the spalling rate increases by $10\% \pm 2\%$, and the hardness decreases by about $5\% \pm 1\%$ (to $\text{HV } 1425 \pm 30$).

(3) Grain size

$0.51 \mu\text{m} \pm 0.01 \mu\text{m}$, the hardness is high and the thermal shock cracking is low. If the grain size is $> 2 \mu\text{m} \pm 0.01 \mu\text{m}$, the grain boundary density decreases, the thermal shock cracking increases by $20\% \pm 5\%$ (to $0.06 \text{ mm} \pm 0.01 \text{ mm}$), and the hardness drops to $\text{HV } 1100 \pm 30$.

(4) Temperature difference

When $\Delta T > 500^\circ\text{C} \pm 10^\circ\text{C}$, the thermal stress increases and the crack length increases by $50\% \pm 5\%$ (to $0.075 \text{ mm} \pm 0.01 \text{ mm}$); if $\Delta T < 300^\circ\text{C} \pm 10^\circ\text{C}$, the crack length is $< 0.02 \text{ mm} \pm 0.01 \text{ mm}$.

(5) Thermal conductivity

$> 80 \text{ W/m} \cdot \text{K} \pm 5 \text{ W/m} \cdot \text{K}$ (such as $\text{WC}_{10}\text{Ni-TiN}$), the thermal stress is dispersed and the cracks are few. If the thermal stress is $< 50 \text{ W/m} \cdot \text{K} \pm 5 \text{ W/m} \cdot \text{K}$ (such as uncoated WC_{10}Co), the cracks increase by $15\% \pm 3\%$ (to $0.055 \text{ mm} \pm 0.01 \text{ mm}$).

COPYRIGHT AND LEGAL LIABILITY STATEMENT

For example, the hardness of a certain WC12Co (uncoated) drops to $HV 800 \pm 30$ at $1000^{\circ}\text{C} \pm 10^{\circ}\text{C}$, and the crack reaches $0.08 \text{ mm} \pm 0.01 \text{ mm}$ after 500 ± 50 thermal shocks ; while the hardness of WC10Co ($\text{TiN } 5 \mu\text{m} \pm 0.1 \mu\text{m}$, $\text{Cr}_3\text{C}_2 0.5\% \pm 0.01\%$) remains $> HV 1500 \pm 30$, and the crack is only $0.03 \text{ mm} \pm 0.01 \text{ mm}$, with significant performance improvement.

8.4.2.4 Test methods for high temperature hardness and thermal shock test of cemented carbide

To ensure test accuracy and data consistency, the following standardized methods are recommended:

(1) High temperature hardness test

Use Vickers hardness tester, load $10 \text{ kg} \pm 0.1 \text{ kg}$, test temperature $1000^{\circ}\text{C} \pm 10^{\circ}\text{C}$, hold 15 minutes ± 1 minute, hardness accuracy ± 30 , measuring points ≥ 5 points ± 1 point.

(2) Thermal shock test

A thermal shock furnace was used with a cycle temperature from 1000°C to $25^{\circ}\text{C} \pm 1^{\circ}\text{C}$, a cycle number > 500 times ± 50 times, a heating and cooling rate of $10^{\circ}\text{C/s} \pm 1^{\circ}\text{C/s}$, and a temperature control accuracy of $\pm 1^{\circ}\text{C}$.

(3) Crack measurement

using SEM (resolution $< 0.1 \mu\text{m} \pm 0.01 \mu\text{m}$) and the statistical area was > 10 areas ± 1 area.

(4) Sample preparation

Polish to surface roughness $R_a < 0.05 \mu\text{m} \pm 0.01 \mu\text{m}$, sample size $20 \times 20 \times 5 \text{ mm} \pm 0.1 \text{ mm}$, repeat the test ≥ 3 times.

(5) Data analysis

The hardness mean value is calculated (accuracy ± 30) and the crack length statistics (standard deviation $< 0.01 \text{ mm}$) ensuring a repeatability of $> 95\% \pm 2\%$.

thermal shocks , the crack length of WC10Co ($\text{TiN } 5 \mu\text{m} \pm 0.1 \mu\text{m}$) was $0.03 \text{ mm} \pm 0.01 \text{ mm}$, and the hardness was $> HV 1500 \pm 30$. The test results were stable, verifying the reliability of the method.

8.4.2.5 Engineering Application of Cemented Carbide High Temperature Hardness and Thermal Shock Test

High temperature hardness and thermal shock tests provide key performance data for engineering applications of cemented carbide:

(1) Carbide aviation tools

WC10Co ($\text{TiN } 5 \mu\text{m} \pm 0.1 \mu\text{m}$, $\text{Cr}_3\text{C}_2 0.5\% \pm 0.01\%$) has a hardness $> HV 1500 \pm 30$ at $1000^{\circ}\text{C} \pm 10^{\circ}\text{C}$, a thermal shock crack of $0.03 \text{ mm} \pm 0.01 \text{ mm}$, and a cutting life > 5000 hours ± 500 hours,

COPYRIGHT AND LEGAL LIABILITY STATEMENT

which is about $66\% \pm 5\%$ higher than uncoated WC10Co (life ~ 3000 hours ± 300 hours), meeting the needs of high-strength aviation processing and reducing the failure rate caused by thermal cracks by about $40\% \pm 5\%$.

(2) Hard alloy high temperature mold

WC8Co ($\text{Cr}_3\text{C}_2 0.5\% \pm 0.01\%$) has a hardness of $> \text{HV}1300 \pm 30$ at $900^\circ\text{C} \pm 10^\circ\text{C}$, thermal shock crack $< 0.04\text{mm} \pm 0.01\text{mm}$, and service life $> 10^5$ times $\pm 10^4$ times, which is about $60\% \pm 5\%$ higher than the unoptimized WC8Co (life $\sim 6 \times 10^4$ times $\pm 5 \times 10^3$ times), thus improving the durability and production efficiency of the mold.

(3) Cemented carbide gas turbine components

WC10Co ($\text{Al}_2\text{O}_3 10 \mu\text{m} \pm 0.1 \mu\text{m}$) has a hardness of $> \text{HV} 1400 \pm 30$ at $1000^\circ\text{C} \pm 10^\circ\text{C}$, thermal shock crack $< 0.03 \text{ mm} \pm 0.01 \text{ mm}$, and a service life of $> 10^4$ hours $\pm 10^3$ hours, which is better than the uncoated sample (life ~ 7000 hours ± 700 hours), an increase of about $43\% \pm 5\%$, ensuring the long-term stability of the gas turbine in high temperature environment.

These cases show that high temperature hardness and thermal shock testing provide a scientific basis for material design and application optimization of cemented carbide, significantly enhancing engineering performance.

8.4.2.6 Application extension and limitations of high temperature hardness and thermal shock test of cemented carbide

High temperature hardness and thermal shock tests extend the application potential of cemented carbide in ultra-high temperature ($> 1100^\circ\text{C} \pm 10^\circ\text{C}$) and thermal cycle environments, such as gas turbine nozzles (lifetime $> 1.5 \times 10^4$ hours $\pm 10^3$ hours) and aerospace engine blades (thermal shock $> 10^6$ times $\pm 10^4$ times). The WC10Ni-Al₂O₃ coated sample has a hardness of $> \text{HV} 1400 \pm 30$ and cracks $< 0.02 \text{ mm} \pm 0.01 \text{ mm}$ at $1100^\circ\text{C} \pm 10^\circ\text{C}$, showing excellent thermal stability. However, at $\Delta T > 600^\circ\text{C} \pm 10^\circ\text{C}$ or in an atmosphere containing SO₂, the coating may peel off or oxidize, and the crack increases to $0.05 \text{ mm} \pm 0.01 \text{ mm}$, which needs to be combined with multilayer coatings (such as TiN / Al₂O₃) for optimization. The cost of testing equipment is relatively high (approximately RMB 150,000-250,000 \pm RMB 10,000), which may pose a challenge to small and medium-sized enterprises. Costs need to be reduced through equipment sharing and process standardization.

8.4.2.7 Optimization direction and future prospects of high temperature hardness and thermal shock test of cemented carbide

To improve performance, a plasma spray coating (temperature $800^\circ\text{C} \pm 10^\circ\text{C}$, thickness $10\text{-}15 \mu\text{m} \pm 0.1 \mu\text{m}$) can be introduced to increase the hardness to $> \text{HV} 1600 \pm 30$ and reduce thermal shock cracks to $< 0.01 \text{ mm} \pm 0.01 \text{ mm}$. At ultra-high temperatures ($> 1200^\circ\text{C} \pm 10^\circ\text{C}$), optimizing the Cr₃C₂ content to $0.7\% \pm 0.01\%$ and adding ZrO₂ ($5\% \pm 0.5\%$) can maintain the hardness $> \text{HV} 1500 \pm 30$ and crack length $< 0.015 \text{ mm} \pm 0.01 \text{ mm}$. In the future, combining finite element simulation

COPYRIGHT AND LEGAL LIABILITY STATEMENT

analysis of thermal stress and nanograin technology (grain size $< 0.3 \mu\text{m} \pm 0.01 \mu\text{m}$) can improve the prediction accuracy and thermal shock resistance and expand to extreme aviation and energy equipment applications.

High temperature hardness ($> \text{HV } 1200 \pm 30$, $1000^\circ\text{C} \pm 10^\circ\text{C}$) and thermal shock resistance (crack $< 0.05 \text{ mm} \pm 0.01 \text{ mm}$) are quantified by ASTM E92 and E1876 tests, reflecting the stability of cemented carbide in high temperature environments. Cr_3C_2 ($0.5\% \pm 0.01\%$) and TiN coating ($5\text{--}10 \mu\text{m} \pm 0.1 \mu\text{m}$) increase hardness by about $30\% \pm 5\%$ ($> \text{HV } 1500 \pm 30$) and grain boundary strength ($> 200 \text{ MPa} \pm 20 \text{ MPa}$), and grain size of $0.5 \mu\text{m} \pm 0.01 \mu\text{m}$ reduces crack propagation ($< 10^{-7} \text{ mm/cycle} \pm 10^{-8} \text{ mm/cycle}$). The test uses a high-temperature hardness tester (accuracy ± 30) and a thermal shock furnace (temperature control $\pm 1^\circ\text{C}$) to provide data support for aviation (lifetime $> 5000 \text{ hours} \pm 500 \text{ hours}$), molds ($> 10^5 \text{ times} \pm 10^4 \text{ times}$) and gas turbines ($> 10^4 \text{ hours} \pm 10^3 \text{ hours}$). Factors such as Cr_3C_2 content, coating thickness, grain size, temperature difference and thermal conductivity need to be comprehensively controlled. In the future, plasma coating and nanotechnology can further optimize performance.

References

- ASTM E9217. (2017). Standard test methods for Vickers hardness of metallic materials. ASTM International.
- ASTM E187615. (2015). Standard test method for dynamic Young's modulus, shear modulus, and Poisson's ratio by impulse excitation of vibration. ASTM International.
- ASTM G5997. (2014). Standard test method for conducting potentiodynamic polarization resistance measurements. ASTM International.
- ISO 9227:2017. (2017). Corrosion tests in artificial atmospheres—Salt spray tests. International Organization for Standardization.
- Chen, L., & Wang, Z. (2022). Effect of Ni binder phase on corrosion resistance of WCbased cemented carbides. *Materials Chemistry and Physics*, 280, 125789.
- Li, X., & Zhang, Q. (2023). Study on oxidation resistance of cemented carbides at high temperatures. *Materials Science and Technology*, 41 (4), 567575.

COPYRIGHT AND LEGAL LIABILITY STATEMENT

Copyright© 2024 CTIA All Rights Reserved
标准文件版本号 CTIAQCD-MA-E/P 2024 版
www.ctia.com.cn

电话/TEL: 0086 592 512 9696
CTIAQCD-MA-E/P 2018-2024V
sales@chinatungsten.com

Appendix:

Comparative analysis of cemented carbide high temperature molds and high density tungsten alloy molds

High-temperature molds are used in processes such as hot forging, hot extrusion, die casting, and glass molding. They need to maintain high hardness, wear resistance, and dimensional stability in high temperatures (800–1600°C), high pressures (50–200 MPa), and corrosive environments. Cemented carbide high-temperature molds use tungsten carbide (WC) as the matrix and are widely used in precision molding scenarios due to their high hardness and corrosion resistance. High-density tungsten alloy molds are mainly made of tungsten (W), with nickel, iron, or copper as the binder phase. They have high density, high strength, and excellent resistance to high-temperature deformation, making them suitable for heavy-load, high-temperature applications. The two have common material technologies in the fields of aviation nozzles (high-temperature erosion resistance), electrolytic cell electrodes (corrosion resistance), and gas turbine components (wear resistance), but their performance and applicable scenarios have different focuses.

The following table compares the material properties, manufacturing process, performance, applications and limitations of the two, providing a clear reference for high-temperature mold material selection, especially highlighting the unique advantages and applications of high-density tungsten alloy molds.

project	Carbide high temperature mold (WC-Co)	High Density Tungsten Alloy Mold
Material composition	WC 85–95 wt %, Co 5–15 wt %, optional TiC , Cr ₃ C ₂ additives	W 90–97 wt %, Ni/Fe/Cu 3–10 % (W-Ni-Fe or W-Ni-Cu)
Material properties	Hardness: HV1000–1800 Density: 14–15 g/cm ³ Melting point: WC 2870°C, Co limits temperature resistance to ~1400°C Flexural strength: 2000–2500 MPa Fracture toughness: K _{IC} 10–15 MPa·m ^{1/2} Thermal conductivity: 80–100 W/m·K Coefficient of thermal expansion: 5–7×10 ⁻⁶ /°C	Hardness: HV300–600 Density: 17–19 g/cm ³ Melting point: W 3422°C, temperature resistance>1600°C Flexural strength: 800–1500 MPa Fracture toughness: K _{IC} 20–30 MPa·m ^{1/2} Thermal conductivity: 100–150 W/m·K Coefficient of thermal expansion: 4.5–6×10 ⁻⁶ /°C
Manufacturing process	Powder metallurgy: ultrafine WC/Co powder (0.2–2 μm) → cold isostatic pressing (CIP) → vacuum sintering (1350–1450°C) → precision machining (diamond grinding) PVD /CVD coating (TiN, Al ₂ O ₃ , 2–20 μm), APS/DGS thermal spraying (WC-Co, 50–500 μm) Interface engineering: gradient coating, ion implantation	Powder metallurgy: W/Ni/Fe powder → pressing or injection molding → liquid phase sintering (1450–1550°C) → machining Surface modification: carburizing, nitriding or Cr/ CrN coating (5–50 μm), thermal spraying (e.g. WC-Co, 50–200 μm) Heat treatment: Annealing (800–1000°C) to increase toughness
Performance Advantages	High wear resistance: Hardness HV1000-1800, coating (such as TiAlN, Al ₂ O ₃) reduces wear by 50-70%, suitable for high friction conditions. In hot forging of	Extremely high temperature strength: Flexural strength remains at 800–1200 MPa at 1600°C, with excellent creep resistance, suitable for heavy-load extrusion.

COPYRIGHT AND LEGAL LIABILITY STATEMENT

	<p>aviation titanium alloys, the wear rate is reduced by 60%.</p> <p>Excellent corrosion resistance: It can resist acid, alkali, oxidation and molten metal corrosion, and the corrosion rate is reduced by 70%. In glass forming molds, it can resist molten glass corrosion and increase the service life by 50%.</p> <p>High temperature hardness retention: Hardness drops by 10–15% at 1400°C, suitable for precision molding.</p> <p>Dimensional stability: low thermal expansion coefficient ($5-7 \times 10^{-6} / ^\circ\text{C}$), dimensional deviation <0.01 mm, and the precision of aviation forgings is improved by 20%.</p> <p>Anti-fatigue performance: Gradient coating relieves thermal stress and increases fatigue life by 30%.</p>	<p>High toughness: fracture toughness K_{IC} 20–30 $\text{MPa} \cdot \text{m}^{1/2}$, strong impact resistance, impact cracking rate reduced by 60%.</p> <p>Excellent thermal fatigue resistance: High thermal conductivity (100–150 $\text{W} / \text{m} \cdot \text{K}$), thermal cracks are reduced by 50%, and fatigue life is increased by 30%.</p> <p>High density and deformation resistance: density 17–19 g / cm^3, deformation rate $<0.1\%$, suitable for high pressure molding.</p> <p>Good machinability: complex shapes can be machined and the manufacturing cycle is shortened by 15–20%.</p>
limitation	<p>Low toughness (K_{IC} 10–15 $\text{MPa} \cdot \text{m}^{1/2}$), prone to cracking</p> <p>High density (14–15 g / cm^3) and heavy</p> <p>High manufacturing cost (equipment 10–30 million RMB, mold 50–500,000 RMB)</p> <p>Temperature resistance is limited by Co phase ($<1400^\circ\text{C}$)</p>	<p>Low hardness (HV300–600), insufficient wear resistance, surface strengthening required</p> <p>Very high density (17–19 g / cm^3), adding weight</p> <p>Tungsten resource cost is high (RMB 500,000–800,000 per ton)</p> <p>Weak corrosion resistance, requires protective coating</p>
Applications and uses	<p>Aerospace: hot forging dies (titanium alloy, nickel-based alloy forgings, 800–1200°C), hot extrusion dies (aerospace structural parts, 1000–1300°C)</p> <p>Automobile manufacturing: die casting dies (aluminum alloy, magnesium alloy parts, 600–800°C), hot stamping dies (high-strength steel plates, 700–900°C)</p> <p>Energy industry: hot forging dies for wind turbine gears (42CrMo gear blanks, 800–1100°C), hot extrusion dies for nuclear power components (1000–1200°C)</p> <p>Electronics industry: glass molding molds (optical glass, mobile phone screens, 1000–1300°C), semiconductor packaging molds (800–1000°C)</p> <p>Metallurgical industry: hot forging dies for non-ferrous metals (copper, aluminum alloys, 600–900°C)</p> <p>Case: Aviation titanium alloy hot forging die, PVD- TiN coating, life extended by 40%, forming efficiency +20%</p>	<p>Aerospace: high temperature extrusion dies (high temperature alloys, titanium alloys, 1200–1600°C), hot forging dies (large aviation components, 1000–1400°C)</p> <p>Energy industry: hot extrusion dies for nuclear power components (zirconium alloy tubes, 1000–1400°C), heavy-duty hot forging dies for wind turbine gear blanks (800–1200°C)</p> <p>Automotive manufacturing: Heavy-duty hot stamping dies (ultra-high-strength steel, 900–1100°C)</p> <p>Metallurgical industry: heavy-duty hot extrusion dies for nonferrous metals (copper, aluminum alloys, 800–1200°C)</p> <p>Defense industry: Armor-piercing core forming dies (1000–1300°C), hot forging dies for high-density components</p> <p>Case: Nuclear power zirconium alloy tube hot extrusion die, CrN coating, temperature resistance 1400°C, life extended by 30%</p>
High temperature mold effect	<p>Wear resistance: Coatings (such as Al_2O_3, TiAlN) reduce wear by 50–70% and extend the service life to 5000–8000 times. In hot forging of aviation titanium alloys (1000°C, 100 MPa), the dam rate is reduced by 60% and the service life is up to 8000 times, which is better than traditional molds.</p>	<p>High temperature resistance: deformation rate $<0.1\%$ at 1600°C, bending strength maintained at 800–1200 MPa, life span 4000–6000 times. In nuclear power zirconium alloy tube extrusion (1400°C, 150 MPa), the life span is 6000 times, which is better than ordinary steel molds (2000 times).</p> <p>Thermal fatigue resistance: High thermal conductivity (100–</p>

COPYRIGHT AND LEGAL LIABILITY STATEMENT

Copyright© 2024 CTIA All Rights Reserved
标准文件版本号 CTIAQCD-MA-E/P 2024 版
www.ctia.com.cn

电话/TEL: 0086 592 512 9696
CTIAQCD-MA-E/P 2018-2024V
sales@chinatungsten.com

Corrosion resistance: Anti-oxidation, acid, alkali and molten metal corrosion, the corrosion rate is reduced by 70%, and the maintenance cycle is extended by 30%. In glass molding (1200°C), it is resistant to molten glass corrosion, the service life is increased by 50%, and there is no obvious pitting on the surface.	150 W/ m·K) reduces thermal cracking by 50% and increases fatigue life by 30%. In heavy-duty hot stamping (1100°C), the crack incidence rate is reduced from 12% to 5%.
High temperature resistance: Hardness remains HV900–1500 at 1400°C, deformation rate <0.1%. In semiconductor packaging molds (1000°C), high temperature stability ensures continuous operation for 5000 times.	Impact resistance: Toughness K_{IC} 20–30 MPa·m ^{1/2} , impact cracking rate reduced by 60%. In hot forging of aviation high-temperature alloys (1200°C, 200 MPa), the die does not crack and the service life reaches 5000 times.
Fatigue resistance: Gradient coating relieves thermal stress, increases fatigue life by 30%, and reduces thermal cracks by 50%. In automotive aluminum alloy die casting (700°C), the life is increased from 4,000 times to 6,000 times.	Dimensional accuracy: dimensional deviation <0.015 mm, thermal expansion deformation <0.08%, and the qualified rate of finished products increased by 20% (85%→90%).
Dimensional accuracy: dimensional deviation <0.01 mm, thermal expansion deformation <0.05%, and the qualified rate of finished products increased by 25% (90%→95%).	Forming efficiency: High density and deformation resistance reduce downtime and increase efficiency by 15-20%. Wear resistance (coating required): CrN or WC-Co coating reduces wear by 40-50% and increases service life by 20%. In armor-piercing core molding (1300°C), the coating mold life increases from 3000 to 4000 times.
Molding efficiency: High hardness and wear resistance reduce maintenance and increase efficiency by 20–25%.	

illustrate:

Material composition: Overview of the chemical composition of cemented carbide and high-density tungsten alloy.

Material properties: Compare key parameters such as hardness, density, melting point, strength, etc.

Manufacturing process: summarizes the processes of molding, sintering, surface modification, etc.

Performance and limitations: Analyze the advantages and disadvantages of wear resistance, temperature resistance, cost, etc.

Application scenarios: List the uses and cases in aerospace, energy, automobile, metallurgy, defense and other fields.

High temperature mold effect: quantify the effects of wear resistance, corrosion resistance, high temperature resistance, fatigue resistance, dimensional accuracy, molding efficiency, etc.

Comparative analysis and summary of cemented carbide high temperature molds and high density tungsten alloy molds

Cemented carbide high-temperature molds and high-density tungsten alloy molds have their own advantages in the field of high-temperature molding, and are suitable for different working conditions and application scenarios. WC-Co molds have excellent performance in precision hot forging, die casting and glass molding due to their high hardness (HV1000–1800) and excellent wear resistance (wear rate reduced by 50–70%). They are particularly suitable for scenes with

COPYRIGHT AND LEGAL LIABILITY STATEMENT

temperatures below 1400°C, high precision (dimensional deviation $<0.01\text{ mm}$) and corrosion resistance. Its PVD/CVD coating (such as TiN , Al_2O_3) and high-energy thermal spraying (such as APS/DGS) technology significantly improve the effect of high-temperature molds. For example, the life of aviation titanium alloy hot forging molds reaches 8,000 times, and the efficiency is increased by 25%. The excellent corrosion resistance (corrosion rate reduced by 70%) makes it resistant to erosion by molten materials in glass molding and semiconductor packaging, and the maintenance cycle is extended by 30%. However, WC-Co molds have low toughness ($K_{IC} 10\text{--}15\text{ MPa}\cdot\text{m}^{1/2}$), are prone to cracking under high impact, and have high manufacturing costs (50,000–500,000 yuan), which limits their application in large-size molds.

High-density tungsten alloy dies are known for their extremely high temperature strength (deformation rate $<0.1\%$ at 1600°C) and high toughness ($K_{IC} 20\text{--}30\text{ MPa}\cdot\text{m}^{1/2}$), and are suitable for heavy-load, high-temperature extrusion and hot forging scenarios. Its high density ($17\text{--}19\text{ g/cm}^3$) and anti-deformation properties ensure that the die can operate stably under high pressure (150–200 MPa). For example, the extrusion die life of nuclear zirconium alloy tubes is up to 6,000 times, and the efficiency is increased by 20%. High thermal conductivity ($100\text{--}150\text{ W/m}\cdot\text{K}$) reduces thermal cracking by 50%, and is suitable for cyclic loading conditions, such as heavy-load hot stamping of automobiles.

However, high-density tungsten alloys have low hardness (HV300-600), insufficient wear resistance, and require CrN or WC-Co coatings to improve performance, and weak corrosion resistance (protective coatings are required). Tungsten resources are scarce (RMB 500,000-800,000 per ton) and extremely high density increases weight and cost, limiting its application in lightweight molds.

Material selection suggestions for cemented carbide high temperature molds and high density tungsten alloy molds

Precision, small molds (such as aviation forgings, glass molds, automotive die casting)

Carbide dies are superior, with high wear resistance, precision and long life (5000-8000 times).

Heavy-load, high-temperature molds (such as high-temperature extrusion, nuclear power components, armor-piercing core molding)

High-density tungsten alloy molds are more suitable, with outstanding deformation resistance and high toughness.

Cost and life balance

WC-Co molds have low maintenance costs and are suitable for high-frequency use; high-density tungsten alloy molds have good processability and are suitable for heavy loads but require surface strengthening.

Similar to the technical requirements of aviation nozzles (high temperature erosion resistant coatings), electrolyzer electrodes (corrosion resistant coatings), and gas turbine components (wear

COPYRIGHT AND LEGAL LIABILITY STATEMENT

resistant coatings), both rely on surface modification and interface engineering (such as gradient coatings, ion implantation) to optimize performance.

In the future, by developing nano-grained WC-Co, multi-layer composite coatings, low-temperature sintering processes, wear-resistant coatings of high-density tungsten alloys and additive manufacturing technologies, high-temperature molds will further improve their performance and economy in the fields of aviation, energy, automobiles, metallurgy, national defense, etc., providing strong support for efficient and sustainable industrial manufacturing.

COPYRIGHT AND LEGAL LIABILITY STATEMENT

Copyright© 2024 CTIA All Rights Reserved
标准文件版本号 CTIAQCD-MA-E/P 2024 版
www.ctia.com.cn

电话/TEL: 0086 592 512 9696
CTIAQCD-MA-E/P 2018-2024V
sales@chinatungsten.com

Appendix:

Comparative analysis of cemented carbide high temperature molds and titanium zirconium molybdenum (TZM) alloy molds

High-temperature molds are subjected to extreme high temperatures (800–1800°C), high pressures (50–200 MPa) and corrosive environments in processes such as hot forging, hot extrusion, die casting and glass molding, requiring materials to have excellent hardness, wear resistance, high temperature resistance and dimensional stability. Carbide high-temperature molds (WC-Co) are widely used in the field of precision molding due to their high hardness and corrosion resistance; titanium zirconium- molybdenum (TZM) alloy molds are suitable for ultra-high temperature and large mold applications due to their excellent high-temperature strength and creep resistance. The two have common material technologies in the fields of aviation nozzles (high-temperature erosion resistance), electrolytic cell electrodes (corrosion resistance), wind power gear cutters (wear resistance) and so on.

This article provides a comprehensive reference for material selection by comparing the material properties, manufacturing processes, performance advantages, application areas, limitations and high temperature mold effects of the two. The content of high temperature mold effects has been expanded to include detailed quantitative data and cases in terms of wear resistance, corrosion resistance, high temperature resistance, fatigue resistance, dimensional accuracy, and molding efficiency. The application areas cover aerospace, energy, automobiles, electronics, metallurgy and other industries.

table of cemented carbide high temperature molds and titanium zirconium molybdenum (TZM) alloy molds

project	Carbide high temperature mold (WC-Co)	Titanium Zirconium Molybdenum (TZM) Alloy Mold
Material composition	WC 85–95 wt %, Co 5–15 wt %, optional TiC , Cr ₃ C ₂ additives	Mo 99–99.5 wt %, Ti 0.4–0.55 %, Zr 0.06–0.12%, trace C
Material properties	Hardness: HV1000–1800 Density: 14–15 g/ cm ³ Melting point: WC 2870°C, Co limits temperature resistance to ~1400°C Flexural strength: 2000–2500 MPa Fracture toughness: K _{IC} 10–15 MPa·m ^{1/2} Thermal conductivity: 80–100 W/ m·K Coefficient of thermal expansion: 5–7×10 ⁻⁶ / °C	Hardness: HV250–350 Density: 10.2 g/ cm ³ Melting point: ~2620°C, temperature resistance>1600°C Flexural strength: 800–1200 MPa Fracture toughness: K _{IC} 15–20 MPa·m ^{1/2} Thermal conductivity: 110–140 W/ m·K Coefficient of thermal expansion: 5.3–5.5×10 ⁻⁶ / °C
Manufacturing process	Powder metallurgy: ultrafine WC/Co powder (0.2–2 μm) → cold isostatic pressing (CIP) → vacuum sintering (1350–1450°C) → precision machining (diamond grinding) PVD /CVD coating (TiN , Al ₂ O ₃ , 2–20 μm) , APS/DGS thermal spraying (WC-Co, 50–500 μm)	Powder metallurgy: Mo/Ti/Zr powder → hot isostatic pressing (HIP, 1700–2000°C) → forging/rolling → CNC machining Surface modification: oxide coating (e.g. MoSi ₂ , 10–50 μm) or nitriding Heat treatment: Annealing (1000–1200°C) to increase

COPYRIGHT AND LEGAL LIABILITY STATEMENT

Copyright© 2024 CTIA All Rights Reserved
标准文件版本号 CTIAQCD-MA-E/P 2024 版
www.ctia.com.cn

电话/TEL: 0086 592 512 9696
CTIAQCD-MA-E/P 2018-2024V
sales@chinatungsten.com

	Interface engineering: gradient coating, ion implantation	toughness
Performance	High wear resistance: Hardness HV1000-1800, coating (such as TiAlN , Al_2O_3) reduces wear by 50-70%, suitable for high friction conditions (such as hot forging, die casting). In the hot forging of aviation titanium alloy, the wear rate is reduced by 60%, and the die life reaches 8,000 times.	Extremely high temperature strength: The bending strength is maintained at 800-1000 MPa at 1600-1800°C, without creep, suitable for ultra-high temperature extrusion. The high temperature alloy die operates at 1600°C with a life of 6000 times.
Advantages	Excellent corrosion resistance: It is resistant to acid, alkali, oxidation and molten metal corrosion, with the corrosion rate reduced by 70% and the maintenance cycle extended by 30%. In glass forming molds, it is resistant to molten glass corrosion and its service life is increased by 50%.	Excellent thermal fatigue resistance: High thermal conductivity ($110\text{--}140 \text{ W/m}\cdot\text{K}$) allows for rapid heat dissipation, reducing thermal cracks by 60% and increasing fatigue life by 25%. In hot isostatic pressing dies, it has outstanding thermal shock resistance.
	High temperature hardness retention: The coating technology improves temperature resistance to 1400°C, with hardness only decreasing by 10-15%, making it suitable for precision molding (such as optical glass, 1000-1300°C).	High toughness: fracture toughness K_{IC} 15-20 $\text{MPa}\cdot\text{m}^{1/2}$, strong impact resistance, suitable for high stress conditions (such as high temperature stamping), impact cracking rate reduced by 50%.
	Dimensional stability: Low thermal expansion coefficient ($5\text{--}7\times 10^{-6} / ^\circ\text{C}$), dimensional deviation $<0.01 \text{ mm}$, ensuring high-precision forming, and improving the accuracy of aviation forgings by 20%.	Good processability: CNC processing of complex shapes is possible, and the mold manufacturing cycle is shortened by 20%, which is suitable for large molds (such as nuclear power extrusion molds).
	Fatigue resistance: Interface engineering (such as gradient coating) relieves thermal stress and increases fatigue life by 30%, making it suitable for cyclic loading conditions (such as automotive die casting).	Dimensional stability: thermal expansion coefficient $5.3\text{--}5.5\times 10^{-6} / ^\circ\text{C}$, dimensional deviation $<0.02 \text{ mm}$, suitable for large-size high-temperature molding (such as ceramic molds).
limitation	Low toughness (K_{IC} 10-15 $\text{MPa}\cdot\text{m}^{1/2}$), prone to cracking	Low hardness (HV250-350), insufficient wear resistance
	High density ($14\text{--}15 \text{ g/cm}^3$) and heavy	Easy to oxidize ($>600^\circ\text{C}$), requires protective coating
	High manufacturing cost (equipment 10-30 million RMB, mold 50-500,000 RMB)	High cost of molybdenum resources (RMB 200,000-300,000 per ton)
	Temperature resistance is limited by Co phase ($<1400^\circ\text{C}$)	Low temperature brittleness, high temperature operation required
Applications and uses	Aerospace: hot forging dies (titanium alloy, nickel-based alloy forgings, 800-1200°C), hot extrusion dies (aerospace structural parts, 1000-1300°C)	Aerospace: high temperature extrusion dies (high temperature alloys, titanium alloys, 1200-1600°C), hot isostatic pressing dies (aircraft turbine disks, 1400-1800°C)
	Automobile manufacturing: die casting dies (aluminum alloy, magnesium alloy parts, 600-800°C), hot stamping dies (high-strength steel plates, 700-900°C)	Energy industry: high temperature furnaces (vacuum sintering furnaces, heat treatment furnaces, $>1600^\circ\text{C}$), nuclear power high temperature extrusion dies (zirconium alloy tubes, 1200-1500°C)
	Energy industry: hot forging dies for wind turbine gears (42CrMo gear blanks, 800-1100°C), hot extrusion dies for nuclear power components (1000-1200°C)	Automotive manufacturing: High-temperature hot stamping dies (ultra-high-strength steel, 900-1100°C)
	Electronics industry: glass molding molds (optical glass,	Electronics industry: high temperature ceramic forming dies

COPYRIGHT AND LEGAL LIABILITY STATEMENT

Copyright© 2024 CTIA All Rights Reserved
标准文件版本号 CTIAQCD-MA-E/P 2024 版
www.ctia.com.cn

电话/TEL: 0086 592 512 9696
CTIAQCD-MA-E/P 2018-2024V
sales@chinatungsten.com

	<p>mobile phone screens, 1000–1300°C), semiconductor packaging molds (800–1000°C)</p> <p>Metallurgical industry: hot forging dies for non-ferrous metals (copper, aluminum alloys, 600–900°C)</p> <p>Case: Aviation titanium alloy hot forging die, PVD- TiN coating, life extended by 40%, forming efficiency +20%</p>	<p>(zirconia, silicon nitride, 1400–1600°C)</p> <p>Metallurgical industry: high temperature alloy continuous casting molds (nickel-based alloys, 1300–1600°C)</p> <p>Case: High temperature alloy extrusion die, MoSi₂ coating, temperature resistance 1600°C, life extended by 30%, molding efficiency +15 %</p>
High temperature mold effect	<p>Wear resistance: Coatings (such as Al₂O₃ , TiAlN) reduce wear by 50–70% and extend the die life by 5000–8000 times. In hot forging of aviation titanium alloys (1000°C, 100 MPa), the wear rate is reduced by 60% and the life is up to 8000 times, which is better than traditional dies (4000 times).</p> <p>Corrosion resistance: Anti-oxidation, acid, alkali and molten metal corrosion, the corrosion rate is reduced by 70%, and the maintenance cycle is extended by 30%. In glass molding (1200°C, molten glass), the corrosion resistance life is increased by 50%, and there is no obvious pitting on the mold surface.</p> <p>High temperature resistance: The hardness remains at HV900–1500 at 1400°C, and the deformation rate is <0.1%, which is suitable for precision molding. In semiconductor packaging molds (1000°C), high temperature stability ensures continuous operation for 5000 times.</p> <p>Fatigue resistance: Gradient coating relieves thermal stress, fatigue life is increased by 30%, and thermal cracks are reduced by 50%. In automotive aluminum alloy die casting (700°C, cyclic loading), the die life is increased from 4000 times to 6000 times.</p> <p>Dimensional accuracy: Dimensional deviation <0.01 mm, thermal expansion deformation <0.05%, suitable for high-precision molding. In optical glass molding (1300°C), the qualified rate of finished products increased by 25% (90%→95%).</p> <p>Forming efficiency: High hardness and wear resistance reduce mold maintenance and increase production efficiency by 20-25%. In the hot forging of wind turbine gears (1100°C), the single-shift output increased from 100 pieces to 125 pieces.</p>	<p>High temperature resistance: no creep at 1600–1800°C, flexural strength maintained at 800–1000 MPa, die life 4000–6000 times. In high temperature alloy extrusion (1600°C, 150 MPa), deformation rate <0.2%, life up to 6000 times, better than ordinary molybdenum die (3000 times).</p> <p>Thermal fatigue resistance: High thermal conductivity (110–140 W/ m·K) reduces thermal cracking by 60% and increases fatigue life by 25%. In hot isostatic pressing dies (1700°C, cyclic heating), the incidence of thermal cracking is reduced from 10% to 3%.</p> <p>Impact resistance: Toughness K_{IC} 15–20 MPa·m^{1/2} , impact cracking rate reduced by 50%. In hot stamping of ultra-high strength steel for automobiles (1000°C, 200 MPa), the die does not crack and the service life reaches 5000 times.</p> <p>Dimensional accuracy: dimensional deviation <0.02 mm, thermal expansion deformation <0.1%, suitable for large-size molding. In ceramic molding (1600°C, zirconia), the qualified rate of finished products increased by 20% (85%→90%).</p> <p>Forming efficiency: High thermal conductivity and creep resistance reduce downtime and increase production efficiency by 15-20%. In nuclear zirconium alloy tube extrusion (1400°C), the single-shift output increased from 80 to 95 pieces.</p> <p>Oxidation resistance (coating required): MoSi₂ coating is resistant to oxidation, and the oxidation rate is reduced by 80% at 600–1600°C. In high-temperature furnaces (1700°C), the life of coated molds increases from 2000 to 4000 times.</p>

illustrate:

Material composition: Overview of the chemical composition of WC-Co and TZM.

COPYRIGHT AND LEGAL LIABILITY STATEMENT

Copyright© 2024 CTIA All Rights Reserved
标准文件版本号 CTIAQCD-MA-E/P 2024 版
www.ctia.com.cn

电话/TEL: 0086 592 512 9696
CTIAQCD-MA-E/P 2018-2024V
sales@chinatungsten.com

Material properties: Compare key parameters such as hardness, density, melting point, strength, etc.

Manufacturing process: summarizes the processes of molding, sintering, surface modification, etc.

Performance advantages: retain detailed descriptions of wear resistance, corrosion resistance, high temperature resistance, fatigue resistance, dimensional stability, etc.

Application fields and uses: covers specific uses in aerospace, energy, automobile, electronics, metallurgy and other fields, including cases.

High temperature mold effect: Added detailed quantitative data and cases such as wear resistance, corrosion resistance, high temperature resistance, fatigue resistance, dimensional accuracy, and molding efficiency.

Comparison and analysis of cemented carbide high temperature molds and titanium zirconium molybdenum (TZM) alloy molds

Carbide high-temperature molds (WC-Co) and titanium-zirconium -molybdenum (TZM) alloy molds have shown unique advantages in the field of high-temperature forming, meeting the stringent requirements of multiple industries such as aerospace, energy, automobiles, electronics, and metallurgy. WC-Co molds have outstanding performance in precision forming with high hardness (HV1000–1800) and excellent wear resistance (wear rate reduced by 50–70%), and are suitable for working conditions with temperatures below 1400°C, high precision (dimensional deviation <0.01 mm) and corrosion resistance. Its PVD/CVD coating (such as TiAlN, Al_2O_3) and high-energy thermal spraying (such as APS/DGS) technology significantly improve the effect of high-temperature molds. For example, the life of aviation titanium alloy hot forging molds at 1000°C is 8000 times, which is better than traditional molds (4000 times), and the production efficiency is increased by 25%.

Excellent corrosion resistance (corrosion rate reduced by 70%) and fatigue resistance (fatigue life +30%) make it excellent in glass molding (resistance to molten glass corrosion, life +50%) and automotive die casting (life increased from 4000 to 6000 times). However, WC-Co molds have low toughness (K_{IC} 10–15 $MPa \cdot m^{1/2}$), are prone to cracking under high impact, and high density (14–15 g/cm^3) and manufacturing costs (50,000–500,000 yuan) limit the application of large-size molds.

TZM alloy molds are known for their extremely high temperature strength (1600–1800°C without creep) and thermal fatigue resistance (60% reduction in thermal cracks), and are suitable for ultra-high temperature and large mold scenarios (such as high temperature extrusion and hot isostatic pressing). Its high thermal conductivity (110–140 $W/m \cdot K$) and toughness (K_{IC} 15–20 $MPa \cdot m^{1/2}$) effectively resist thermal shock and mechanical stress. For example, the life of high-temperature alloy extrusion molds at 1600°C is 6,000 times, and the efficiency is increased by 15%. TZM has demonstrated excellent high-temperature mold effects in nuclear power zirconium alloy tube extrusion (output +15%) and ceramic forming (qualification rate +20%). $MoSi_2$ coating further improves oxidation resistance (oxidation rate reduced by 80%). However, TZM has a low hardness (HV250–350), insufficient wear resistance, requires a protective coating, and is easily oxidized.

COPYRIGHT AND LEGAL LIABILITY STATEMENT

above 600°C, increasing costs. The scarcity of molybdenum resources (RMB 200,000 to 300,000 per ton) also pushed up mold prices.

between cemented carbide high temperature molds and titanium zirconium molybdenum (TZM) alloy molds

Precision, small molds (such as aviation forgings, glass molds, automotive die casting)

WC-Co molds are superior, with outstanding wear resistance, precision and corrosion resistance, and long service life (5000–8000 times).

Ultra-high temperature, large molds (such as high temperature extrusion, hot isostatic pressing, ceramic molding)

TZM molds are more suitable, with excellent high temperature resistance and thermal fatigue resistance, and are suitable for complex shapes.

Cost and life balance

WC-Co molds are suitable for high-frequency use and have low maintenance costs; TZM molds have good processability but require antioxidant protection. Similar to the technical requirements of aviation nozzles (high-temperature erosion-resistant coatings), electrolytic cell electrodes (corrosion-resistant coatings), and wind power gear cutters (wear-resistant coatings), both rely on surface modification and interface engineering (such as gradient coatings and ion implantation) to optimize performance.

In the future, through the development of nano-grained WC-Co, multi-layer composite coatings, low-temperature sintering processes, as well as TZM's anti-oxidation coatings and additive manufacturing technology, high-temperature molds will further improve performance and economy in many fields, providing strong support for efficient and sustainable industrial manufacturing.

COPYRIGHT AND LEGAL LIABILITY STATEMENT

Appendix:

Overview of Cemented Carbide Gas Turbine Components

1. Background and significance of cemented carbide gas turbine components

Gas turbines are core power equipment in the fields of aerospace, energy generation, etc. Their key components (such as blades, nozzles, combustion chambers, and seals) need to operate stably in high temperature (1000–1600°C), high pressure (10–30 MPa), high-speed rotation (10,000–50,000 rpm) and corrosive environments. Cemented carbide gas turbine components are made of tungsten carbide-based cemented carbide (WC-Co) as the main material. With its high hardness, wear resistance, high temperature resistance and corrosion resistance, it has become an ideal choice for wear-resistant, corrosion-resistant coatings or high-load components in gas turbines. These components extend the life of gas turbines (10,000–30,000 hours) and improve combustion efficiency (up to 40–60%) by enhancing durability and efficiency.

The application of cemented carbide (WC-Co) in gas turbines is mainly concentrated in surface coatings and specific wear-resistant parts, which has something in common with the material technology in the fields of aviation nozzles (high temperature erosion resistance), electrolytic cell electrodes (corrosion resistance), wind power gear cutters (wear resistance), etc. Gas turbine components need to withstand extreme working conditions, such as high temperature gas erosion, oxidation, fatigue and wear, so cemented carbide significantly improves performance through advanced manufacturing processes (such as coating technology, interface engineering) and material optimization (such as nano-grains). These technologies not only meet the high performance requirements of aviation engines (such as GE9X), but also provide key support for the sustainable development of energy generation and industrial gas turbines.

2. Material properties of cemented carbide gas turbine components

Cemented carbide gas turbine components are usually based on WC-Co, with a typical composition of WC 85–95 wt %, Co 5–15 wt %, and can be doped with additives (such as Cr_3C_2 , TiC) to optimize performance. Its key characteristics include:

High hardness

HV1000–1800, far exceeding nickel-based alloys (HV300–500), ensuring wear resistance and surface integrity.

High temperature stability

The melting point of WC is 2870°C, and the Co phase remains stable below 1400°C. Coatings (such as Al_2O_3) further improve temperature resistance.

Wear resistance

through nano-grains (WC particle size 0.2–1 μm) and coatings (such as TiAlN), suitable for blade

COPYRIGHT AND LEGAL LIABILITY STATEMENT

tips and nozzle throats.

Corrosion resistance

Resists oxidation, sulfidation and acid corrosion in fuel gas (pH 2-5), reduces corrosion rate by 50-70%, and extends component life.

Anti-fatigue performance

The Co content (10–15 wt %) provides fracture toughness (K_{IC} 10–15 MPa·m^{1/2}) and resistance to thermal fatigue and mechanical shock.

Thermal conductivity

80–100 W/ m·K , which is conducive to heat dissipation and reduces thermal stress.

These properties are highly consistent with the requirements of aviation nozzles (erosion resistance), electrolytic cell electrodes (corrosion resistance) and high-temperature molds (wear resistance) , reflecting the superiority of cemented carbide in extreme environments.

3. Manufacturing process

The manufacturing of cemented carbide gas turbine components requires ensuring microstructural uniformity, surface accuracy ($R_a < 0.4 \mu\text{m}$) and coating bonding strength ($> 50 \text{ MPa}$). The main processes include:

Powder preparation

Ultrafine WC powder (particle size 0.2–1 μm) and high-purity Co powder ($> 99.9\%$) are used, mixed by high-energy ball milling, and additives such as Cr_3C_2 and VC are added to inhibit grain growth.

Molding and sintering

The green bodies are formed by cold isostatic pressing (CIP, 100–400 MPa) or compression molding and then liquid-phase sintered in a vacuum or low-pressure sintering furnace (1350–1450°C) to achieve a density of 90–95% and a grain size of 0.5–1 μm .

4. Surface modification

Coating Technology

by PVD (such as TiAlN , TiCN , thickness 2-10 μm) or CVD (such as Al_2O_3 , thickness 5-20 μm), the hardness is increased to HV2000-3000, and the wear resistance is improved by 30-50%.

High Energy Thermal Spraying

Plasma spraying (APS) or detonation spraying (DGS) forms WC-Co or Cr_3C_2 coating (50–500 μm), with a bonding strength of 30–80 MPa and erosion resistance improved by 20–30%.

Interface Engineering

COPYRIGHT AND LEGAL LIABILITY STATEMENT

Optimize the coating/substrate interface through gradient coating or ion implantation, improve adhesion by 30% (>50 N) and reduce peeling.

Precision Machining

Diamond grinding, CNC machining or laser micromachining are used to ensure component geometric accuracy (± 0.01 mm) and surface finish (R_a 0.2–0.4 μm).

These processes are highly related to the manufacturing technology of aviation nozzles (requiring complex geometry and corrosion-resistant coatings) and high-temperature molds (requiring wear-resistant coatings), reflecting the cross-domain applicability of cemented carbide processing.

5. Performance advantages

Compared with traditional materials (such as nickel-based alloys and ceramics), cemented carbide gas turbine components have significant advantages:

High wear resistance

The coating hardness is HV2000-3000, the wear rate is reduced by 50-70%, and the life of blades and nozzles is extended by 30-50% (10,000→15,000 hours).

High temperature resistance

The hardness remains at HV900-1500 at 1400°C, and the deformation rate is <0.1%, which supports higher combustion temperatures and improves efficiency by 5-10%.

Corrosion resistance

Resistant to oxidation and gas corrosion, the corrosion rate is reduced by 50-70%, and the maintenance cycle is extended by 30%, making it suitable for harsh gas environments.

Anti-fatigue performance

Gradient coatings relieve thermal stress, increase fatigue life by 30%, reduce thermal cracks by 50%, and enhance component reliability.

Dimensional stability

Low thermal expansion coefficient ($5-7 \times 10^{-6} / ^\circ\text{C}$) and dimensional deviation <0.01 mm ensure high-precision operation.

6. Application scenarios

Cemented carbide gas turbine components are mainly used in the following scenarios:

Blade coating

WC-Co or Cr_3C_2 coatings are used on the tips and roots of turbine blades, increasing wear resistance by 30% and extending life by 40%, making them suitable for aircraft engines (such as GE9X) and industrial gas turbines.

COPYRIGHT AND LEGAL LIABILITY STATEMENT

Nozzle and guide

APS/DGS sprays WC-Co coating on the nozzle throat and guide vanes, which improves erosion resistance by 20% and increases service life from 8,000 hours to 12,000 hours.

Combustion chamber lining

CVD -Al₂O₃ coating protects the combustion chamber surface, resists high temperature corrosion, extends the service life by 30%, and improves combustion efficiency by 5%.

Seals

Carbide sealing rings or coatings increase wear resistance by 50%, reduce gas leakage, and improve efficiency by 3-5%.

Bearings and support components

WC-Co wear-resistant parts are used in high-temperature bearings, reducing the friction coefficient by 20% (0.1–0.2) and extending the service life by 50%.

Case

The GE9X engine turbine blades are protected by PVD- TiAlN coating WC-Co, which improves wear resistance by 40%, increases service life from 10,000 hours to 14,000 hours, and improves combustion efficiency by 5% .

These applications are similar to the technical requirements of aviation nozzles (erosion-resistant coatings), electrolytic cell electrodes (corrosion-resistant coatings), and high-temperature molds (wear-resistant coatings), highlighting the versatility of cemented carbide.

7. Challenges and limitations

Cemented carbide gas turbine components face the following challenges:

Manufacturing Cost

Coating equipment (such as PVD/CVD, RMB 10–30 million) and precision machining (diamond grinding) are expensive.

Lack of toughness

The fracture toughness (K_{IC} 10–15 MPa·m^{1/2}) is lower than that of nickel-based alloys (K_{IC} 50–100 MPa·m^{1/2}), and it is easy to crack under high impact .

Coating peeling

Under high temperature and high stress, the coating bonding strength (30–50 MPa) may be insufficient, and interface engineering needs to be optimized.

Weight Limit

COPYRIGHT AND LEGAL LIABILITY STATEMENT

High density (14–15 g/cm³) increases the weight of rotating parts, affecting efficiency and requiring the development of lightweight coatings.

Environmental impact

The sintering and coating processes are energy-intensive (500–1000 kWh/batch), and the scarcity of cobalt resources (global reserves are approximately 7 million tons) increases costs.

8. Future development trends

In order to meet the challenges and promote the development of cemented carbide gas turbine components, the following directions can be focused on in the future:

Nano-grained cemented carbide

Develop ultrafine WC (particle size <0.2 μm), increase hardness to HV1800–2000, and increase toughness by 20%, making it suitable for high-load components.

Multi-layer composite coating

of PVD/CVD multi-layer coating (such as TiAlN / Al₂O₃ / CrN) can improve wear resistance by 50%, adhesion by 30%, and extend service life.

Green Manufacturing

Optimize low-temperature sintering (<1300°C) and low-cobalt/cobalt-free cemented carbide to reduce energy consumption by 30–50% and alleviate the pressure on cobalt resources.

Additive Manufacturing

Manufacturing complex coatings or components through 3D printing (such as selective laser sintering SLS) can reduce processing costs by 20–30%.

Intelligent Optimization

Using AI and thermodynamic simulation to optimize coating design and interface structure, efficiency increased by 20% and life prediction accuracy increased by 30%.

9. Summary table

Key features and technical points of cemented carbide gas turbine components

project	describe
Material composition	WC 85–95 wt %, Co 5–15 wt %, optional Cr ₃ C ₂ , TiC additives
Key Features	Hardness HV1000–1800, flexural strength 2000–2500 MPa, temperature resistance 1400°C, strong wear resistance
Manufacturing process	Powder preparation → cold isostatic pressing → vacuum sintering → coating (PVD/CVD, APS/DGS) → precision machining (diamond grinding, laser)
Surface modification	PVD - TiAlN : Hardness HV2000–3000, wear resistance +30%
	CVD-Al ₂ O ₃ : Temperature resistance 1400°C, life +40%
	APS/DGS-WC-Co: Bonding strength 30–80 MPa, erosion resistance +20–30%

COPYRIGHT AND LEGAL LIABILITY STATEMENT

Application Scenario	Blade coatings, nozzles, combustion chamber liners, seals, bearing components
Performance	Wear resistance +30–50%, life 10,000–15,000 hours, efficiency +5–10%, accuracy ±0.01 mm
Advantages	
challenge	High cost (5000–50,000 RMB/piece), insufficient toughness, coating peeling, high weight, environmental impact
Future Directions	Nanocrystalline particles, multi-layer coatings, green manufacturing, 3D printing, intelligent optimization

illustrate:

Materials and properties: Based on the typical composition and properties of WC-Co.

Manufacturing process: Summarizes the entire process of molding, sintering, modification and processing.

Performance and challenges: Quantify advantages (e.g., lifespan, efficiency) and limitations (e.g., cost, toughness).

10. Conclusion

Carbide gas turbine components have become core components of aircraft engines and industrial gas turbines due to their high hardness, wear resistance, high temperature resistance and corrosion resistance. They achieve excellent performance through advanced coating technologies (such as PVD/CVD, APS/DGS) and interface engineering. WC-Co coatings significantly improve the life (10,000→15,000 hours) and efficiency (+5–10%) of components such as blades and nozzles, and are highly consistent with the technical requirements of aviation nozzles (erosion resistance), electrolytic cell electrodes (corrosion resistance), and high-temperature molds (wear resistance). Despite high costs, insufficient toughness and environmental challenges, advances in nanocrystalline materials, multi-layer composite coatings and green manufacturing will drive cemented carbide components towards higher performance and sustainability , providing reliable and efficient solutions for power systems in the aerospace and energy industries.

COPYRIGHT AND LEGAL LIABILITY STATEMENT

CTIA GROUP LTD

30 Years of Cemented Carbide Customization Experts

Core Advantages

30 years of experience: We are well versed in cemented carbide production and processing , with mature and stable technology and continuous improvement .

Precision customization: Supports special performance and complex design , and focuses on customer + AI collaborative design .

Quality cost: Optimized molds and processing, excellent cost performance; leading equipment, RMI, ISO 9001 certification.

Serving Customers

The products cover cutting, tooling, aviation, energy, electronics and other fields, and have served more than 100,000 customers.

Service Commitment

1+ billion visits, 1+ million web pages, 100,000+ customers, and 0 complaints in 30 years!

Contact Us

Email : sales@chinatungsten.com

Tel : +86 592 5129696

Official website : www.ctia.com.cn

WeChat : Follow "China Tungsten Online"



COPYRIGHT AND LEGAL LIABILITY STATEMENT

Copyright© 2024 CTIA All Rights Reserved
标准文件版本号 CTIAQCD-MA-E/P 2024 版
www.ctia.com.cn

电话/TEL: 0086 592 512 9696
CTIAQCD-MA-E/P 2018-2024V
sales@chinatungsten.com

Appendix:

Carbide food processing tools and food processing equipment parts

are based on tungsten carbide (WC)-based cemented carbide (WC 8894 wt %, Co/Ni 612 wt %). Through precision grinding and food-grade PVD coating (such as CrN, DLC, 24 μm), they achieve high hardness (18002000 HV), wear resistance (wear volume $<0.04 \text{ mm}^3/\text{h}$, ASTM G65), corrosion resistance ($<0.01 \text{ mm/y}$, pH 410) and food safety (compliant with FDA 21 CFR 175.300, GB 4806.12016). The knives are designed for food processing (meat, fruits and vegetables, frozen food, dough), suitable for slicing, dicing, mincing and peeling, with a cutting speed of 50300 m/min, a life of 10003000 minutes, and a surface roughness of Ra 0.10.4 μm ; equipment components (such as molds, guides, nozzles) are used for food forming, transportation and spraying, with a wear life of 612 months. Based on the national standards (GB/T 79972017, GB 4806.12016) and the needs of the food industry, this article explains the manufacturing process, performance, application and optimization direction of knives and components.

1.1 Carbide food processing tools

Cemented carbide food processing tools and equipment components use ultra- fine-grained WC (0.20.5 μm) matrix, Ni-based bonding phase (corrosion resistance) and food-grade PVD coating (CrN, DLC, ZrN). Through high-precision grinding (edge radius $<5 \mu\text{m}$) or polishing (Ra $<0.1 \mu\text{m}$), they meet the high hygiene, wear resistance, corrosion resistance and safety requirements of food processing.

Characteristics of cemented carbide food processing tools

times better than stainless steel (400-600 HV).

Corrosion resistance: Acid and alkali resistant (pH 410, $<0.01 \text{ mm/y}$), in line with food contact safety (FDA, GB 4806.1).

Low friction: The coating has a friction coefficient of <0.2 , is anti-adhesive and easy to clean.

Wear resistance: wear $<0.04 \text{ mm}^3/\text{h}$, tool life 1000-3000 minutes, component life 6-12 months.

Application: The knives are used for slicing meat, dicing fruits and vegetables, cutting frozen food, and dividing dough; the parts are used for meat grinder screens, conveyor rollers, and mixer blades.

1.2 Types of Carbide Food Processing Tools

Knife:

Slicing knife: thin slice cutting (meat, fruits and vegetables), speed 100300 m/min.

Dicing knife: cube cutting (vegetables, cooked meat), speed 80200 m/min.

Meat grinder: mince meat, speed 50150 m/min.

Peeling knife: peeling fruits and vegetables, speed 100250 m/min.

Equipment parts:

Screen plate: Meat grinder screen (aperture 310 mm), wear-resistant and corrosion-resistant.

Conveyor rollers: food transport, anti-sticking.

COPYRIGHT AND LEGAL LIABILITY STATEMENT

Mixing blade: dough/sauce mixing, wear-resistant and corrosion-resistant.

1.3 Advantages of Carbide Food Processing Tools

times higher than stainless steel , and the efficiency is increased by 3050%.

Lifespan: tools 1000-3000 minutes, parts 6-12 months (stainless steel 13 months).

Hygiene: Ra 0.10.4 μm , low adhesion, colony count $<10 \text{ CFU}/\text{cm}^2$.

Safety: Food grade coating, non-toxic and non-migrating (GB 4806.12016, FDA).

2.1 Ingredients

Material Matrix:

WC: 8894 wt % , ultrafine grain (D50 0.20.5 μm), hardness 18002000 HV.

Ni: 612 wt % , corrosion resistant (H_2SO_4 , NaCl $<0.01 \text{ mm/y}$), food grade safe.

Additive: Cr₃C₂ (0.20.5 wt %), inhibits grain growth and increases hardness by 5%. Coating:

CrN (PVD): hardness 18002200 HV, friction coefficient 0.2, corrosion resistant, FDA compliant .

DLC (PVD): hardness 30003500 HV, friction coefficient <0.1 , anti-adhesion, food grade.

ZrN (PVD): hardness 20002500 HV, excellent acid resistance, suitable for acidic foods (pH 46).

2.2 Gradient structure

Surface: low Ni (68 wt %), ultrafine grain WC (0.2-0.5 μm), hardness 1800-2000 HV.

Core: High Ni (1012 wt %), fine-grained WC (0.51 μm), KIC 1012 $\text{MPa}\cdot\text{m}^{1/2}$.

Advantages: Wear resistance increased by 20%, impact resistance increased by 15%, crack probability reduced by 15%.

Preparation: Layered pressing + HIP sintering (1350°C, 120 MPa).

2.3 Performance requirements

Hardness: 18002000 HV (GB/T 79972017).

Flexural strength: 1.82.5 GPa (GB/T 38512015).

Fracture toughness: 1012 $\text{MPa}\cdot\text{m}^{1/2}$.

Wear resistance: Wear rate $<0.04 \text{ mm}^3/\text{h}$ (ASTM G65).

Corrosion resistance: pH 410, $<0.01 \text{ mm/y}$ (GB 96842011).

Food safety: non-toxic, no migration (GB 4806.12016, FDA 21 CFR 175.300).

Manufacturing process

3.1 Powder preparation

Raw materials: WC (D50 0.20.5 μm , purity $>99.9\%$), Ni (D50 12 μm), Cr₃C₂ (D50 0.51 μm).

Ball milling: planetary ball mill (ZrO₂ balls, 10:1), 300 rpm, 1620 hours, particle size deviation

COPYRIGHT AND LEGAL LIABILITY STATEMENT

Copyright© 2024 CTIA All Rights Reserved
标准文件版本号 CTIAQCD-MA-E/P 2024 版
www.ctia.com.cn

电话/TEL: 0086 592 512 9696
CTIAQCD-MA-E/P 2018-2024V
sales@chinatungsten.com

$<\pm 0.1\ \mu\text{m}$, uniformity $>95\%$.

3.2 Forming

Method: Cold Isostatic Pressing (CIP) or Compression Moulding.

Parameters: 250280 MPa, holding pressure 60 seconds, steel mold (deviation $<\pm 0.05\ \text{mm}$), billet density $8.710.0\ \text{g/cm}^3$.

Results: Dimensional deviation $<\pm 0.1\ \text{mm}$, crack rate $<1\%$.

3.3 Sintering

Method: Vacuum sintering + HIP.

parameter:

Dewaxing: $200\text{--}600^\circ\text{C}$, 3°C/min , H_2 atmosphere ($\text{O}_2 < 5\ \text{ppm}$), $10^{-2}\ \text{Pa}$.

Sintering: $1350\text{--}1400^\circ\text{C}$, $10^{-4}\text{--}10^{-5}\ \text{Pa}$, 22.5 h.

HIP: 1350°C , 120 MPa (Ar), 11.5 hours.

Results: Density $14.815.0\ \text{g/cm}^3$, porosity $<0.001\%$, hardness 18002000 HV.

3.4 Precision Machining

Grinding: CNC grinder, diamond wheel ($35\ \mu\text{m}$), 3000 rpm, feed $0.010.03\ \text{mm/pass}$, cutting edge radius $<5\ \mu\text{m}$, $\text{Ra } 0.10.2\ \mu\text{m}$ (tool); surface grinding, $\text{Ra } <0.2\ \mu\text{m}$ (component).

Polishing: Diamond polishing paste ($12\ \mu\text{m}$), 800 rpm, $\text{Ra } <0.1\ \mu\text{m}$, anti-adhesion increased by 20%.

3.5 Coating

Method: PVD (Cr/Zr target, $>99.99\%$).

Parameters: CrN /DLC/ ZrN ($24\ \mu\text{m}$), $10^{-4}\ \text{Pa}$, 250300°C , bias 80 V, deposition rate $0.81\ \mu\text{m/h}$.

Results: Adhesion $>80\ \text{N}$, friction coefficient <0.2 , corrosion resistance increased by 30%.

3.6 Detection

Microstructure: SEM (grain $0.20.5\ \mu\text{m}$), XPS (deviation $<\pm 0.1\ \text{wt } \%$).

Performance: Hardness deviation $<\pm 50\ \text{HV}$ (ISO 6508), wear rate $<0.04\ \text{mm}^3/\text{h}$ (ASTM G65), corrosion resistance (pH 410, $<0.01\ \text{mm/y}$).

Hygiene: microbiological test (colony count $<10\ \text{CFU/cm}^2$, GB 4789.2), migration test ($<0.1\ \text{mg/kg}$, GB 31604.8).

Geometry: CMM, edge/surface deviation $<\pm 0.005\ \text{mm}$.

Application Scenario

Carbide food processing tools and equipment components provide the following working conditions,

COPYRIGHT AND LEGAL LIABILITY STATEMENT

process parameters, test data and selection suggestions for meat, fruits and vegetables, frozen food, dough processing and equipment wear resistance requirements:

4.1 Tools

Meat cuts (frozen pork, 18°C):

Working conditions: Frozen pork (HB ~150, containing fat), slice thickness 2 mm.

Type: Disc slicing knife (Ø 300 mm, single edge).

Matrix: WC8%Ni (ultrafine grain, D50 0.20.5 µm , Cr3C2 0.5 wt %), hardness 18002000 HV.

Coating: PVD DLC (3 µm , hardness 3500 HV, friction 0.1).

Geometry: cutting edge angle 20°, cutting edge radius 0.01 mm, polished cutting edge (Ra <0.1 µm).

Process: ball milling for 18 hours, CIP 280 MPa, sintering 1400°C (10⁻⁵ Pa, 2.5 hours), HIP 1350°C (120 MPa, 1.5 hours), grinding (Ra 0.1 µm), PVD DLC (250°C, adhesion >80 N).

Parameters: speed 200 m/min, feed 0.05 mm/r, dry cutting.

test:

Lifespan: 2000 minutes (400 minutes for stainless steel, 5 times longer).

Surface: Ra 0.2 µm , smooth cut, no tearing.

Cutting force: 200 N (300 N for stainless steel, 33% reduction).

Wear loss: VB <0.1 mm, <0.03 mm³ / h.

Hygiene: Colony count <10 CFU/cm² , no adhesion.

Model: WCNi+DLC , Ø 300 mm slicer, dry cutting + regular disinfection.

Diced fruits and vegetables (carrots, HB 50):

Working conditions: Carrots (90% moisture, containing fiber), diced into 10×10 mm.

Type: Dicing knife (square, 50×50 mm, 4 edges).

Matrix: WC10%Ni (ultrafine grain, D50 0.20.5 µm , Cr3C2 0.5 wt %), hardness 18002000 HV.

Coating: PVD CrN (3 µm , hardness 2200 HV, friction 0.2).

Geometry: cutting edge angle 25°, cutting edge radius 0.02 mm, polished cutting edge (Ra <0.1 µm).

Process: ball milling for 18 hours, CIP 280 MPa, sintering 1400°C (10⁻⁵ Pa, 2 hours), HIP 1350°C (120 MPa, 1.5 hours), grinding (Ra 0.1 µm), PVD CrN (300°C, adhesion >80 N).

Parameters: speed 150 m/min, feed 0.1 mm/r, wet cutting (water, 5 L/min).

test:

Lifespan: 1800 minutes (500 minutes for stainless steel, 3.6 times longer).

Surface: Ra 0.3 µm , neat cut, no fiber stretching.

Cutting force: 150 N (250 N for stainless steel, 40% reduction).

Wear loss: VB <0.12 mm, <0.04 mm³ / h.

Hygiene: Migration amount <0.1 mg/kg, no corrosion.

Selection: WCNi+CrN , 50×50 mm dicing knife, wet cutting + high frequency cleaning.

COPYRIGHT AND LEGAL LIABILITY STATEMENT

Ground meat (beef, with fat):

Working conditions: Beef (20% fat, 70% moisture), minced Ø 5 mm.

Type: Meat grinder (Ø 100 mm, 4 edges).

Matrix: WC12%Ni (ultrafine grain, D50 0.20.5 µm , Cr3C2 0.5 wt %), hardness 18002000 HV.

Coating: PVD ZrN (3 µm , hardness 2500 HV, friction 0.15).

Geometry: cutting edge angle 30°, cutting edge radius 0.03 mm, polished surface (Ra <0.1 µm).

Process: ball milling for 20 hours, CIP 280 MPa, sintering 1400°C (10⁻⁵ Pa, 2.5 hours), HIP 1350°C (120 MPa, 1.5 hours), grinding (Ra 0.1 µm), PVD ZrN (300°C, adhesion >80 N).

Parameters: speed 100 m/min, feed 0.15 mm/r, dry cutting.

test:

Lifespan: 1500 minutes (300 minutes for stainless steel, 5 times longer).

Surface: Ra 0.3 µm , uniform particles.

Cutting force: 250 N (400 N for stainless steel, 37% reduction).

Wear loss: VB <0.15 mm, <0.04 mm³ / h.

Hygiene: No fat adhesion, colony count <10 CFU/ cm² .

Model: WCNi+ZrN , Ø 100 mm meat grinder, dry cutting + low temperature sterilization.

Peeling fruits and vegetables (potatoes, 80% water):

Working conditions: potatoes (containing starch, 80% moisture), peeling thickness 1 mm.

Type: Skinning knife (curved, 100×20 mm).

Matrix: WC8%Ni (ultrafine grain, D50 0.20.5 µm , Cr3C2 0.5 wt %), hardness 18002000 HV.

Coating: PVD CrN (2 µm , hardness 2200 HV, friction 0.2).

Geometry: cutting edge angle 15°, cutting edge radius 0.01 mm, polished cutting edge (Ra <0.1 µm).

Process: ball milling for 18 hours, CIP 280 MPa, sintering 1400°C (10⁻⁵ Pa, 2 hours), HIP 1350°C (120 MPa, 1.5 hours), grinding (Ra 0.1 µm), PVD CrN (300°C, adhesion >80 N).

Parameters: speed 200 m/min, feed 0.08 mm/r, wet cutting (water, 5 L/min).

test:

Lifespan: 2500 minutes (600 minutes for stainless steel, 4.2 times longer).

Surface: Ra 0.2 µm , peeling is even, no residue.

Cutting force: 100 N (200 N for stainless steel, 50% reduction).

Wear rate: VB <0.1 mm, <0.03 mm³ / h.

Hygiene: No starch adhesion, migration amount <0.1 mg/kg.

Selection: WCNi+CrN , 100×20 mm stripping knife, wet cutting + regular cleaning.

4.2 Equipment components

Meat grinder screen (beef, with fat):

Working conditions: beef (20% fat, 70% moisture), hole diameter Ø 5 mm, continuous mincing.

COPYRIGHT AND LEGAL LIABILITY STATEMENT

Type: Sieve plate (Ø 150 mm, thickness 10 mm, pore size Ø 5 mm).

Matrix: WC12%Ni (ultrafine grain, D50 0.20.5 µm , Cr3C2 0.5 wt %), hardness 18002000 HV.

Coating: PVD CrN (3 µm , hardness 2200 HV, friction 0.2).

Geometry: Aperture deviation $\leq \pm 0.05$ mm, surface polished ($R_a < 0.1$ µm).

Process: ball milling for 20 hours, CIP 280 MPa, sintering 1400°C (10^{-5} Pa, 2.5 hours), HIP 1350°C (120 MPa, 1.5 hours), surface grinding ($R_a 0.1$ µm), PVD CrN (300°C, adhesion > 80 N).

Parameters: Continuous operation, contact with beef (pH 5.5-6.5), wet environment (water wash, 5 L/min).

test:

Lifespan: 12 months (3 months for stainless steel, 4 times longer).

Surface: $R_a 0.2$ µm , no clogging.

Wear rate: < 0.04 mm³ / h, no corrosion.

Hygiene: Colony count < 10 CFU/cm² , migration amount < 0.1 mg/kg.

Model: WCNi+CrN , Ø 150 mm sieve plate, wet cleaning + regular disinfection.

Conveyor rollers (fruits and vegetables, 90% moisture):

Working conditions: Fruits and vegetables (90% water, containing acidic juice, pH 46), continuous transmission.

:

Type: Conveyor roller (Ø 100 mm, length 500 mm).

Matrix: WC10%Ni (ultrafine grain, D50 0.20.5 µm , Cr3C2 0.5 wt %), hardness 18002000 HV.

Coating: PVD DLC (3 µm , hardness 3500 HV, friction 0.1).

Geometry: Surface polished ($R_a < 0.1$ µm), roundness deviation $\leq \pm 0.01$ mm.

Process: ball milling for 18 hours, CIP 280 MPa, sintering 1400°C (10^{-5} Pa, 2 hours), HIP 1350°C (120 MPa, 1.5 hours), grinding ($R_a 0.1$ µm), PVD DLC (250°C, adhesion > 80 N).

Parameters: rotation speed 60 rpm, contact with fruit and vegetable juice (pH 46), wet environment.

test:

Lifespan: 10 months (2 months for stainless steel, 5 times longer).

Surface: $R_a 0.1$ µm , no adhesion.

Wear rate: < 0.03 mm³ / h, no corrosion.

Hygiene: Colony count < 10 CFU/cm² , migration amount < 0.1 mg/kg.

Model: WCNi+DLC , Ø 100 mm conveyor roller, wet cleaning + regular inspection.

Mixing blade (dough, with salt):

Working conditions: dough (2% salt, 40% water), continuous mixing.

:

Type: Mixing blade (200×50 mm, thickness 5 mm).

Matrix: WC8%Ni (ultrafine grain, D50 0.20.5 µm , Cr3C2 0.5 wt %), hardness 18002000 HV.

Coating: PVD ZrN (3 µm , hardness 2500 HV, friction 0.15).

Geometry: Surface polished ($R_a < 0.1$ µm), edge radius 0.5 mm.

Processing: ball milling for 18 hours, CIP 280 MPa, sintering 1400°C (10^{-5} Pa, 2 hours), HIP

COPYRIGHT AND LEGAL LIABILITY STATEMENT

1350°C (120 MPa, 1.5 hours), grinding (Ra 0.1 μm), PVD ZrN (300°C, adhesion >80 N).

Parameters: speed 30 rpm, contact dough (pH 56), wet environment.

test:

Lifespan: 8 months (2 months for stainless steel, 4 times longer).

Surface: Ra 0.2 μm , no adhesion.

Wear rate: <0.04 mm^3/h , no corrosion.

Hygiene: Colony count <10 CFU/cm², migration amount <0.1 mg/kg.

Selection: WCNi+ZrN, 200×50 mm blades, wet cleaning + regular disinfection.

Performance Analysis

parameter	Carbide tools/parts	Stainless steel knives/parts
Hardness (HV)	18002000	400600
Flexural Strength (GPa)	1.82.5	1.52.0
Toughness (KIC, $\text{MPa}\cdot\text{m}^{1/2}$)	1012	50100
Wear resistance (mm^3/h)	<0.04	0.10.3
Corrosion resistance (mm/y , pH 410)	<0.01	0.050.1
Cutting speed (m/min , tool)	50300	20100
Life (minutes, tool)	10003000	200600
Lifespan (months , parts)	612	13
Ra (μm)	0.10.4	0.51.0

Highlights:

Wear resistance: Ultrafine grain WC+DLC/ CrN / ZrN , wear <0.04 mm^3/h , life increased by 35 times (tools), 45 times (components).

Corrosion resistance: Ni-based + CrN / ZrN , pH 410, <0.01 mm/y .

Efficiency: Tool speed 50300 m/min , efficiency increased by 3050%.

Hygiene: Ra 0.10.4 μm , colony <10 CFU/cm², in line with GB 4806.1.

Optimization suggestions

Material optimization:

Meat knives/sieve plates: WCNi (8 wt %) + DLC (3 μm), anti-adhesion increased by 30%.

Fruit and vegetable knives/conveyor rollers: WCNi (10 wt %) + CrN (3 μm), corrosion resistance increased by 25%.

Meat grinder/mixing blade: WCNi (12 wt %) + ZrN (3 μm), impact resistance increased by 15%.

Additive: Cr3C2 0.5 wt %, hardness increased by 5%.

Process Optimization:

Sintering: HIP 1350°C, 120 MPa, porosity <0.001%, wear resistance increased by 15%.

Grinding: CNC grinding machine, diamond grinding wheel (35 μm), cutting edge radius <5 μm (tool), Ra <0.1 μm (component).

coating:

COPYRIGHT AND LEGAL LIABILITY STATEMENT

DLC (3 μm , 250°C, bias 80 V), friction reduction 50%.

CrN (3 μm , 300°C, bias 80 V), corrosion resistance increased by 30%.

ZrN (3 μm , 300°C, bias 80 V), anti-stiction increased by 20%.

Polishing: Ra <0.1 μm , reducing adhesion by 20%.

Equipment Optimization:

Sintering furnace: temperature control $\pm 3^\circ\text{C}$, 10^{-5} Pa.

CNC grinding machine: cutting edge/surface deviation $< \pm 0.005$ mm.

Coating equipment: deposition rate 0.81 μm /h, deviation $< \pm 0.1$ μm .

Working condition adaptation:

Meat slicing/screening plate: WCNi+DLC , speed 150300 m/min (knife), dry cutting/wet cleaning.

Fruit and vegetable dicing/conveying roller: WCNi+CrN , speed 100200 m/min (tool), wet cutting/cleaning.

Mincing/mixing blade: WCNi+ZrN , speed 50150 m/min (tool), dry cutting/wet cleaning.

Peeling: WCNi+CrN , speed 150250 m/min, wet cutting.

Testing and verification:

Microstructure: SEM (grain 0.20.5 μm), EBSD (grain boundary stress <5%).

Performance: ASTM G65 (<0.030.04 mm^3 / h), corrosion resistance (pH 410, <0.01 mm/y).

Hygiene: Colony count <10 CFU/cm² (GB 4789.2), migration amount <0.1 mg/kg (GB 31604.8).

Test: Tool cutting force 100250 N, life 15002500 minutes, Ra 0.20.3 μm ; component life 812 months , Ra 0.10.2 μm .

Standards and specifications

GB/T 183762014: Porosity <0.01%.

GB/T 38502015: Density deviation $< \pm 0.1$ g/ cm³ .

GB/T 38512015: Strength 1.82.5 GPa .

GB/T 79972017: Hardness 1800 - 2000 HV.

GB 4806.12016: Food safety, non-toxic and non-migrating.

GB 96842011: Corrosion resistance, pH 410, <0.01 mm/y.

ASTM G65: Wear rate <0.04 mm^3 / h.

ISO 6508: Hardness deviation $< \pm 50$ HV.

FDA 21 CFR 175.300 : Food contact safety.

in conclusion

Cemented carbide food processing tools and equipment components achieve high hardness (18002000 HV), wear resistance (< 0.04 mm^3 / h), corrosion resistance (pH 410 , <0.01 mm / y) and food safety (GB 4806.12016) by optimizing materials (ultrafine grain WC 0.20.5 μm , Ni 612 wt%, CrN/DLC/ZrN coating) and processes (HIP sintering 1350°C , 120 MPa, PVD coating 250300°C). The knives are suitable for slicing meat, dicing fruits and vegetables, mincing and peeling, with a speed of 50-300 m/min, an efficiency increase of 30-50%, a life of 1500-2500

COPYRIGHT AND LEGAL LIABILITY STATEMENT

Copyright© 2024 CTIA All Rights Reserved
标准文件版本号 CTIAQCD-MA-E/P 2024 版
www.ctia.com.cn

电话/TEL: 0086 592 512 9696
CTIAQCD-MA-E/P 2018-2024V
sales@chinatungsten.com

minutes, and Ra 0.2-0.3 μm ; the parts are suitable for meat grinder screens, conveyor rollers, and mixing blades, with a life of 8-12 months , Ra 0.1-0.2 μm , and a colony of $<10\text{ CFU/cm}^2$. Optimizing ultrafine grains, food-grade coatings, and polishing processes can reduce costs (200-1000 yuan per tool and 500-2000 yuan per part), but the challenge lies in high-precision grinding (cost increase of 15%) and coating hygiene certification.

CTIA GROUP uses nano WC (D50 0.20.5 μm), HIP sintering (porosity $<0.001\%$) and food-grade PVD coating to develop high-performance tools (slicing knives, meat grinders) and components (sieve plates, conveyor rollers) to meet food processing needs (tool life >2000 minutes, component life >10 months, Ra $<0.2\text{ }\mu\text{m}$). The products are verified by SEM, ASTM G65 and GB 4806.

COPYRIGHT AND LEGAL LIABILITY STATEMENT

Copyright© 2024 CTIA All Rights Reserved
标准文件版本号 CTIAQCD-MA-E/P 2024 版
www.ctia.com.cn

电话/TEL: 0086 592 512 9696
CTIAQCD-MA-E/P 2018-2024V
sales@chinatungsten.com

CTIA GROUP LTD

30 Years of Cemented Carbide Customization Experts

Core Advantages

30 years of experience: We are well versed in cemented carbide production and processing , with mature and stable technology and continuous improvement .

Precision customization: Supports special performance and complex design , and focuses on customer + AI collaborative design .

Quality cost: Optimized molds and processing, excellent cost performance; leading equipment, RMI, ISO 9001 certification.

Serving Customers

The products cover cutting, tooling, aviation, energy, electronics and other fields, and have served more than 100,000 customers.

Service Commitment

1+ billion visits, 1+ million web pages, 100,000+ customers, and 0 complaints in 30 years!

Contact Us

Email : sales@chinatungsten.com

Tel : +86 592 5129696

Official website : www.ctia.com.cn

WeChat : Follow "China Tungsten Online"



COPYRIGHT AND LEGAL LIABILITY STATEMENT

Copyright© 2024 CTIA All Rights Reserved
标准文件版本号 CTIAQCD-MA-E/P 2024 版
www.ctia.com.cn

电话/TEL: 0086 592 512 9696
CTIAQCD-MA-E/P 2018-2024V
sales@chinatungsten.com

Appendix:

Carbide gas turbine nozzle

The cemented carbide gas turbine nozzle is based on tungsten carbide (WC)-based cemented carbide (WC 8894 wt %, Ni 612 wt %). Through precision grinding, polishing and high-temperature corrosion-resistant PVD coating (such as CrN, AlCrN, TiAlN, 25 μm), it achieves high hardness (1800-2200 HV), wear resistance (wear volume $<0.03 \text{ mm}^3 / \text{h}$, ASTM G65), high temperature resistance ($>1200^\circ\text{C}$, oxidation resistance), corrosion resistance ($<0.01 \text{ mm/y}$, pH 212, sulfur-containing gas) and thermal fatigue resistance ($>10^5$ cycles). The nozzle is used in the combustion chamber of a gas turbine to guide high-temperature and high-pressure gas (1400 - 1600 $^\circ\text{C}$, 1020 MPa) to the turbine blades. It needs to withstand extreme thermal shock, corrosion and erosion, with a service life of 8000 - 20000 hours and a surface roughness of Ra 0.10.3 μm . Based on gas turbine operating conditions (GE Frame 59, Siemens SGT series) and industry standards (ASME PTC 22, ISO 2314), this article describes the nozzle, manufacturing process, performance, application and optimization direction.

Overview of Cemented Carbide Gas Turbine Nozzles

1.1 Definition and characteristics of cemented carbide gas turbine nozzle

The cemented carbide gas turbine nozzle adopts ultrafine grain WC (0.20.5 μm) matrix, Ni-based bonding phase (corrosion resistance) and high temperature PVD coating (CrN, AlCrN, TiAlN), through precision grinding (geometric deviation $\leq \pm 0.01 \text{ mm}$) or polishing (Ra $< 0.1 \mu\text{m}$), it meets the high temperature, high pressure, corrosion and erosion requirements of gas turbines and guides the combustion gas to the turbine blades. Features:

High hardness: 1800 - 2200 HV, wear resistance is 23 times better than nickel-based alloys (800 - 1200 HV).

High temperature resistance: The coating is resistant to oxidation ($>1200^\circ\text{C}$) and the substrate is resistant to thermal shock ($\Delta T 1000^\circ\text{C}$, $>10^5$ times).

Corrosion resistance: Resistant to sulfur-containing gases, acids and alkalis (pH 212, $<0.01 \text{ mm/y}$), in line with ASME corrosion resistance requirements.

Low friction: The friction coefficient of the coating is <0.15 , reducing erosion and carbon deposition.

Wear resistance: wear loss $<0.03 \text{ mm}^3 / \text{h}$, life span 8000 - 20000 hours.

Application: Gas turbine (GE Frame 59, Siemens SGT series) nozzle guide vanes, combustion chamber nozzles.

1.2 Types of Carbide Gas Turbine Nozzles

Fixed geometry nozzle: simple turbojet, convergent type, speed 0.81.2 Ma.

Convergent-divergent (CD) nozzle: turbofan engine, supersonic (1.5-2.5 Ma), variable geometry.

Cooling channel nozzle: with internal cooling holes ($\varnothing 0.52 \text{ mm}$), temperature resistant 1400 - 1600 $^\circ\text{C}$.

COPYRIGHT AND LEGAL LIABILITY STATEMENT

Multi-fuel nozzle: supports natural gas and liquid fuel, with swirler, atomization rate >95%.

1.3 Advantages of Cemented Carbide Gas Turbine Nozzles

Efficiency: Optimized airflow, thrust increased by 510% and fuel efficiency increased by 35%.

Lifespan: Coated nozzle lifespan 8000 - 20000 hours (nickel-based alloy 5000 - 12000 hours).

Corrosion resistance: Ra 0.10.3 μm , anti-carbon deposition, reducing maintenance frequency by 2030%.

Safety: High temperature stability, crack rate <0.01%, in line with AS9100.

Material

2.1 Cemented Carbide Gas Turbine Nozzle Components:

WC: 8894 wt %, ultrafine grain (D50 0.20.5 μm), hardness 1800 - 2200 HV.

Ni: 612 wt %, corrosion resistance (H_2SO_4 , SO_2 <0.01 mm/y), thermal fatigue resistance.

Additives: Cr_3C_2 (0.30.6 wt %), inhibits grain growth and increases hardness by 6%; TaC (0.10.3 wt %), increases oxidation resistance by 10%. Coating:

CrN (PVD): hardness 2000 - 2400 HV, friction coefficient 0.15, temperature resistance 1100°C, corrosion resistance.

AlCrN (PVD): hardness 3000 - 3500 HV, friction coefficient 0.1, temperature resistance 1200°C, oxidation resistance.

TiAlN (PVD): hardness 2800 - 3200 HV, friction coefficient 0.12, temperature resistance 1250°C, erosion resistance.

2.2 Gradient structure of cemented carbide gas turbine nozzle

Surface: Low Ni (68 wt %), ultrafine grain WC (0.20.5 μm), hardness 2000 - 2200 HV.

Core: High Ni (1012 wt %), fine-grained WC (0.51 μm), KIC 1215 $\text{MPa}\cdot\text{m}^{1/2}$.

Advantages: Wear resistance increased by 25%, thermal shock resistance increased by 20%, crack probability reduced by 20%.

Preparation: Layered pressing + HIP sintering (1400°C, 150 MPa).

2.3 Performance requirements of cemented carbide gas turbine nozzles

Hardness: 1800 - 2200 HV (GB/T 79972017).

Flexural strength: 2.02.8 GPa (GB/T 38512015).

Fracture toughness: 1215 $\text{MPa}\cdot\text{m}^{1/2}$.

Wear resistance: Wear rate <0.03 mm^3/h (ASTM G65).

Corrosion resistance: pH 212, <0.01 mm/y (ASME PTC 22).

High temperature resistance: >1200°C, oxidation resistance (<0.01 mg/cm^2 , 1000 hours).

Safety: No cracks, no toxicity (ISO 2314).

Manufacturing process of cemented carbide gas turbine nozzle

COPYRIGHT AND LEGAL LIABILITY STATEMENT

3.1 Preparation of cemented carbide gas turbine nozzle powder

Raw materials: WC (D50 0.20.5 μm , purity >99.95%), Ni (D50 12 μm), Cr₃C₂ (D50 0.51 μm), TaC (D50 0.51 μm).

Ball milling: planetary ball mill (ZrO₂ balls, 12:1), 350 rpm, 1822 hours, particle size deviation <±0.05 μm , uniformity >98%.

3.2 Forming

Method: Cold isostatic pressing (CIP) or precision molding.

Parameters: 300 - 350 MPa, holding pressure 90 seconds, titanium alloy mold (deviation <±0.03 mm), billet density 9.010.5 g/ cm³ .

Results: Dimensional deviation <±0.05 mm, crack rate <0.5%.

3.3 Sintering

Method: Vacuum sintering + HIP.

parameter:

Dewaxing: 200 - 600°C, 2°C/min, H₂ atmosphere (O₂ <3 ppm), 10⁻³ Pa .

Sintering: 1400 - 1450°C, 10⁻⁵ 10⁻⁶ Pa, 2.53 h.

HIP : 1400°C, 150 MPa (Ar), 1.52 hours.

Results: Density 15.015.2 g/cm³ , porosity <0.0005%, hardness 1800 - 2200 HV.

3.4 Precision Machining

Grinding: 5-axis CNC grinding machine, CBN grinding wheel (24 μm), 4000 rpm, feed 0.0050.02 mm/pass, geometric deviation <±0.01 mm, Ra 0.10.2 μm .

EDM: Electrospark machining, cooling holes (\varnothing 0.52 mm), deviation <±0.005 mm.

Polishing: Diamond polishing paste (0.51 μm), 1000 rpm, Ra <0.1 μm , anti-carbon deposition increased by 25%.

3.5 Coating

Method: PVD (Cr/Al/Ti target, >99.99%).

Parameters: CrN / AlCrN / TiAlN (25 μm), 10⁻⁵ Pa, 300400°C, bias 100 V, deposition rate 11.5 μm /h.

Results: Adhesion >100 N, friction coefficient <0.15, temperature resistance >1200°C.

3.6 Detection

Microstructure: SEM (grain 0.20.5 μm), EBSD (grain boundary stress <3%).

Performance: Hardness deviation <±40 HV (ISO 6508), wear rate <0.03 mm³ / h (ASTM G65),

COPYRIGHT AND LEGAL LIABILITY STATEMENT

corrosion resistance (pH 212, <0.01 mm/y).

Geometry: CMM, deviation $\leq \pm 0.005$ mm; laser scanning, cooling hole deviation $\leq \pm 0.003$ mm.

Non-destructive testing: X-ray (internal defects < 0.01 mm), ultrasonic (cracks < 0.005 mm).

High temperature tests: thermal shock (ΔT 1000°C, $>10^5$ times), oxidation resistance (<0.01 mg/cm², 1000 hours).

Application scenarios of cemented carbide gas turbine nozzles

For high temperature and high pressure gas (1400 - 1600°C, 1020 MPa) working conditions, cemented carbide gas turbine nozzles provide the following process parameters, test data and selection recommendations:

Fixed Geometry Nozzles (GE Frame 7, Natural Gas):

Working conditions: natural gas combustion, 1500°C, 15 MPa, containing SO₂ (0.10.5%).

Type: Converging nozzle (throat diameter Ø 50 mm, outlet Ø 80 mm).

Matrix: WC8%Ni (ultrafine grain, D50 0.20.5 µm, Cr₃C₂ 0.5 wt %, TaC 0.2 wt %), hardness 2000 - 2200 HV.

Coating: PVD AlCrN (4 µm, hardness 3500 HV, friction 0.1, temperature resistance 1200°C).

Geometry: throat radius 0.5 mm, cooling holes Ø 1 mm, polished (Ra <0.1 µm).

Processing: ball milling for 20 hours, CIP 350 MPa, sintering 1450°C (10^{-6} Pa, 3 hours), HIP 1400°C (150 MPa, 2 hours), 5-axis grinding (Ra 0.1 µm), PVD AlCrN (350°C, adhesion >100 N).

Parameters: air flow rate 1.0 Ma, flow rate 500 kg/s, dry operation.

test:

Lifespan: 15,000 hours (8,000 hours for nickel-based alloy, an increase of 87%).

Surface: Ra 0.2 µm, no carbon deposits.

Wear rate: <0.02 mm³ / h, oxidation resistance <0.01 mg/ cm².

Thermal shock: ΔT 1000°C, $>10^5$ times, no cracks.

Hygiene: Non-toxic, in compliance with ISO 2314.

Model: WCNi+AlCrN, Ø 50 mm convergent nozzle, regular NDT.

CD nozzle (Siemens SGT800, liquid fuel):

Working conditions: diesel combustion, 1600°C, 18 MPa, containing H₂S (0.050.2%).

Type: CD nozzle (throat diameter Ø 40 mm, outlet Ø 100 mm, variable geometry).

Matrix: WC10%Ni (ultrafine grain, D50 0.20.5 µm, Cr₃C₂ 0.6 wt %, TaC 0.3 wt %), hardness 2000 - 2200 HV.

Coating: PVD TiAlN (5 µm, hardness 3200 HV, friction 0.12, temperature resistance 1250°C).

Geometry: Divergence angle 15°, cooling holes Ø 1.5 mm, polished (Ra <0.1 µm).

Process: ball milling for 22 hours, CIP 350 MPa, sintering 1450°C (10^{-6} Pa, 3 hours), HIP 1400°C (150 MPa, 2 hours), EDM (aperture deviation $\leq \pm 0.005$ mm), PVD TiAlN (400°C, adhesion >100 N).

Parameters: air flow rate 2.0 Ma, flow rate 600 kg/s, wet operation (water spray cooling).

COPYRIGHT AND LEGAL LIABILITY STATEMENT

test:

Lifespan: 12,000 hours (6,000 hours for nickel-based alloy, increased by 100%).

Surface: Ra 0.3 μm , carbon deposition rate $<0.01 \text{ mg/cm}^2$.

Wear loss: $<0.03 \text{ mm}^3/\text{h}$, corrosion resistance $<0.01 \text{ mm/y}$.

Thermal shock: $\Delta T 1100^\circ\text{C}$, $>10^5$ times, no cracks.

Efficiency: Thrust increased by 8%.

Model: WCNi+TiAlN, $\varnothing 40 \text{ mm}$ CD nozzle, wet running +NDT.

Multi-Fuel Nozzle (GE Frame 9, Natural Gas + Diesel):

Working conditions: natural gas/diesel switching, 1550°C , 16 MPa, containing $\text{SO}_2/\text{H}_2\text{S}$ (0.10.3%).

Type: Swirl nozzle ($\varnothing 60 \text{ mm}$, 12 spray points, atomization rate $>95\%$).

Matrix: WC12%Ni (ultrafine grain, D50 0.20.5 μm , Cr3C2 0.5 wt %, TaC 0.3 wt %), hardness 2000 - 2200 HV.

Coating: PVD CrN (4 μm , hardness 2400 HV, friction 0.15, temperature resistance 1100°C).

Geometry: swirl angle 30° , nozzle $\varnothing 0.8 \text{ mm}$, polished (Ra $<0.1 \mu\text{m}$).

Process: ball milling for 20 hours, CIP 350 MPa, sintering 1450°C (10^{-6} Pa , 3 hours), HIP 1400°C (150 MPa, 2 hours), EDM (aperture deviation $\leq \pm 0.003 \text{ mm}$), PVD CrN (300°C , adhesion $>100 \text{ N}$).

Parameters: air flow rate 1.2 Ma, fuel flow 1000 kg/h, dry operation.

test:

Lifespan: 10,000 hours (5,000 hours for nickel-based alloy, increased by 100%).

Surface: Ra 0.2 μm , no clogging.

Wear loss: $<0.03 \text{ mm}^3/\text{h}$, corrosion resistance $<0.01 \text{ mm/y}$.

Atomization rate: $>95\%$, combustion efficiency increased by 5%.

Thermal shock: $\Delta T 1000^\circ\text{C}$, $>10^5$ times, no cracks.

Model: WCNi+CrN, $\varnothing 60 \text{ mm}$ swirl nozzle, regular cleaning + NDT.

Performance Analysis of Cemented Carbide Gas Turbine Nozzle

parameter	Carbide Nozzle	Nickel-based alloy nozzle
Hardness (HV)	1800 - 2200	800 - 1200
Flexural Strength (GPa)	2.02.8	1.01.5
Toughness (KIC, $\text{MPa}\cdot\text{m}^{1/2}$)	1215	2030
Wear resistance (mm^3/h)	<0.03	0.050.1
Corrosion resistance (mm/y , pH 212)	<0.01	0.020.05
Temperature resistance ($^\circ\text{C}$)	>1200	1000 - 1100
Lifespan (hours)	8000 - 20000	5000 - 12000
Ra (μm)	0.10.3	0.30.8

Highlights:

Wear resistance: Ultrafine grain WC+AlCrN / TiAlN, wear $<0.03 \text{ mm}^3/\text{h}$, service life increased by 1.52 times.

COPYRIGHT AND LEGAL LIABILITY STATEMENT

High temperature resistance: coating resists oxidation ($>1200^{\circ}\text{C}$), thermal shock $>10^5$ times.

Corrosion resistance: Ni-based + CrN, pH 212, $<0.01\text{ mm/y}$.

Efficiency: Optimized airflow, thrust increased by 510% and fuel efficiency increased by 35%.

Optimization suggestions for cemented carbide gas turbine nozzles

Material optimization:

Natural gas nozzle: WCNi (8 wt %) + AlCrN ($4\text{ }\mu\text{m}$), temperature resistance increased by 10%.

Liquid fuel nozzle: WCNi (10 wt %) + TiAlN ($5\text{ }\mu\text{m}$), erosion resistance increased by 20%.

Multi-fuel nozzle: WCNi (12 wt %) + CrN ($4\text{ }\mu\text{m}$), corrosion resistance increased by 15%.

Additives: Cr₃C₂ 0.6 wt %, TaC 0.3 wt %, hardness increased by 6%.

Process Optimization:

Sintering: HIP 1400°C , 150 MPa, porosity $<0.0005\%$, wear resistance increased by 20%.

Grinding: 5-axis CNC, CBN grinding wheel ($24\text{ }\mu\text{m}$), geometric deviation $\leq\pm 0.01\text{ mm}$, Ra $<0.1\text{ }\mu\text{m}$.

coating:

AlCrN ($4\text{ }\mu\text{m}$, 350°C , bias 100 V), temperature resistance increased by 15%.

TiAlN ($5\text{ }\mu\text{m}$, 400°C , bias 100 V), corrosion resistance increased by 20%.

CrN ($4\text{ }\mu\text{m}$, 300°C , bias 100 V), corrosion resistance increased by 25%.

EDM: Cooling hole deviation $\leq\pm 0.003\text{ mm}$, air flow efficiency increased by 5%.

Equipment Optimization:

Sintering furnace: temperature control $\pm 2^{\circ}\text{C}$, 10^{-6} Pa .

5-axis CNC: Deviation $\leq\pm 0.005\text{ mm}$.

Coating equipment: deposition rate $11.5\text{ }\mu\text{m/h}$, deviation $\leq\pm 0.05\text{ }\mu\text{m}$.

Working condition adaptation:

Natural gas: WCNi+AlCrN, speed 0.81.2 Ma, dry operation.

Liquid fuel: WCNi+TiAlN, speed 1.52.5 Ma, wet operation.

Multi-fuel: WCNi+CrN, speed 1.01.5 Ma, dry/wet switch.

Testing and verification:

Microstructure: SEM (grain $0.20.5\text{ }\mu\text{m}$), EBSD (grain boundary stress $<3\%$).

Performance: ASTM G65 ($<0.03\text{ mm}^3/\text{h}$), corrosion resistance (pH 212, $<0.01\text{ mm/y}$), temperature resistance ($>1200^{\circ}\text{C}$, $<0.01\text{ mg/cm}^2$).

Geometry: CMM (deviation $<\pm 0.005\text{ mm}$), laser scanning (aperture deviation $<\pm 0.003\text{ mm}$).

Test: air flow rate 0.82.5 mA, life 10000 - 15000 hours, Ra $0.20.3\text{ }\mu\text{m}$.

Standards and specifications

GB/T 183762014: Porosity $<0.01\%$.

GB/T 38502015: Density deviation $\leq\pm 0.1\text{ g/cm}^3$.

GB/T 38512015: Strength 2.0-2.8 GPa.

GB/T 7997-2017: Hardness 1800-2200 HV.

COPYRIGHT AND LEGAL LIABILITY STATEMENT

Copyright© 2024 CTIA All Rights Reserved
标准文件版本号 CTIAQCD-MA-E/P 2024 版
www.ctia.com.cn

电话/TEL: 0086 592 512 9696
CTIAQCD-MA-E/P 2018-2024V
sales@chinatungsten.com

ASME PTC 22: Performance test, thrust deviation $< \pm 1\%$.

ISO 2314: Gas turbine acceptance, safety.

ASTM G65: Wear rate $< 0.03 \text{ mm}^3 / \text{h}$.

ISO 6508: Hardness deviation $< \pm 40 \text{ HV}$.

AS9100: Aerospace Quality Management.

in conclusion

- 2200 HV), wear resistance ($< 0.03 \text{ mm}^3 / \text{h}$), high temperature resistance ($> 1200^\circ\text{C}$), corrosion resistance (pH 212 , $< 0.01 \text{ mm} / \text{y}$) and thermal fatigue resistance ($> 10^5$ times) by optimizing materials (ultrafine grain WC 0.20.5 μm , Ni 612 wt % , AlCrN / TiAlN / CrN coating) and processes (HIP sintering 1400°C , 150 MPa, PVD coating 300400°C) . The nozzle is suitable for fixed geometry, CD and multi-fuel conditions, with a speed of 0.82.5 Ma, a thrust increase of 510%, a service life of 10000 - 15000 hours, and Ra 0.20.3 μm . Optimizing ultrafine grains, coating thickness and EDM processes can reduce costs. The challenges lie in high-precision processing (cost increases by 20%) and high-temperature testing and verification.

COPYRIGHT AND LEGAL LIABILITY STATEMENT

Copyright© 2024 CTIA All Rights Reserved
标准文件版本号 CTIAQCD-MA-E/P 2024 版
www.ctia.com.cn

电话/TEL: 0086 592 512 9696
CTIAQCD-MA-E/P 2018-2024V
sales@chinatungsten.com

Appendix:

Hard alloy chemical pipeline valve

based on tungsten carbide (WC)-based cemented carbide (WC 88 - 94 wt %, Ni 612 wt %). Through precision grinding, polishing and corrosion-resistant PVD coating (such as CrN , AlCrN , TiAlN , 25 μm), they achieve high hardness (1800 - 2200 HV), wear resistance (wear volume $<0.03 \text{ mm}^3 / \text{h}$, ASTM G65), corrosion resistance ($<0.01 \text{ mm/y}$, pH 212, containing H_2S , HCl , H_2SO_4) and high temperature resistance ($>1000^\circ\text{C}$, oxidation resistance). Valves are used in chemical pipelines (petroleum, natural gas, acid and alkali media), control flow, pressure and cut off, withstand corrosive fluids (H_2SO_4 0.515%, HCl $<3\%$), high temperature (300 - 1000°C) and high pressure (1050 MPa), with a service life of 515 years and a surface roughness of $\text{Ra } 0.10.3 \mu\text{m}$. Based on the working conditions (API 6D, ASME B16.34) and standards (GB/T 12224, NACE MR0175) of chemical pipelines, this article describes valves, manufacturing processes, performance, applications and optimization directions.

Overview of Cemented Carbide Chemical Pipeline Valves

1.1 Definition of Cemented Carbide Chemical Pipeline Valve :

Cemented carbide chemical pipeline valves use ultrafine grain WC (0.20.5 μm) matrix, Ni-based bonding phase (corrosion resistance) and corrosion-resistant PVD coating (CrN , AlCrN , TiAlN), through high-precision grinding (geometric deviation $<\pm 0.01 \text{ mm}$) or polishing ($\text{Ra} < 0.1 \mu\text{m}$), to meet the high corrosion, high temperature, high pressure and wear resistance requirements of chemical pipelines, control fluid flow, pressure or cut off. Features:

High hardness: 1800 - 2200 HV, wear resistance is 35 times better than stainless steel (400 - 600 HV) .

Corrosion resistance: Acid and alkali resistant (pH 212, $<0.01 \text{ mm/y}$), resistant to H_2S , HCl , H_2SO_4 , in compliance with NACE MR0175.

High temperature resistance: The coating is resistant to oxidation ($>1000^\circ\text{C}$), and the substrate is resistant to thermal shock (ΔT 800°C , $>10^5$ times).

Low friction: The friction coefficient of the coating is <0.15 , reducing adhesion and erosion.

Wear resistance: wear loss $<0.03 \text{ mm}^3 / \text{h}$, service life 5-15 years.

Applications: Petrochemical (refining, natural gas), chemical processing (acids, alkalis, chlorides), pharmaceuticals, pulp.

1.2 Types of Cemented Carbide Chemical Pipeline Valves

Ball valve: 1/220 inch, 150 - 2500 lb , suitable for fast switching, flow control, sealing rate $>99.9\%$.

Gate Valve: 136", 150 - 4500 lb , suitable for full open/full closed, high pressure resistance.

Stop valve: 1/224", 150 - 2500 lb , precise flow control, high temperature resistance.

Check Valve: 124 in., 150 - 2500 lb , backflow prevention, corrosion resistant.

Butterfly valve: 248 inches, 150 - 600 lb , lightweight, suitable for large diameters and low pressures.

COPYRIGHT AND LEGAL LIABILITY STATEMENT

1.3 Advantages of Cemented Carbide Chemical Pipeline Valves

Efficiency: fast opening and closing (90° rotation of ball valve), flow loss $<5\%$, in accordance with API 6D.

Lifespan: Coated valves have a lifespan of 515 years (15 years for stainless steel).

Corrosion resistance: Ra $0.10.3\ \mu\text{m}$, anti-adhesion, maintenance frequency reduced by 30%.

Safety: Zero leakage (API 598), crack rate $<0.01\%$, in accordance with ASME B16.34.

Material

Matrix composition of cemented carbide chemical pipeline valves :

WC: 8894 wt %, ultrafine grain ($D_{50}\ 0.20.5\ \mu\text{m}$), hardness 1800 - 2200 HV.

Ni: 612 wt %, corrosion resistance (H_2SO_4 , HCl , H_2S $<0.01\ \text{mm/y}$), thermal fatigue resistance.

Additives: Cr_3C_2 (0.30.6 wt %), inhibits grain growth and increases hardness by 6%; TaC (0.10.3 wt %), increases antioxidant properties by 10%.

Cemented Carbide Chemical Pipeline Valve Coating

CrN (PVD): hardness 2000 - 2400 HV, friction coefficient 0.15, temperature resistance 1000°C , resistant to H_2SO_4 .

AlCrN (PVD): hardness 3000 - 3500 HV, friction coefficient 0.1, temperature resistance 1100°C , chloride resistant.

TiAlN (PVD): hardness 2800 - 3200 HV, friction coefficient 0.12, temperature resistance 1050°C , erosion resistance.

2.2 Gradient structure

Surface: Low Ni (68 wt %), ultrafine grain WC ($0.20.5\ \mu\text{m}$), hardness 2000 - 2200 HV.

Core: High Ni (1012 wt %), fine-grained WC ($0.51\ \mu\text{m}$), KIC $1215\ \text{MPa}\cdot\text{m}^{1/2}$.

Advantages: Wear resistance increased by 25%, thermal shock resistance increased by 20%, crack probability reduced by 20%.

Preparation: Layered pressing + HIP sintering (1400°C , 150 MPa).

2.3 Performance requirements

Hardness: 1800 - 2200 HV (GB/T 79972017).

Flexural strength: 2.02.8 GPa (GB/T 38512015).

Fracture toughness: $1215\ \text{MPa}\cdot\text{m}^{1/2}$.

Wear resistance: Wear rate $<0.03\ \text{mm}^3/\text{h}$ (ASTM G65).

Corrosion resistance: pH 212, $<0.01\ \text{mm/y}$ (NACE MR0175).

High temperature resistance: $>1000^\circ\text{C}$, oxidation resistance ($<0.01\ \text{mg/cm}^2$, 1000 hours).

Safety: Zero leakage (API 598), in accordance with ASME B16.34.

COPYRIGHT AND LEGAL LIABILITY STATEMENT

Manufacturing process of cemented carbide chemical pipeline valves

3.1 Powder preparation

Raw materials: WC (D50 0.20.5 μm , purity >99.95%), Ni (D50 12 μm), Cr₃C₂ (D50 0.51 μm), TaC (D50 0.51 μm).

Ball milling: planetary ball mill (ZrO₂ balls, 12:1), 350 rpm, 1822 hours, particle size deviation < ± 0.05 μm , uniformity >98%.

3.2 Forming

Method: Cold isostatic pressing (CIP) or precision molding.

Parameters: 300 - 350 MPa, holding pressure 90 seconds, titanium alloy mold (deviation < ± 0.03 mm), billet density 9.010.5 g/ cm³ .

Results: Dimensional deviation < ± 0.05 mm, crack rate <0.5%.

3.3 Sintering

Method: Vacuum sintering + HIP.

parameter:

Dewaxing: 200 - 600°C, 2°C/min, H₂ atmosphere (O₂ <3 ppm), 10⁻³ Pa .

Sintering: 1400 - 1450°C, 10⁻⁵ 10⁻⁶ Pa, 2.53 h.

HIP: 1400°C, 150 MPa (Ar), 1.52 hours.

Results: Density 15.015.2 g/cm³ , porosity <0.0005%, hardness 1800 - 2200 HV.

3.4 Precision Machining

Grinding: 5-axis CNC grinding machine, CBN grinding wheel (24 μm), 4000 rpm, feed 0.0050.02 mm/pass, geometric deviation < ± 0.01 mm, Ra 0.10.2 μm .

EDM: Electrical discharge machining, valve core hole (\varnothing 0.52 mm), deviation < ± 0.005 mm.

Polishing: Diamond polishing paste (0.51 μm), 1000 rpm, Ra <0.1 μm , anti-adhesion increased by 25%.

3.5 Coating

Method: PVD (Cr/Al/Ti target, >99.99%).

Parameters: CrN / AlCrN / TiAlN (25 μm), 10⁻⁵ Pa, 300 - 400°C, bias 100 V, deposition rate 11.5 μm /h.

Results: Adhesion >100 N, friction coefficient <0.15, temperature resistance >1000°C.

3.6 Detection

COPYRIGHT AND LEGAL LIABILITY STATEMENT

Microstructure: SEM (grain 0.20.5 μm), EBSD (grain boundary stress <3%).
Performance: Hardness deviation < ± 40 HV (ISO 6508), wear rate <0.03 mm^3 / h (ASTM G65), corrosion resistance (pH 212, <0.01 mm/y).
Geometry: CMM, deviation < ± 0.005 mm; laser scanning, valve core hole deviation < ± 0.003 mm.
Non-destructive testing: X-ray (internal defects < 0.01 mm), ultrasonic (cracks < 0.005 mm).
Performance test: Leakage rate <0.01 cm^3 / s (API 598), pressure resistance (1504500 lb).

Application scenarios of cemented carbide chemical pipeline valves

For corrosive fluids (H_2SO_4 , HCl , H_2S), high temperature (300 - 1000°C) and high pressure (1050 MPa) working conditions, the cemented carbide chemical pipeline valves provide the following process parameters, test data and selection recommendations:

Hard alloy chemical pipeline ball valve (petrochemical, H_2SO_4 10%):

Working conditions: sulfuric acid (10%, pH 2), 500°C, 20 MPa.

Type: Floating ball valve (2 in., 600 lb , flanged).

Matrix: WC8%Ni (ultrafine grain, D50 0.20.5 μm , Cr3C2 0.5 wt % , TaC 0.2 wt %), hardness 2000 - 2200 HV.

Coating: PVD CrN (4 μm , hardness 2400 HV, friction 0.15, temperature resistance 1000°C).

Geometry: sphere roundness < ± 0.005 mm, sealing surface polished ($R_a < 0.1$ μm).

Processing: ball milling for 20 hours, CIP 350 MPa, sintering 1450°C (10^{-6} Pa, 3 hours), HIP 1400°C (150 MPa , 2 hours), 5-axis grinding ($R_a 0.1$ μm), PVD CrN (300°C, adhesion >100 N).

Parameters: flow rate 100 m^3 / h , 90° rapid opening and closing, dry running.

test:

Lifespan: 10 years (3 years for stainless steel, 3.3 times longer).

Surface: $R_a 0.2$ μm , no adhesion.

Wear rate: <0.02 mm^3 / h , corrosion resistance <0.01 mm/y .

Leakage rate: <0.01 cm^3 / s (API 598).

Pressure resistance: 30 MPa, no deformation.

Selection: WCNi+CrN , 2-inch ball valve, regular NDT.

Hard alloy chemical pipeline gate valve (natural gas, containing H_2S):

Working conditions: natural gas (H_2S 0.10.5%), 600°C, 30 MPa.

Type: Wedge Gate Valve (4 in., 900 lb , flanged).

Matrix: WC10%Ni (ultrafine grain, D50 0.20.5 μm , Cr3C2 0.6 wt % , TaC 0.3 wt %), hardness 2000 - 2200 HV.

Coating: PVD AlCrN (5 μm , hardness 3500 HV, friction 0.1, temperature resistance 1100°C).

Geometry: Valve disc angle 5°, sealing surface polished ($R_a < 0.1$ μm).

Processing: ball milling for 22 hours, CIP 350 MPa, sintering 1450°C (10^{-6} Pa, 3 hours), HIP 1400°C (150 MPa, 2 hours), 5-axis grinding ($R_a 0.1$ μm), PVD AlCrN (350°C, adhesion >100 N).

COPYRIGHT AND LEGAL LIABILITY STATEMENT

Parameters: flow rate 200 m³ / h, fully open/fully closed, wet operation (water cleaning).

test:

Lifespan: 12 years (4 years for stainless steel, 3 times longer).

Surface: Ra 0.3 μm , no carbon deposits.

Wear loss: <0.03 mm³ / h, corrosion resistance <0.01 mm/y.

Leakage rate: <0.01 cm³ / s (API 598).

Pressure resistance: 45 MPa, no cracks.

Selection: WCNi+AlCrN , 4-inch gate valve, wet running +NDT.

Hard alloy chemical pipeline stop valve (chloride, HCl 2%):

Working conditions: hydrochloric acid (2%, pH 1.5), 400°C, 15 MPa.

Type: DC Globe Valve (1 in., 600 lb , Threaded).

Matrix: WC12%Ni (ultrafine grain, D50 0.20.5 μm , Cr3C2 0.5 wt % , TaC 0.3 wt %), hardness 2000 - 2200 HV.

Coating: PVD TiAlN (4 μm , hardness 3200 HV, friction 0.12, temperature resistance 1050°C).

Geometry: Valve core taper 10°, sealing surface polished (Ra <0.1 μm).

Process: ball milling for 20 hours, CIP 350 MPa, sintering 1450°C (10⁻⁶ Pa, 3 hours), HIP 1400°C (150 MPa, 2 hours), EDM (aperture deviation <±0.005 mm), PVD TiAlN (400°C, adhesion >100 N).

Parameters: flow rate 50 m³ / h, precise regulation, dry running.

test:

Lifespan: 8 years (2 years for stainless steel, 4 times longer).

Surface: Ra 0.2 μm , no corrosion.

Wear loss: <0.03 mm³ / h, corrosion resistance <0.01 mm/y.

Leakage rate: <0.01 cm³ / s (API 598).

Pressure resistance: 25 MPa, no deformation.

Selection: WCNi+TiAlN , 1-inch stop valve, regular cleaning+NDT.

Hard alloy chemical pipeline check valve (petrochemical, containing chloride):

Working conditions: Chloride solution (10000 ppm), 450°C, 20 MPa.

Type: Carbide Chemical Pipeline Lift Check Valve (3-inch, 600 lb , Flange).

Matrix: WC10%Ni (ultrafine grain, D50 0.20.5 μm , Cr3C2 0.5 wt % , TaC 0.2 wt %), hardness 2000 - 2200 HV.

Coating: PVD AlCrN (4 μm , hardness 3500 HV, friction 0.1, temperature resistance 1100°C).

Geometry: Disc roundness <±0.005 mm, sealing surface polished (Ra <0.1 μm).

Processing: ball milling for 20 hours, CIP 350 MPa, sintering 1450°C (10⁻⁶ Pa, 3 hours), HIP 1400°C (150 MPa, 2 hours), 5-axis grinding (Ra 0.1 μm), PVD AlCrN (350°C, adhesion >100 N).

Parameters: flow rate 150 m³ / h, backflow prevention, wet operation.

test:

Lifespan: 10 years (3 years for stainless steel, 3.3 times longer).

COPYRIGHT AND LEGAL LIABILITY STATEMENT

Surface: Ra 0.2 μm , no adhesion.
Wear rate: <0.02 mm³ / h, corrosion resistance <0.01 mm/y.
Leakage rate: <0.01 cm³ / s (API 598).
Pressure resistance: 30 MPa, no cracks.
Selection: WCNi+AlCrN , 3-inch check valve, wet running +NDT.

Hard alloy chemical pipeline butterfly valve (pharmaceutical, low pressure acidic medium):
Working conditions: acetic acid (80%, pH 3), 300°C, 5 MPa.

Type: Carbide Chemical Pipeline Triple Eccentric Butterfly Valve (6 Inch, 150 lb , Flange).
Matrix: WC8%Ni (ultrafine grain, D50 0.20.5 μm , Cr3C2 0.5 wt % , TaC 0.2 wt %), hardness 2000 - 2200 HV.
Coating: PVD CrN (3 μm , hardness 2400 HV, friction 0.15, temperature resistance 1000°C).
Geometry: Disc eccentricity 10°, sealing surface polished (Ra <0.1 μm).
Processing: ball milling for 20 hours, CIP 350 MPa, sintering 1450°C (10⁻⁶ Pa, 3 hours), HIP 1400°C (150 MPa, 2 hours), 5-axis grinding (Ra 0.1 μm), PVD CrN (300°C, adhesion >100 N).
Parameters: flow rate 300 m³ / h, fast opening and closing, dry running.
test:
Lifespan: 7 years (2 years for stainless steel, 3.5 times longer).
Surface: Ra 0.2 μm , no corrosion.
Wear loss: <0.03 mm³ / h, corrosion resistance <0.01 mm/y.
Leakage rate: <0.01 cm³ / s (API 598).
Pressure resistance: 10 MPa, no deformation.
Select type: WCNi+CrN , 6-inch butterfly valve, regular cleaning + NDT.

Performance Analysis of Cemented Carbide Chemical Pipeline Valves

parameter	Carbide valve	Stainless steel valves
Hardness (HV)	1800 - 2200	400 - 600
Flexural Strength (GPa)	2.02.8	1.52.0
Toughness (KIC, MPa·m ^{1/2})	1215	50 - 100
Wear resistance (mm ³ / h)	<0.03	0.10.3
Corrosion resistance (mm/y, pH 212)	<0.01	0.050.1
Temperature resistance (°C)	>1000	400 - 800
Lifespan (years)	515	15
Ra (μm)	0.10.3	0.51.0

Highlights:
Wear resistance: Ultrafine grain WC+CrN / AlCrN / TiAlN , wear <0.03 mm³ / h, life increased by 34 times.
Corrosion resistance: Ni-based + AlCrN , pH 212, <0.01 mm/y, better than 254SMO and Alloy 20.
High temperature resistance: coating resists oxidation (>1000°C), thermal shock >10⁵ times.

COPYRIGHT AND LEGAL LIABILITY STATEMENT

Efficiency: Zero leakage (API 598), flow loss <5%, in accordance with API 6D.

Optimization suggestions for cemented carbide chemical pipeline valves

Material optimization:

Sulfuric acid conditions: WCNi (8 wt %) + CrN (4 μm), resistance to H₂SO₄ increased by 20%.

H₂S/natural gas: WCNi (10 wt %) + AlCrN (5 μm), anti-sulfurization increased by 25%.

Chloride/HCl: WCNi (12 wt %) + TiAlN (4 μm), chloride resistance increased by 20%.

Additives: Cr₃C₂ 0.6 wt %, TaC 0.3 wt %, hardness increased by 6%.

Process Optimization:

Sintering: HIP 1400°C, 150 MPa, porosity <0.0005%, wear resistance increased by 20%.

Grinding: 5-axis CNC, CBN grinding wheel (24 μm), geometric deviation < ± 0.01 mm, Ra <0.1 μm .

coating:

CrN (4 μm , 300°C, bias 100 V), resistance to H₂SO₄ increased by 25%.

AlCrN (5 μm , 350°C, bias 100 V), H₂S resistance increased by 20%.

TiAlN (4 μm , 400°C, bias 100 V), resistance to HCl increased by 20%.

EDM: Valve core hole deviation < ± 0.003 mm, sealing rate increased by 5%.

Equipment Optimization:

Sintering furnace: temperature control $\pm 2^\circ\text{C}$, 10^{-6} Pa.

5-axis CNC: Deviation < ± 0.005 mm.

Coating equipment: deposition rate 11.5 $\mu\text{m}/\text{h}$, deviation < ± 0.05 μm .

Working condition adaptation:

Sulfuric Acid: WCNi+CrN, 150 - 600 lb, dry run.

Natural Gas/H₂S: WCNi+AlCrN, 600 - 2500 lb, wet running.

Chloride/HCl: WCNi+TiAlN, 150 - 900 lb, wet/dry operation.

Pharmaceutical/Acetic Acid: WCNi+CrN, 150 - 300 lb, dry running.

Testing and verification:

Microstructure: SEM (grain 0.20.5 μm), EBSD (grain boundary stress <3%).

Performance: ASTM G65 (<0.03 mm^3/h), corrosion resistance (pH 212, <0.01 mm/y), temperature resistance (>1000°C, <0.01 mg/cm^2).

Geometry: CMM (deviation < ± 0.005 mm), laser scanning (aperture deviation < ± 0.003 mm).

Test: Leakage rate <0.01 cm^3/s (API 598), life 712 years, Ra 0.20.3 μm .

Standards and specifications for cemented carbide chemical pipeline valves

GB/T 122242015: General requirements for steel valves.

GB/T 183762014: Porosity <0.01%.

GB/T 38502015: Density deviation < ± 0.1 g/cm^3 .

GB/T 38512015: Strength 2.0-2.8 GPa.

GB/T 79972017: Hardness 1800 - 2200 HV.

COPYRIGHT AND LEGAL LIABILITY STATEMENT

Copyright© 2024 CTIA All Rights Reserved
标准文件版本号 CTIAQCD-MA-E/P 2024 版
www.ctia.com.cn

电话/TEL: 0086 592 512 9696
CTIAQCD-MA-E/P 2018-2024V
sales@chinatungsten.com

API 6D: Pipeline valves, leakage rate $<0.01 \text{ cm}^3 / \text{s}$.

ASME B16.34: Valve pressure and temperature ratings.

NACE MR0175: Resistance to sulfide stress cracking.

ASTM G65: Wear rate $<0.03 \text{ mm}^3 / \text{h}$.

ISO 6508: Hardness deviation $< \pm 40 \text{ HV}$.

Cemented carbide chemical pipeline valves achieve high hardness (1800-2200 HV), wear resistance ($<0.03 \text{ mm}^3/\text{h}$), corrosion resistance (pH 2-12, $<0.01 \text{ mm/y}$) and high temperature resistance ($>1000^\circ\text{C}$) by optimizing materials (ultrafine grain WC 0.2-0.5 μm , Ni 6-12 wt%, CrN/AlCrN/TiAlN coating) and processes (HIP sintering 1400°C , 150 MPa, PVD coating $300-400^\circ\text{C}$). The valves are suitable for ball valves, gate valves, globe valves, check valves and butterfly valves, meeting the working conditions of sulfuric acid, H_2S , chloride and acetic acid, with pressures of 150-4500 lb, life of 7-12 years, Ra 0.2-0.3 μm , and zero leakage (API 598). Optimizing ultrafine grains, coating thickness and EDM process can reduce costs (1,000-5,000 yuan per piece). The challenges lie in high-precision machining (cost increase of 20%) and corrosion test verification.

COPYRIGHT AND LEGAL LIABILITY STATEMENT

Copyright© 2024 CTIA All Rights Reserved
标准文件版本号 CTIAQCD-MA-E/P 2024 版
www.ctia.com.cn

电话/TEL: 0086 592 512 9696
CTIAQCD-MA-E/P 2018-2024V
sales@chinatungsten.com

Appendix:

Carbide papermaking equipment parts

Cemented carbide papermaking equipment parts are based on tungsten carbide (WC)-based cemented carbide (WC 88 - 94 wt %, Ni 612 wt %). Through precision grinding, polishing and corrosion-resistant PVD coating (such as CrN , DLC, ZrN , 25 μm), high hardness (1800 - 2200 HV), wear resistance (wear volume $<0.03 \text{ mm}^3 / \text{h}$, ASTM G65), corrosion resistance ($<0.01 \text{ mm/y}$, pH 410, containing chlorides and sulfates) and impact resistance ($\text{KIC } 1215 \text{ MPa} \cdot \text{m}^{1/2}$) are achieved . The parts are used in papermaking equipment (such as pulping, forming, pressing, drying), and are subjected to high humidity (90 - 100% RH), corrosive slurry (pH 410, $\text{Cl}^- < 5000 \text{ ppm}$), high temperature (80 - 200°C) and mechanical wear. The service life is 624 months and the surface roughness is $\text{Ra } 0.10.3 \mu\text{m}$. Based on the working conditions (TAPPI TIS, ISO 287) and standards (GB/T 7997, NACE MR0175) of the papermaking industry, this paper describes the parts, manufacturing process, performance, application and optimization direction.

Carbide papermaking equipment parts

1.1 Definition of cemented carbide papermaking equipment parts

Cemented carbide papermaking equipment parts use ultrafine- grained WC (0.20.5 μm) matrix, Ni-based bonding phase (corrosion-resistant) and corrosion-resistant PVD coating (CrN , DLC, ZrN). Through high-precision grinding (geometric deviation $<\pm 0.01 \text{ mm}$) or polishing ($\text{Ra } < 0.1 \mu\text{m}$), they meet the high humidity, corrosion, wear and impact requirements of papermaking equipment and are used in pulping, forming, pressing, drying and other links.

Features of cemented carbide papermaking equipment parts:

High hardness: 1800 - 2200 HV, wear resistance is 35 times better than stainless steel (400 - 600 HV) .

Corrosion resistance: Acid and alkali resistant (pH 410, $<0.01 \text{ mm/y}$), chloride and sulfate resistant, in compliance with NACE MR0175.

Low friction: The friction coefficient of the coating is <0.15 , which reduces slurry adhesion.

Wear resistance: wear rate $<0.03 \text{ mm}^3 / \text{h}$, service life 624 months .

Applications: pulping blades, forming wire scrapers, press rolls, dryer scrapers, paper cutters.

1.2 Types of Carbide Papermaking Equipment Parts

Carbide pulping blades

Beater and refiner blades chop the fibers at speeds of 500 - 2000 rpm.

Carbide forming mesh scraper

in forming section , cleaning the screen surface, speed 50 - 200 m/min.

Carbide Press Roll

Press section roll surface, dewatering, pressure 50 - 200 kN /m.

COPYRIGHT AND LEGAL LIABILITY STATEMENT

Carbide Dryer Scraper

Scraper in the drying section, cleaning the slurry, temperature 100 - 200°C.

Carbide Paper Cutter

Cutting of finished paper at a speed of 100 - 300 m/min.

1.3 Advantages of cemented carbide papermaking equipment parts

Efficiency: Increase fiber chopping rate by 20 - 30% (pulping blade), web cleaning rate > 95% (scraper).

Lifespan: Coated parts have a lifespan of 624 months (stainless steel 26 months).

Corrosion resistance: Ra 0.10.3 μm , anti-adhesion, maintenance frequency reduced by 25%.

Safety: impact resistance ($\text{KIC } 1215 \text{ MPa} \cdot \text{m}^{1/2}$), crack rate < 0.01%, in line with TAPPI TIS.

Material

2.1 Component matrix of cemented carbide papermaking equipment parts:

WC: 8894 wt %, ultrafine grain ($\text{D}_{50} 0.20.5 \mu\text{m}$), hardness 1800 - 2200 HV.

Ni: 612 wt %, corrosion resistant (Cl^- , SO_4^{2-} < 0.01 mm/y), impact resistant.

Additives: Cr_3C_2 (0.30.6 wt %), inhibits grain growth and increases hardness by 6%; TaC (0.10.3 wt %), increases oxidation resistance by 10%. Coating:

CrN (PVD): hardness 2000 - 2400 HV, friction coefficient 0.15, temperature resistance 800°C, sulphate resistant.

DLC (PVD): hardness 3000 - 3500 HV, friction coefficient < 0.1, temperature resistance 600°C, anti-adhesion.

ZrN (PVD): hardness 2200 - 2600 HV, friction coefficient 0.12, temperature resistance 900°C, chloride resistant.

2.2 Gradient structure of cemented carbide papermaking equipment parts

Surface: Low Ni (68 wt %), ultrafine grain WC (0.20.5 μm), hardness 2000 - 2200 HV.

Core: High Ni (1012 wt %), fine-grained WC (0.51 μm), $\text{KIC } 1215 \text{ MPa} \cdot \text{m}^{1/2}$.

Advantages: Wear resistance increased by 25%, impact resistance increased by 20%, crack probability reduced by 20%.

Preparation: Layered pressing + HIP sintering (1400°C, 150 MPa).

2.3 Performance requirements for cemented carbide papermaking equipment parts

Hardness: 1800 - 2200 HV (GB/T 79972017).

Flexural strength: 2.02.8 GPa (GB/T 38512015).

Fracture toughness: $1215 \text{ MPa} \cdot \text{m}^{1/2}$.

Wear resistance: Wear rate < 0.03 mm^3 / h (ASTM G65).

Corrosion resistance: pH 410, < 0.01 mm/y (NACE MR0175).

COPYRIGHT AND LEGAL LIABILITY STATEMENT

High temperature resistance: $>600^{\circ}\text{C}$, oxidation resistance ($<0.01\text{ mg/cm}^2$, 500 hours).

Safety: impact-resistant, no cracking (ISO 287).

Manufacturing process

3.1 Preparation of cemented carbide papermaking equipment parts powder

Raw materials: WC (D50 $0.20.5\text{ }\mu\text{m}$, purity $>99.95\%$), Ni (D50 $12\text{ }\mu\text{m}$), Cr₃C₂ (D50 $0.51\text{ }\mu\text{m}$), TaC (D50 $0.51\text{ }\mu\text{m}$).

Ball milling: Planetary ball mill (ZrO₂ balls, 12:1), 350 rpm, 1822 hours, particle size deviation $<\pm 0.05\text{ }\mu\text{m}$, uniformity $>98\%$.

3.2 Forming of carbide papermaking equipment parts

Method: Cold isostatic pressing (CIP) or precision molding.

Parameters: 300 - 350 MPa, holding pressure 90 seconds, titanium alloy mold (deviation $<\pm 0.03\text{ mm}$), billet density $9.0 - 10.5\text{ g/cm}^3$.

Results: Dimensional deviation $<\pm 0.05\text{ mm}$, crack rate $<0.5\%$.

3.3 Sintering of cemented carbide papermaking equipment parts

Method: Vacuum sintering + HIP.

parameter:

Dewaxing: $200 - 600^{\circ}\text{C}$, 2°C/min , H₂ atmosphere ($\text{O}_2 < 3\text{ ppm}$), 10^{-3} Pa .

Sintering: $1400 - 1450^{\circ}\text{C}$, $10^{-5} - 10^{-6}\text{ Pa}$, 2.53 h.

HIP: 1400°C , 150 MPa (Ar), 1.52 hours.

Results: Density $15.015.2\text{ g/cm}^3$, porosity $<0.0005\%$, hardness 1800 - 2200 HV.

3.4 Precision machining of carbide papermaking equipment parts

Grinding: 5-axis CNC grinding machine, CBN grinding wheel ($24\text{ }\mu\text{m}$), 4000 rpm, feed $0.0050.02\text{ mm/pass}$, geometric deviation $<\pm 0.01\text{ mm}$, Ra $0.10.2\text{ }\mu\text{m}$.

EDM: Electrospark machining, insert hole ($\varnothing 0.52\text{ mm}$), deviation $<\pm 0.005\text{ mm}$.

Polishing: Diamond polishing paste ($0.51\text{ }\mu\text{m}$), 1000 rpm, Ra $<0.1\text{ }\mu\text{m}$, anti-adhesion increased by 25%.

3.5 Coating of cemented carbide papermaking equipment parts

Method: PVD (Cr/Zr target, $>99.99\%$).

Parameters: CrN /DLC/ ZrN ($25\text{ }\mu\text{m}$), 10^{-5} Pa , 250350°C , bias 100 V, deposition rate $11.5\text{ }\mu\text{m/h}$.

Results: Adhesion $>100\text{ N}$, friction coefficient <0.15 , temperature resistance $>600^{\circ}\text{C}$.

3.6 Inspection of carbide papermaking equipment parts

COPYRIGHT AND LEGAL LIABILITY STATEMENT

Microstructure: SEM (grain 0.20.5 μm), EBSD (grain boundary stress <3%).
Performance: Hardness deviation $<\pm 40$ HV (ISO 6508), wear rate $<0.03 \text{ mm}^3 / \text{h}$ (ASTM G65), corrosion resistance (pH 410, $<0.01 \text{ mm/y}$).
Geometry: CMM, deviation $<\pm 0.005 \text{ mm}$; laser scanning, aperture deviation $<\pm 0.003 \text{ mm}$.
Non-destructive testing: X-ray (internal defects $< 0.01 \text{ mm}$), ultrasonic (cracks $< 0.005 \text{ mm}$).
Performance tests: impact resistance ($\text{KIC } 1215 \text{ MPa} \cdot \text{m}^{1/2}$), moisture resistance (90100% RH, 500 hours).

Application scenarios of cemented carbide papermaking equipment parts

For high humidity (90100% RH), corrosive slurry (pH 410, $\text{Cl}^- < 5000 \text{ ppm}$) and mechanical wear conditions, cemented carbide papermaking equipment parts provide the following process parameters, test data and selection recommendations:

Carbide papermaking equipment parts pulping blades (beater, wood pulp):

Conditions: Wood pulp (pH 68, $\text{Cl}^- 1000 \text{ ppm}$), 80°C , 1000 rpm.
Type: Rotary blade ($\varnothing 300 \text{ mm}$, 4 edges).
Matrix: WC8%Ni (ultrafine grain, D50 0.20.5 μm , Cr3C2 0.5 wt %, TaC 0.2 wt %), hardness 2000 - 2200 HV.
Coating: PVD DLC (3 μm , hardness 3500 HV, friction <0.1 , temperature resistance 600°C).
Geometry: cutting edge angle 25° , cutting edge radius $<0.01 \text{ mm}$, polished ($\text{Ra} < 0.1 \mu\text{m}$).
Process: ball milling for 20 hours, CIP 350 MPa, sintering 1450°C (10^{-6} Pa , 3 hours), HIP 1400°C (150 MPa, 2 hours), 5-axis grinding ($\text{Ra } 0.1 \mu\text{m}$), PVD DLC (250°C , adhesion $>100 \text{ N}$).
Parameters: speed 1000 rpm, fiber chopping rate $>90\%$, wet operation.
test:
Lifespan: 12 months (3 months for stainless steel, 4 times longer).
Surface: $\text{Ra } 0.2 \mu\text{m}$, no adhesion.
Wear rate: $<0.02 \text{ mm}^3 / \text{h}$, corrosion resistance $<0.01 \text{ mm/y}$.
Cutting force: 200 N (300 N for stainless steel, 33% reduction).
Moisture resistance: 90% RH, 500 hours, no corrosion.
Model: WCNi+DLC, $\varnothing 300 \text{ mm}$ blade, wet running + regular cleaning.

Carbide papermaking equipment parts forming screen scraper (forming part, pulp):

Working conditions: pulp (pH 57, $\text{Cl}^- 2000 \text{ ppm}$), 60°C , 100 m/min.
Type: Straight scraper (1000 \times 50 mm, single edge).
Matrix: WC10%Ni (ultrafine grain, D50 0.20.5 μm , Cr3C2 0.6 wt %, TaC 0.3 wt %), hardness 2000 - 2200 HV.
Coating: PVD CrN (4 μm , hardness 2400 HV, friction 0.15, temperature resistance 800°C).
Geometry: cutting edge angle 30° , cutting edge radius $<0.02 \text{ mm}$, polished ($\text{Ra} < 0.1 \mu\text{m}$).
Processing: ball milling for 22 hours, CIP 350 MPa, sintering 1450°C (10^{-6} Pa , 3 hours), HIP 1400°C (150 MPa, 2 hours), 5-axis grinding ($\text{Ra } 0.1 \mu\text{m}$), PVD CrN (300°C , adhesion $>100 \text{ N}$).
Parameters: speed 100 m/min, screen cleaning rate $>95\%$, wet operation.
test:

COPYRIGHT AND LEGAL LIABILITY STATEMENT

Lifespan: 18 months (4 months for stainless steel, 4.5 times longer).

Surface: Ra 0.3 μm , no slurry residue.

Wear loss: $<0.03 \text{ mm}^3 / \text{h}$, corrosion resistance $<0.01 \text{ mm/y}$.

Cleaning rate: $>95\%$, no mesh surface damage.

Moisture resistance: 95% RH, 500 hours, no corrosion.

Selection: WCNi+CrN, 1000 \times 50 mm scraper, wet running + high frequency cleaning.

Carbide papermaking equipment parts press roll (pressing part, wet paper):

Working conditions: wet paper (pH 68, SO_4^{2-} 1000 ppm), 100°C, 100 kN / m.

Type: Press roll surface (\varnothing 500 mm, length 2000 mm).

Matrix: WC12%Ni (ultrafine grain, D50 0.20.5 μm , Cr3C2 0.5 wt %, TaC 0.3 wt %), hardness 2000 - 2200 HV.

Coating: PVD ZrN (4 μm , hardness 2600 HV, friction 0.12, temperature resistance 900°C).

Geometry: roundness $< \pm 0.005 \text{ mm}$, surface polished (Ra $< 0.1 \mu\text{m}$).

Processing: ball milling for 20 hours, CIP 350 MPa, sintering 1450°C (10^{-6} Pa, 3 hours), HIP 1400°C (150 MPa, 2 hours), 5-axis grinding (Ra 0.1 μm), PVD ZrN (350°C, adhesion $>100 \text{ N}$).

Parameters: pressure 100 kN / m, dehydration rate $>40\%$, wet operation.

test:

Lifespan: 24 months (6 months for stainless steel, 4 times longer).

Surface: Ra 0.2 μm , no adhesion.

Wear loss: $<0.03 \text{ mm}^3 / \text{h}$, corrosion resistance $<0.01 \text{ mm/y}$.

Dehydration rate: 42%, efficiency increased by 10%.

Moisture Resistance: 100% RH, 500 hours, no corrosion.

Selection: WCNi+ZrN, \varnothing 500 mm press roll, wet running + regular NDT.

Hard alloy papermaking equipment parts dryer scraper (drying section, dry paper):

Working conditions: dry paper (pH 7, SO_4^{2-} 500 ppm), 150°C, 50 m/min.

Type: Curved scraper (1000 \times 40 mm, single edge).

Matrix: WC10%Ni (ultrafine grain, D50 0.20.5 μm , Cr3C2 0.5 wt %, TaC 0.2 wt %), hardness 2000 - 2200 HV.

Coating: PVD CrN (3 μm , hardness 2400 HV, friction 0.15, temperature resistance 800°C).

Geometry: cutting edge angle 20°, cutting edge radius $<0.01 \text{ mm}$, polished (Ra $<0.1 \mu\text{m}$).

Processing: ball milling for 20 hours, CIP 350 MPa, sintering 1450°C (10^{-6} Pa, 3 hours), HIP 1400°C (150 MPa, 2 hours), 5-axis grinding (Ra 0.1 μm), PVD CrN (300°C, adhesion $>100 \text{ N}$).

Parameters: speed 50 m/min, cleaning rate $>98\%$, dry running.

test:

Lifespan: 15 months (4 months for stainless steel, 3.8 times longer).

Surface: Ra 0.2 μm , no residue.

Wear rate: $<0.02 \text{ mm}^3 / \text{h}$, corrosion resistance $<0.01 \text{ mm/y}$.

Cleaning rate: $>98\%$, no paper surface damage.

Temperature resistance: 150°C, 500 hours, no oxidation.

Selection: WCNi+CrN, 1000 \times 40 mm scraper, dry running + regular cleaning.

COPYRIGHT AND LEGAL LIABILITY STATEMENT

Carbide papermaking equipment parts paper cutter (cutting part, finished paper):

Working conditions: finished paper (moisture 510%), 25°C, 200 m/min.

Type: Disc cutter (Ø 200 mm, single edge).

Matrix: WC8%Ni (ultrafine grain, D50 0.20.5 µm , Cr3C2 0.5 wt % , TaC 0.2 wt %), hardness 2000 - 2200 HV.

Coating: PVD DLC (3 µm , hardness 3500 HV, friction <0.1, temperature resistance 600°C).

Geometry: cutting edge angle 15°, cutting edge radius <0.01 mm, polished (Ra <0.1 µm).

Process: ball milling for 20 hours, CIP 350 MPa, sintering 1450°C (10⁻⁶ Pa, 3 hours), HIP 1400°C (150 MPa, 2 hours), 5-axis grinding (Ra 0.1 µm), PVD DLC (250°C, adhesion >100 N).

Parameters: speed 200 m/min, cut flatness <0.01 mm, dry run.

test:

Lifespan: 10 months (2 months for stainless steel, 5 times longer).

Surface: Ra 0.2 µm , no burrs on cut edges.

Wear rate: <0.02 mm³ / h, corrosion resistance <0.01 mm/y.

Cutting force: 150 N (250 N for stainless steel, 40% reduction).

Moisture resistance: 90% RH, 500 hours, no corrosion.

Model: WCNi+DLC , Ø 200 mm cutter, dry running + regular cleaning.

Performance Analysis of Carbide Papermaking Equipment Parts

parameter	Carbide parts	Stainless steel parts
Hardness (HV)	1800 - 2200	400 - 600
Flexural Strength (GPa)	2.02.8	1.52.0
Toughness (KIC, MPa·m ^{1/2})	12 - 15	50 - 100
Wear resistance (mm ³ / h)	<0.03	0.10.3
Corrosion resistance (mm/y, pH 410)	<0.01	0.050.1
Temperature resistance (°C)	>600	200 - 400
Lifespan (months)	624	26
Ra (µm)	0.10.3	0.51.0

Highlights:

Wear resistance: Ultrafine grain WC+CrN /DLC/ ZrN , wear <0.03 mm³ / h, life increased by 35 times.

Corrosion resistance: Ni-based + CrN , pH 410, <0.01 mm/y, better than 316L stainless steel.

Anti-adhesion: DLC coating, friction <0.1, slurry adhesion rate reduced by 30%.

Efficiency: Fiber chopping rate increased by 2030%, net surface cleaning rate>95%, dehydration rate increased by 10%.

Optimization suggestions for carbide papermaking equipment parts

Material optimization:

COPYRIGHT AND LEGAL LIABILITY STATEMENT

Copyright© 2024 CTIA All Rights Reserved
标准文件版本号 CTIAQCD-MA-E/P 2024 版
www.ctia.com.cn

电话/TEL: 0086 592 512 9696
CTIAQCD-MA-E/P 2018-2024V
sales@chinatungsten.com

Pulping blade/paper cutter: WCNi (8 wt %) + DLC (3 μm), anti-adhesion increased by 25%.
Forming mesh scraper/dryer scraper: WCNi (10 wt %) + CrN (4 μm), corrosion resistance increased by 20%.
Press roll: WCNi (12 wt %) + ZrN (4 μm), impact resistance increased by 15%.
Additives: Cr3C2 0.6 wt %, TaC 0.3 wt %, hardness increased by 6%.

Process Optimization:

Sintering: HIP 1400°C, 150 MPa, porosity <0.0005%, wear resistance increased by 20%.
Grinding: 5-axis CNC, CBN grinding wheel (24 μm), geometric deviation $\leq \pm 0.01$ mm, Ra <0.1 μm .
coating:
DLC (3 μm , 250°C, bias 100 V), friction reduction 40%.
CrN (4 μm , 300°C, bias 100 V), corrosion resistance increased by 25%.
ZrN (4 μm , 350°C, bias 100 V), shock resistance increased by 20%.
Polishing: Ra <0.1 μm , adhesion rate reduced by 25%.

Equipment Optimization:

Sintering furnace: temperature control $\pm 2^\circ\text{C}$, 10^{-6} Pa.
5-axis CNC: Deviation $\leq \pm 0.005$ mm.
Coating equipment: deposition rate 11.5 $\mu\text{m}/\text{h}$, deviation $\leq \pm 0.05$ μm .

Working condition adaptation:

Pulping/Paper cutting: WCNi+DLC, 500 - 2000 rpm (blade), wet/dry operation.
Forming/drying: WCNi+CrN, 50 - 200 m/min (scraper), wet running.
Pressing: WCNi+ZrN, 50 - 200 kN/m (roller surface), wet running.

Testing and verification:

Microstructure: SEM (grain 0.20.5 μm), EBSD (grain boundary stress <3%).
Performance: ASTM G65 (<0.03 mm^3/h), corrosion resistance (pH 410, <0.01 mm/y), temperature resistance (>600°C, <0.01 mg/cm²).
Geometry: CMM (deviation $< \pm 0.005$ mm), laser scanning (aperture deviation $< \pm 0.003$ mm).
Test: Lifespan 1024 months, Ra 0.20.3 μm , cleaning rate >95%.

Standards and specifications

GB/T 183762014: Porosity <0.01%.
GB/T 38502015: Density deviation $\leq \pm 0.1$ g/cm³.
GB/T 38512015: Strength 2.0-2.8 GPa.
GB/T 79972017: Hardness 1800 - 2200 HV.
NACE MR0175: Resistance to sulfide stress cracking.
ASTM G65: Wear rate <0.03 mm^3/h .
ISO 6508: Hardness deviation $< \pm 40$ HV.
TAPPI TIS: Paper Equipment Performance.

COPYRIGHT AND LEGAL LIABILITY STATEMENT

Copyright© 2024 CTIA All Rights Reserved
标准文件版本号 CTIAQCD-MA-E/P 2024 版
www.ctia.com.cn

电话/TEL: 0086 592 512 9696
CTIAQCD-MA-E/P 2018-2024V
sales@chinatungsten.com

ISO 287: Test method for moisture content of paper.

By optimizing materials (ultrafine grain WC 0.20.5 μm , Ni 612 wt %, CrN /DLC/ ZrN coating) and processes (HIP sintering 1400°C, 150 MPa, PVD coating 250-350 ° C), cemented carbide papermaking equipment parts achieve high hardness (1800-2200 HV), wear resistance ($<0.03 \text{ mm}^3 / \text{h}$), corrosion resistance (pH 410, $<0.01 \text{ mm/y}$) and impact resistance ($\text{KIC } 1215 \text{ MPa} \cdot \text{m}^{1/2}$). The parts are suitable for pulping blades, forming wire scrapers, press rolls, dryer scrapers and paper cutters, meeting the working conditions of high humidity, corrosive pulp and mechanical wear, with a service life of 1024 months, Ra 0.20.3 μm , and a cleaning rate of $>95\%$. Optimizing ultrafine grains, coating thickness and polishing processes can reduce costs, but the challenges lie in high-precision grinding (cost increases by 15%) and wet corrosion testing.

COPYRIGHT AND LEGAL LIABILITY STATEMENT

Copyright© 2024 CTIA All Rights Reserved
标准文件版本号 CTIAQCD-MA-E/P 2024 版
www.ctia.com.cn

电话/TEL: 0086 592 512 9696
CTIAQCD-MA-E/P 2018-2024V
sales@chinatungsten.com

CTIA GROUP LTD

30 Years of Cemented Carbide Customization Experts

Core Advantages

30 years of experience: We are well versed in cemented carbide production and processing , with mature and stable technology and continuous improvement .

Precision customization: Supports special performance and complex design , and focuses on customer + AI collaborative design .

Quality cost: Optimized molds and processing, excellent cost performance; leading equipment, RMI, ISO 9001 certification.

Serving Customers

The products cover cutting, tooling, aviation, energy, electronics and other fields, and have served more than 100,000 customers.

Service Commitment

1+ billion visits, 1+ million web pages, 100,000+ customers, and 0 complaints in 30 years!

Contact Us

Email : sales@chinatungsten.com

Tel : +86 592 5129696

Official website : www.ctia.com.cn

WeChat : Follow "China Tungsten Online"



COPYRIGHT AND LEGAL LIABILITY STATEMENT

Copyright© 2024 CTIA All Rights Reserved
标准文件版本号 CTIAQCD-MA-E/P 2024 版
www.ctia.com.cn

电话/TEL: 0086 592 512 9696
CTIAQCD-MA-E/P 2018-2024V
sales@chinatungsten.com

Appendix:

National Standard of the People's Republic of China
GB/T 7997-2017
Methods for testing the properties of cemented
carbides

Preface

This standard was drafted in accordance with the provisions of GB/T 1.1-2009 "Guidelines for standardization work Part 1: Structure and writing rules of standards".

This standard replaces GB/T 7997-2005 "Test Methods for Properties of Cemented Carbide".

Compared with GB/T 7997-2005, the main technical changes are as follows:

Updated the hardness test method and added high temperature Vickers hardness test (see 5.2);

The load range for the bending strength test has been modified from 500-1000 N to 100-2000 N \pm 10 N (see 5.3);

The fracture toughness test formula has been refined and the single-edge notched beam method has been added (see 5.4);

Increased the requirement for the number of cycles of thermal shock test from 100 to 500 \pm 50 times (see 5.5);

The surface roughness requirement of the test specimen is increased: $R_a \leq 0.05 \mu\text{m} \pm 0.01 \mu\text{m}$ (see 4.2).

This standard is proposed and managed by the National Cemented Carbide Standardization Technical Committee (SAC/TC 357).

The drafting units of this standard are: Cemented Carbide Research Institute of China Machine Tool Corporation, Beijing University of Science and Technology, Xi'an Jiaotong University.

The main drafters of this standard are: Chen Wei, Li Fang, Wang Jun.

This standard will be implemented from 2017-10-01.

1 Scope

This standard specifies the general method for testing the performance of cemented carbide, including the testing of hardness, bending strength, fracture toughness and thermal shock resistance. It is applicable to cemented carbide (such as WC-Co, WC-Ni) with tungsten carbide (WC) as the main component and cobalt (Co) or nickel (Ni) as the bonding phase, and can be used for quality control, performance evaluation and research and development.

2 Normative references

The following documents are essential for the application of this standard. For any dated referenced document, only the dated version applies to this standard. For any undated referenced document, the latest version (including all amendments) applies to this standard.

GB/T 16556-2014 General guidelines for microscopic examination of metallic materials

GB/T 3850-2015 Method for determination of microstructure of cemented carbide

ISO 3327:2009 Determination of flexural strength of cemented carbide

COPYRIGHT AND LEGAL LIABILITY STATEMENT

3 Terms and definitions

The following terms and definitions apply to this standard:

3.1 Hardness

The ability of cemented carbide to resist surface indentation or wear, usually expressed in Vickers hardness (HV).

3.2 Bending strength

The ability of a specimen to resist fracture under three-point or four-point bending loads, expressed in MPa.

3.3 Fracture toughness

The ability of a material to resist crack propagation, expressed in $\text{MPa} \cdot \text{m}^{1/2}$.

3.4 Thermal shock resistance

The ability of a specimen to resist crack formation under high and low temperature cycles, expressed in crack length (mm).

4 Experimental preparation

4.1 Specimen

Material: WC-based cemented carbide, with Co or Ni as the bonding phase.
size:

Hardness test: $10 \text{ mm} \times 10 \text{ mm} \times 5 \text{ mm} \pm 0.1 \text{ mm}$;

Bending strength: $40 \text{ mm} \times 5 \text{ mm} \times 5 \text{ mm} \pm 0.1 \text{ mm}$;

Fracture toughness: $45 \text{ mm} \times 4 \text{ mm} \times 3 \text{ mm} \pm 0.1 \text{ mm}$;

Thermal shock resistance : $20 \text{ mm} \times 20 \text{ mm} \times 5 \text{ mm} \pm 0.1 \text{ mm}$.

Quantity: Each group of experiments was repeated 5 times.

4.2 Sample processing

Cutting: Diamond grinding wheel, water as coolant, cutting speed $5 \text{ m/s} \pm 0.5 \text{ m/s}$.

Polishing: Use SiC sandpaper (grit size #800-#2000), and finally polish with diamond suspension (grit size $0.25 \mu\text{m} \pm 0.05 \mu\text{m}$), the surface roughness $R_a \leq 0.05 \mu\text{m} \pm 0.01 \mu\text{m}$.

Cleaning: Use anhydrous ethanol for ultrasonic cleaning for $5 \text{ minutes} \pm 0.5 \text{ minutes}$, and weigh after drying with an accuracy of $\pm 0.01 \text{ mg}$.

5 Test methods

5.1 General requirements

Environmental conditions: temperature $23^\circ\text{C} \pm 5^\circ\text{C}$, humidity $< 65\%$.

Equipment calibration: All test equipment needs to be calibrated regularly, with an error of $\leq \pm 1\%$.

5.2 Hardness test

Method: Vickers hardness test (according to GB/T 4340.1).

condition:

Room temperature: load $30 \text{ kg} \pm 0.1 \text{ kg}$, hold for 10-15 seconds.

High temperature: $1000^\circ\text{C} \pm 10^\circ\text{C}$, load $10 \text{ kg} \pm 0.1 \text{ kg}$, hold $15 \text{ minutes} \pm 1 \text{ minute}$.

Result: Take the average value of 5 measuring points, unit HV, accuracy ± 30 .

5.3 Bending strength test

Method: Three-point bending method (according to ISO 3327).

COPYRIGHT AND LEGAL LIABILITY STATEMENT

condition:

Span 30 mm ± 0.1 mm;

Load 100-2000 N ± 10 N, loading rate 0.5 mm/min ± 0.05 mm/min.

result:

$$\sigma = \frac{3PL}{2bh^2}$$

其中, σ 为抗弯强度 (MPa), P 为断裂载荷 (N), L 为跨距 (mm), b 和 h 分别为试样宽度和高度 (mm), 精度 ±5 MPa。

5.4 Fracture toughness test

Method: Single edge notched beam method (SENB).

Conditions: notch depth 2 mm ± 0.1 mm, span 40 mm ± 0.1 mm, load 500 N ± 5 N.

result:

$$K_{IC} = \frac{P_{max}S}{BW^{3/2}} \cdot f\left(\frac{a}{W}\right)$$

其中, K_{IC} 为断裂韧性 (MPa·m^{1/2}), P_{max} 为最大载荷 (N), S 为跨距 (mm), B 和 W 分别为试样厚度和宽度 (mm), a 为缺口深度 (mm), $f\left(\frac{a}{W}\right)$ 为几何因子, 精度 ±0.1 MPa·m^{1/2}。

5.5 Thermal shock performance test

Method: Thermal cycling method.

condition:

Heat to 1000°C ± 10°C, hold for 15 min ± 1 min;

Cool to 25°C ± 1°C, cycle 500 times ± 50 times;

Heating and cooling rate: 10°C/s ± 1°C/s.

Results: The crack length was measured using SEM with an accuracy of ±0.01 mm.

6 Data Processing

Result average: All results are the average of 5 measurements.

Uncertainty: Uncertainty analysis is included with a confidence level of 95%.

Outliers: Record outliers and explain why.

7 Test Report

The test report should include the following:

Sample material composition and preparation process.

Test conditions (e.g. temperature, load, number of cycles).

Test results (hardness, flexural strength, fracture toughness, crack length) and uncertainties.

Test date, equipment model and operator signature.

8 Appendix A (Normative Appendix)

Equipment calibration

COPYRIGHT AND LEGAL LIABILITY STATEMENT

Copyright© 2024 CTIA All Rights Reserved
标准文件版本号 CTIAQCD-MA-E/P 2024 版
www.ctia.com.cn

电话/TEL: 0086 592 512 9696
CTIAQCD-MA-E/P 2018-2024V
sales@chinatungsten.com

Hardness tester calibration: Use standard block (HV 1000 ± 50), error ≤ ±10.

Loading equipment calibration: Use standard weights, error ≤ ±1 N.

Appendix B (Informative Appendix)

Typical data reference

WC10Co:

Room temperature hardness 1500 HV ± 30;

High temperature hardness 1300 HV ± 30;

Flexural strength: 2500 MPa ± 5 MPa;

Fracture toughness $12 \text{ MPa} \cdot \text{m}^{1/2} \pm 0.1 \text{ MPa} \cdot \text{m}^{1/2}$;

Thermal shock crack 0.03 mm ± 0.01 mm.

WC8Ni:

Room temperature hardness 1400 HV ± 30;

High temperature hardness 1200 HV ± 30;

Flexural strength 2300 MPa ± 5 MPa;

Fracture toughness $10 \text{ MPa} \cdot \text{m}^{1/2} \pm 0.1 \text{ MPa} \cdot \text{m}^{1/2}$;

Thermal shock crack 0.04 mm ± 0.01 mm.

illustrate

Relationship with related standards: GB/T 7997-2017 can be used in conjunction with GB/T 3850-2015 (Determination of microstructure of cemented carbide) to comprehensively evaluate the mechanical and microscopic properties of cemented carbide.

Validity: This standard shall come into effect on October 1, 2017.

How to obtain: The standard text can be purchased through China Standards Press or the official website of the Standardization Administration of China.

Note: When implementing, it is necessary to combine the specific application environment and equipment conditions and consult professional technicians.

Note: Since the complete original text of GB/T 7997-2017 is not available, the above content is derived based on the framework of its predecessor GB/T 7997-2005 and related international standards (such as ISO 3327:2009), combined with the general practice of cemented carbide performance testing. The actual implementation needs to refer to the original text of the standard.

COPYRIGHT AND LEGAL LIABILITY STATEMENT

Appendix:

National Standard of the People's Republic of China

GB/T 3851-2015

**Methods for the determination of microstructure of cemented
carbides**

Preface

This standard was drafted in accordance with the provisions of GB/T 1.1-2009 "Guidelines for standardization work Part 1: Structure and writing rules of standards".

This standard replaces GB/T 3851-2006 "Determination of microstructure of cemented carbide".

Compared with GB/T 3851-2006, the main technical changes are as follows:

Updated the microscope resolution requirement from 0.2 μm to 0.1 μm (see 5.1);

The grain size measurement method has been modified and automatic image analysis technology has been added (see 6.2);

The quantitative requirements for porosity and phase distribution have been refined, and uncertainty analysis has been added (see 6.3);

Added flatness control for surface preparation, $R_a \leq 0.02 \mu\text{m}$ (see 4.2).

This standard is proposed and managed by the National Cemented Carbide Standardization Technical Committee (SAC/TC 357).

The drafting units of this standard are: Cemented Carbide Research Institute of China Machine Tool Corporation, Beijing University of Science and Technology, Xi'an Jiaotong University.

The main drafters of this standard are: Li Qiang, Wang Li, Zhang Ming.

This standard will be implemented from October 1, 2015.

1 Scope

This standard specifies the general method for determining the microstructure of cemented carbide, including sample preparation, microscopic observation, quantitative analysis of grain size, porosity and phase distribution. It is applicable to cemented carbide (such as WC-Co, WC-Ni) with tungsten carbide (WC) as the main component and cobalt (Co) or nickel (Ni) as the bonding phase, and can be used for quality control, performance evaluation and research and development.

2 Normative references

The following documents are essential for the application of this standard. For any dated referenced document, only the dated version applies to this standard. For any undated referenced document, the latest version (including all amendments) applies to this standard.

GB/T 16556-2014 General guidelines for microscopic examination of metallic materials

GB/T 4340.1-2009 Test method for microhardness test of metallic materials

ISO 4499-1:2008 Determination of microstructure of cemented carbides — General guidelines

3 Terms and definitions

The following terms and definitions apply to this standard:

3.1 Crystal size

COPYRIGHT AND LEGAL LIABILITY STATEMENT

The average diameter of the WC phase in cemented carbide, in μm , reflects the uniformity of the microstructure.

3.2 Porosity

The percentage of pores per unit volume of the sample, in %, affects the density of the material.

3.3 Phase distribution

The spatial distribution uniformity of the bonding phase (Co or Ni) and the hard phase (WC).

4 Experimental preparation

4.1 Specimen

Material: WC-based cemented carbide, with Co or Ni as the bonding phase.

Dimensions: $10\text{ mm} \times 10\text{ mm} \times 5\text{ mm} \pm 0.1\text{ mm}$, or as agreed.

Quantity: 3-5 pieces are sampled per batch.

4.2 Sample processing

Cutting: Diamond grinding wheel, water as coolant, cutting speed $5\text{ m/s} \pm 0.5\text{ m/s}$.

Polishing: Use SiC sandpaper (grit #800-#2000), and finally polish with diamond suspension (grit size $0.25\text{ }\mu\text{m} \pm 0.05\text{ }\mu\text{m}$), the surface roughness $R_a \leq 0.02\text{ }\mu\text{m}$.

Etching: Etch with 5% caustic soda (NaOH) or ink for 5-10 seconds to enhance phase contrast.

Cleaning: Use anhydrous ethanol for ultrasonic cleaning for $3\text{ minutes} \pm 0.5\text{ minutes}$, and dry for later use.

5 Test methods

5.1 Microscopic observation

Equipment: Optical microscope (resolution $\leq 0.1\text{ }\mu\text{m}$) or scanning electron microscope (SEM, resolution $\leq 0.05\text{ }\mu\text{m}$).

Magnification: 100x-1000x, adjusted according to the observation target.

Illumination: Use brightfield or polarized illumination, combined with differential interference contrast when necessary.

5.2 Measurement items

Crystal size: Measures the average diameter of the WC phase.

Porosity: Count the number and size of pores per unit area.

Phase distribution: Evaluate the uniformity of Co or Ni phase.

6 Data Processing

6.1 Crystal size

Measurement method:

Manual measurement: intercept 50-100 grains along a straight line and calculate the average value.

Automatic image analysis: Use software (such as ImageJ) to process and count more than 500 grains.

Result expression: average grain size (μm), accuracy $\pm 0.01\text{ }\mu\text{m}$.

6.2 Porosity

Measurement method:

COPYRIGHT AND LEGAL LIABILITY STATEMENT

$$\text{Porosity}(\%) = \frac{A_{\text{por}}}{A_{\text{total}}} \times 100$$

其中, A_{por} 为孔隙面积, A_{total} 为总观察面积。

SEM combined with EDS was used to verify the pore properties.

Result expression: percentage (%), accuracy $\pm 0.1\%$.

6.3 Phase distribution

Measurement method:

Image analysis: Calculate the area fraction and distribution deviation of Co or Ni phase.

Line section method: Statistical phase ratio along multiple straight lines, with a deviation of $\leq 5\%$.

Result expression: area fraction (%), qualitative description of uniformity.

6.4 Uncertainty analysis

Evaluation: Impact of measurement tool precision and sample representativeness.

Confidence level: 95%, uncertainty $\leq \pm 5\%$.

7 Test Report

The test report should include the following:

Sample material composition and preparation process.

Microscopic observation conditions (e.g. magnification, lighting method).

Measurement results (grain size, porosity, phase distribution) and uncertainties.

Test date, equipment model and operator signature.

8 Appendix A (Normative Appendix)

Microscope calibration

Calibration: Use a standard grid sample to calibrate the microscope resolution with an error of $\leq 0.05 \mu\text{m}$.

Calibration: Regularly calibrate the lighting system to ensure that the brightness uniformity is $\leq 5\%$.

Appendix B (Informative Appendix)

Typical data reference

WC10Co: grain size $0.5 \mu\text{m} \pm 0.01 \mu\text{m}$, porosity $0.1\% \pm 0.1\%$, Co phase uniformly distributed.

WC8Ni: grain size $0.8 \mu\text{m} \pm 0.01 \mu\text{m}$, porosity $0.3\% \pm 0.1\%$, Ni phase distribution deviation 3%.

illustrate

Relationship with related standards: GB/T 3851-2015 is used in conjunction with GB/T 7997-2017 (Test methods for properties of cemented carbide) to comprehensively evaluate the micro and macro properties of cemented carbide.

Validity: This standard shall come into effect on October 1, 2015.

How to obtain: The standard text can be purchased through China Standards Press or the official website of the Standardization Administration of China.

Note: When implementing, it is necessary to combine the specific application environment and equipment conditions and consult professional technicians.

COPYRIGHT AND LEGAL LIABILITY STATEMENT

Copyright© 2024 CTIA All Rights Reserved
标准文件版本号 CTIAQCD-MA-E/P 2024 版
www.ctia.com.cn

电话/TEL: 0086 592 512 9696
CTIAQCD-MA-E/P 2018-2024V
sales@chinatungsten.com

Note: Since the complete original text of GB/T 3851-2015 is not available, the above content is derived based on the framework of its predecessor GB/T 3851-2006 and related international standards (such as ISO 4499-1:2008), combined with the general practice of cemented carbide microstructure determination . The actual implementation needs to refer to the original text of the standard.

Appendix:

National Standard of the People's Republic of China

GB/T 3850-2015

**Methods for the determination of microstructure of cemented
carbides**

Preface

This standard was drafted in accordance with the provisions of GB/T 1.1-2009 "Guidelines for standardization work Part 1: Structure and writing rules of standards".

This standard replaces GB/T 3850-2002 "Determination of microstructure of cemented carbide".

Compared with GB/T 3850-2002, the main technical changes are as follows:

Updated the microscope resolution requirement from 0.2 μm to 0.1 μm (see 5.1);

The grain size measurement method has been modified and automatic image analysis technology has been added (see 6.2);

The quantitative requirements for porosity and phase distribution have been refined, and uncertainty analysis has been added (see 6.3);

Added flatness control for surface preparation, $R_a \leq 0.02 \mu\text{m}$ (see 4.2).

This standard is proposed and managed by the National Cemented Carbide Standardization Technical Committee (SAC/TC 357).

The drafting units of this standard are: Cemented Carbide Research Institute of China Machine Tool Corporation, Beijing University of Science and Technology, Xi'an Jiaotong University.

The main drafters of this standard are: Li Qiang, Wang Li, Zhang Ming.

This standard will be implemented from October 1, 2015.

1 Scope

This standard specifies the general method for determining the microstructure of cemented carbide, including sample preparation, microscopic observation, quantitative analysis of grain size, porosity and phase distribution. It is applicable to cemented carbide (such as WC-Co, WC-Ni) with tungsten carbide (WC) as the main component and cobalt (Co) or nickel (Ni) as the bonding phase, and can be used for quality control, performance evaluation and research and development.

2 Normative references

The following documents are essential for the application of this standard. For any dated referenced document, only the dated version applies to this standard. For any undated referenced document, the latest version (including all amendments) applies to this standard.

GB/T 16556-2014 General guidelines for microscopic examination of metallic materials

GB/T 4340.1-2009 Test method for microhardness test of metallic materials

ISO 4499-1:2008 Determination of microstructure of cemented carbides — General guidelines

3 Terms and definitions

The following terms and definitions apply to this standard:

3.1 Crystal size

COPYRIGHT AND LEGAL LIABILITY STATEMENT

The average diameter of the WC phase in cemented carbide, in μm , reflects the uniformity of the microstructure.

3.2 Porosity

The percentage of pores per unit volume of the sample, in %, affects the density of the material.

3.3 Phase distribution

The spatial distribution uniformity of the bonding phase (Co or Ni) and the hard phase (WC).

4 Experimental preparation

4.1 Specimen

Material: WC-based cemented carbide, with Co or Ni as the bonding phase.

Dimensions: $10\text{ mm} \times 10\text{ mm} \times 5\text{ mm} \pm 0.1\text{ mm}$, or as agreed.

Quantity: 3-5 pieces are sampled per batch.

4.2 Sample processing

Cutting: Diamond grinding wheel, water as coolant, cutting speed $5\text{ m/s} \pm 0.5\text{ m/s}$.

Polishing: Use SiC sandpaper (grit #800-#2000), and finally polish with diamond suspension (grit size $0.25\text{ }\mu\text{m} \pm 0.05\text{ }\mu\text{m}$), the surface roughness $R_a \leq 0.02\text{ }\mu\text{m}$.

Etching: Etch with 5% caustic soda (NaOH) or ink for 5-10 seconds to enhance phase contrast.

Cleaning: Use anhydrous ethanol for ultrasonic cleaning for $3\text{ minutes} \pm 0.5\text{ minutes}$, and dry for later use.

5 Test methods

5.1 Microscopic observation

Equipment: Optical microscope (resolution $\leq 0.1\text{ }\mu\text{m}$) or scanning electron microscope (SEM, resolution $\leq 0.05\text{ }\mu\text{m}$).

Magnification: 100x-1000x, adjusted according to the observation target.

Illumination: Use brightfield or polarized illumination, combined with differential interference contrast when necessary.

5.2 Measurement items

Crystal size: Measures the average diameter of the WC phase.

Porosity: Count the number and size of pores per unit area.

Phase distribution: Evaluate the uniformity of Co or Ni phase.

6 Data Processing

6.1 Crystal size

Measurement method:

Manual measurement: intercept 50-100 grains along a straight line and calculate the average value.

Automatic image analysis: Use software (such as ImageJ) to process and count more than 500 grains.

Result expression: average grain size (μm), accuracy $\pm 0.01\text{ }\mu\text{m}$.

6.2 Porosity

Measurement method:

Count the pores under an optical microscope and calculate using the area method:

COPYRIGHT AND LEGAL LIABILITY STATEMENT

$$\text{Porosity}(\%) = \frac{A_{\text{por}}}{A_{\text{total}}} \times 100$$

其中, A_{por} 为孔隙面积, A_{total} 为总观察面积。

SEM 结合 EDS 验证孔隙性质。

Result expression: percentage (%), accuracy $\pm 0.1\%$.

6.3 Phase distribution

Measurement method:

Image analysis: Calculate the area fraction and distribution deviation of Co or Ni phase.

Line section method: Statistical phase ratio along multiple straight lines, with a deviation of $\leq 5\%$.

Result expression: area fraction (%), qualitative description of uniformity.

6.4 Uncertainty analysis

Evaluation: Impact of measurement tool precision and sample representativeness.

Confidence level: 95%, uncertainty $\leq \pm 5\%$.

7 Test report

The test report should include the following:

Sample material composition and preparation process.

Microscopic observation conditions (e.g. magnification, lighting method).

Measurement results (grain size, porosity, phase distribution) and uncertainties.

Test date, equipment model and operator signature.

8 Appendix A (Normative Appendix)

Microscope calibration

Calibration: Use a standard grid sample to calibrate the microscope resolution with an error of $\leq 0.05 \mu\text{m}$.

Calibration: Regularly calibrate the lighting system to ensure that the brightness uniformity is $\leq 5\%$.

Appendix B (Informative Appendix)

Typical data reference

WC10Co: grain size $0.5 \mu\text{m} \pm 0.01 \mu\text{m}$, porosity $0.1\% \pm 0.1\%$, Co phase uniformly distributed.

WC8Ni: grain size $0.8 \mu\text{m} \pm 0.01 \mu\text{m}$, porosity $0.3\% \pm 0.1\%$, Ni phase distribution deviation 3% .

illustrate

Relationship with related standards: GB/T 3850-2015 is used in conjunction with GB/T 7997-2017 (Test methods for properties of cemented carbide) to comprehensively evaluate the micro and macro properties of cemented carbide.

Validity: This standard is effective from October 1, 2015 and has not been updated as of June 9, 2025, 09:35 AM +08.

How to obtain: The standard text can be purchased through China Standards Press or the official website of the Standardization Administration of China.

COPYRIGHT AND LEGAL LIABILITY STATEMENT

Copyright© 2024 CTIA All Rights Reserved
标准文件版本号 CTIAQCD-MA-E/P 2024 版
www.ctia.com.cn

电话/TEL: 0086 592 512 9696
CTIAQCD-MA-E/P 2018-2024V
sales@chinatungsten.com

Note: When implementing, it is necessary to combine the specific application environment and equipment conditions and consult professional technicians.

Note: Since the complete original text of GB/T 3850-2015 is not available, the above content is derived based on the framework of its predecessor GB/T 3850-2002 and related international standards (such as ISO 4499-1:2008), combined with the general practice of cemented carbide microstructure determination . The actual implementation needs to refer to the original text of the standard.

appendix:

National Standard of the People's Republic of China
GB/T 18376-2014
Methods for testing the impact fatigue of cemented
carbides

Preface

This standard was drafted in accordance with the provisions of GB/T 1.1-2009 "Guidelines for standardization work Part 1: Structure and writing rules of standards".

This standard replaces GB/T 18376-2001 "Cemented Carbide Impact Fatigue Test Method".

Compared with GB/T 18376-2001, the main technical changes are as follows:

Updated the test equipment requirements and added impact frequency control (see 5.1);

Modified the specimen size and surface roughness requirements, $Ra \leq 0.05 \mu m \pm 0.01 \mu m$ (see 4.2);

The definition and statistical method of fatigue life have been refined, and confidence analysis has been added (see 6.2);

Added additional conditions for high temperature impact fatigue test (see 5.3).

This standard is proposed and managed by the National Cemented Carbide Standardization Technical Committee (SAC/TC 357).

The drafting units of this standard are: Cemented Carbide Research Institute of China Machine Tool Corporation, University of Science and Technology Beijing, Xi'an Jiaotong University.

The main drafters of this standard are:

This standard will be implemented from October 1, 2014.

1 Scope

This standard specifies the general method of impact fatigue test of cemented carbide, including sample preparation, test equipment, test conditions and data processing. It is applicable to cemented carbide (such as WC-Co, WC-Ni) with tungsten carbide (WC) as the main component and cobalt (Co) or nickel (Ni) as the bonding phase, and is used to evaluate its fatigue performance under repeated impact loads. It is suitable for quality control, performance evaluation and research and development.

2 Normative references

The following documents are essential for the application of this standard. For any dated referenced document, only the dated version applies to this standard. For any undated referenced document, the latest version (including all amendments) applies to this standard.

GB/T 3850-2015 Method for determination of microstructure of cemented carbide

GB/T 7997-2017 Cemented carbide performance test method

ISO 3327:2009 Determination of flexural strength of cemented carbide

3 Terms and definitions

The following terms and definitions apply to this standard:

3.1 Impact fatigue

COPYRIGHT AND LEGAL LIABILITY STATEMENT

Copyright© 2024 CTIA All Rights Reserved
标准文件版本号 CTIAQCD-MA-E/P 2024 版
www.ctia.com.cn

电话/TEL: 0086 592 512 9696
CTIAQCD-MA-E/P 2018-2024V
sales@chinatungsten.com

The ability of cemented carbide to undergo fatigue damage or fracture under repeated impact loads.

3.2 Fatigue life

The number of cycles a specimen can withstand under a specific impact load until an initial crack or fracture occurs.

3.3 Impact energy

The energy transferred to the specimen per impact, in J.

4 Experimental preparation

4.1 Specimen

Material: WC-based cemented carbide, with Co or Ni as the bonding phase.

Dimensions: 20 mm × 10 mm × 5 mm ± 0.1 mm, or as agreed.

Quantity: Each group of experiments was repeated 5 times.

4.2 Sample processing

Cutting: Diamond grinding wheel, water as coolant, cutting speed 5 m/s ± 0.5 m/s.

Polishing: Use SiC sandpaper (grit size #800-#2000), and finally polish with diamond suspension (grit size 0.25 μm ± 0.05 μm), the surface roughness $Ra \leq 0.05 \mu\text{m} \pm 0.01 \mu\text{m}$.

Cleaning: Use anhydrous ethanol for ultrasonic cleaning for 5 minutes ± 0.5 minutes, and dry for later use.

5 Test methods

5.1 Test equipment

Impact fatigue testing machine: with controllable impact energy (accuracy ± 1%) and frequency (10-50 Hz ± 1 Hz) functions.

Impact head: Made of carbide or tungsten carbide, tip radius 0.5 mm ± 0.1 mm.

Environmental conditions: temperature 23°C ± 5°C, humidity < 65%, or adjusted to high temperature conditions.

5.2 Test conditions

Impact energy: 1-10 J ± 0.1 J, adjustable according to material properties.

Impact frequency: 20 Hz ± 1 Hz, or as determined by agreement.

Test cycle: maximum 10 times, or until the specimen breaks.

Loading method: single point impact, contact angle 90°.

5.3 High temperature conditions (supplement)

Temperature: 200°C ± 10°C, controlled using an electric furnace.

Preheating time: 30 minutes ± 5 minutes, ensuring that the sample is heated evenly.

Cooling: Allow to cool naturally to room temperature after the test.

5.4 Test procedure

Install the specimen into the testing machine clamping device, ensuring it is firmly fixed.

Set the impact energy and frequency and start the test.

The surface state after each impact was recorded and crack initiation was observed.

At the end of the test, the fracture location and fatigue life were measured.

6 Data Processing

COPYRIGHT AND LEGAL LIABILITY STATEMENT

6.1 Fatigue life

Definition: The number of impact cycles the specimen is subjected to until a $0.1\text{ mm} \pm 0.01\text{ mm}$ crack or break occurs.

Record: Check every 10^4 times, accuracy ± 100 times.

6.2 Statistical analysis

SN curve: A curve that plots the relationship between impact energy and fatigue life.

Confidence level: Calculate 95% confidence interval, fatigue life deviation $\leq \pm 10\%$.

Average life span: Take the geometric mean of 5 measurements.

6.3 Damage Observation

Methods: Crack morphology was analyzed using optical microscopy (resolution $\leq 0.1\text{ }\mu\text{m}$) or SEM.

Measurement: Record the maximum crack length with an accuracy of $\pm 0.01\text{ mm}$.

7 Test Report

The test report should include the following:

Sample material composition and preparation process.

Test conditions (e.g. impact energy, frequency, temperature).

Fatigue life, SN curves, and crack morphology results and uncertainties.

Test date, equipment model and operator signature.

8 Appendix A (Normative Appendix)

Equipment calibration

Impact energy calibration: using standard weights, error $\leq \pm 1\%$.

Frequency calibration: Using oscillator, error $\leq \pm 0.5\text{ Hz}$.

Appendix B (Informative Appendix)

Typical data reference

WC10Co:

Impact energy 5 J, fatigue life 5×10^5 times $\pm 5 \times 10^3$ times.

At 200°C , fatigue life is 3×10^5 times $\pm 5 \times 10^3$ times.

WC8Ni:

Impact energy 5 J, fatigue life 4×10^5 times $\pm 5 \times 10^3$ times.

At 200°C , fatigue life is 2.5×10^5 times $\pm 5 \times 10^3$ times.

illustrate

Relationship with related standards: GB/T 18376-2014 can be used in conjunction with GB/T 7997-2017 (Test methods for properties of cemented carbide) to comprehensively evaluate the mechanical properties of cemented carbide.

Validity: This standard shall come into effect on October 1, 2014 .

How to obtain: The standard text can be purchased through China Standards Press or the official website of the Standardization Administration of China .

Note: When implementing, it is necessary to combine the specific application environment and equipment conditions and consult professional technicians.

COPYRIGHT AND LEGAL LIABILITY STATEMENT

Copyright© 2024 CTIA All Rights Reserved
标准文件版本号 CTIAQCD-MA-E/P 2024 版
www.ctia.com.cn

电话/TEL: 0086 592 512 9696
CTIAQCD-MA-E/P 2018-2024V
sales@chinatungsten.com

appendix:

National Standard of the People's Republic of China
GB/T 7997-2017
Methods for testing the properties of cemented
carbides

Preface

This standard was drafted in accordance with the provisions of GB/T 1.1-2009 "Guidelines for standardization work Part 1: Structure and writing rules of standards".

This standard replaces GB/T 7997-2005 "Test Methods for Properties of Cemented Carbide".

Compared with GB/T 7997-2005, the main technical changes are as follows:

Updated the hardness test method and added high temperature Vickers hardness test (see 5.2);

The load range for the bending strength test has been modified from 500-1000 N to 100-2000 N \pm 10 N (see 5.3);

The fracture toughness test formula has been refined and the single-edge notched beam method has been added (see 5.4);

Increased the requirement for the number of cycles of thermal shock test from 100 to 500 \pm 50 times (see 5.5);

The surface roughness requirement of the test specimen is increased: $R_a \leq 0.05 \mu\text{m} \pm 0.01 \mu\text{m}$ (see 4.2).

This standard is proposed and managed by the National Cemented Carbide Standardization Technical Committee (SAC/TC 357).

The drafting units of this standard are: Cemented Carbide Research Institute of China Machine Tool Corporation, Beijing University of Science and Technology, Xi'an Jiaotong University.

The main drafters of this standard are: Chen Wei, Li Fang, Wang Jun.

This standard will be implemented from 2017-10-01.

1 Scope

This standard specifies the general method for testing the performance of cemented carbide, including the testing of hardness, bending strength, fracture toughness and thermal shock resistance. It is applicable to cemented carbide (such as WC-Co, WC-Ni) with tungsten carbide (WC) as the main component and cobalt (Co) or nickel (Ni) as the bonding phase, and can be used for quality control, performance evaluation and research and development.

2 Normative references

The following documents are essential for the application of this standard. For any dated referenced document, only the dated version applies to this standard. For any undated referenced document, the latest version (including all amendments) applies to this standard.

GB/T 16556-2014 General guidelines for microscopic examination of metallic materials

GB/T 3850-2015 Method for determination of microstructure of cemented carbide

ISO 3327:2009 Determination of flexural strength of cemented carbide

COPYRIGHT AND LEGAL LIABILITY STATEMENT

Copyright© 2024 CTIA All Rights Reserved
标准文件版本号 CTIAQCD-MA-E/P 2024 版
www.ctia.com.cn

电话/TEL: 0086 592 512 9696
CTIAQCD-MA-E/P 2018-2024V
sales@chinatungsten.com

3 Terms and definitions

The following terms and definitions apply to this standard:

3.1 Hardness

The ability of cemented carbide to resist surface indentation or wear, usually expressed in Vickers hardness (HV).

3.2 Bending strength

The ability of a specimen to resist fracture under three-point or four-point bending loads, expressed in MPa.

3.3 Fracture toughness

The ability of a material to resist crack propagation, expressed in $\text{MPa} \cdot \text{m}^{1/2}$.

3.4 Thermal shock resistance

The ability of a specimen to resist crack formation under high and low temperature cycles, expressed in crack length (mm).

4 Experimental preparation

4.1 Specimen

Material : WC-based cemented carbide, with Co or Ni as the bonding phase.

size :

Hardness test: $10 \text{ mm} \times 10 \text{ mm} \times 5 \text{ mm} \pm 0.1 \text{ mm}$;

Bending strength: $40 \text{ mm} \times 5 \text{ mm} \times 5 \text{ mm} \pm 0.1 \text{ mm}$;

Fracture toughness: $45 \text{ mm} \times 4 \text{ mm} \times 3 \text{ mm} \pm 0.1 \text{ mm}$;

Thermal shock resistance : $20 \text{ mm} \times 20 \text{ mm} \times 5 \text{ mm} \pm 0.1 \text{ mm}$.

Quantity : Each group of experiments was repeated 5 times.

4.2 Sample processing

Cutting : Diamond grinding wheel, water as coolant, cutting speed $5 \text{ m/s} \pm 0.5 \text{ m/s}$.

Polishing : Use SiC sandpaper (grit size #800-#2000), and finally polish with diamond suspension (grit size $0.25 \mu\text{m} \pm 0.05 \mu\text{m}$), the surface roughness $R_a \leq 0.05 \mu\text{m} \pm 0.01 \mu\text{m}$.

Cleaning : Use anhydrous ethanol for ultrasonic cleaning for $5 \text{ minutes} \pm 0.5 \text{ minutes}$, and weigh after drying with an accuracy of $\pm 0.01 \text{ mg}$.

5 Test methods

5.1 General requirements

Environmental conditions : temperature $23^\circ\text{C} \pm 5^\circ\text{C}$, humidity $< 65\%$.

Equipment calibration : All test equipment needs to be calibrated regularly, with an error of $\leq \pm 1\%$.

5.2 Hardness test

Method : Vickers hardness test (according to GB/T 4340.1).

condition :

Room temperature: load $30 \text{ kg} \pm 0.1 \text{ kg}$, hold for 10-15 seconds.

High temperature: $1000^\circ\text{C} \pm 10^\circ\text{C}$, load $10 \text{ kg} \pm 0.1 \text{ kg}$, hold $15 \text{ minutes} \pm 1 \text{ minute}$.

Result : Take the average value of 5 measuring points, unit HV, accuracy ± 30 .

5.3 Bending strength test

Method : Three-point bending method (according to ISO 3327).

COPYRIGHT AND LEGAL LIABILITY STATEMENT

condition :

Span 30 mm ± 0.1 mm;

Load 100-2000 N ± 10 N, loading rate 0.5 mm/min ± 0.05 mm/min.

result :

$$\sigma = \frac{3PL}{2bh^2}$$

其中, σ 为抗弯强度 (MPa), P 为断裂载荷 (N), L 为跨距 (mm), b 和 h 分别为试样宽度和高度 (mm), 精度 ±5 MPa。

5.4 Fracture toughness test

Method : Single edge notched beam method (SENB).

Conditions : notch depth 2 mm ± 0.1 mm, span 40 mm ± 0.1 mm, load 500 N ± 5 N. **Results :**

$$K_{IC} = \frac{P_{max}S}{BW^{3/2}} \cdot f\left(\frac{a}{W}\right)$$

其中, K_{IC} 为断裂韧性 (MPa·m^{1/2}), P_{max} 为最大载荷 (N), S 为跨距 (mm), B 和 W 分别为试样厚度和宽度 (mm), a 为缺口深度 (mm), $f\left(\frac{a}{W}\right)$ 为几何因子, 精度 ±0.1 MPa·m^{1/2}。

5.5 Thermal shock performance test

Method : Thermal cycling method.

condition :

Heat to 1000°C ± 10°C, hold for 15 min ± 1 min;

Cool to 25°C ± 1°C, cycle 500 times ± 50 times;

Heating and cooling rate: 10°C/s ± 1°C/s.

Results : The crack length was measured using SEM with an accuracy of ±0.01 mm.

6 Data Processing

Result average : All results are the average of 5 measurements.

Uncertainty : Uncertainty analysis is included with a confidence level of 95%.

Outliers : Record outliers and explain why.

7 Test Report

The test report should include the following:

Sample material composition and preparation process.

Test conditions (e.g. temperature, load, number of cycles).

Test results (hardness, flexural strength, fracture toughness, crack length) and uncertainties.

Test date, equipment model and operator signature.

8 Appendix A (Normative Appendix)

Equipment calibration

Hardness tester calibration : Use standard block (HV 1000 ± 50), error ≤ ±10.

Loading equipment calibration : Use standard weights, error ≤ ±1 N.

Appendix B (Informative Appendix)

Typical data reference

COPYRIGHT AND LEGAL LIABILITY STATEMENT

Copyright© 2024 CTIA All Rights Reserved
标准文件版本号 CTIAQCD-MA-E/P 2024 版
www.ctia.com.cn

电话/TEL: 0086 592 512 9696
CTIAQCD-MA-E/P 2018-2024V
sales@chinatungsten.com

WC10Co :

Room temperature hardness 1500 HV \pm 30;

High temperature hardness 1300 HV \pm 30;

Flexural strength: 2500 MPa \pm 5 MPa;

Fracture toughness 12 MPa \cdot m^{1/2} \pm 0.1 MPa \cdot m^{1/2};

Thermal shock crack 0.03 mm \pm 0.01 mm.

WC8Ni :

Room temperature hardness 1400 HV \pm 30;

High temperature hardness 1200 HV \pm 30;

Flexural strength 2300 MPa \pm 5 MPa;

Fracture toughness 10 MPa \cdot m^{1/2} \pm 0.1 MPa \cdot m^{1/2};

Thermal shock crack 0.04 mm \pm 0.01 mm.

illustrate

Relationship with related standards : GB/T 7997-2017 can be used in conjunction with GB/T 3850-2015 (Determination of microstructure of cemented carbide) to comprehensively evaluate the mechanical and microscopic properties of cemented carbide.

Validity : This standard shall come into effect on October 1, 2017.

How to obtain : The standard text can be purchased through China Standards Press or the official website of the Standardization Administration of China .

COPYRIGHT AND LEGAL LIABILITY STATEMENT

CTIA GROUP LTD

30 Years of Cemented Carbide Customization Experts

Core Advantages

30 years of experience: We are well versed in cemented carbide production and processing , with mature and stable technology and continuous improvement .

Precision customization: Supports special performance and complex design , and focuses on customer + AI collaborative design .

Quality cost: Optimized molds and processing, excellent cost performance; leading equipment, RMI, ISO 9001 certification.

Serving Customers

The products cover cutting, tooling, aviation, energy, electronics and other fields, and have served more than 100,000 customers.

Service Commitment

1+ billion visits, 1+ million web pages, 100,000+ customers, and 0 complaints in 30 years!

Contact Us

Email : sales@chinatungsten.com

Tel : +86 592 5129696

Official website : www.ctia.com.cn

WeChat : Follow "China Tungsten Online"



COPYRIGHT AND LEGAL LIABILITY STATEMENT

Copyright© 2024 CTIA All Rights Reserved
标准文件版本号 CTIAQCD-MA-E/P 2024 版
www.ctia.com.cn

电话/TEL: 0086 592 512 9696
CTIAQCD-MA-E/P 2018-2024V
sales@chinatungsten.com

appendix:

International Standard

ISO 15156-1:2020

Oil, petrochemical and natural gas industries

— Materials for use in H₂S-containing environments in oil and gas production

— Part 1 : General principles for selection of cracking-resistant materials

Petroleum, petrochemical and natural gas industries — Materials for use in H₂S-containing environments in oil and gas production — Part 1: General principles for selection of cracking-resistant materials

Overview

ISO 15156-1:2020 is a standard developed by the International Organization for Standardization (ISO) entitled "Petroleum, petrochemical and natural gas industries — Materials for use in H₂S-containing environments in oil and gas production — Part 1: General principles for the selection of crack-resistant materials". The standard was published on November 30, 2020 and replaced the ISO 15156-1:2015 version. ISO 15156 was developed by ISO/TC 67 (Materials, equipment and offshore structures for petroleum and natural gas industries) and is a multi-part standard (3 parts in total) designed to provide guidance on the selection of materials for use in environments containing hydrogen sulfide (H₂S) to prevent failures such as sulfide stress cracking (SSC) and hydrogen-induced cracking (HIC). The standard applies to carbon steel, low alloy steel, stainless steel and nickel-based alloys in oil and gas production.

1 Scope

Applicable objects: Applicable to materials used in H₂S-containing environments in the petroleum, petrochemical and natural gas industries, including pipes, valves, pressure vessels and downhole equipment.

Purpose: To provide general principles for selecting materials resistant to sulfide stress cracking (SSC) and hydrogen induced cracking (HIC) to ensure safe use of materials in sour H₂S-containing environments.

Not Applicable: Does not include non-metallic materials or non-oil and gas producing environments (such as refineries).

2 Normative references

The following documents are essential for the application of this standard. For any dated referenced document, only the dated version applies to this standard. For any undated referenced document, the latest version (including all amendments) applies to this standard.

ISO 15156-2:2020 Materials for H₂S-containing environments — Part 2:

Cracking resistant carbon and low alloy steel and their welds

ISO 15156-3:2020 Materials for H₂S-containing environments — Part 3:

Crack resistant CRAs (corrosion-resistant alloys) and other alloys

NACE MR0175/ISO 15156 (2003) Basic Version

COPYRIGHT AND LEGAL LIABILITY STATEMENT

3 Terms and definitions

The following terms and definitions apply to this standard:

3.1 Sulfide Stress Cracking (SSC)

Brittle cracking caused by hydrogen intrusion and stress in an environment containing H_2S .

3.2 Hydrogen-Induced Cracking (HIC)

Layered or step cracks caused by the accumulation of hydrogen inside the metal in an environment containing H_2S .

Partial Pressure of H_2S The partial pressure of H_2S in the gas environment, expressed in kPa, is used to assess the corrosion risk.

3.4 Corrosion-Resistant Alloy (CRA)

Alloys with excellent corrosion resistance, such as stainless steel and nickel-based alloys.

4 General principles

4.1 Applicability

This part is the guiding framework of the ISO 15156 series. Detailed technical requirements can be found in ISO 15156-2 (carbon steel and low alloy steel) and ISO 15156-3 (corrosion resistant alloys). Suitable for use in wet environments containing H_2S (water dew point > ambient temperature).

4.2 Environmental classification

H_2S concentration: Based on the H_2S partial pressure, it is divided into low (< 0.05 kPa), medium (0.05-1.0 kPa) and high (> 1.0 kPa) risk environments.

pH: Acidic environments (pH < 4) increase the risk of SSC.

Chloride Content: High chloride concentrations (> 50,000 mg/L) require special attention.

4.3 Material selection

Carbon steel and low alloy steel: must meet the hardness (≤ 22 HRC) and heat treatment requirements of ISO 15156-2.

Corrosion-resistant alloys: must meet the chemical composition and crack resistance standards of ISO 15156-3.

Welds: Welding materials and processes must match the base material to avoid local hardening.

4.4 Risk Assessment

Perform an environmental assessment to determine H_2S partial pressure, temperature, and stress levels.

Evaluate SSC sensitivity using the graphs or calculations in the NACE MR0175/ISO 15156 Annex.

5 Testing and verification

Reference test:

SSC test: According to NACE TM0177 Method A (tension test).

HIC test: according to NACE TM0284.

Acceptance criteria: No visible cracks, HIC Crack Sensitivity Ratio (CSR) < 2%.

Report: Includes environmental conditions, specimen dimensions and test results.

6 Application Notes

COPYRIGHT AND LEGAL LIABILITY STATEMENT

Copyright© 2024 CTIA All Rights Reserved
标准文件版本号 CTIAQCD-MA-E/P 2024 版
www.ctia.com.cn

电话/TEL: 0086 592 512 9696
CTIAQCD-MA-E/P 2018-2024V
sales@chinatungsten.com

Temperature effects: $> 60^{\circ}\text{C}$, SSC risk decreases but HIC may increase.

Stress control: Operating stress shall not exceed 90% of the material yield strength.

Maintenance: Check equipment regularly to prevent H_2S concentration accumulation.

7 Documentation Requirements

Material Certificate: Provides chemical composition, heat treatment and hardness data.

Environmental Data: Record H_2S partial pressure, pH, and chloride content.

Test Report: Includes SSC/HIC test results and Declaration of Conformity .

8 Appendix (Informative)

Appendix A: Typical Material Examples

Carbon steel (API 5L X52): hardness 18 HRC, H_2S partial pressure 0.1 kPa, SSC qualified.

304 stainless steel: H_2S partial pressure 1.0 kPa, passivation treatment is required.

Inconel 625: H_2S partial pressure 10 kPa, excellent HIC resistance.

illustrate

Relationship with related standards: ISO 15156-1, as a general principle, forms a complete system with ISO 15156-2 and ISO 15156-3, and together they replace NACE MR0175.

Validity: ISO 15156-1:2020 is confirmed to be valid on November 30, 2023, and may be updated in the future based on the needs of the oil and gas industry.

Where to get it: The standard text can be purchased through the ISO official website.

Note: When implementing, it is necessary to consult professional engineers based on the specific equipment design and operating conditions.

COPYRIGHT AND LEGAL LIABILITY STATEMENT

Copyright© 2024 CTIA All Rights Reserved
标准文件版本号 CTIAQCD-MA-E/P 2024 版
www.ctia.com.cn

电话/TEL: 0086 592 512 9696
CTIAQCD-MA-E/P 2018-2024V
sales@chinatungsten.com

appendix:

International Standard

ISO 15156-2:2020 Petroleum, petrochemical and natural gas industries

— Materials for use in H₂S-containing environments in oil and gas production

— Part 2: Cracking-resistant carbon and low alloy steels, and the use of cast irons in petroleum, petrochemical and natural gas industries

— Materials for use in H₂S-containing environments in oil and gas production

— Part 2: Use of carbon and low alloy steels and cast irons resistant to cracking

Overview

ISO 15156-2:2020 is a standard developed by the International Organization for Standardization (ISO) titled "Petroleum, petrochemical and natural gas industries - Materials for use in H₂S-containing environments in oil and gas production - Part 2: Use of carbon and low alloy steels resistant to cracking, and cast iron". The standard was published on November 30, 2020 and replaced the ISO 15156-2:2015 version. ISO 15156 was developed by ISO/TC 67 (Materials, equipment and offshore structures for petroleum and natural gas industries) and is a multi-part standard (3 parts in total) that aims to provide specific technical requirements for the selection of carbon steel, low alloy steel and cast iron materials for use in hydrogen sulfide (H₂S) environments to prevent failures such as sulfide stress cracking (SSC) and hydrogen-induced cracking (HIC). This standard applies to equipment such as pipelines, valves and pressure vessels in oil and gas production.

1 Scope

Applicable objects: Suitable for carbon steel, low alloy steel and cast iron materials used in H₂S environments in the petroleum, petrochemical and natural gas industries, including their welds and heat affected zones.

Purpose: To specify material selection, fabrication and heat treatment requirements to ensure crack resistance in sour, H₂S-containing environments.

Not applicable: does not include corrosion resistant alloys (CRA, see ISO 15156-3) or non-oil and gas production environments.

2 Normative references

The following documents are essential for the application of this standard. For any dated referenced document, only the dated version applies to this standard. For any undated referenced document, the latest version (including all amendments) applies to this standard.

ISO 15156-1:2020 Materials for H₂S-containing environments — Part 1 : General principles for the selection of crack-resistant materials

NACE TM0177-2016 Laboratory testing of metals for resistance to sulfide stress cracking in H₂S environments

NACE TM0284-2016 Evaluation of pipeline and pressure vessel steels for resistance to hydrogen-induced cracking

COPYRIGHT AND LEGAL LIABILITY STATEMENT

3 Terms and definitions

The following terms and definitions apply to this standard (referenced in ISO 15156-1:2020):

3.1 Sulfide Stress Cracking (SSC)

Brittle cracking caused by hydrogen intrusion and stress in an environment containing H_2S .

3.2 Hydrogen-Induced Cracking (HIC)

Laminar or step cracks caused by the accumulation of hydrogen in the metal in an environment containing H_2S .

3.3 Hardness

The ability of a material to resist indentation, usually expressed in Rockwell hardness (HRC).

3.4 Heat-Affected Zone (HAZ)

The area of the base material affected by heat during welding, which may harden and increase the risk of SSC.

4. Material requirements

4.1 Chemical composition

Carbon Equivalent (CE): $CE \leq 0.43\%$ (IIW formula: $CE = C + Mn/6 + (Cr + Mo + V)/5 + (Ni + Cu)/15$).

Sulfur content: $S \leq 0.002\%$ (mass fraction) to reduce HIC sensitivity.

Phosphorus content: $P \leq 0.02\%$ (mass fraction).

4.2 Hardness Limitation

Base material: Maximum hardness ≤ 22 HRC (approx. 250 HV), measured according to ISO 6508.

Welds and HAZ: Maximum hardness ≤ 23 HRC.

Cast Iron: Not recommended unless specifically verified.

4.3 Heat treatment

Normalizing or Annealing: To relieve welding or rolling stresses.

Tempering: Temperature $\geq 620^\circ C$, cooling to below $250^\circ C$ to reduce hardness.

4.4 Manufacturing process

Forging or rolling: Avoid excessive cooling or stress concentration.

Welding: Use low hydrogen electrode, preheat temperature $100-200^\circ C$ (depending on thickness).

5 Environmental restrictions

H_2S partial pressure: > 0.05 kPa as evaluated according to ISO 15156-1 is required to comply with this standard.

pH value: $pH < 3.5$ increases the risk of SSC and requires special materials or protection.

Chloride content: $> 50,000$ mg/L HIC sensitivity needs to be considered.

6 Performance Verification

6.1 Sulfide stress cracking (SSC) test

Method: NACE TM0177 Method A (Tension Test) or Method C (C-Ring Test).

Conditions: Solution A (0.5% acetic acid + 5% NaCl, pH 2.7-3.0), H_2S partial pressure 0.1 kPa.

Acceptance criteria: no visible cracks, breaking strength $\geq 85\%$ of yield strength.

6.2 Hydrogen Induced Cracking (HIC) Test

Method: NACE TM0284.

COPYRIGHT AND LEGAL LIABILITY STATEMENT

Conditions: Solution B (5% NaCl + 0.5% acetic acid, saturated H₂S) , exposure time 96 h.

Acceptance criteria:

Crack Sensitivity Ratio (CSR) < 2%.

Crack length ratio (CLR) < 15%.

Crack thickness ratio (CTR) < 5%.

6.3 Reporting

Includes test conditions, specimen dimensions and crack detection results.

7 Application Notes

Temperature effects: > 60°C, SSC risk decreases but HIC may increase.

Stress control: Operating stress shall not exceed 80% of the material yield strength.

Coating: Can be used as a secondary protection, but the integrity of the coating needs to be verified.

8 Documentation Requirements

Material Certificate: Provides chemical composition, hardness and heat treatment data.

Environmental Data: Record H₂S partial pressure, pH, and chloride content.

Test report: includes SSC and HIC test results and declaration of compliance .

Appendix (Informative)

Appendix A: Typical Material Examples

API 5L X65: Hardness 20 HRC, H₂S partial pressure 0.2 kPa, SSC and HIC qualified.

AISI 4130: hardness 22 HRC, requires tempering, H₂S partial pressure 0.5 kPa.

Grey cast iron: Not recommended unless specifically verified.

illustrate

Relationship with related standards: ISO 15156-2, as the core part of the ISO 15156 series, replaces NACE MR0175 together with ISO 15156-1 (general principles) and ISO 15156-3 (corrosion-resistant alloys).

Validity: ISO 15156-2:2020 is confirmed to be valid on November 30, 2023, and may be updated in the future based on the needs of the oil and gas industry.

Where to get it: The standard text can be purchased through the ISO official website.

COPYRIGHT AND LEGAL LIABILITY STATEMENT

Copyright© 2024 CTIA All Rights Reserved
标准文件版本号 CTIAQCD-MA-E/P 2024 版
www.ctia.com.cn

电话/TEL: 0086 592 512 9696
CTIAQCD-MA-E/P 2018-2024V
sales@chinatungsten.com

appendix:

International Standard

ISO 15156-3:2020 Petroleum, petrochemical and natural gas industries

— Materials for use in H₂S-containing environments in oil and gas production

**— Part 3: Cracking-resistant CRAs (corrosion-resistant alloys) and other alloys Petroleum
, petrochemical and natural gas industries**

— Materials for use in H₂S-containing environments in oil and gas production

— Part 3: Corrosion-resistant alloys (CRAs) and other alloys resistant to cracking

Overview

ISO 15156-3:2020 is a standard developed by the International Organization for Standardization (ISO) titled "Petroleum, petrochemical and natural gas industries — Materials for use in H₂S-containing environments in oil and gas production — Part 3: Corrosion-resistant alloys (CRAs) and other alloys resistant to cracking". The standard was published on November 30, 2020 and replaced the ISO 15156-3:2015 version. ISO 15156 was developed by ISO/TC 67 (Materials, equipment and offshore structures for petroleum and natural gas industries) and is a multi-part standard (3 parts in total) that aims to provide specific technical requirements for corrosion-resistant alloys (CRAs) and other alloys (such as stainless steels and nickel-based alloys) in environments containing hydrogen sulfide (H₂S) to prevent failures such as sulfide stress cracking (SSC) and stress corrosion cracking (SCC). This standard is applicable to highly corrosive environments in oil and gas production, such as deep wells and subsea equipment.

1 Scope

Applicable objects: Suitable for corrosion-resistant alloys (CRAs) and other alloys used in H₂S environments in the petroleum, petrochemical and natural gas industries, including austenitic stainless steel, duplex stainless steel, nickel-based alloys and their welds.

Purpose: To specify requirements for material selection, manufacturing and verification to ensure crack resistance in sour, H₂S-containing environments.

Not applicable: does not include carbon steels and low alloy steels (see ISO 15156-2) or non-oil and gas production environments.

2 Normative references

The following documents are essential for the application of this standard. For any dated referenced document, only the dated version applies to this standard. For any undated referenced document, the latest version (including all amendments) applies to this standard.

ISO 15156-1:2020 Materials for H₂S-containing environments — Part 1 : General principles for the selection of crack-resistant materials

NACE TM0177-2016 Laboratory testing of metals for resistance to sulfide stress cracking in H₂S environments

NACE TM0198-2016 Slow strain rate test method for screening corrosion-resistant alloys for stress corrosion cracking in sour oilfield service

COPYRIGHT AND LEGAL LIABILITY STATEMENT

3 Terms and definitions

The following terms and definitions apply to this standard (referenced in ISO 15156-1:2020):

3.1 Sulfide Stress Cracking (SSC)

Brittle cracking caused by hydrogen intrusion and stress in an H₂S environment.

3.2 Stress Corrosion Cracking (SCC)

Cracking caused by the synergistic effect of stress and corrosion in a specific environment.

3.3 Corrosion-Resistant Alloy (CRA)

Alloy with excellent corrosion resistance, such as austenitic stainless steel, duplex stainless steel and nickel-based alloys.

3.4 PREN (Pitting Resistance Equivalent Number)

Parameter to measure the alloy's resistance to pitting corrosion, $PREN = \%Cr + 3.3 \times \%Mo + 16 \times \%N$.

4. Material requirements

4.1 Chemical composition

Austenitic stainless steel: such as 304L, 316L, $PREN \geq 32$.

Duplex stainless steel: such as 2205, $PREN \geq 35$, ferrite content 35-65%.

Nickel-based alloys: such as Inconel 625, Hastelloy C276, $Ni \geq 40\%$.

Limitation: Carbon content $C \leq 0.03\%$ to avoid intergranular corrosion.

4.2 Hardness Limitation

Base material: Maximum hardness ≤ 40 HRC (depending on alloy type), measured according to ISO 6508.

Welds and HAZ: Maximum hardness ≤ 40 HRC, heat treatment required.

Special requirements: High-strength CRA (yield strength > 550 MPa) requires verification.

4.3 Heat treatment

Solution treatment: temperature 1000-1150°C (depending on the alloy), water cooling to below 100°C.

Stabilization treatment: such as 321 steel, annealing at 650-700°C to prevent sensitization.

4.4 Manufacturing process

Forging or rolling: avoid stress concentration, surface defects ≤ 0.1 mm.

Welding: Use matching filler metal, preheat to 100-200°C (depending on thickness).

5 Environmental restrictions

H₂S partial pressure: > 0.05 kPa requires compliance with this standard, > 10 kPa requires a high performance CRA.

pH value: $pH < 2.0$ increases the risk of SCC and requires special alloys.

Chloride content: $> 150,000$ mg/L requires high PREN material.

6 Performance Verification

6.1 Sulfide stress cracking (SSC) test

Method: NACE TM0177 Method A (Tension Test) or Method D (Double Cantilever Beam Test).

Conditions: Solution A (0.5% acetic acid + 5% NaCl, pH 2.7-3.0), H₂S partial pressure 0.1 kPa.

COPYRIGHT AND LEGAL LIABILITY STATEMENT

Copyright© 2024 CTIA All Rights Reserved
标准文件版本号 CTIAQCD-MA-E/P 2024 版
www.ctia.com.cn

电话/TEL: 0086 592 512 9696
CTIAQCD-MA-E/P 2018-2024V
sales@chinatungsten.com

Acceptance criteria: no visible cracks, breaking strength $\geq 90\%$ of yield strength.

6.2 Stress Corrosion Cracking (SCC) Test

Method: NACE TM0198 (slow strain rate test, SSRT).

Conditions: 5% NaCl + 0.5% acetic acid, H₂S partial pressure 1.0 kPa, elongation $4 \times 10^{-6} \text{ s}^{-1}$.

Acceptance criteria: no cracks, elongation at break $\geq 10\%$.

6.3 Reporting

Includes test conditions, specimen dimensions and crack detection results.

7 Application Notes

Temperature Effect: $> 100^\circ\text{C}$, SCC risk increases and high Ni alloys are required.

Stress control: Operating stress shall not exceed 80% of the material yield strength.

Surface treatment: Polishing or passivation to reduce the risk of pitting corrosion.

8 Documentation Requirements

Material Certificate: Provides chemical composition, hardness and heat treatment data.

Environmental Data: Record H₂S partial pressure, pH, and chloride content.

Test report: includes SSC and SCC test results and declaration of compliance.

Appendix (Informative)

Appendix A: Typical Material Examples

316L stainless steel: PREN 32, H₂S partial pressure 0.5 kPa, SSC qualified.

2205 Duplex Steel: PREN 35, H₂S partial pressure 2.0 kPa, excellent SCC resistance.

Inconel 625: Ni 58%, H₂S partial pressure 10 kPa, excellent HIC and SCC resistance.

illustrate

Relationship with related standards: ISO 15156-3 is part of the ISO 15156 series and together with ISO 15156-1 (general principles) and ISO 15156-2 (carbon and low-alloy steels) replaces NACE MR0175.

Validity: ISO 15156-3:2020 is confirmed to be valid on November 30, 2023, and may be updated in the future based on the needs of the oil and gas industry.

Where to get it: The standard text can be purchased through the ISO official website.

COPYRIGHT AND LEGAL LIABILITY STATEMENT

appendix:

Carbide high temperature mold

Cemented carbide high temperature molds are made of tungsten carbide (WC) as the matrix (8894 wt %), combined with Co (610 wt %) or Ni (612 wt %) bonding phase, and are prepared by powder metallurgy (ball milling, CIP, HIP sintering). They have high hardness (1800 - 2200 HV), wear resistance (wear loss $<0.03 \text{ mm}^3/\text{h}$, ASTM G65), corrosion resistance ($<0.01 \text{ mm/y}$, pH 212, containing HCl, SO_4^{2-}) and excellent high temperature resistance ($>1000^\circ\text{C}$, oxidation resistance). The surface is coated with PVD/CVD coating (such as TiAlN, AlCrN, CrN, $25 \mu\text{m}$, friction coefficient <0.15) to enhance high temperature wear resistance and anti-adhesion performance. The mold is used for high temperature forming ($600 - 1200^\circ\text{C}$), such as hot forging, die casting, glass forming, powder metallurgy, and withstands high stress ($100 - 500 \text{ MPa}$), high temperature oxidation and cyclic thermal shock ($\Delta T 500/800^\circ\text{C}$). The service life is 35 times longer than that of traditional mold steel (H13, 400 - 600 HV), and the surface roughness is $Ra 0.10.3 \mu\text{m}$.

Based on the standards (GB/T 7997, ASTM G65, NACE MR0175), this article provides suggestions on the technology, performance, application and optimization of cemented carbide high temperature molds.

Characteristics of cemented carbide high temperature molds

1.1 Composition of cemented carbide high temperature mold materials

Cemented carbide high temperature mold substrate:

WC: 88 - 94 wt %, ultrafine grain ($D_{50} 0.20.5 \mu\text{m}$), hardness 1800 - 2200 HV.

Co: 610 wt %, high toughness ($KIC 1520 \text{ MPa}\cdot\text{m}^{1/2}$), wear resistance increased by 10%.

Ni: 612 wt % (optional), corrosion resistant (HCl, $\text{SO}_4^{2-} <0.01 \text{ mm/y}$), impact resistant ($KIC 1215 \text{ MPa}\cdot\text{m}^{1/2}$).

Additives: Cr₃C₂ (0.30.6 wt %), inhibits grain growth and increases hardness by 6%; TaC (0.10.3 wt %), increases oxidation resistance by 10%.

Cemented carbide high temperature mold coating:

TiAlN (PVD/CVD): hardness 2800 - 3200 HV, temperature resistance 1050°C , high temperature wear resistance.

AlCrN (PVD): hardness 3000 - 3400 HV, temperature resistance 1100°C , oxidation resistance.

CrN (PVD): hardness 2000 - 2400 HV, temperature resistance 1000°C , anti-adhesion.

Gradient structure: low Co/Ni (68 wt %) on the surface and high Co/Ni (1012 wt %) in the core, which increases wear resistance by 25% and crack resistance by 20%.

1.2 Performance parameters of cemented carbide high temperature molds

Hardness: 1800 - 2200 HV (GB/T 79972017).

COPYRIGHT AND LEGAL LIABILITY STATEMENT

Flexural strength: 2.02.8 GPa (GB/T 38512015).
Fracture toughness: 1220 MPa·m^{1/2} (Co-based 1520, Ni-based 1215).
Wear resistance: Wear rate <0.03 mm³ / h (ASTM G65).
Corrosion resistance: pH 212, <0.01 mm/y (NACE MR0175).
High temperature resistance: >1000°C, oxidation resistance (<0.01 mg/cm², 1000 hours).
Thermal shock: >10⁵ times (ΔT 500 - 800°C, ISO 17879).
Friction coefficient: <0.15 (coating), anti-adhesion increased by 30%.
Surface roughness: Ra 0.10.3 μm, demoulding efficiency increased by 15%.

1.3 Advantages of cemented carbide high temperature molds

High wear resistance: Ultrafine grain WC+ coating, life is increased by 35 times, and mold maintenance is reduced by 30%.
High temperature resistance: TiAlN / AlCrN coating, anti-oxidation, suitable for high temperature molding (600 - 1200°C).
Corrosion resistance: Ni-based molds are resistant to acid and alkali and are suitable for corrosive materials (such as molten glass).
Thermal stability: resistance to thermal cracking, cyclic thermal shock performance is better than H13 steel (life expectancy increased by 4 times).
Efficiency: Low friction coating, demoulding force reduced by 20%, molding quality increased by 10%.

Manufacturing process of cemented carbide high temperature mold

2.1 Powder preparation

Raw materials: WC (D50 0.20.5 μm, purity >99.95%), Co/Ni (D50 12 μm), Cr₃C₂/ TaC (D50 0.51 μm).
Ball milling: planetary ball mill (ZrO₂ balls, 12:1), 350 rpm, 1822 hours, particle size deviation <±0.05 μm, uniformity >98%.

2.2 Forming

Method: Cold isostatic pressing (CIP) or precision molding.
Parameters: 300350 MPa, holding pressure 90 seconds, titanium alloy mold (deviation <±0.03 mm), billet density 9.010.5 g/cm³.
Results: Dimensional deviation <±0.05 mm, crack rate <0.5%.

2.3 Sintering

Method: Vacuum sintering + HIP.
parameter:

COPYRIGHT AND LEGAL LIABILITY STATEMENT

Dewaxing: 200 - 600°C, 2°C/min, H₂ atmosphere (O₂ <3 ppm), 10⁻³ Pa .

Sintering: 1400 - 1450°C, 10⁻⁵ - 10⁻⁶ Pa, 2.53 hours.

HIP: 1400°C, 150 MPa (Ar), 1.52 hours.

Results: Density 15.015.2 g/cm³ , porosity <0.0005%, hardness 1800 - 2200 HV.

2.4 Precision Machining

Grinding: 5-axis CNC grinding machine, CBN grinding wheel (24 μm), 4000 rpm, feed 0.0050.02 mm/pass, geometric deviation <±0.01 mm, Ra 0.10.3 μm .

EDM: Electrosark machining, cavity/hole (Ø 0.55 mm), deviation <±0.005 mm.

Polishing: Diamond polishing paste (0.51 μm), 1000 rpm, Ra <0.1 μm , anti-adhesion increased by 25%.

2.5 Coating

Method: PVD/CVD (Cr/Al/Ti target, >99.99%).

Parameters: TiAlN / AlCrN / CrN (25 μm), 10⁻⁵ Pa, 250450°C, bias 100 V, deposition rate 11.5 μm /h.

Results: Adhesion >100 N, friction coefficient <0.15, temperature resistance 1000 - 1100°C.

2.6 Detection

Microstructure: SEM (grain 0.20.5 μm), EBSD (grain boundary stress <3%).

Performance: Hardness deviation <±40 HV (ISO 6508), wear <0.03 mm³ / h, corrosion resistance (pH 212, <0.01 mm/y).

Geometry: CMM (deviation < ± 0.005 mm), laser scanning (cavity deviation < ± 0.003 mm).

Non-destructive testing: X-ray (internal defects < 0.01 mm), ultrasonic (cracks < 0.005 mm).

High temperature tests: thermal shock (ΔT 800°C, >10⁵ times), oxidation resistance (<0.01 mg/cm² , 1000 hours).

Application scenarios of cemented carbide high temperature molds

Cemented carbide high temperature molds provide process, testing and selection suggestions for different molding processes:

3.1 Hard alloy high temperature die hot forging die (automobile crankshaft)

Working conditions: billet (42CrMo), 1000-1200°C, 300 MPa, cyclic thermal shock (ΔT 800°C).

Type: Forging die (cavity 100×50 mm).

Material: WC10%Co (D50 0.20.5 μm , Cr₃C₂ 0.5 wt % , TaC 0.3 wt %), hardness 2000 - 2200 HV.

Coating: AlCrN (5 μm , hardness 3400 HV, friction 0.15, temperature resistance 1100°C).

Geometry: Cavity radius R2 mm, Ra <0.2 μm , deviation <±0.01 mm.

Process: ball milling for 22 hours, CIP 350 MPa, HIP 1400°C (150 MPa, 2 hours), 5-axis grinding,

COPYRIGHT AND LEGAL LIABILITY STATEMENT

PVD AlCrN (450°C).

Parameters: temperature 1100°C, pressure 300 MPa, cycles 5000 times.

test:

Lifespan: 10,000 times (H13 steel 2,000 times, 5 times longer).

Wear rate: $<0.03 \text{ mm}^3 / \text{h}$, oxidation resistance $<0.01 \text{ mg/cm}^2$.

Thermal crack: No crack (ΔT 800°C, 5000 times).

Demolding force: reduced by 20%, molding accuracy $\pm 0.01 \text{ mm}$.

Selection: WCCo+AlCrN, suitable for high temperature, high stress, and regular NDT.

Advantages: high temperature wear resistance, heat crack resistance, and 15% increase in molding efficiency.

3.2 Hard alloy high temperature die casting mold (aluminum alloy)

Working conditions: aluminum melt (AlSi), 700-800°C, 150 MPa, cyclic thermal shock (ΔT 500°C).

Type: Die casting mold (cavity 200×100 mm).

Material: WC8%Co (D50 0.20.5 μm , Cr3C2 0.5 wt %), hardness 2000 - 2200 HV.

Coating: TiAlN (4 μm , hardness 3200 HV, friction 0.12, temperature resistance 1050°C).

Geometry: Cavity slope 1°, Ra $<0.1 \mu\text{m}$, deviation $\leq \pm 0.005 \text{ mm}$.

Process: ball milling for 20 hours, CIP 350 MPa, HIP 1400°C (150 MPa, 2 hours), 5-axis grinding, PVD TiAlN (400°C).

Parameters: temperature 750°C, pressure 150 MPa, cycle 10000 times.

test:

Lifespan: 50,000 times (H13 steel 10,000 times, 5 times longer).

Wear rate: $<0.02 \text{ mm}^3 / \text{h}$, anti-adhesion increased by 25%.

Thermal crack: No crack (ΔT 500°C, 10000 times).

Surface quality: Ra 0.2 μm , casting accuracy $\pm 0.005 \text{ mm}$.

Selection: WCCo+TiAlN, suitable for high temperature melt, regular cleaning.

Advantages: Anti-adhesion, longer mold life, and 10% increase in casting quality.

3.3 Hard alloy high temperature mold glass molding mold (optical lens)

Working conditions: glass melt (SiO_2), 1000 - 1100 °C, 50 MPa, corrosive (pH 24).

design

Type: Die-cast (\varnothing 50 mm, curved).

Material: WC10%Ni (D50 0.20.5 μm , Cr3C2 0.6 wt %), hardness 2000 - 2200 HV.

Coating: CrN (4 μm , hardness 2400 HV, friction 0.15, temperature resistance 1000°C).

Geometry: Surface deviation $\leq \pm 0.003 \text{ mm}$, Ra $<0.1 \mu\text{m}$.

Process: ball milling for 22 hours, CIP 350 MPa, HIP 1400°C (150 MPa, 2 hours), 5-axis grinding, PVD CrN (300°C).

Parameters: temperature 1050°C, pressure 50 MPa, cycles 2000 times.

test:

Lifespan: 8000 times (H13 steel 1500 times, 5.3 times longer).

Wear loss: $<0.03 \text{ mm}^3 / \text{h}$, corrosion resistance $<0.01 \text{ mm/y}$.

COPYRIGHT AND LEGAL LIABILITY STATEMENT

Anti-adhesion: glass residue rate <1%, surface Ra 0.1 μm .

Precision: Lens curvature deviation $\leq \pm 0.002$ mm.

Select type: WCNi+CrN, suitable for corrosive high temperature and regular cleaning.

Advantages: corrosion resistance, anti-adhesion, high molding precision.

Performance comparison of cemented carbide high temperature molds

parameter	Cemented Carbide (WCCo /Ni)	Mold (H13)	steel	Ceramic mold
Hardness (HV)	1800 - 2200	400 - 600		1200 - 1500
Flexural Strength (GPa)	2.02.8	1.52.0		0.51.0
Toughness (KIC, $\text{MPa} \cdot \text{m}^{1/2}$)	1220	2030		35
Wear resistance (mm^3 / h)	<0.03	0.10.3		0.05 - 0.1
Corrosion resistance (mm/y, pH 212)	<0.01	0.050.1		0.01 - 0.03
Temperature resistance ($^{\circ}\text{C}$)	>1000	600 - 800		1200 - 1500
Thermal shock (ΔT 800 $^{\circ}\text{C}$)	>10 ⁵ times	10 ³ - 10 ⁴ times		10 ² - 10 ³ times
Life span multiple (relative to H13)	35	1		1.52
Coefficient of friction (coating)	<0.15	0.3 - 0.5		0.2 - 0.4

cemented carbide high temperature molds:

High temperature resistance: TiAlN / AlCrN coating, anti-oxidation, suitable for 1200 $^{\circ}\text{C}$ molding.

Wear resistance: Ultrafine grain WC, wear <0.03 mm^3 / h , lifespan increased by 35 times.

Corrosion resistance: Ni-based + CrN, resistant to glass melt corrosion, better than H13 steel.

Thermal stability: resistance to thermal cracking and cyclic thermal shock performance is better than ceramic molds.

Optimization suggestions for cemented carbide high temperature molds

Material selection:

Hot forging: WC10%Co+AlCrN, high temperature wear resistance increased by 15%.

Die casting: WC8%Co+TiAlN, anti-adhesion increased by 25%.

Glass molding: WC10%Ni+CrN, corrosion resistance increased by 20%.

Additives: Cr3C2 0.6 wt %, TaC 0.3 wt %, hardness increased by 6%.

Process Optimization:

Sintering: HIP 1400 $^{\circ}\text{C}$, 150 MPa, porosity <0.0005%, wear resistance increased by 20%.

Grinding: 5-axis CNC, CBN grinding wheel (24 μm), deviation $\leq \pm 0.01$ mm, Ra <0.1 μm .

coating:

COPYRIGHT AND LEGAL LIABILITY STATEMENT

Copyright© 2024 CTIA All Rights Reserved
标准文件版本号 CTIAQCD-MA-E/P 2024 版
www.ctia.com.cn

电话/TEL: 0086 592 512 9696
CTIAQCD-MA-E/P 2018-2024V
sales@chinatungsten.com

TiAlN (4 μm , 400°C), high temperature resistance increased by 15%.

AlCrN (5 μm , 450°C), oxidation resistance increased by 20%.

CrN (4 μm , 300°C), anti-adhesion increased by 25%.

EDM: Cavity deviation $\leq \pm 0.003$ mm, accuracy increased by 5%.

Equipment Optimization:

Sintering furnace: temperature control $\pm 2^\circ\text{C}$, 10^{-6} Pa.

5-axis CNC: Deviation $\leq \pm 0.005$ mm.

Coating equipment: deposition rate 11.5 μm /h, deviation $\leq \pm 0.05$ μm .

Working condition adaptation:

Hot forging: WCCo+AlCrN , 1000 - 1200°C, 300 - 500 MPa.

Die casting: WCCo+TiAlN , 700 - 800°C, 100 - 200 MPa.

Glass molding: WCNi+CrN , 1000 - 1100°C, 50 - 100 MPa.

Testing and verification:

Microstructure: SEM (grain 0.20.5 μm), EBSD (grain boundary stress $< 3\%$).

Performance: ASTM G65 (< 0.03 mm^3 / h), corrosion resistance (pH 212, < 0.01 mm/y), temperature resistance ($> 1000^\circ\text{C}$, < 0.01 mg/cm^2) .

Geometry: CMM (deviation $< \pm 0.005$ mm), laser scanning (cavity deviation $< \pm 0.003$ mm).

High temperature tests: thermal shock (ΔT 800°C, $> 10^5$ times), anti-oxidation (1000 hours).

Standards and specifications

GB/T 183762014: Porosity $< 0.01\%$.

GB/T 38502015: Density deviation $\leq \pm 0.1$ g/cm^3 .

GB/T 38512015: Strength 2.0-2.8 GPa .

GB/T 7997-2017: Hardness 1800-2200 HV.

ASTM G65: Wear rate < 0.03 mm^3 / h.

NACE MR0175: Resistance to sulfide stress cracking.

ISO 6508: Hardness deviation $< \pm 40$ HV.

ISO 17879: Thermal shock test.

in conclusion

By optimizing ultrafine grain WC (0.20.5 μm), Co/Ni bonding phase (612 wt %) and PVD/CVD coating (TiAlN / AlCrN / CrN , 25 μm), cemented carbide high temperature molds achieve high hardness (1800-2200 HV), wear resistance (< 0.03 mm^3 / h), corrosion resistance (pH 212, < 0.01 mm/y) and high temperature resistance ($> 1000^\circ\text{C}$). The molds are suitable for hot forging (steel billets), die casting (aluminum alloys), and glass molding (optical lenses). The service life is increased by 35 times, Ra 0.10.3 μm , and the molding efficiency is increased by 1015%. Optimizing grain size, coating thickness and EDM accuracy can reduce costs (5000-20000 yuan per piece) , and the challenges lie in high-precision processing (cost increase of 15%) and high-temperature thermal shock testing (cycle $> 10^5$ times).

COPYRIGHT AND LEGAL LIABILITY STATEMENT

Copyright© 2024 CTIA All Rights Reserved
标准文件版本号 CTIAQCD-MA-E/P 2024 版
www.ctia.com.cn

电话/TEL: 0086 592 512 9696
CTIAQCD-MA-E/P 2018-2024V
sales@chinatungsten.com

appendix:

CTIA GROUP
Carbide Paper Cutter

1. Overview

CTIA GROUP develops , designs and produces carbide industrial cutting tools , and customizes a piece of finished product for customers. CTIA GROUP Carbide Paper Cutter uses tungsten-based carbide (such as WC-Co, WC-Ni) as the blade material, and is specially used for the precise cutting of paper, cardboard, film, aluminum foil and other materials. Its high hardness (HV1600-2000), excellent wear resistance and high temperature stability (600-800°C maintain strength) ensure high-speed and continuous cutting performance, and is widely used in printing, packaging, papermaking and stationery industries to meet the needs of high-precision (tolerance <0.01mm) and high-quality surface cutting.

As a customized manufacturer of cemented carbide cutting tools in China with unique advantages and decades of experience, CTIA GROUP Technology Co. , Ltd. integrates the industry's advanced design and manufacturing processes with intelligent technologies to provide global customers with high-performance paper cutting tools, helping the printing and packaging industries to develop green and efficiently .

2. Materials and manufacturing

2.1 Material composition

Main Ingredients

The blade is made of a composite of tungsten carbide (WC, 82–92%) and a binder (such as Co, 6–12%; Ni, 0–5%), with trace amounts of TiC (0.5–2%) and TaC (0.3–1%) added to enhance wear resistance.

WC-8Co: Co content is 8%, high toughness, suitable for high-speed cutting of ordinary paper and cardboard.

WC-6Co-Ni: Co content is 6%, Ni content is 2%, corrosion resistant, suitable for wet environments or special paper (such as bank paper).

Ultrafine grain

The WC particle size is 0.4–1.2μm, which increases the hardness to HV1900 and improves the chipping resistance by 30%.

Advantages

Compared with high carbon steel, carbide paper cutters are 3 times harder and 5 times more wear-resistant; compared with ceramic cutters, they are more resilient and 50% more impact-resistant.

2.2 Manufacturing process

Powder Metallurgy:

COPYRIGHT AND LEGAL LIABILITY STATEMENT

Ingredients

High-purity WC (purity>99.9%) and Co powders were mixed in a ball mill for 24 hours to ensure uniformity (particle distribution deviation<5%).

suppress

Molded under 400 MPa isostatic pressing, the billet density is >95%, reducing sintering defects.

sintering

Sintered in a vacuum sintering furnace at 1400±10°C for 2 hours under hydrogen protection, the hardness reaches HV1800–1900 and the porosity is <0.1%.

Precision grinding:

Use a CNC five-axis grinder and a diamond grinding wheel to machine the blade to a sharpness of <2μm, a straightness of <0.005mm, and a surface roughness of Ra <0.08μm.

blade angles (15–25° on one side, 30–45° on both sides) ensure smooth cutting without burrs.

Coating technology:

PVD coating

TiN and TiAlN coatings are used with a thickness of 1.5-3μm, a deposition temperature of 400-500°C, a hardness of HV2800, a friction coefficient of 0.2-0.3, and a wear resistance improvement of 60%.

DLC coating

Some high-end cutting tools use diamond-like coating (DLC) with a thickness of 1-2μm, a friction coefficient as low as 0.1, and a lifespan extended by 100%, making them suitable for high-finish cutting.

Quality Control

Each batch of cutting tools is tested for composition by X-ray fluorescence (XRF) and for cutting edge defects by microscope, in compliance with ISO 9001 and ISO 14001 standards.

3. Specifications of China Tungsten Intelligent Carbide Paper Cutter

CTIA GROUP Carbide Paper Cutters provide a variety of specifications to meet the needs of different cutting equipment and materials. The following is the main specification table:

type	Dimensions (mm)	Blade Angle	Appropriate thickness Degree mm	Applicable Materials	Applicable devices
Straight Edge Paper Cutter	500×80×10–1500×120×15	15–20° on one side	0.1–8	Coated paper, newsprint, cardboard	Polar, Wohlenberg, Perfecta
Circular paper cutter	Diameter 50–300, thickness 2–10	Bilateral 30–40°	0.05–5	Film, aluminum foil, paper roll	Slitting machine, coil cutting machine
Toothed paper cutter	300×50×5–800×80×8	20–25° on one side	0.1–3	Label paper, stamp paper, punched paper	Die cutting machine, label cutting machine

COPYRIGHT AND LEGAL LIABILITY STATEMENT

Copyright© 2024 CTIA All Rights Reserved
标准文件版本号 CTIAQCD-MA-E/P 2024 版
www.ctia.com.cn

电话/TEL: 0086 592 512 9696
CTIAQCD-MA-E/P 2018-2024V
sales@chinatungsten.com

Custom Paper Cutter	According to customer needs (maximum 2000×150×20)	15–45° adjustable	0.05–10	Bank paper, composite materials, special films	Customized equipment (eg Heidelberg, Muller)
---------------------	---	-------------------	---------	--	--

tolerance

Length/width $\pm 0.02\text{mm}$, thickness $\pm 0.01\text{mm}$, cutting edge straightness $< 0.005\text{mm}$.

Customization

Support non-standard sizes and blade shapes (such as bevel, wavy blade), with a delivery cycle of 7-14 days.

Package

The knife is equipped with a micro smart Hardbox (size 15×10×5cm, with built-in RFID and QR code) for easy recycling and in line with green manufacturing standards.

Types and applications of carbide paper cutters

Straight Edge Paper Cutter

Used for flat sheet cutting, cutting thickness 0.1-8mm, accuracy $< 0.01\text{mm}$, suitable for printing plants to cut coated paper, newsprint, cardboard, compatible with Polar, Wohlenberg and other equipment.

Circular paper cutter

Used for coil slitting, speed $> 200\text{ m/min}$, suitable for packaging film, aluminum foil, roll paper slitting, tolerance $< 5\mu\text{m}$, widely used in high-speed production lines.

Toothed paper cutter

Used for punching or sawtooth cutting, the cut flatness is improved by 30%, suitable for label paper and stamp paper processing, and used in die-cutting machines.

Custom Paper Cutter

blade angles and coatings are designed for special materials (such as bank paper and composite materials), such as the TiAlN bevel cutter manufactured by China Tungsten Intelligence, which extends the service life by 25%.

Carbide Paper Cutter Application Cases

CTIA GROUP Straight Edge Paper Cutter (1000×100×12mm, TiN coating) is used in Polar 115 paper trimmer to cut A4 coated paper (70g/m^2), with an annual output of 200 million sheets, a tool life of 600,000 times, a 60% reduction in tool change frequency, and a 30% reduction in cutting costs.

Circular paper cutter (200 diameter x 5 mm thickness, DLC coating) for BOPP film slitting, speed 250 m/min, tolerance $< 3\mu\text{m}$, annual output 50 million meters, tool life 1 million meters, customer satisfaction increased by 35%.

The toothed paper cutter (500×60×6mm, TiAlN coating) is used for punching holes in label paper, with a cutting accuracy of $< 0.008\text{mm}$ and an annual output of 100 million sheets. The tool durability is increased by 40% and the scrap rate is reduced by 50%.

COPYRIGHT AND LEGAL LIABILITY STATEMENT

5. Technical features of carbide paper cutter

High efficiency

Cutting speed is 50–200 m/min, single cutting thickness is 0.05–10 mm, and production efficiency is increased by 40–60%.

High precision

The cutting tolerance is $<0.01\text{mm}$ and the cutting smoothness is $Ra < 0.15\mu\text{m}$, meeting ISO 9001 and printing industry standards (such as ISO 12647).

Durability

The hardness of the carbide tool is 62-65 HRC, the service life is 500,000-1,000,000 cuts, and the tool change frequency is reduced by 50%.

Recyclability

Waste cutting tools are recycled through a micro-intelligent Hardbox (with built-in RFID and 5G data upload). Combined with zinc melting or electrochemical methods, the tungsten recovery rate is $>90\%$, and the cost is reduced by 30-40%.

Features of CTIA GROUP

The independently developed ultra-fine-grained cemented carbide and DLC coating technology increase tool life by 20% compared to the industry average, supporting the high-speed demands of the printing and packaging industries ().

6. Maintenance and regrinding of carbide paper cutters

Daily maintenance

clean

After cutting, wipe the blade with anhydrous ethanol to remove paper scraps and stickies to prevent corrosion.

store

Store in a dry environment (humidity $<60\%$), using China Tungsten customized tool box (including shockproof foam and rust inhibitor).

examine

Check the edge wear after every 100,000 cuts (magnification 50 times under a microscope) to ensure there is no chipping .

Regrinding Technology

Regrinding cycle

The tool can be reground when the wear depth is less than 0.1mm. It is recommended to reground it every 300,000 to 500,000 cuts.

Technology

Diamond grinding wheel (grit size D15) and CNC grinding machine are used for processing, with blade angle error $<0.5^\circ$ and surface roughness $Ra < 0.1\mu\text{m}$.

frequency

straight- edged knife can be resharpened 3–5 times, a round-edged knife 2–4 times. After

COPYRIGHT AND LEGAL LIABILITY STATEMENT

resharpening, the performance is restored to 90% and the cost is reduced by 40%.

7. Development trend of carbide paper cutters

Intelligent Manufacturing

Introducing digital twin technology to monitor tool wear and cutting performance in real time, predict maintenance cycles, and reduce downtime by 20%.

Combined with AI to optimize blade angle (15–45°) and coating parameters, cutting efficiency is increased by 25% ().

Green Manufacturing

Research and develop low- Co (<4%) cemented carbide to reduce cobalt resource consumption and reduce environmental impact by 50%.

Promote the micro-intelligent Hardbox recycling system, which integrates RFID, QR code and 5G technology, improves recycling efficiency by 40% and reduces waste liquid emissions by 60% (refer to China's green manufacturing trend for cutting tools).

Super Hard Coating

Develop nano multi-layer coatings (such as TiAlN / CrN , DLC/Si3N4) with a hardness of HV3500, a 70% increase in wear resistance, and a 2-fold increase in service life.

Optimize the coating deposition process (arc ion plating, deposition rate increased by 30%) and reduce production costs by 15%.

Customization and modularity

blades and coatings for digital printing papers (such as HP Indigo paper) and high-strength composite materials, which improve cutting accuracy by 20%. Promote modular tool design (such as replaceable blades), shorten installation time by 50%, and reduce inventory costs by 25%.

CTIA GROUP's carbide paper cutters have become the core cutting tools in the printing, packaging and papermaking industries due to their high hardness (HV1800-1900), wear resistance and high precision (tolerance <0.01mm). Its ultra-fine-grain carbide, DLC coating and micro-intelligent Hardbox recycling system significantly improve tool life (500,000-1 million cuts), efficiency (speed 200 m/min) and green performance (tungsten recovery rate >90%). Through many application cases such as printing plants and packaging production lines, the cutters have demonstrated excellent cost-effectiveness (reduced by 30-40%) and customer satisfaction (increased by 35%).

In the future, CTIA GROUP will continue to research, develop and design carbide paper cutters through intelligent manufacturing (digital twins, AI optimization) and green recycling (low-Co alloys, ionic liquid technology), to help the printing and packaging industry develop in a green and efficient manner and enhance its global market competitiveness .

COPYRIGHT AND LEGAL LIABILITY STATEMENT

appendix:

ISO 9227:2017

Corrosion test

Salt spray test in artificial atmosphere

1 Scope

This standard specifies the test methods for conducting salt spray tests (Neutral Salt Spray, NSS), acetic acid salt spray tests (Acetic Acid Salt Spray, AASS) and copper accelerated acetic acid salt spray tests (Copper-Accelerated Acetic Acid Salt Spray, CASS) in artificial atmospheres to evaluate the corrosion resistance of metal materials and their protective coatings (such as cemented carbide, galvanized layer, coated steel plate). The test methods are applicable to the comparison of corrosion performance of materials, components or assemblies, but do not directly predict their service life in actual environments. This standard is not applicable to the evaluation of the corrosion resistance of non-metallic materials.

2 Normative references

The clauses listed in the following documents become the clauses of this standard through reference in this standard. For referenced documents with dates, only the referenced versions apply; for referenced documents without dates, the latest versions (including all amendments) apply.

ISO 1514:2016 Paints and varnishes — Standard test panels for testing

ISO 2808:2019 Paints and varnishes — Determination of film thickness

ISO 3574:2012 Cold-rolled carbon steel sheets and strip — Specifications

General requirements for the competence of testing and calibration laboratories

3 Terms and definitions

The following terms and definitions apply to this document:

Salt spray test: Under controlled conditions, a salt solution is dispersed into fine droplets through a spray device to form an artificial corrosive atmosphere to evaluate the corrosion resistance of a material.

NSS (Neutral Salt Spray Test): A salt spray test performed using a neutral salt solution (pH 6.5-7.2).

AASS (Acetic Acid Salt Spray Test): A salt spray test conducted by adding acetic acid to a neutral salt solution and adjusting the pH to 3.1-3.3.

chloride (CuCl_2) to the acetate salt spray test solution accelerates the corrosion test.

Weight loss: The change in mass of a sample before and after a test, usually expressed in mg/cm^2 .

4 Test Principle

The salt spray test simulates the corrosion conditions in marine or industrial environments by exposing the specimen to an artificial atmosphere containing salt droplets. The NSS test simulates a neutral salt spray environment, and the AASS and CASS tests accelerate corrosion by acidification and adding catalysts (such as CuCl_2), which are suitable for more demanding corrosion performance evaluations. The corrosion rate is evaluated by weight loss, corrosion product analysis, or surface defects (such as pitting and spalling).

COPYRIGHT AND LEGAL LIABILITY STATEMENT

5 Test equipment

5.1 Salt spray test chamber

Volume ≥ 400 L, ensuring uniform airflow around the sample.

The box body is made of corrosion-resistant material (such as glass fiber reinforced plastic) to avoid metal material pollution.

Equipped with spray device, heating system and humidity control system.

5.2 Spray device

The nozzle material is corrosion-resistant material (such as polytetrafluoroethylene).

Spray pressure: 0.07-0.17 MPa (0.7-1.7 bar).

Spray droplet size: 1-10 μm .

5.3 Environmental Control

Temperature in the test chamber:

NSS: $35^{\circ}\text{C} \pm 2^{\circ}\text{C}$.

AASS and CASS: $50^{\circ}\text{C} \pm 2^{\circ}\text{C}$.

Humidity: $\geq 95\%$ RH.

6 Test solution

6.1 NSS test solution

Sodium chloride (NaCl) concentration: $50 \text{ g/L} \pm 5 \text{ g/L}$.

pH: 6.5-7.2 (at 25°C).

Solution purity: Impurities (such as Cu, Ni) $< 0.001\%$.

6.2 AASS test solution

Add glacial acetic acid to the NSS solution and adjust the pH to 3.1-3.3 (at 25°C).

6.3 CASS test solution

$\text{CuCl}_2 \cdot 2\text{H}_2\text{O}$ to the AASS solution at a concentration of $0.26 \text{ g/L} \pm 0.02 \text{ g/L}$.

pH: 3.1-3.3 (at 25°C).

6.4 Solution Collection

Collection rate: 1.0-2.0 mL/h (80 cm^2 horizontal area).

Collection solution NaCl concentration: $50 \text{ g/L} \pm 10 \text{ g/L}$.

7. Sample requirements

7.1 Specimen type

Metallic materials, coated materials or components, with dimensions suitable for the test chamber (recommended 150 mm \times 70 mm \times 1 mm).

The surface roughness of cemented carbide specimen is $R_a \leq 0.2 \mu\text{m}$.

7.2 Number of samples

At least 3 samples were included in each group to ensure statistical reliability.

7.3 Sample preparation

Clean the sample to remove oil and oxides (can be cleaned with anhydrous ethanol).

The edges of the specimens should be smooth to avoid sharp edges and corners that may cause local corrosion.

Record the initial mass of the sample (accuracy $\pm 0.001 \text{ g}$).

COPYRIGHT AND LEGAL LIABILITY STATEMENT

7.4 Sample placement

The specimen is placed at an angle of 15°-30° to the vertical.

The distance between the samples should be ≥ 20 mm to ensure that the droplets do not drip onto each other.

8 Test procedures

8.1 Test conditions

NSS: $35^{\circ}\text{C} \pm 2^{\circ}\text{C}$, pH 6.5-7.2.

AASS: $50^{\circ}\text{C} \pm 2^{\circ}\text{C}$, pH 3.1-3.3.

CASS: $50^{\circ}\text{C} \pm 2^{\circ}\text{C}$, pH 3.1-3.3, with CuCl_2 .

8.2 Test time

Recommended test cycles: 24 h, 48 h, 96 h, 240 h, 720 h (select according to application requirements).

720 h is recommended for cemented carbide to evaluate long-term corrosion resistance.

8.3 Test operation

Preheat the test chamber to the specified temperature. Add the test solution and start the spray device. Place the sample, close the test chamber, and record the test start time. Check the solution pH and collection rate every 24 hours.

8.4 End of the test

The samples were removed and rinsed with distilled water to remove salt deposits.

Wash with anhydrous ethanol and dry ($60^{\circ}\text{C} \pm 5^{\circ}\text{C}$, 30 min).

Record the final mass of the sample (accuracy ± 0.001 g).

9 Results Evaluation

9.1 Weight loss calculation

Weight loss rate (mg/cm^2) = (initial mass - final mass) / sample surface area.

cm^2 after 720 h of NSS $\pm 0.01 \text{ mg}/\text{cm}^2$.

9.2 Surface analysis

Use an optical microscope (magnification 50×-200×) to observe pitting, spalling or corrosion products.

Record the number, size (diameter, depth) and distribution of corrosion pits.

9.3 Evaluation criteria

According to the application requirements, the qualified standards of weight loss rate or surface defects are established.

For example: Chemical valve carbide weight loss $< 0.1 \text{ mg}/\text{cm}^2$, pitting depth $< 5 \mu\text{m}$.

10 Test Report

The test report should include the following:

Specimen information: material type, size, surface condition.

Test conditions: test type (NSS/AASS/CASS), temperature, pH, test time.

Results: weight loss rate, number and size of corrosion pits, surface photos.

Evaluation conclusion: whether it meets the application requirements.

COPYRIGHT AND LEGAL LIABILITY STATEMENT

Test date and operator signature.

Appendix A (Informative Appendix) Reference Values of Salt Spray Resistance of Typical Materials

Material Type	Test Type	Test time (h)	Weight loss rate (mg/cm ²)	Typical Applications
Cemented Carbide (WC-10Co)	NSS	720	0.08 ± 0.01	Marine equipment
Galvanized steel sheet	AASS	240	0.15 ± 0.02	Building Components
Stainless steel (304)	CASS	96	0.05 ± 0.01	Food processing equipment

Appendix B (Informative Appendix) Environmental Requirements

Test chamber temperature: 15°C to 35°C, 23±2°C recommended.
Humidity: 30%-70%, 50±10% recommended.
No vibration, no corrosive gas environment.
Test bench levelness: deviation < 0.02 mm/m.

Summarize

ISO 9227:2017 "Corrosion tests - Salt spray tests in artificial atmospheres" provides standardized methods for evaluating the corrosion resistance of metal materials and protective coatings, including three test types: NSS, AASS and CASS. Through standardized test conditions and procedures, the performance of materials in simulated corrosive environments can be effectively compared, providing a scientific basis for material selection and engineering applications (such as the use of cemented carbide in marine equipment).

COPYRIGHT AND LEGAL LIABILITY STATEMENT

appendix:

National Standard of the People's Republic of China
GB/T 18376-2014
Methods for testing the corrosion resistance and wear resistance
of cemented carbides

Preface

This standard was drafted in accordance with the provisions of GB/T 1.1-2009 "Guidelines for standardization work Part 1: Structure and writing rules of standards".

This standard replaces GB/T 18376-2001 "Test methods for corrosion resistance and wear resistance of cemented carbide".

Compared with GB/T 18376-2001, the main technical changes are as follows:

Added electrochemical test method (see 5.3);

The salt spray test conditions were adjusted, and the temperature was changed from 40°C to 35°C $\pm 2^\circ\text{C}$ (see 5.1);

The load and number of cycles of the abrasive wear test were modified. The load was changed from 30 N to 20 N ± 0.5 N, and the number of cycles was changed from 500 to 1000 ± 10 (see 6.2).

The sample surface roughness requirement is increased to $R_a < 0.8 \mu\text{m} \pm 0.1 \mu\text{m}$ (see 4.2).

This standard is proposed and managed by the National Cemented Carbide Standardization Technical Committee (SAC/TC 357).

The drafting units of this standard are: Cemented Carbide Research Institute of China Machine Tool Corporation, University of Science and Technology Beijing, Xi'an Jiaotong University.

The main drafters of this standard are:

This standard will be implemented from October 1, 2014.

1 Scope

This standard specifies the test methods for the corrosion resistance and wear resistance of cemented carbides. It is applicable to cemented carbides with tungsten carbide (WC) as the main component and cobalt (Co) or nickel (Ni) as the bonding phase, including but not limited to WC-Co and WC-Ni systems.

2 Normative references

The following documents are essential for the application of this standard. For any dated referenced document, only the dated version applies to this standard. For any undated referenced document, the latest version (including all amendments) applies to this standard.

GB/T 12444-2006 Test methods for sliding friction and wear of metallic materials

GB/T 16545-2008 Salt spray corrosion test method for metal materials

ISO 9227-2017 Corrosion test - Corrosivity in artificial atmosphere

3 Terms and definitions

The following terms and definitions apply to this standard:

3.1 Corrosion resistance

COPYRIGHT AND LEGAL LIABILITY STATEMENT

Copyright© 2024 CTIA All Rights Reserved
标准文件版本号 CTIAQCD-MA-E/P 2024 版
www.ctia.com.cn

电话/TEL: 0086 592 512 9696
CTIAQCD-MA-E/P 2018-2024V
sales@chinatungsten.com

The ability of cemented carbide to resist mass loss or surface damage in corrosive media (such as acidic solutions or salt spray), usually expressed in weight loss rate (mg/cm^2) and corrosion current density (i_{corr} , A/cm^2).

3.2 Wear resistance

The ability of cemented carbide to resist material wear under mechanical friction or abrasive action, usually expressed in wear mass loss (mg) or wear volume (mm^3).

3.3 Corrosion current density (i_{corr})

In electrochemical testing, it is a parameter reflecting the corrosion rate of the material, with the unit of A/cm^2 .

4 Experimental preparation

4.1 Sample

4.1.1 Sample material: WC-based cemented carbide, with Co or Ni as the bonding phase, and the composition should meet the product technical requirements.

4.1.2 Sample size: $10\text{ mm} \times 10\text{ mm} \times 5\text{ mm} \pm 0.1\text{ mm}$.

4.1.3 Number of samples: Each group of tests should be repeated more than 3 times.

4.2 Sample processing

4.2.1 Surface treatment: The sample surface is mechanically polished, with a roughness of $R_a < 0.8\text{ }\mu\text{m} \pm 0.1\text{ }\mu\text{m}$.

4.2.2 Cleaning: Ultrasonic cleaning with anhydrous ethanol for $5\text{ minutes} \pm 0.5\text{ minutes}$, drying for use.

4.2.3 Initial mass: Measured with an analytical balance, with an accuracy of $\pm 0.01\text{ mg}$.

5 Corrosion resistance test

5.1 Salt spray test

5.1.1 Test conditions:

Solution: $5\% \pm 0.1\%$ NaCl solution (mass fraction), pH 6.5-7.2.

Temperature: $35^\circ\text{C} \pm 2^\circ\text{C}$.

Duration: $48\text{ hours} \pm 2\text{ hours}$.

5.1.2 Test equipment

Salt spray chamber, spray volume $1\text{-}2\text{ mL}/(80\text{ cm}^2 \cdot \text{h})$.

5.1.3 Result evaluation:

Weight loss rate = $(m_0 - m_1) / A$, unit: mg/cm^2 , accuracy: $\pm 0.01\text{ mg}/\text{cm}^2$, where m_0 is the mass before the test, m_1 is the mass after the test, and A is the surface area of the specimen.

Observe the surface corrosion morphology and record the depth of the corrosion pit (accuracy $\pm 0.5\text{ }\mu\text{m}$).

5.2 Acid immersion test

5.2.1 Test conditions:

Solution: $1\% \pm 0.1\%$ H_2SO_4 solution (volume fraction).

Temperature: $25^\circ\text{C} \pm 1^\circ\text{C}$.

Immersion time: $24\text{ hours} \pm 1\text{ hour}$.

5.2.2 Test equipment

COPYRIGHT AND LEGAL LIABILITY STATEMENT

Constant temperature water bath.

5.2.3 Result evaluation:

The weight loss rate is calculated according to 5.1.3.

Measure the depth of corrosion pits with an accuracy of $\pm 0.5 \mu\text{m}$.

5.3 Electrochemical testing

5.3.1 Test conditions:

Electrolyte: $3.5\% \pm 0.1\%$ NaCl solution, temperature $25^\circ\text{C} \pm 1^\circ\text{C}$.

Electrode system: working electrode (hard alloy), reference electrode (saturated calomel electrode SCE), auxiliary electrode (platinum electrode).

Scan rate: $1 \text{ mV/s} \pm 0.1 \text{ mV/s}$, potential range $\pm 0.25 \text{ V}$ vs. E_{corr} .

5.3.2 Test equipment

Electrochemical workstation, potential accuracy $\pm 0.001 \text{ V}$, current accuracy $\pm 10^{-9} \text{ A}$.

5.3.3 Result evaluation:

Measures corrosion potential (E_{corr} , accuracy $\pm 0.02 \text{ V}$) and corrosion current density (i_{corr} , accuracy $\pm 10^{-7} \text{ A/cm}^2$).

Tafel fitting analysis was used, and the test was repeated ≥ 3 times.

6 Wear resistance test

6.1 Friction and wear test

6.1.1 Test conditions:

Load: $50 \text{ N} \pm 1 \text{ N}$.

Sliding speed: $0.1 \text{ m/s} \pm 0.01 \text{ m/s}$.

Test time: $30 \text{ minutes} \pm 1 \text{ minute}$.

Friction pair: carbide pin, paired material is hardened steel disc (hardness $\text{HV } 600 \pm 50$).

6.1.2 Test equipment

Friction and wear testing machine, load accuracy $\pm 1 \text{ N}$, speed accuracy $\pm 0.01 \text{ m/s}$.

6.1.3 Result evaluation:

Wear mass loss = $m_0 - m_1$, unit: mg, accuracy: $\pm 0.01 \text{ mg}$.

Observe the wear scar depth and width with an accuracy of $\pm 0.5 \mu\text{m}$.

6.2 Abrasive wear test

6.2.1 Test conditions:

Abrasive: SiC, particle size $100\text{-}150 \mu\text{m}$.

Load: $20 \text{ N} \pm 0.5 \text{ N}$.

Number of test cycles: $1000 \text{ cycles} \pm 10 \text{ cycles}$.

Friction pair: carbide specimen, the mating material is abrasive disc.

6.2.2 Test equipment

Abrasive wear testing machine, load accuracy $\pm 0.5 \text{ N}$, circle accuracy ± 10 circles.

6.2.3 Result evaluation:

Wear volume = $(m_0 - m_1) / \rho$, unit: mm^3 , accuracy: $\pm 0.01 \text{ mm}^3$, where ρ is the material density, accuracy: $\pm 0.1 \text{ g/cm}^3$.

Measure the wear scar profile with an accuracy of $\pm 0.5 \mu\text{m}$.

COPYRIGHT AND LEGAL LIABILITY STATEMENT

7 Data Processing

- 7.1 All test results are the average of more than 3 measurements.
- 7.2 Corrosion resistance is expressed as weight loss rate (mg/cm^2 , accuracy $\pm 0.01 \text{ mg}/\text{cm}^2$) and i_{corr} (A/cm^2 , accuracy $\pm 10^{-7} \text{ A}/\text{cm}^2$).
- 7.3 Wear resistance is expressed as wear mass loss (mg , accuracy $\pm 0.01 \text{ mg}$) or wear volume (mm^3 , accuracy $\pm 0.01 \text{ mm}^3$).
- 7.4 The results are accompanied by uncertainty analysis with a confidence level of 95%.

8 Test report

The test report should include the following:

Sample material composition and preparation process.

Test conditions (such as temperature, time, load, etc.).

Test results (weight loss, i_{corr} , wear loss, etc.) and uncertainties.

Test date and operator signature.

Appendix A (Normative Appendix)

Sample preparation example

- A.1 Sample cutting: Use diamond grinding wheel, water as coolant, cutting speed $10 \text{ m/s} \pm 1 \text{ m/s}$.
- A.2 Polishing: Use SiC sandpaper (grit #800-#1200), and finally polish with diamond suspension (grit $1 \mu\text{m} \pm 0.1 \mu\text{m}$).
- A.3 Cleaning: Ultrasonic cleaning for $5 \text{ minutes} \pm 0.5 \text{ minutes}$, weigh after drying.

Appendix B (Informative Appendix)

Typical data reference

- B.1 WC10Ni: Salt spray weight loss rate $0.04 \text{ mg}/\text{cm}^2 \pm 0.01 \text{ mg}/\text{cm}^2$, $i_{\text{corr}} 10^{-6} \text{ A}/\text{cm}^2 \pm 10^{-7} \text{ A}/\text{cm}^2$, wear mass loss $0.08 \text{ mg} \pm 0.01 \text{ mg}$.
- B.2 WC10Co: Salt spray weight loss rate $0.07 \text{ mg}/\text{cm}^2 \pm 0.01 \text{ mg}/\text{cm}^2$, $i_{\text{corr}} 10^{-5} \text{ A}/\text{cm}^2 \pm 10^{-6} \text{ A}/\text{cm}^2$, wear mass loss $0.12 \text{ mg} \pm 0.01 \text{ mg}$.

For

matters not covered in this standard, please refer to relevant international standards (such as ISO 3738, ISO 28079) or consult with the technical committee.

This standard was issued by the National Standardization Administration on July 9, 2014 and implemented on October 1, 2014.

COPYRIGHT AND LEGAL LIABILITY STATEMENT

Copyright© 2024 CTIA All Rights Reserved
标准文件版本号 CTIAQCD-MA-E/P 2024 版
www.ctia.com.cn

电话/TEL: 0086 592 512 9696
CTIAQCD-MA-E/P 2018-2024V
sales@chinatungsten.com

appendix:

International Standard
ISO 4287:1997
Geometric Product Specifications
— **Surface texture: Contour method**
— **Terms, definitions and surface texture parameters**
Geometrical Product Specifications (GPS)
— **Surface texture: Profile method**
— **Terms, definitions and surface texture parameters**

Overview

ISO 4287:1997 is a standard developed by the International Organization for Standardization (ISO), titled "Geometrical Product Specifications (GPS) — Surface texture: Profile method — Terms, definitions and surface texture parameters". The standard was published on August 1, 1997. The latest version is ISO 4287:1997 (Amd 1:2009) and is confirmed to be valid in 2018. ISO 4287 was developed by ISO/TC 213 (Geometrical Product Specifications and Verification) to provide unified terms, definitions and parameters for the profile method of surface texture, which is applicable to the surface quality assessment of mechanical parts, tools and materials. This standard is widely used in manufacturing, quality control and engineering design.

1 Scope

Applicable objects: Applicable to parts that measure and evaluate surface texture using the profile method, including metals, plastics and ceramics.

Purpose: To define the terminology and calculation methods of surface texture parameters and to provide guidance for surface roughness measurement and reporting.

Not applicable: Not applicable to non-profile measurement of surface topography (such as the area method) or microstructure analysis.

2 Normative references

The following documents are essential for the application of this standard. For any dated referenced document, only the dated version applies to this standard. For any undated referenced document, the latest version (including all amendments) applies to this standard.

ISO 3274:1996 Geometrical Product Specifications (GPS)

— Surface texture: Profile method — Nominal characteristics of contact (stylus) instruments

ISO 4288:1996 Geometrical Product Specifications (GPS)

— Surface texture: Profile method — Rules and procedures for the assessment of surface texture

3 Terms and definitions

The following terms and definitions apply to this standard:

3.1 Basic concepts

3.1.1 Surface texture

The surface of a part is the sum of its roughness, waviness and error of form. 3.1.2 Profile

COPYRIGHT AND LEGAL LIABILITY STATEMENT

The two-dimensional cross section of the surface texture, representing the curve of height versus length.

3.2 Roughness parameters

3.2.1 Ra (Arithmetic mean deviation)

Profile Arithmetic mean deviation, defined as the average of the absolute values of the profile deviation within the sampling length, in μm (Micrometers).

3.2.2 Rq (Root mean square deviation) Profile Root mean square deviation, defined as the square root of the average of the squares of the profile deviation within the sampling length, in μm (Micrometers).

3.2.3 Rz (Maximum height of the profile) Maximum height of the profile, defined as the height difference between the highest peak and the lowest valley within the sampling length, in μm (Micrometers).

3.2.4 Rt (Total height of the profile) Total height of the profile, defined as the maximum height difference between the highest peak and the lowest valley within the evaluation length, in μm (Micrometers).

3.2.5 Rp (Maximum profile peak height) Peak height within the sampling length, in μm (Micrometers).

3.2.6 Rv (Maximum profile valley depth) is

the deepest valley depth within the sampling length, in μm (Micrometers).

3.3 Sampling and evaluation lengths

3.3.1 Sampling length (lr)

The reference length used to calculate the roughness parameters, usually 0.25 mm, 0.8 mm or 2.5 mm.

3.3.2 Evaluation length (ln)

The sum of multiple sampling lengths, used for comprehensive evaluation of surface texture, usually 5lr.

3.3.3 Traversing length (lt)

The total length actually scanned during the measurement process, usually 1.5ln.

3.4 Other parameters

3.4.1 Sk (Core roughness depth)

Profile Core roughness depth, reflects the material bearing properties, unit is μm (Micrometers).

3.4.2 Rsk (Skewness)

Profile Skewness, describes the asymmetry of the height distribution, unit is not specified.

3.4.3 Rku (Kurtosis) Profile

Kurtosis, describes the sharpness of the height distribution, unit is not specified.

4 Parameter calculation methods

4.1 Roughness parameters

Calculation of Ra:

$$Ra = \frac{1}{lr} \int_0^{lr} |z(x)| dx$$

其中, $z(x)$ 为轮廓偏差 (Profile deviation), lr 为采样长度 (Sampling length)。

COPYRIGHT AND LEGAL LIABILITY STATEMENT

Rq 计算 (Calculation of Rq):

$$Rq = \sqrt{\frac{1}{lr} \int_0^{lr} z(x)^2 dx}$$

Rz 计算 (Calculation of Rz): 取 采样长度 (Sampling length) 内最大 峰高 (Peak height) 与最低 谷深 (Valley depth) 的和。

Rt 计算 (Calculation of Rt): 取 评估长度 (Evaluation length) 内最大 峰高 (Peak height) 与最低 谷深 (Valley depth) 的和。

4.2 Measurement conditions

Instrument: Contact (stylus) instrument conforming to ISO 3274, with a stylus radius $\leq 5 \mu\text{m}$.

Filtering: Use high-pass filtering to remove the effect of waviness. The cutoff wavelength λ_c is usually 0.8 mm.

5 Reporting requirements

Parameter values: Report R_a , R_q , R_z and other parameter values (Parameter values), the unit is μm (Micrometers), the accuracy is $\pm 0.01 \mu\text{m}$.

Measurement conditions: including sampling length, evaluation length, filtering conditions and stylus type.

Uncertainty: Measurement uncertainty is provided within a 95% confidence level.

6 Appendix

Appendix A: Typical Data

Machined steel part: $R_a = 0.8 \mu\text{m} \pm 0.01 \mu\text{m}$, $R_z = 4.5 \mu\text{m} \pm 0.1 \mu\text{m}$.

Polished cemented carbide: $R_a = 0.02 \mu\text{m} \pm 0.01 \mu\text{m}$, $R_z = 0.15 \mu\text{m} \pm 0.01 \mu\text{m}$.

Appendix B: Measurement example

The sampling length is 0.8 mm, the evaluation length is 4 mm, and the R_a measurement value is 1.2 μm .

illustrate

Related standards: ISO 3274 specifies the characteristics of measuring instruments. ISO4288 provides rules and procedures for surface texture assessment.

Validity: ISO 4287:1997 (Amd 1:2009) confirmed as valid in 2018, may be updated in the future based on the GPS framework.

Where to get it: The standard text can be purchased through the ISO official website.

Note: When implementing, it is necessary to combine the specific surface treatment process and measurement equipment calibration, and consult professional technicians.

COPYRIGHT AND LEGAL LIABILITY STATEMENT

Copyright© 2024 CTIA All Rights Reserved
标准文件版本号 CTIAQCD-MA-E/P 2024 版
www.ctia.com.cn

电话/TEL: 0086 592 512 9696
CTIAQCD-MA-E/P 2018-2024V
sales@chinatungsten.com

appendix:

International Standard
ISO 3274:1996
Geometrical Product Specifications (GPS)
— Surface texture: Contour method
Geometrical Product Specifications (GPS) for contact instruments
— Surface texture: Profile method
— Nominal characteristics of contact (stylus) instruments

Overview

ISO 3274:1996 is a standard developed by the International Organization for Standardization, titled "Geometric product specifications - Surface texture: Profile method - Nominal characteristics of contact instruments". The standard was published on August 1, 1996, and the latest version is ISO 3274:1996 (Amd 1:2009), which was confirmed to be valid in 2019. ISO 3274 was developed by ISO/TC 213 (Geometric product specifications and verification) to specify the nominal characteristics of contact instruments used for surface texture profilometry measurement, including probes, drive devices and filter requirements. This standard provides a technical basis for surface roughness measurement and is widely used in manufacturing, mechanical engineering and material testing.

1 Scope

Applicable to : Profilometry for measuring surface texture using contact instruments, covering materials such as metals, plastics and ceramics.

Purpose : To define the nominal characteristics of contact instruments to ensure comparability and consistency of measurement results.

Not Applicable : Not suitable for use with non-contact measuring instruments (such as optical or laser equipment) or for microstructural analysis.

2 Normative references

The following documents are essential for the application of this standard. For any dated referenced document, only the dated version applies to this standard. For any undated referenced document, the latest version (including all amendments) applies to this standard.

ISO 4287:1997 Geometrical product specifications — Surface texture: Profile method — Terms, definitions and surface texture parameters

ISO 4288:1996 Geometrical product specifications — Surface texture: Profile method — Rules and procedures for the evaluation of surface texture

3 Terms and definitions

The following terms and definitions apply to this standard:

3.1 Contact instrument

A device that uses a physical probe to contact the surface for measurement, used to obtain surface

COPYRIGHT AND LEGAL LIABILITY STATEMENT

profile data. 3.2 The part at the end of the **probe** instrument that contacts the surface and is responsible for sensing height changes. 3.3 **Sampling length**

The reference length used to measure surface texture, usually 0.25 mm, 0.8 mm or 2.5 mm. 3.4 **Cut-off wavelength**

filter The critical length used to separate roughness and waviness, a common value is 0.8 mm.

4 Instrument characteristics requirements

4.1 Probe

Shape : Conical or spherical tip, tip radius typically 2 μm to 10 μm .

Materials : Wear-resistant materials such as diamond or carbide.

Contact force : 0.5 mN to 4 mN , depending on surface hardness and roughness.

4.2 Drive device

Moving speed : 0.1 mm/s to 1 mm/s, accuracy ± 0.02 mm/s.

Straightness : The straightness error of the moving path is ≤ 0.5 μm .

Resolution : height resolution ≤ 0.01 μm , length resolution ≤ 0.1 μm .

4.3 Filters

Type : 2RC or phase corrected high pass filter.

Cut-off wavelength (λ_c) : 0.08 mm, 0.25 mm, 0.8 mm or 2.5 mm, select according to measurement requirements.

Transfer characteristics : in accordance with ISO 11562 requirements, attenuation rate $\geq 75\%$.

5 Measurement conditions

Environmental conditions : temperature $20^\circ\text{C} \pm 2^\circ\text{C}$, humidity 40%-60%.

Surface preparation : The sample surface should be clean, free of oil and dirt, with a roughness of $R_a \leq 0.8$ μm .

Measuring direction : measure along the main processing direction or vertical direction of the part.

6 Data collection and processing

Sampling interval : automatically adjusted according to the sampling length, the maximum interval is ≤ 0.1 μm .

Number of data points : At least 5000 data points per sampling length.

Filtering : Use a specified cutoff wavelength to remove the effects of waviness.

7 Test Report

The test report should include the following:

Specimen material and surface condition.

Instrument model, probe type and contact force.

Measurement conditions (e.g. sampling length, cut-off wavelength).

Measurement results and uncertainties.

Test date and operator signature.

COPYRIGHT AND LEGAL LIABILITY STATEMENT

8 Appendix (Informative)

Appendix A: Typical Data

Machined steel parts : probe radius 5 μm , sampling length 0.8 mm, $R_a = 0.8 \mu\text{m}$.

Polishing carbide : probe radius 2 μm , sampling length 0.25 mm, $R_a = 0.02 \mu\text{m}$.

illustrate

Related standards :

ISO 4287 provides definitions of surface texture parameters.

ISO 4288 provides rules and procedures for assessment.

Validity : ISO 3274:1996 (Amd 1:2009) confirmed as valid in 2019 and may be updated in the future based on technological advances.

Where to get it : The standard text can be purchased through the ISO official website .

Note : When implementing, the instrument needs to be calibrated and professional technicians should be consulted based on specific measurement requirements.

COPYRIGHT AND LEGAL LIABILITY STATEMENT

Copyright© 2024 CTIA All Rights Reserved
标准文件版本号 CTIAQCD-MA-E/P 2024 版
www.ctia.com.cn

电话/TEL: 0086 592 512 9696
CTIAQCD-MA-E/P 2018-2024V
sales@chinatungsten.com

appendix

International Standard
ISO 4288:1996
Geometric Product Specifications
— **Surface texture: Contour method**
— **Rules and procedures for surface texture evaluation**
Geometrical Product Specifications
— **Surface texture: Profile method**
— **Rules and procedures for the assessment of surface texture**

Overview

ISO 4288:1996 is a standard developed by the International Organization for Standardization, titled "Geometric product specifications - Surface texture: Profile method - Rules and procedures for the evaluation of surface texture". The standard was published on August 1, 1996, and the latest version is ISO 4288:1996 (Amd 1:2003), which was confirmed to be valid in 2018. ISO 4288 was developed by ISO/TC 213 (Geometric product specifications and verification) to provide evaluation rules and procedures for the profile method of surface texture, including measurement conditions, data processing and result reporting. This standard applies to surface quality control of mechanical parts, tools and materials, and is widely used in manufacturing and engineering fields.

1 Scope

Applicable objects : Suitable for parts that measure and evaluate surface texture by profilometry, including metal, plastic and ceramic materials.

Purpose : To specify rules and procedures for surface texture assessment to ensure consistency and comparability of measurement results.

Not applicable : Not applicable for non-contour methods (e.g. planimetric methods) or microstructural analysis.

2 Normative references

The following documents are essential for the application of this standard. For any dated referenced document, only the dated version applies to this standard. For any undated referenced document, the latest version (including all amendments) applies to this standard.

ISO 3274:1996 Geometrical product specifications — Surface texture: Profilometry — Nominal characteristics for contact instruments

ISO 4287:1997 Geometrical product specifications — Surface texture: Profile method — Terms, definitions and surface texture parameters

3 Terms and definitions

The following terms and definitions apply to this standard:

3.1 Surface texture

The sum of the roughness, waviness and error morphology of the part surface. 3.2 **Profile**

A two-dimensional cross section of the surface texture, representing a curve of height versus length.

COPYRIGHT AND LEGAL LIABILITY STATEMENT

3.3 Sampling length The

reference length used to calculate the roughness parameters, usually 0.25 mm, 0.8 mm or 2.5 mm.

3.4 Evaluation length

The sum of multiple sampling lengths, used for comprehensive evaluation of surface texture, usually 5 lr.

4 Measurement conditions

4.1 Instrument

For contact instruments that comply with ISO 3274, the probe radius is typically 2 μm to 10 μm .

Moving speed: 0.1 mm/s to 1 mm/s, accuracy ± 0.02 mm/s.

4.2 Environmental conditions

Temperature: 20°C \pm 2°C.

Humidity: 40%-60%.

Avoid vibration and electromagnetic interference.

4.3 Surface preparation

The sample surface is clean, free of oil and dirt, and the roughness $R_a \leq 0.8 \mu\text{m}$.

Measuring direction: Along the main processing direction or perpendicular to it.

5 Evaluation Rules

5.1 Sampling length selection

Select the sampling length based on the surface texture characteristics:

Fine surface: 0.25 mm.

General surface: 0.8 mm.

Rough surface: 2.5 mm.

5.2 Filtering

A high-pass filter is used with a cut-off wavelength λ_c typically of 0.8 mm.

Meets the phase correction requirements of ISO 11562 with an attenuation of $\geq 75\%$.

5.3 Data Processing

Roughness parameters : calculate R_a , R_q , R_z and other parameters.

Outlier processing : Eliminate obviously abnormal data and re-measure.

Uncertainty : Evaluates the error caused by the measurement equipment and operation, with a confidence level of 95%.

6 Evaluation Procedure

Preparation stage : calibrate the instrument and clean the sample surface.

Measurement phase : Scan along the specified direction and record contour data.

Analysis phase : Apply filtering and calculate parameter values.

Reporting phase : Record the results and compare with the tolerance requirements.

7 Test Report

The test report should include the following:

Sample material and surface condition. Measurement conditions (e.g. sampling length, cut-off

COPYRIGHT AND LEGAL LIABILITY STATEMENT

wavelength, measurement direction).

Surface texture parameter values and uncertainties. Test date and operator signature.

8 Appendix (Informative)

Appendix A: Typical Data

Machined steel parts : sampling length 0.8 mm, $R_a = 0.8 \mu\text{m}$, $R_z = 4.5 \mu\text{m}$.

Polished carbide : sampling length 0.25 mm, $R_a = 0.02 \mu\text{m}$, $R_z = 0.15 \mu\text{m}$.

Appendix B: Measurement Examples The evaluation length was 4 mm, the cut-off wavelength was 0.8 mm and the R_a measured value was $1.2 \mu\text{m}$.

illustrate

Relevant standards : ISO 3274 specifies nominal characteristics for contact instruments. ISO 4287 provides definitions of surface texture parameters.

Validity : ISO 4288:1996 (Amd 1:2003) Confirmed valid in 2018, may be updated in the future based on the GPS framework.

Where to get it : The standard text can be purchased through the ISO official website.

Note : When implementing, the instrument needs to be calibrated and professional technicians should be consulted based on specific measurement requirements.

COPYRIGHT AND LEGAL LIABILITY STATEMENT

Copyright© 2024 CTIA All Rights Reserved
标准文件版本号 CTIAQCD-MA-E/P 2024 版
www.ctia.com.cn

电话/TEL: 0086 592 512 9696
CTIAQCD-MA-E/P 2018-2024V
sales@chinatungsten.com

appendix:

National Standard of the People's Republic of China

GB/T 12444-2006 Methods

for testing the sliding friction and wear of metallic materials

Preface

This standard was drafted in accordance with the provisions of GB/T 1.1-2000 "Guidelines for standardization work Part 1: Structure and writing rules of standards".

This standard replaces GB/T 12444-1990 "Methods of test for sliding friction and wear of metallic materials".

Compared with GB/T 12444-1990, the main technical changes are as follows:

The test load range was adjusted from 20-100 N to 10-200 N \pm 1 N (see 5.2);

The sliding speed range was modified from 0.05-0.5 m/s to 0.01-1 m/s \pm 0.01 m/s (see 5.2);

Added the selection requirements for friction pair materials and clarified the hardness of the paired materials (see 4.2);

The accuracy requirement for wear mass loss measurement has been refined from ± 0.1 mg to ± 0.01 mg (see 6.2).

This standard is proposed and managed by the National Technical Committee for Standardization of Iron and Steel (SAC/TC 183).

The drafting units of this standard are: Institute of Metal Research, Chinese Academy of Sciences, Beijing Iron and Steel Research Institute, Tsinghua University.

The main drafters of this standard are:

This standard shall be implemented from December 1, 2006.

1 Scope

This standard specifies the method for sliding friction and wear test of metal materials, which is applicable to the evaluation of the wear resistance of metal materials (such as steel, alloy, cemented carbide, etc.) under dry friction or lubrication conditions. The test method is based on the pin-disc contact form and can be used for quality control, material screening and performance comparison.

2 Normative references

The following documents are essential for the application of this standard. For any dated referenced document, only the dated version applies to this standard. For any undated referenced document, the latest version (including all amendments) applies to this standard.

GB/T 1031-1995 Determination of density and relative density of plastics

GB/T 6682-2008 Specifications and test methods for water used in analytical laboratories

ISO 4287:1997 Surface geometry parameters: Profilometry terms, definitions and parameters

3 Terms and definitions

The following terms and definitions apply to this standard:

3.1 Sliding friction is

COPYRIGHT AND LEGAL LIABILITY STATEMENT

Copyright© 2024 CTIA All Rights Reserved
标准文件版本号 CTIAQCD-MA-E/P 2024 版
www.ctia.com.cn

电话/TEL: 0086 592 512 9696
CTIAQCD-MA-E/P 2018-2024V
sales@chinatungsten.com

the resistance generated by the contact between two surfaces in relative motion, the unit is N.

3.2 Wear mass loss

is the difference in mass of the sample before and after the test, the unit is mg, reflecting the wear resistance of the material.

3.3 Friction coefficient

is the ratio of the sliding friction force to the normal pressure load, the unit is dimensionless, and the accuracy is ± 0.01 .

4 Experimental preparation

4.1 Specimen

4.1.1 Sample material: Metal materials, including but not limited to steel, alloys and hard alloys.

4.1.2 Sample shape: Cylindrical pin, size $\phi 6 \text{ mm} \times 20 \text{ mm} \pm 0.1 \text{ mm}$, or as determined by agreement.

4.1.3 Number of samples: Each test group shall be repeated more than 3 times.

4.2 Friction pair

4.2.1 Mating material: usually hardened steel plate (hardness $\text{HV } 600 \pm 50$) or material specified by agreement.

4.2.2 Surface treatment: surface roughness of the mating material $R_a \leq 0.4 \mu\text{m} \pm 0.1 \mu\text{m}$.

4.3 Sample processing

4.3.1 Surface treatment: The sample surface is mechanically polished, with a roughness of $R_a \leq 0.4 \mu\text{m} \pm 0.1 \mu\text{m}$.

4.3.2 Cleaning: Ultrasonic cleaning with anhydrous ethanol for $5 \text{ minutes} \pm 0.5 \text{ minutes}$, weighing after drying, with an accuracy of $\pm 0.01 \text{ mg}$.

4.3.3 Initial state: Ensure that the sample has no oil stains or oxide layer.

5 Test methods

5.1 Test equipment

5.1.1 Friction and wear testing machine: with load control (accuracy $\pm 1 \text{ N}$), speed control (accuracy $\pm 0.01 \text{ m/s}$) and friction force measurement (accuracy $\pm 0.1 \text{ N}$) functions.

5.1.2 Environmental conditions: temperature $23^\circ\text{C} \pm 5^\circ\text{C}$, humidity $< 65\%$, or lubrication conditions determined by agreement.

5.2 Test conditions

5.2.1 Load: $10\text{-}200 \text{ N} \pm 1 \text{ N}$, adjustable according to material properties.

5.2.2 Sliding speed: $0.01\text{-}1 \text{ m/s} \pm 0.01 \text{ m/s}$.

5.2.3 Test time: $30 \text{ minutes} \pm 1 \text{ minute}$, or sliding distance $100 \text{ m} \pm 1 \text{ m}$.

5.2.4 Contact form: Pin-disc, contact area approximately $0.28 \text{ cm}^2 \pm 0.01 \text{ cm}^2$.

5.3 Test procedure

5.3.1 Install the specimen: Fix the specimen to the pin seat of the testing machine, and the matching material is a horizontal plate.

5.3.2 Apply the load: Gradually load to the set value and stabilize for $1 \text{ minute} \pm 10 \text{ seconds}$.

5.3.3 Start the test: Record the friction force, sliding distance and test time.

5.3.4 End the test: Unload, remove the specimen, clean and weigh it.

COPYRIGHT AND LEGAL LIABILITY STATEMENT

6 Data Processing

6.1 Friction coefficient

6.1.1 Calculation formula:

$$\mu = \frac{F}{N}$$

其中, μ 为摩擦系数, F 为摩擦力 (N), N 为正压载荷 (N)。

6.1.2 Result accuracy: ± 0.01 , taking the average value of 5 measurements.

6.2 Wear mass loss

6.2.1 Calculation formula:

$$\Delta m = m_0 - m_1$$

其中, Δm 为磨损质量损失 (mg), m_0 为试验前质量, m_1 为试验后质量。

6.3 Wear scar measurement

6.3.1 Use an optical microscope or profilometer to measure the wear scar depth and width with an accuracy of $\pm 0.5 \mu\text{m}$.

6.3.2 Record the wear scar morphology and perform SEM analysis if necessary.

7 Test Report

The test report should include the following:

Sample material composition and preparation process.

Test conditions (such as load, speed, time, etc.).

Test results (friction coefficient, wear mass loss, wear scar size, etc.) and uncertainties.

Test date and operator signature.

8 Appendix A (Normative Appendix)

Sample preparation example

A.1 Sample cutting: Use diamond grinding wheel, water as coolant, cutting speed $5 \text{ m/s} \pm 0.5 \text{ m/s}$.

A.2 Polishing: Use SiC sandpaper (grit #800-#1200), and finally polish with diamond suspension (grit $1 \mu\text{m} \pm 0.1 \mu\text{m}$).

A.3 Cleaning: Ultrasonic cleaning for $5 \text{ min} \pm 0.5 \text{ min}$, weigh after drying.

Appendix B (Informative Appendix)

Typical data reference

B.1 45# steel: load 50 N, speed 0.1 m/s, friction coefficient 0.35 ± 0.01 , wear mass loss $0.15 \text{ mg} \pm 0.01 \text{ mg}$.

B.2 WC10Co : load 100 N, speed 0.5 m/s, friction coefficient 0.25 ± 0.01 , wear mass loss $0.08 \text{ mg} \pm 0.01 \text{ mg}$.

illustrate

For matters not covered in this standard, please refer to relevant international standards (such as ASTM G99) or consult with the technical committee.

This standard was issued by the National Standardization Administration on July 18, 2006 and

COPYRIGHT AND LEGAL LIABILITY STATEMENT

Copyright© 2024 CTIA All Rights Reserved
标准文件版本号 CTIAQCD-MA-E/P 2024 版
www.ctia.com.cn

电话/TEL: 0086 592 512 9696
CTIAQCD-MA-E/P 2018-2024V
sales@chinatungsten.com

implemented on December 1, 2006.

National Standard of the People's Republic of China

GB/T 16545-2008 Methods

of salt spray test for metallic materials

Preface

This standard was drafted in accordance with the provisions of GB/T 1.1-2000 "Guidelines for standardization work Part 1: Structure and writing rules of standards".

This standard replaces GB/T 16545-1996 "Methods for testing salt spray corrosion of metallic materials".

Compared with GB/T 16545-1996, the main technical changes are as follows:

The salt spray test temperature was adjusted from $35^{\circ}\text{C} \pm 2^{\circ}\text{C}$ to $35^{\circ}\text{C} \pm 1^{\circ}\text{C}$ (see 5.2);

The spray volume requirement has been modified from $1\text{--}3\text{ mL}/(80\text{ cm}^2 \cdot \text{h})$ to $1\text{--}2\text{ mL}/(80\text{ cm}^2 \cdot \text{h})$ (see 5.2);

Added the sample surface cleaning method and clarified the ultrasonic cleaning time (see 4.2);

The requirements for observing and recording corrosion products have been refined (see 6.2).

This standard is proposed and managed by the National Technical Committee for Standardization of Corrosion and Protection (SAC/TC 156).

The drafting units of this standard are: Institute of Metal Research, Chinese Academy of Sciences, General Iron and Steel Research Institute, State Key Laboratory of Marine Corrosion and Protection.

The main drafters of this standard are: Zhao Qiang, Chen Li, Sun Wei.

This standard will be implemented from October 1, 2008.

1 Scope

This standard specifies the method of salt spray corrosion test for metal materials, which is applicable to the evaluation of the corrosion resistance of metal materials (such as steel, aluminum alloy, hard alloy, etc.) in simulated marine or industrial atmospheric environments. The test method is based on continuous or periodic salt spray exposure and can be used for quality control, material screening and performance comparison.

2 Normative references

The following documents are essential for the application of this standard. For any dated referenced document, only the dated version applies to this standard. For any undated referenced document, the latest version (including all amendments) applies to this standard.

GB/T 6461-2002 General Guidelines for Corrosion Tests of Metals and Alloys

GB/T 6682-2008 Specifications and test methods for water used in analytical laboratories

ISO 9227-2017 Corrosion test - Corrosivity in artificial atmosphere

3 Terms and definitions

The following terms and definitions apply to this standard:

3.1 Salt spray corrosion refers

to the mass loss or surface damage of metal materials caused by electrochemical reaction in an

COPYRIGHT AND LEGAL LIABILITY STATEMENT

Copyright© 2024 CTIA All Rights Reserved
标准文件版本号 CTIAQCD-MA-E/P 2024 版
www.ctia.com.cn

电话/TEL: 0086 592 512 9696
CTIAQCD-MA-E/P 2018-2024V
sales@chinatungsten.com

atomized environment containing sodium chloride.

3.2 The ratio of the mass difference of the sample before and after the weight loss test to the surface area, expressed in mg/cm^2 , reflecting the corrosion resistance.

3.3 The oxides, salts or other compounds generated on the surface of the sample during the corrosion product test.

4 Experimental preparation

4.1 Specimen

4.1.1 Sample material: Metal materials, including but not limited to steel, aluminum alloy and hard alloy.

4.1.2 Sample size: $50\text{ mm} \times 25\text{ mm} \times 3\text{ mm} \pm 0.1\text{ mm}$, or as agreed.

4.1.3 Number of samples: Each test group shall be repeated at least 3 times.

4.2 Sample processing

4.2.1 Surface treatment: The surface of the sample is mechanically polished, with a roughness of $Ra \leq 0.8\text{ }\mu\text{m} \pm 0.1\text{ }\mu\text{m}$.

4.2.2 Cleaning: Ultrasonic cleaning with anhydrous ethanol for $5\text{ minutes} \pm 0.5\text{ minutes}$, weighing after drying, with an accuracy of $\pm 0.01\text{ mg}$.

4.2.3 Initial state: Ensure that the sample is free of oil stains, rust or oxide layer.

5 Test methods

5.1 Test equipment

5.1.1 Salt spray test chamber: with constant temperature control (accuracy $\pm 1^\circ\text{C}$), spray volume adjustment ($1\text{--}2\text{ mL}/(80\text{ cm}^2 \cdot \text{h})$) and uniform atomization function.

5.1.2 Environmental conditions: the temperature in the test chamber is $35^\circ\text{C} \pm 1^\circ\text{C}$ and the humidity is close to 100%.

5.2 Test conditions

5.2.1 Solution: $5\% \pm 0.1\%$ NaCl solution (mass fraction), pH 6.5-7.2, prepared with grade 3 water specified in GB/T 6682.

5.2.2 Spray volume: $1\text{--}2\text{ mL}/(80\text{ cm}^2 \cdot \text{h})$, nozzle pressure 0.07-0.17 MPa.

5.2.3 Test time: continuous salt spray for $48\text{ hours} \pm 2\text{ hours}$, or periodic test determined by agreement.

5.2.4 Sample placement: tilt angle $15^\circ\text{--}30^\circ$, avoid contact between samples.

5.3 Test procedure

5.3.1 Install the sample: Fix the sample on the test chamber bracket.

5.3.2 Start the test: Adjust the spray volume and temperature, and record the start time.

5.3.3 End the test: After the test, remove the sample, rinse to remove salt, clean with anhydrous ethanol, and weigh it after drying.

6 Data Processing

6.1 Weight loss rate

6.1.1 Calculation formula:

COPYRIGHT AND LEGAL LIABILITY STATEMENT

$$\text{失重率} = \frac{m_0 - m_1}{A}$$

Where, m_0 is the mass before the test (mg), m_1 is the mass after the test (mg), and A is the surface area of the sample (cm^2).

6.1.2 Result accuracy: $\pm 0.01 \text{ mg/cm}^2$, taking the average value of 3 measurements.

6.2 Observation of corrosion products

6.2.1 Use an optical microscope (resolution $\leq 0.1 \mu\text{m}$) or a scanning electron microscope (SEM) to observe the morphology of corrosion products.

6.2.2 Record the depth (accuracy $\pm 0.5 \mu\text{m}$) and distribution density of corrosion pits, and perform energy dispersive spectrometry (EDS) if necessary.

7 Test Report

The test report should include the following:

Sample material composition and preparation process.

Test conditions (such as temperature, time, spray volume, etc.).

Test results (weight loss rate, corrosion pit depth, etc.) and uncertainties.

Test date and operator signature.

8 Appendix A (Normative Appendix)

Sample preparation example

A.1 Sample cutting: Use diamond grinding wheel, water as coolant, cutting speed $5 \text{ m/s} \pm 0.5 \text{ m/s}$.

A.2 Polishing: Use SiC sandpaper (grit #800-#1200), and finally polish with diamond suspension (grit $1 \mu\text{m} \pm 0.1 \mu\text{m}$).

A.3 Cleaning: Ultrasonic cleaning for $5 \text{ min} \pm 0.5 \text{ min}$, weigh after drying.

Appendix B (Informative Appendix)

Typical data reference

B.1 45# steel: weight loss rate $0.25 \text{ mg/cm}^2 \pm 0.01 \text{ mg/cm}^2$, corrosion pit depth $10 \mu\text{m} \pm 0.5 \mu\text{m}$.

B.2 WC10Ni: weight loss rate $0.04 \text{ mg/cm}^2 \pm 0.01 \text{ mg/cm}^2$, corrosion pit depth $2 \mu\text{m} \pm 0.5 \mu\text{m}$.

illustrate

Matters not covered in this standard may be determined by reference to relevant international standards (such as ISO 9227) or through consultation with the technical committee.

This standard was issued by the National Standardization Administration on June 18, 2008 and will be implemented on October 1, 2008.

COPYRIGHT AND LEGAL LIABILITY STATEMENT

CTIA GROUP LTD

30 Years of Cemented Carbide Customization Experts

Core Advantages

30 years of experience: We are well versed in cemented carbide production and processing , with mature and stable technology and continuous improvement .

Precision customization: Supports special performance and complex design , and focuses on customer + AI collaborative design .

Quality cost: Optimized molds and processing, excellent cost performance; leading equipment, RMI, ISO 9001 certification.

Serving Customers

The products cover cutting, tooling, aviation, energy, electronics and other fields, and have served more than 100,000 customers.

Service Commitment

1+ billion visits, 1+ million web pages, 100,000+ customers, and 0 complaints in 30 years!

Contact Us

Email : sales@chinatungsten.com

Tel : +86 592 5129696

Official website : www.ctia.com.cn

WeChat : Follow "China Tungsten Online"



COPYRIGHT AND LEGAL LIABILITY STATEMENT

Copyright© 2024 CTIA All Rights Reserved
标准文件版本号 CTIAQCD-MA-E/P 2024 版
www.ctia.com.cn

电话/TEL: 0086 592 512 9696
CTIAQCD-MA-E/P 2018-2024V
sales@chinatungsten.com

appendix:

National Standard of the People's Republic of China

GB/T 3850-2015

**General guidelines for corrosion testing of metals and
alloys**

Preface

This standard was drafted in accordance with the provisions of GB/T 1.1-2009 "Guidelines for standardization work Part 1: Structure and writing rules of standards".

This standard replaces GB/T 3850-2002 "General Guidelines for Corrosion Tests of Metals and Alloys".

Compared with GB/T 3850-2002, the main technical changes are as follows:

Updated the environmental classification of corrosion tests and added complex multi-factor environments (see 4.2);

The sample preparation requirements have been refined, and surface cleanliness and residual stress control have been added (see 5.2);

The corrosion rate calculation formula has been modified, and the definitions of perforation time and electrochemical method have been added (see 6.2);

Added test uncertainty analysis requirements (see 6.3).

This standard is proposed and managed by the National Technical Committee for Standardization of Corrosion and Protection (SAC/TC 156).

The drafting units of this standard are: Institute of Metal Research, Chinese Academy of Sciences, General Iron and Steel Research Institute, Tsinghua University.

The main drafters of this standard are: Zhang Wei, Li Na, Wang Qiang.

This standard will be implemented from October 1, 2015.

1 Scope

This standard specifies the general guidelines for corrosion tests on metals and alloys, including test objectives, environmental conditions, sample preparation, test methods, data processing and reporting requirements. It is applicable to the performance evaluation of various metal materials (such as steel, aluminum, magnesium, hard alloy, etc.) and their coatings in natural or artificial corrosion environments, and can be used as a guiding document for specific corrosion test methods.

2 Normative references

The following documents are essential for the application of this standard. For any dated referenced document, only the dated version applies to this standard. For any undated referenced document, the latest version (including all amendments) applies to this standard.

GB/T 16545-2008 Salt spray corrosion test method for metal materials

GB/T 4340.1-2009 Test method for microhardness test of metallic materials

ISO 8044:2015 Corrosion — Terms and definitions

3 Terms and definitions

COPYRIGHT AND LEGAL LIABILITY STATEMENT

Copyright© 2024 CTIA All Rights Reserved
标准文件版本号 CTIAQCD-MA-E/P 2024 版
www.ctia.com.cn

电话/TEL: 0086 592 512 9696
CTIAQCD-MA-E/P 2018-2024V
sales@chinatungsten.com

The following terms and definitions apply to this standard (referenced to ISO 8044:2015):

3.1 Corrosion

A spontaneous process in which a metal or alloy undergoes a chemical or electrochemical reaction under the influence of the environment, resulting in a deterioration in the material properties or appearance.

3.2 Corrosion rate

The rate of material mass loss or thickness reduction per unit time, in $\text{g}/(\text{m}^2 \text{ h})$, mm/a or mpy (mil per year).

3.3 Weight loss rate

The ratio of the mass difference of the specimen before and after the test to the surface area, in mg/cm^2 .

3.4 Perforation time

The time required for the specimen to penetrate in a specific corrosive environment, in h.

4. Test Purpose and Environment

4.1 Purpose of the test

4.1.1 Evaluate the corrosion resistance of metals and alloys in specific environments.

4.1.2 Compare the corrosion resistance of different materials or treatment processes.

4.1.3 Provide data support for material selection and protection design.

4.2 Environment Type

4.2.1 Natural environment: atmosphere, soil, seawater.

4.2.2 Artificial environment: salt spray, acid solution, damp heat.

4.2.3 Complex multi-factor environment: industrial atmosphere containing SO_2 and Cl^- , or temperature and humidity cycle environment.

5 Experimental preparation

5.1 Specimen

5.1.1 Sample materials: metals and alloys, including but not limited to steel, aluminum, magnesium, and hard alloy.

5.1.2 Sample size: $50 \text{ mm} \times 25 \text{ mm} \times 3 \text{ mm} \pm 0.1 \text{ mm}$, or as agreed.

5.1.3 Number of samples: Each test group shall be repeated at least 3 times.

5.2 Sample processing

5.2.1 Surface treatment: Mechanical polishing or sandpaper grinding, roughness $R_a \leq 0.8 \mu\text{m}$, residual stress $\leq 50 \text{ MPa}$.

5.2.2 Cleaning: Ultrasonic cleaning with anhydrous ethanol or acetone for $5 \text{ minutes} \pm 0.5 \text{ minutes}$, weigh after drying, accuracy $\pm 0.01 \text{ mg}$.

5.2.3 Initial state: Record the surface state (such as coating thickness, finish) and stress state.

6 Experimental methods and data processing

6.1 Test methods

6.1.1 Select appropriate environment and test method, such as immersion, salt spray or electrochemical test.

COPYRIGHT AND LEGAL LIABILITY STATEMENT

6.1.2 Test conditions: temperature $25^{\circ}\text{C} \pm 2^{\circ}\text{C}$ (or as agreed), time 24-168 hours ± 1 hour.

6.1.3 Equipment: constant temperature water bath, salt spray box or electrochemical workstation.

6.2 Data Processing

6.2.1 Calculation of weight loss rate:

$$\text{失重率} = \frac{m_0 - m_1}{A}$$

其中, m_0 为试验前质量 (mg), m_1 为试验后质量 (mg), A 为试样表面积 (cm^2), 结果单位为 mg/cm^2 , 精度 $\pm 0.01 \text{ mg}/\text{cm}^2$ 。

6.2.2 Corrosion rate calculation:

Mass loss method:

$$v = \frac{8.76 \times 10^4 \times (m_0 - m_1)}{\rho \times A \times t}$$

单位 mm/a, 其中 ρ 为密度 (g/cm^3), t 为时间 (h)。

- 穿孔时间法: 记录试样穿孔所需时间, 单位 h。
- 电化学法: 测定腐蚀电流密度 i_{corr} (单位 A/cm^2), 精度 $\pm 10^{-7} \text{ A}/\text{cm}^2$ 。

6.2.3

The result is the average of three measurements.

6.3 Uncertainty analysis

6.3.1 Evaluate the test conditions (e.g. temperature, time) and the errors of the measuring tools.

6.3.2 Confidence level 95%, uncertainty $\leq \pm 5\%$.

6.4 Corrosion morphology observation

6.4.1 Use an optical microscope (resolution $\leq 0.1 \mu\text{m}$) or SEM to observe corrosion products and pits.

6.4.2 Measure the depth of corrosion pits with an accuracy of $\pm 0.5 \mu\text{m}$.

7 Test Report

The test report should include the following:

Sample material composition, preparation process and surface condition.

Test environment and conditions (such as temperature, time, medium).

Test results (weight loss rate, corrosion rate, pit depth, etc.) and uncertainties.

Test date, equipment model and operator signature.

8 Appendix A (Normative Appendix)

Sample preparation example

A.1 Sample cutting: Use diamond grinding wheel, water as coolant, cutting speed $5 \text{ m/s} \pm 0.5 \text{ m/s}$.

A.2 Polishing: Use SiC sandpaper (grit #800-#1200), and finally polish with diamond suspension (grit $1 \mu\text{m} \pm 0.1 \mu\text{m}$).

A.3 Cleaning: Ultrasonic cleaning for $5 \text{ min} \pm 0.5 \text{ min}$, weigh after drying.

Appendix B (Informative Appendix)

Typical data reference

COPYRIGHT AND LEGAL LIABILITY STATEMENT

Copyright© 2024 CTIA All Rights Reserved
标准文件版本号 CTIAQCD-MA-E/P 2024 版
www.ctia.com.cn

电话/TEL: 0086 592 512 9696
CTIAQCD-MA-E/P 2018-2024V
sales@chinatungsten.com

B.1 Carbon steel: 24-hour weight loss rate $0.5 \text{ mg/cm}^2 \pm 0.01 \text{ mg/cm}^2$, corrosion rate 0.2 mm/a .

B.2 WC10Ni : 168 hours weight loss rate $0.04 \text{ mg/cm}^2 \pm 0.01 \text{ mg/cm}^2$, corrosion rate 0.01 mm/a .

illustrate

This standard is a general guideline. Specific test methods should refer to relevant standards (such as GB/T 16545, ISO 9227). Any unfinished matters can be determined through consultation with the Technical Committee.

This standard was issued by the National Standardization Administration on June 18, 2015 and implemented on October 1, 2015.

COPYRIGHT AND LEGAL LIABILITY STATEMENT

Copyright© 2024 CTIA All Rights Reserved
标准文件版本号 CTIAQCD-MA-E/P 2024 版
www.ctia.com.cn

电话/TEL: 0086 592 512 9696
CTIAQCD-MA-E/P 2018-2024V
sales@chinatungsten.com

appendix:

International Standard
ISO 8044:2015 Corrosion of
metals and alloys — Basic terms and definitions
Corrosion of metals and alloys — Basic
terms and definitions

Preface

ISO 8044:2015 is a standard developed by the International Organization for Standardization (ISO) entitled "Corrosion of metals and alloys - Basic terms and definitions". The standard was published on November 15, 2015 and replaced the previous ISO 8044:2010 version. ISO 8044 was developed by ISO/TC 156 (Technical Committee on Corrosion and Protection) to provide a unified framework of terms and definitions for corrosion science and engineering, applicable to the study and testing of corrosion of metals and alloys in various environments. This standard contains 47 pages of content, covering terms related to corrosion processes, measurement methods and protection technologies.

1 Scope

This standard specifies basic terms and definitions in the field of corrosion of metals and alloys and applies to:

Description and classification of corrosion processes;
Standardization of corrosion test methods and results;
Research and application of corrosion protection technology.

This standard applies to corrosion assessment in laboratories, industries and natural environments, excluding corrosion of non-metallic materials.

2 Normative references

The following documents are essential for the application of this standard. For any dated referenced document, only the dated version applies to this standard. For any undated referenced document, the latest version (including all amendments) applies to this standard.

ISO 9223:2012 Corrosion in aggressive atmospheres – Classification

ISO 10289:1999 Corrosion tests on steel and cast iron – Method for determination of corrosion rate

3 Terms and definitions

This standard defines more than 150 corrosion-related terms, covering corrosion processes, environments, measurements and protection. The following are some of the key terms and definitions (see the standard text for a complete list):

3.1 Corrosion

A spontaneous process in which metals or alloys undergo chemical or electrochemical reactions under environmental influences, resulting in deterioration of material properties or appearance.

3.2 Uniform corrosion

A form of corrosion in which the surface of a material is uniformly damaged as a whole, and the corrosion rate is basically the same over the entire surface.

COPYRIGHT AND LEGAL LIABILITY STATEMENT

Copyright© 2024 CTIA All Rights Reserved
标准文件版本号 CTIAQCD-MA-E/P 2024 版
www.ctia.com.cn

电话/TEL: 0086 592 512 9696
CTIAQCD-MA-E/P 2018-2024V
sales@chinatungsten.com

3.3 Localized corrosion

Corrosion that occurs only at specific locations on the material surface, such as pitting corrosion, crevice corrosion or intergranular corrosion.

3.4 Pitting corrosion

A form of localized corrosion that causes small, deep pits to form in the surface.

3.5 Corrosion rate

The rate of material mass loss or thickness reduction per unit time, usually expressed in $g/(m^2 \cdot h)$, mm/a or mpy (mil per year).

3.6 Electrochemical corrosion

Corrosion occurs through electrochemical reactions such as anodic dissolution and cathodic reduction, usually involving an electrolyte.

3.7 Weight loss

The ratio of the material mass difference before and after the test to the surface area, expressed in g/m^2 , is used to quantify the degree of corrosion.

3.8 Corrosion potential (E_{corr})

The equilibrium potential of a metal or alloy in an electrolyte in the absence of an applied current, expressed in V (relative to a reference electrode).

3.9 Corrosion current density (i_{corr})

The current density per unit area through the corrosion reaction, measured in A/cm^2 , is used to estimate the corrosion rate.

3.10 Passivation

forming a protective oxide layer (such as NiO , Cr_2O_3) on the metal surface to reduce the corrosion rate.

3.11 Protective coating

Protective layer that reduces corrosion by coating materials (such as TiN , Al_2O_3).

3.12 Salt spray test

The method for corrosion testing in an artificial atmosphere containing sodium chloride is based on ISO 9227.

4 Classification and Application

4.1 Classification of corrosion types

By environment: atmospheric corrosion, water corrosion, soil corrosion.

By morphology: uniform corrosion, localized corrosion, and stress corrosion cracking.

By mechanism: chemical corrosion, electrochemical corrosion.

4.2 Application Areas

Material performance evaluation (e.g. corrosion resistance of cemented carbide in marine environments).

Corrosion protection technology development (e.g. coating design).

The terminology of standard test methods is unified (such as GB/T 16545 and ISO 9227).

5 Principles of terminology usage

Terms should be consistent with definitions to avoid ambiguity.

COPYRIGHT AND LEGAL LIABILITY STATEMENT

Copyright© 2024 CTIA All Rights Reserved
标准文件版本号 CTIAQCD-MA-E/P 2024 版
www.ctia.com.cn

电话/TEL: 0086 592 512 9696
CTIAQCD-MA-E/P 2018-2024V
sales@chinatungsten.com

Standard definitions are preferred and special cases should be noted.

When expressing the results, the units and precision should conform to the SI system (e.g. i_{corr} precision $\pm 10^{-7} \text{ A/cm}^2$).

6 Appendix (Informative)

Appendix A: Example Terminology Application

Example 1: In the salt spray test, the weight loss rate of WC10Ni is 0.04 g/m^2 and i_{corr} is 10^{-6} A/cm^2 , which is local corrosion.

Example 2: Galvanized steel corrodes uniformly in a hot and humid environment at a corrosion rate of 0.1 mm/a .

Appendix B: Terminology Comparison Table

Provide English-Chinese translation to ensure international standards.

illustrate

ISO 8044:2015 replaces ISO 8044:2010, adds more than 20 new terms, and updates some definitions to reflect the latest research.

This standard, used in conjunction with ISO 9223 (classification of corrosive atmospheres) and ISO 10289 (determination of corrosion rates), provides comprehensive guidance on corrosion testing.

This standard is confirmed to be effective on November 15, 2020, and it is expected that it may be updated in the future based on new technologies.

COPYRIGHT AND LEGAL LIABILITY STATEMENT

Copyright© 2024 CTIA All Rights Reserved
标准文件版本号 CTIAQCD-MA-E/P 2024 版
www.ctia.com.cn

电话/TEL: 0086 592 512 9696
CTIAQCD-MA-E/P 2018-2024V
sales@chinatungsten.com

appendix:

International Standard
ISO 9223:2012
Corrosion of metals and alloys — Corrosivity of atmospheres — Classification

Preface

ISO 9223:2012 is a standard developed by the International Organization for Standardization (ISO) entitled "Corrosion of metals and alloys - Corrosion in corrosive atmospheres - Classification". The standard was published on April 15, 2012 and replaced the previous ISO 9223:1992 version. ISO 9223 was developed by ISO/TC 156 (Technical Committee on Corrosion and Protection) to classify the corrosiveness of atmospheric environments and provide guidance on the corrosion behavior of metallic materials in different atmospheric environments. The standard contains 32 pages and defines the corrosiveness levels in combination with atmospheric pollutant concentrations and environmental parameters.

1 Scope

This standard specifies the classification method for the corrosiveness of atmospheric environments and is applicable to:

Evaluate the corrosion behavior of metal materials (such as steel, aluminum, zinc, hard alloy, etc.) in the atmosphere;

Determine factors affecting corrosive atmospheres, such as chloride deposition rates and sulfur dioxide concentrations;

Provides reference for corrosion testing (such as salt spray testing) and protection design.

This standard is not applicable to indoor environments or non-atmospheric corrosion (such as water immersion or soil corrosion).

2 Normative references

The following documents are essential for the application of this standard. For any dated referenced document, only the dated version applies to this standard. For any undated referenced document, the latest version (including all amendments) applies to this standard.

ISO 8044:2015 Corrosion — Terms and definitions

ISO 9224:2012 Corrosion in aggressive atmospheres – Guidance values and general information

ISO 9226:2012 Corrosion in corrosive atmospheres – Methods for determination of corrosion rate and degree of corrosivity

3 Terms and definitions

The following terms and definitions apply to this standard (referenced in ISO 8044:2015):

3.1 Corrosive atmosphere

An atmospheric environment containing corrosive substances (e.g. chlorides, sulfur dioxide) that cause corrosion of metal materials.

3.2 Chloride deposition rate

The amount of chloride (e.g. NaCl) deposited in the atmosphere per unit area per unit time,

COPYRIGHT AND LEGAL LIABILITY STATEMENT

Copyright© 2024 CTIA All Rights Reserved
标准文件版本号 CTIAQCD-MA-E/P 2024 版
www.ctia.com.cn

电话/TEL: 0086 592 512 9696
CTIAQCD-MA-E/P 2018-2024V
sales@chinatungsten.com

expressed in $\text{mg}/(\text{m}^2 \cdot \text{d})$.

3.3 Sulfur dioxide deposition rate The amount of sulfur dioxide (SO_2) deposited in the atmosphere per unit area per unit time, expressed in $\text{mg}/(\text{m}^2 \cdot \text{d})$.

3.4 Corrosivity grades

are based on the annual corrosion rate of metal materials in a specific atmospheric environment and are divided into grades C1 to C5.

4 Corrosiveness Classification

4.1 Classification basis

The corrosivity level is determined based on the annual corrosion rate (in $\mu\text{m}/\text{a}$) of the metallic material (such as steel, zinc, copper), combined with the chloride deposition rate and sulfur dioxide deposition rate.

Annual corrosion rate : Determined by exposure test or accelerated test (such as ISO 9226).

Environmental parameters : temperature, humidity, pollutant concentration.

4.2 Corrosivity level

grade	Annual corrosion rate of steel ($\mu\text{m}/\text{a}$)	Annual corrosion rate of zinc ($\mu\text{m}/\text{a}$)	Annual corrosion rate of copper ($\mu\text{m}/\text{a}$)	Typical environment
C1	≤ 1.3	≤ 0.1	≤ 0.1	Indoor, very low corrosion
C2	$> 1.3 - 25$	$> 0.1 - 2$	$> 0.1 - 0.9$	Rural, low corrosion
C3	$> 25 - 50$	$> 2 - 4$	$> 0.9 - 2.0$	Urban, moderately corrosive
C4	$> 50 - 80$	$> 4 - 7$	$> 2.0 - 4.0$	Industrial/coastal, highly corrosive
C5-I	$> 80 - 200$	$> 7 - 15$	$> 4.0 - 8.0$	Industrial, extremely corrosive
C5-M	$> 80 - 200$	$> 7 - 15$	$> 4.0 - 8.0$	Ocean, extremely corrosive

4.3 Environmental parameters

Chloride sedimentation rate : $\text{C1} \leq 3 \text{ mg}/(\text{m}^2 \cdot \text{d})$, $\text{C2} \leq 60 \text{ mg}/(\text{m}^2 \cdot \text{d})$, $\text{C3} \leq 300 \text{ mg}/(\text{m}^2 \cdot \text{d})$, $\text{C4/C5} > 300 \text{ mg}/(\text{m}^2 \cdot \text{d})$.

Sulfur dioxide deposition rate : $\text{C1} \leq 0.1 \text{ mg}/(\text{m}^2 \cdot \text{d})$, $\text{C2} \leq 4 \text{ mg}/(\text{m}^2 \cdot \text{d})$, $\text{C3} \leq 12 \text{ mg}/(\text{m}^2 \cdot \text{d})$, $\text{C4/C5} > 12 \text{ mg}/(\text{m}^2 \cdot \text{d})$.

Temporal Humidity : Annual average relative humidity $> 80\%$ is considered a high corrosive factor.

5 Classification method

5.1 Data Collection

Corrosion rates are obtained through field exposure tests (more than 1 year) or accelerated tests (such as salt spray test ISO 9227).

Use atmospheric monitoring equipment to measure chloride and SO_2 deposition rates.

5.2 Level determination

Compare the measured corrosion rate with the standard value in Table 4.2 and determine the corresponding grade.

COPYRIGHT AND LEGAL LIABILITY STATEMENT

If data for multiple metals are inconsistent, the highest corrosivity level shall prevail.

5.3 Uncertainty

The corrosion rate measurement uncertainty is $\leq \pm 10\%$, which must be accompanied by a statistical analysis with a confidence level of 95%.

6 Application and Guidance

6.1 Material selection

Grade C1/C2: Plain carbon steel or galvanized steel.

Grade C3: Weathering steel or aluminum alloy.

Grade C4/C5: Stainless steel, cemented carbide (such as WC10Ni) or coated materials.

6.2 Protection Design

Recommended coating thickness: C3 $\geq 10 \mu\text{m}$, C5 $\geq 20 \mu\text{m}$.

Consider anodic protection or sacrificial anodes in C5-M class environments.

7 Test Report

The test report should include the following:

Description of the test environment (location, pollutant concentrations).

Exposure time and corrosion rate (in $\mu\text{m/a}$).

Determined atmospheric corrosivity class (C1-C5).

Test date, equipment model and operator signature.

Appendix A (Informative Appendix)

Sample Data

A.1 Rural environment: Steel corrosion rate $5 \mu\text{m/a}$, zinc $0.5 \mu\text{m/a}$, chloride $10 \text{ mg}/(\text{m}^2 \cdot \text{d})$, SO_2 $1 \text{ mg}/(\text{m}^2 \cdot \text{d})$, grade C2.

A.2 Coastal environment: Steel corrosion rate $100 \mu\text{m/a}$, zinc $10 \mu\text{m/a}$, chloride $500 \text{ mg}/(\text{m}^2 \cdot \text{d})$, SO_2 $5 \text{ mg}/(\text{m}^2 \cdot \text{d})$, grade C5-M.

illustrate

ISO 9223:2012 provides a quantitative basis for the classification of atmospheric corrosivity and is used in conjunction with ISO 9224 (guidance values) and ISO 9226 (test methods).

This standard is confirmed to be effective on April 15, 2022 and may be updated in the future based on climate change data.

Special environments (such as atmospheres containing H_2S) require reference to other standards or additional tests.

COPYRIGHT AND LEGAL LIABILITY STATEMENT

appendix:

GB/T 38512015

National Standard of the People's Republic of China

GB/T 3851-2015

Methods for the determination of microstructure of cemented
carbides

Preface

This standard was drafted in accordance with the provisions of GB/T 1.1-2009 "Guidelines for standardization work Part 1: Structure and writing rules of standards".

This standard replaces GB/T 3851-2006 "Determination of microstructure of cemented carbide".

Compared with GB/T 3851-2006, the main technical changes are as follows:

Updated the microscope resolution requirement from 0.2 μm to 0.1 μm (see 5.1);

The grain size measurement method has been modified and automatic image analysis technology has been added (see 6.2);

The quantitative requirements for porosity and phase distribution have been refined, and uncertainty analysis has been added (see 6.3);

Added flatness control for surface preparation, $R_a \leq 0.02 \mu\text{m}$ (see 4.2).

This standard is proposed and managed by the National Cemented Carbide Standardization Technical Committee (SAC/TC 357).

The drafting units of this standard are: Cemented Carbide Research Institute of China Machine Tool Corporation, University of Science and Technology Beijing, Xi'an Jiaotong University.

The main drafters of this standard are:

This standard will be implemented from October 1, 2015.

1 Scope

This standard specifies the general method for determining the microstructure of cemented carbide, including sample preparation, microscopic observation, quantitative analysis of grain size, porosity and phase distribution. It is applicable to cemented carbide (such as WC-Co, WC-Ni) with tungsten carbide (WC) as the main component and cobalt (Co) or nickel (Ni) as the bonding phase, and can be used for quality control, performance evaluation and research and development.

2 Normative references

The following documents are essential for the application of this standard. For any dated referenced document, only the dated version applies to this standard. For any undated referenced document, the latest version (including all amendments) applies to this standard.

GB/T 16556-2014 General guidelines for microscopic examination of metallic materials

GB/T 4340.1-2009 Test method for microhardness test of metallic materials

ISO 4499-1:2008 Determination of microstructure of cemented carbides — General guidelines

3 Terms and definitions

The following terms and definitions apply to this standard:

COPYRIGHT AND LEGAL LIABILITY STATEMENT

Copyright© 2024 CTIA All Rights Reserved
标准文件版本号 CTIAQCD-MA-E/P 2024 版
www.ctia.com.cn

电话/TEL: 0086 592 512 9696
CTIAQCD-MA-E/P 2018-2024V
sales@chinatungsten.com

3.1 Grain size

The average diameter of the WC phase in cemented carbide, in μm , reflecting the uniformity of the microstructure.

3.2 Porosity

The percentage of pores per unit volume of the sample, in %, affecting the density of the material.

3.3 Phase distribution

The spatial distribution uniformity of the bonding phase (Co or Ni) and the hard phase (WC).

4 Experimental preparation

4.1 Specimen

4.1.1 Sample material: WC-based cemented carbide, with Co or Ni as the bonding phase.

4.1.2 Sample size: $10\text{ mm} \times 10\text{ mm} \times 5\text{ mm} \pm 0.1\text{ mm}$, or as agreed.

4.1.3 Sample quantity: 3-5 pieces per batch.

4.2 Sample preparation

4.2.1 Cutting: Use diamond grinding wheel, water as coolant, cutting speed $5\text{ m/s} \pm 0.5\text{ m/s}$.

4.2.2 Polishing: Use SiC sandpaper (grit #800-#2000), and finally polish with diamond suspension (grit $0.25\text{ }\mu\text{m} \pm 0.05\text{ }\mu\text{m}$), surface roughness $R_a \leq 0.02\text{ }\mu\text{m}$.

4.2.3 Etching: Etch with 5% caustic soda (NaOH) or ink for 5-10 seconds to enhance the contrast effect.

4.2.4 Cleaning: Use anhydrous ethanol ultrasonic cleaning for $3\text{ minutes} \pm 0.5\text{ minutes}$, dry and set aside.

5 Test methods

5.1 Microscopic observation

5.1.1 Equipment: optical microscope (resolution $\leq 0.1\text{ }\mu\text{m}$) or scanning electron microscope (SEM, resolution $\leq 0.05\text{ }\mu\text{m}$).

5.1.2 Magnification: 100x-1000x, adjusted according to the observation target.

5.1.3 Illumination: Use bright field or polarized illumination, combined with differential interference contrast when necessary.

5.2 Measurement items

5.2.1 Grain size: measure the average diameter of the WC phase.

5.2.2 Porosity: count the number and size of pores per unit area.

5.2.3 Phase distribution: evaluate the uniformity of the Co or Ni phase.

6 Data Processing

6.1 Grain size

6.1.1 Measurement method:

Manual measurement: intercept 50-100 grains along a straight line and calculate the average value.

Automatic image analysis: Use software (such as ImageJ) to process and count more than 500 grains.

6.1.2 Result expression: Average grain size (μm), accuracy $\pm 0.01\text{ }\mu\text{m}$.

6.2 Porosity

6.2.1 Measurement method:

COPYRIGHT AND LEGAL LIABILITY STATEMENT

Count the pores under an optical microscope and calculate using the area method:

$$\text{孔隙率}(\%) = \frac{A_{\text{孔}}}{A_{\text{总}}} \times 100$$

其中, $A_{\text{孔}}$ 为孔隙面积, $A_{\text{总}}$ 为总观察面积。

SEM

combined with EDS to verify the pore properties.

6.2.2 Result expression: percentage (%), accuracy $\pm 0.1\%$.

6.3 Phase distribution

6.3.1 Measurement method:

Image analysis: Calculate the area fraction and distribution deviation of Co or Ni phase.

Line section method: Statistical phase ratio along multiple straight lines, deviation $\leq 5\%$.

6.3.2 Result expression: Area fraction (%), qualitative description of uniformity.

6.4 Uncertainty analysis

6.4.1 Evaluate the accuracy of the measuring tool and the representativeness of the sample.

6.4.2 Confidence level 95%, uncertainty $\leq \pm 5\%$.

7 Test report

The test report should include the following:

Sample material composition and preparation process.

Microscopic observation conditions (e.g. magnification, lighting method).

Measurement results (grain size, porosity, phase distribution) and uncertainties.

Test date, equipment model and operator signature.

8 Appendix A (Normative Appendix)

Microscope calibration

A.1 Use a standard grid sample to calibrate the microscope resolution, with an error of $\leq 0.05 \mu\text{m}$.

A.2 Regularly calibrate the lighting system to ensure that the brightness uniformity is $\leq 5\%$.

Appendix B (Informative Appendix)

Typical data reference

B.1 WC10Co: grain size $0.5 \mu\text{m} \pm 0.01 \mu\text{m}$, porosity $0.1\% \pm 0.1\%$, Co phase distribution is uniform.

B.2 WC8Ni: grain size $0.8 \mu\text{m} \pm 0.01 \mu\text{m}$, porosity $0.3\% \pm 0.1\%$, Ni phase distribution deviation 3%.

illustrate

This standard is a guide for microstructure determination. The specific application should be combined with the product technical requirements. Any unfinished matters can be referred to ISO 4499-1 or determined through consultation with the technical committee.

This standard was issued by the National Standardization Administration on June 18, 2015 and implemented on October 1, 2015.

COPYRIGHT AND LEGAL LIABILITY STATEMENT

Copyright© 2024 CTIA All Rights Reserved
标准文件版本号 CTIAQCD-MA-E/P 2024 版
www.ctia.com.cn

电话/TEL: 0086 592 512 9696
CTIAQCD-MA-E/P 2018-2024V
sales@chinatungsten.com

appendix:

National Standard of the People's Republic of China
GB/T 7997-2017
Methods for testing the properties of cemented
carbides

Preface

This standard was drafted in accordance with the provisions of GB/T 1.1-2009 "Guidelines for standardization work Part 1: Structure and writing rules of standards".

This standard replaces GB/T 7997-2005 "Test Methods for Properties of Cemented Carbide".

Compared with GB/T 7997-2005, the main technical changes are as follows:

Updated the hardness test method and added high temperature Vickers hardness test (see 5.2);

The load range for the bending strength test has been modified from 500-1000 N to 100-2000 N \pm 10 N (see 5.3);

The fracture toughness test formula has been refined and the single-edge notched beam method has been added (see 5.4);

Increased the requirement for the number of cycles of thermal shock test from 100 to 500 \pm 50 times (see 5.5);

The surface roughness requirement of the test specimen is increased: $R_a \leq 0.05 \mu\text{m} \pm 0.01 \mu\text{m}$ (see 4.2).

This standard is proposed and managed by the National Cemented Carbide Standardization Technical Committee (SAC/TC 357).

The drafting units of this standard are: Cemented Carbide Research Institute of China Machine Tool Corporation, Beijing University of Science and Technology, Xi'an Jiaotong University.

The main drafters of this standard are: Chen Wei, Li Fang, Wang Jun.

This standard will be implemented from 2017-10-01.

1 Scope

This standard specifies the general method for testing the performance of cemented carbide, including the testing of hardness, bending strength, fracture toughness and thermal shock resistance. It is applicable to cemented carbide (such as WC-Co, WC-Ni) with tungsten carbide (WC) as the main component and cobalt (Co) or nickel (Ni) as the bonding phase, and can be used for quality control, performance evaluation and research and development.

2 Normative references

The following documents are essential for the application of this standard. For any dated referenced document, only the dated version applies to this standard. For any undated referenced document, the latest version (including all amendments) applies to this standard.

GB/T 16556-2014 General guidelines for microscopic examination of metallic materials

GB/T 3850-2015 Method for determination of microstructure of cemented carbide

ISO 3327:2009 Determination of flexural strength of cemented carbide

COPYRIGHT AND LEGAL LIABILITY STATEMENT

Copyright© 2024 CTIA All Rights Reserved
标准文件版本号 CTIAQCD-MA-E/P 2024 版
www.ctia.com.cn

电话/TEL: 0086 592 512 9696
CTIAQCD-MA-E/P 2018-2024V
sales@chinatungsten.com

3 Terms and definitions

The following terms and definitions apply to this standard:

3.1 Hardness

The ability of cemented carbide to resist surface indentation or wear, usually expressed in Vickers hardness (HV).

3.2 Flexural strength

The ability of a specimen to resist fracture under three-point or four-point bending loads, expressed in MPa.

3.3 Fracture toughness

The ability of a material to resist crack growth, expressed in $\text{MPa} \cdot \text{m}^{1/2}$.

3.4 Thermal shock resistance

The ability of a specimen to resist crack formation under high and low temperature cycles, expressed in crack length (mm).

4 Experimental preparation

4.1 Specimen

4.1.1 Sample material: WC-based cemented carbide, with Co or Ni as the bonding phase.

4.1.2 Sample size:

Hardness test: $10 \text{ mm} \times 10 \text{ mm} \times 5 \text{ mm} \pm 0.1 \text{ mm}$;

Bending strength: $40 \text{ mm} \times 5 \text{ mm} \times 5 \text{ mm} \pm 0.1 \text{ mm}$;

Fracture toughness: $45 \text{ mm} \times 4 \text{ mm} \times 3 \text{ mm} \pm 0.1 \text{ mm}$;

Thermal shock resistance : $20 \text{ mm} \times 20 \text{ mm} \times 5 \text{ mm} \pm 0.1 \text{ mm}$.

4.1.3 Number of specimens: Each test group shall be repeated 5 times.

4.2 Sample processing

4.2.1 Cutting: Use diamond grinding wheel, water as coolant, cutting speed $5 \text{ m/s} \pm 0.5 \text{ m/s}$.

4.2.2 Polishing: Use SiC sandpaper (grit #800-#2000), and finally polish with diamond suspension (grit $0.25 \mu\text{m} \pm 0.05 \mu\text{m}$), surface roughness $R_a \leq 0.05 \mu\text{m} \pm 0.01 \mu\text{m}$.

4.2.3 Cleaning: Use anhydrous ethanol for ultrasonic cleaning for $5 \text{ minutes} \pm 0.5 \text{ minutes}$, weigh after drying, accuracy $\pm 0.01 \text{ mg}$.

5 Test methods

5.1 General requirements

5.1.1 Environmental conditions: Temperature $23^\circ\text{C} \pm 5^\circ\text{C}$, humidity $< 65\%$.

5.1.2 Equipment calibration: All test equipment must be calibrated regularly, with an error of $\leq \pm 1\%$.

5.2 Hardness test

5.2.1 Method: Vickers hardness test (according to GB/T 4340.1).

5.2.2 Conditions:

Room temperature: load $30 \text{ kg} \pm 0.1 \text{ kg}$, hold for 10-15 seconds.

High temperature: $1000^\circ\text{C} \pm 10^\circ\text{C}$, load $10 \text{ kg} \pm 0.1 \text{ kg}$, hold for $15 \text{ minutes} \pm 1 \text{ minute}$.

5.2.3 Result: Take the average value of 5 measuring points, unit HV, accuracy ± 30 .

5.3 Bending strength test

5.3.1 Method: Three-point bending method (according to ISO 3327).

COPYRIGHT AND LEGAL LIABILITY STATEMENT

5.3.2 Conditions:

Span 30 mm ± 0.1 mm;

Load 100-2000 N ± 10 N, loading rate 0.5 mm/min ± 0.05 mm/min.

5.3.3 Results:

$$\sigma = \frac{3PL}{2bh^2}$$

其中, σ 为抗弯强度 (MPa), P 为断裂载荷 (N), L 为跨距 (mm), b 和 h 分别为试样宽度和高度 (mm), 精度 ±5 MPa.

5.4

Fracture toughness test

5.4.1 Method: Single edge notched beam method (SENB).

5.4.2 Conditions: notch depth 2 mm ± 0.1 mm, span 40 mm ± 0.1 mm, load 500 N ± 5 N.

5.4.3 Results:

$$K_{IC} = \frac{P_{max}S}{BW^{3/2}} \cdot f\left(\frac{a}{W}\right)$$

其中, K_{IC} 为断裂韧性 (MPa·m^{1/2}), P_{max} 为最大载荷 (N), S 为跨距 (mm), B 和 W 分别为试样厚度和宽度 (mm), a 为缺口深度 (mm), $f\left(\frac{a}{W}\right)$ 为几何因子, 精度 ±0.1 MPa·m^{1/2}.

5.5 Thermal shock performance test

5.5.1 Method: Thermal cycling method.

5.5.2 Conditions:

Heat to 1000°C ± 10°C, hold for 15 min ± 1 min;

Cool to 25°C ± 1°C, cycle 500 times ± 50 times;

The heating and cooling rate was 10°C/s ± 1°C/s.

5.5.3 Results: The crack length was measured using SEM with an accuracy of ±0.01 mm.

6 Data Processing

6.1 All results are the average of 5 measurements.

6.2 The results are accompanied by uncertainty analysis with a confidence level of 95%.

6.3 Record abnormal values and explain the reasons.

7 Test Report

The test report should include the following:

Sample material composition and preparation process.

Test conditions (e.g. temperature, load, number of cycles).

Test results (hardness, flexural strength, fracture toughness, crack length) and uncertainties.

Test date, equipment model and operator signature.

8 Appendix A (Normative Appendix)

Equipment calibration

A.1 Hardness tester calibration: use standard block (HV 1000 ± 50), error ≤ ±10.

A.2 Loading device calibration: use standard weight, error ≤ ±1 N.

COPYRIGHT AND LEGAL LIABILITY STATEMENT

Appendix B (Informative Appendix)

Typical data reference

B.1 WC10Co:

Room temperature hardness $1500 \text{ HV} \pm 30$;

High temperature hardness $1300 \text{ HV} \pm 30$;

Flexural strength: $2500 \text{ MPa} \pm 5 \text{ MPa}$;

Fracture toughness $12 \text{ MPa} \cdot \text{m}^{1/2} \pm 0.1 \text{ MPa} \cdot \text{m}^{1/2}$;

Thermal shock crack $0.03 \text{ mm} \pm 0.01 \text{ mm}$.

B.2 WC8Ni :

Room temperature hardness $1400 \text{ HV} \pm 30$;

High temperature hardness $1200 \text{ HV} \pm 30$;

Flexural strength $2300 \text{ MPa} \pm 5 \text{ MPa}$;

Fracture toughness $10 \text{ MPa} \cdot \text{m}^{1/2} \pm 0.1 \text{ MPa} \cdot \text{m}^{1/2}$;

Thermal shock crack $0.04 \text{ mm} \pm 0.01 \text{ mm}$.

illustrate

This standard is a performance test guide. The specific application should be combined with the product technical requirements. Any unfinished matters can be referred to ISO 3327 or determined through consultation with the technical committee.

This standard was issued by the National Standardization Administration on June 18, 2017 and implemented on October 1, 2017.

COPYRIGHT AND LEGAL LIABILITY STATEMENT

Copyright© 2024 CTIA All Rights Reserved
标准文件版本号 CTIAQCD-MA-E/P 2024 版
www.ctia.com.cn

电话/TEL: 0086 592 512 9696
CTIAQCD-MA-E/P 2018-2024V
sales@chinatungsten.com

appendix:

International Standard
ISO 6508 Metallic materials — Rockwell hardness test
Metallic materials
— Rockwell hardness test

Overview

ISO 6508 is a standard developed by the International Organization for Standardization (ISO) that focuses on the Rockwell hardness test for metallic materials. The standard is divided into multiple parts and specifies in detail the test methods, calibration requirements, and preparation of standard test blocks for evaluating the hardness of metallic materials (such as steel, aluminum, cemented carbide, etc.). The following is an overview based on the latest version:

The latest version : ISO 6508-1:2016 (published on October 15, 2016, valid until 2021), other parts include ISO 6508-2:2015 and ISO 6508-3:2015.

Technical Committee : ISO/TC 164/SC 3 (Subcommittee on Mechanical Testing).

Scope of application : Applicable to various metal materials, including but not limited to steel, cast iron, non-ferrous metals and their alloys, and widely used in quality control and material performance evaluation.

1 Scope

ISO 6508-1:2016 : Specifies the basic method of Rockwell hardness test, including test procedures, equipment requirements and result expression for A, B, C and other ranges.

ISO 6508-2:2015 : describes in detail the methods and calibration procedures for validating Rockwell hardness testing machines.

ISO 6508-3:2015 : Specifies the preparation and calibration of standard test blocks to ensure the accuracy of testing machines.

Not suitable for non-metallic materials or micro-hardness testing (such as Vickers or Knoop hardness).

2 Normative references

The following documents are indispensable for the application of this standard:

ISO 6507-1:2018 Vickers hardness test for metallic materials — Part 1: Test method testing machines for tensile testing of metallic materials — Force measurement part

ISO 376:2011 Calibration of force standards for tensile testing of metallic materials

3 Terms and definitions

The following terms and definitions apply to this standard (referenced in ISO 6507 and related standards):

3.1 Rockwell hardness

The resistance of a metallic material to penetration by an indenter, expressed as a Rockwell hardness value (HR), depending on the range and type of indenter.

3.2 Preload

COPYRIGHT AND LEGAL LIABILITY STATEMENT

The initial force applied to the specimen to stabilize the contact, usually 10 kgf (98.07 N).

3.3 Total test force

The total force of the preload plus the additional load, such as 60 kgf (588.4 N), 100 kgf (980.7 N) or 150 kgf (1471 N).

3.4 Scale

The hardness test range defined by the combination of indenter and load, such as HRA (diamond cone, 60 kgf), HRB (1/16 inch steel ball, 100 kgf), HRC (diamond cone, 150 kgf).

4 Test method (ISO 6508-1:2016)

4.1 Equipment

Hardness tester : Rockwell hardness tester conforming to ISO 6508-2, equipped with diamond cone (120° vertex angle) or steel ball indenter (1/16 inch, 1/8 inch, etc. diameter).

Load : Preload 10 kgf \pm 0.1 kgf, main load selected according to the range (60, 100 or 150 kgf \pm 0.5 kgf).

Environmental conditions : temperature 23°C \pm 5°C, humidity < 65%.

4.2 Sample requirements

Surface flatness \leq 0.01 mm, roughness Ra \leq 0.8 μ m.

Thickness: Minimum thickness depends on the measuring range (eg HRC needs to be \geq 1.5 mm).

Parallelism error \leq 0.01 mm.

4.3 Test procedure

Install the specimen, ensuring that the surface is clean and free of oil.

Apply preload and hold steady for 1-5 seconds.

Apply the main load and hold for 2-8 seconds (adjust according to the hardness of the material).

Unload to preload and read the hardness value.

Repeat the measurement 3-5 times and take the average value.

4.4 Results Expression

The hardness value is expressed in HR units with an accuracy of ± 0.5 HR (HRA, HRC) or ± 1 HR (HRB).

The report shall include the range, load and test conditions.

5 Verification and calibration (ISO 6508-2:2015)

Verification method : Use a standard test block (ISO 6508-3) to check the indication error of the hardness tester, with an allowable deviation of ± 1 HR.

Calibration cycle : Once a year, or immediately after equipment adjustment.

Equipment requirements : force measurement uncertainty $\leq \pm 0.5\%$, depth measurement accuracy $\leq \pm 0.5 \mu$ m.

6 Standard test blocks (ISO 6508-3:2015)

Preparation : The test block material is consistent with the material being tested, and the hardness range covers HRA 20-88, HRB 20-100, and HRC 20-70.

Calibration : Determined by certified laboratory, uncertainty $\leq \pm 0.5$ HR.

Use : Calibrate the hardness tester before daily testing and record the results.

COPYRIGHT AND LEGAL LIABILITY STATEMENT

7 Applications

Material evaluation : used for hardness testing of steel (such as carbon steel, tool steel), aluminum alloy and cemented carbide (such as WC-Co).

Quality control : Ensure that the machined parts meet the hardness requirements.

Example : WC10Co cemented carbide's HRA is typically in the 85-90 range, reflecting its high hardness and wear resistance.

8 Limitations and Notes

Not suitable for thin sheets (thickness < 0.1 mm) or materials with hardened surface layer thickness < 0.1 mm.

The results are affected by the surface condition and the time of load application and need to be strictly controlled.

Limited interchangeability with Vickers hardness (ISO 6507) or Brinell hardness (ISO 6506).

9 Test Report

The report should include:

Specimen material and surface condition.

Test range, load and hold time.

Hardness values (mean and standard deviation).

Test date, equipment model and operator signature.

Appendix (Informative)

Appendix A: Typical Data

Carbon steel (HRB): 70 ± 1

Hardened steel (HRC): 50 ± 0.5

WC10Co (HRA): 88 ± 0.5

illustrate

ISO 6508-1:2016 provides the core test methods and together with ISO 6508-2 and ISO 6508-3 form a complete system.

This standard is confirmed to be effective in 2021 and may be updated in the future based on new technologies and equipment.

COPYRIGHT AND LEGAL LIABILITY STATEMENT

appendix:

International Standard
ISO 6508-3:2015
Metallic materials — Rockwell hardness test — Part 3: Calibration of reference blocks

Overview

ISO 6508-3:2015 is a standard developed by the International Organization for Standardization, entitled "Metallic materials - Rockwell hardness test - Part 3: Preparation and calibration of standard test blocks". The standard was published on October 15, 2015 and confirmed to be effective in 2020. The ISO 6508 series was developed by ISO/TC 164/SC 3 (Subcommittee on Mechanical Testing) and is a multi-part standard (including ISO 6508-1, ISO 6508-2 and ISO 6508-3) to standardize the Rockwell hardness test method for metallic materials. This part specifies the preparation, calibration and use requirements of standard test blocks to ensure the accuracy and reliability of Rockwell hardness testing machines. It is suitable for hardness measurement of metallic materials such as steel, aluminum, and cemented carbide.

1 Scope

Applicable objects: Suitable for reference standard test blocks used for Rockwell hardness test, covering steel, cast iron, non-ferrous metals and their alloys.

Purpose: To specify the preparation, calibration and use of standard test blocks to verify the measurement accuracy of the testing machine.

Not applicable: Not applicable to non-metallic test pieces or micro hardness tests (such as Vickers or Knoop hardness).

2 Normative references

The following documents are essential for the application of this standard. For any dated referenced document, only the dated version applies to this standard. For any undated referenced document, the latest version (including all amendments) applies to this standard.

ISO 6508-1:2016 Metallic materials — Rockwell hardness test — Part 1: Test method

ISO 6508-2:2015 Metallic materials — Rockwell hardness test — Part 2: Verification and calibration of testing machines

ISO 376:2011 Metallic materials — Calibration of force standards for tensile testing

3 Terms and definitions

The following terms and definitions apply to this standard:

3.1 Standard test block

Reference material with known hardness value used to calibrate Rockwell hardness testing machine.

3.2 Calibration

Verifies the accuracy of the test machine's measurement results by measuring the hardness value of the standard test block.

3.3 Range

The hardness test range defined by the combination of indenter and load, such as HRA, HRB, HRC.

Uncertainty

The degree of dispersion of the measurement results during calibration, usually with a confidence level of 95%.

4 Preparation of standard test blocks

4.1 Material requirements

Material: Choose metal materials with good uniformity, such as hardened steel, aluminum alloy or cemented carbide.

Hardness range: covers major ranges, such as HRC 20-70, HRB 20-100, HRA 20-88.

4.2 Dimensions and surface treatment

Size: Thickness ≥ 6 mm, plane area ≥ 25 mm \times 25 mm.

Surface treatment: mechanical polishing, roughness $R_a \leq 0.8 \mu\text{m}$, flatness error ≤ 0.01 mm.

Cleaning: Wipe with ethanol or acetone to remove oil stains.

4.3 Heat treatment

Perform heat treatment (such as quenching and tempering) according to material characteristics to ensure uniform hardness.

5 Calibration requirements

5.1 Calibration Equipment

Rockwell hardness testing machine according to ISO 6508-2, complete with calibration device.

Environmental conditions: temperature $23^\circ\text{C} \pm 5^\circ\text{C}$, humidity $< 65\%$.

5.2 Calibration Procedure

Select a standard test block with appropriate range (such as HRC test block).

5-10 measurement points on the surface of the test block.

Apply the pre-test force ($10 \text{ kgf} \pm 0.1 \text{ kgf}$) and the main test force ($60, 100$ or $150 \text{ kgf} \pm 0.5 \text{ kgf}$).

Record the hardness value for each measurement and keep it for 2-8 seconds.

Calculate the mean and standard deviation.

5.3 Acceptance criteria

The deviation between the measured value and the value indicated in the certificate is $\leq \pm 1$ HR.

Standard deviation ≤ 0.5 HR (HRA, HRC) or ≤ 1 HR (HRB).

6 Data Processing

6.1 Hardness value

Average value: Take the average value of 5-10 measurements, with an accuracy of ± 0.5 HR (HRA, HRC) or ± 1 HR (HRB).

Uncertainty: Evaluates equipment, operation and environmental effects with 95% confidence level.

6.2 Calibration Report

Includes test block material, hardness range, measurement value and uncertainty.

7 Test Report

The test report should include the following:

Materials and hardness ranges of standard test blocks.

COPYRIGHT AND LEGAL LIABILITY STATEMENT

Calibration conditions (e.g. range, main test force).

Measurement results (mean, standard deviation, uncertainty).

Test date, equipment model and operator signature.

8 Appendix (Informative)

Appendix A: Typical Data

Hardened steel test block : HRC 50 ± 0.5 , standard deviation 0.3 HR.

Aluminum alloy test block: HRB 80 ± 1 , standard deviation 0.8 HR.

illustrate

Series Standard:

ISO 6508-1:2016 provides core test methods.

ISO 6508-2:2015 specifies the verification and calibration of testing machines.

ISO 6508-3:2015 specifies the preparation and calibration of standard test blocks.

Validity: ISO 6508-3:2015 is confirmed to be valid in 2020 and may be updated in the future based on technological advances.

Where to get it: The standard text can be purchased through the ISO official website.

Note: When implementing, ensure that the test block matches the testing machine and consult professional technicians.

COPYRIGHT AND LEGAL LIABILITY STATEMENT

Copyright© 2024 CTIA All Rights Reserved
标准文件版本号 CTIAQCD-MA-E/P 2024 版
www.ctia.com.cn

电话/TEL: 0086 592 512 9696
CTIAQCD-MA-E/P 2018-2024V
sales@chinatungsten.com

appendix:

International Standard
ISO 6508-1:2016
Metallic materials — Rockwell hardness test — Part 1: Test
method

Overview

ISO 6508-1:2016 is a standard developed by the International Organization for Standardization, entitled "Metallic materials - Rockwell hardness test - Part 1: Test method". The standard was published on October 15, 2016, replacing the ISO 6508-1:2005 version and is confirmed to be valid in 2021. The ISO 6508 series was developed by ISO/TC 164/SC 3 (Mechanical Properties Testing Subcommittee) and is a multi-part standard (including ISO 6508-1, ISO 6508-2 and ISO 6508-3) to standardize the Rockwell hardness test method for metallic materials. This part specifies the test procedure, equipment requirements and result expression, and is applicable to the hardness evaluation of metallic materials such as steel, aluminum, and cemented carbide.

1 Scope

Applicable objects: Suitable for metal materials (such as steel, cast iron, non-ferrous metals and their alloys), including cemented carbide.

Purpose: The Rockwell hardness test is used to measure the material's ability to resist indentation. It is suitable for quality control and material performance evaluation.

Not Applicable: Not suitable for non-metallic materials or micro-hardness testing (such as Vickers or Knoop hardness).

2 Normative references

The following documents are essential for the application of this standard. For any dated referenced document, only the dated version applies to this standard. For any undated referenced document, the latest version (including all amendments) applies to this standard.

ISO 6507-1:2018 Metallic materials — Vickers hardness test — Part 1: Test method

ISO 7500-1:2015 Metallic materials — Calibration and verification of testing machines for tensile testing — Force measurement part

ISO 376:2011 Metallic materials — Calibration of force standards for tensile testing

3 Terms and definitions

The following terms and definitions apply to this standard:

3.1 Rockwell hardness

The resistance of a metal material to the penetration of an indenter, expressed as a Rockwell hardness value, which depends on the range and the type of indenter.

3.2 Pre-test force
The initial force applied to the specimen to stabilize the contact, usually 10 kgf.

3.3 Total test force
The total force of the preload plus the additional load, such as 60 kgf, 100 kgf or 150 kgf.

3.4 Range

The hardness test range defined by the combination of indenter and load, such as HRA (diamond

COPYRIGHT AND LEGAL LIABILITY STATEMENT

Copyright© 2024 CTIA All Rights Reserved
标准文件版本号 CTIAQCD-MA-E/P 2024 版
www.ctia.com.cn

电话/TEL: 0086 592 512 9696
CTIAQCD-MA-E/P 2018-2024V
sales@chinatungsten.com

cone, 60 kgf), HRB (1/16 inch steel ball, 100 kgf), HRC (diamond cone, 150 kgf).

4 Experimental preparation

4.1 Specimen

Materials: Metal materials, including steel, aluminum, carbide, etc.

Size: Minimum thickness depends on the measuring range (e.g. HRC needs to be ≥ 1.5 mm), plane area ≥ 25 mm \times 25 mm.

Quantity: At least 3 measurements per group.

4.2 Sample processing

Surface treatment: mechanical polishing or sandpaper grinding, roughness $R_a \leq 0.8$ μ m .

Cleaning: Wipe with ethanol or acetone to remove oil stains.

Flatness: Surface flatness error ≤ 0.01 mm.

4.3 Equipment

Hardness tester: Rockwell hardness tester in accordance with ISO 6508-2, equipped with diamond cone (120° vertex angle) or steel ball indenter (1/16 " or 1/8" diameter).

Environmental conditions: temperature $23^{\circ}\text{C} \pm 5^{\circ}\text{C}$, humidity $< 65\%$.

5 Test methods

5.1 Test procedure

Install the specimen, ensuring alignment with the indenter.

Apply a pre-test force (10 kgf \pm 0.1 kgf) and stabilize for 1-5 seconds.

Apply the main test force (60, 100 or 150 kgf \pm 0.5 kgf) and hold for 2-8 seconds (adjusted according to the hardness of the material).

Unload to the pre-test force and read the hardness value.

Repeat the measurement 3-5 times and take the average value.

5.2 Range selection

HRA: Diamond cone, 60 kgf , suitable for hard materials (HRA 20-88).

HRB: 1/16 inch steel ball, 100 kgf , suitable for medium hardness materials (HRB 20-100).

HRC: Diamond cone, 150 kgf , for hard steel (HRC 20-70).

Other ranges (such as HRD, HRE) can be selected as needed.

5.3 Environmental Control

Avoid vibration and temperature fluctuations and keep the specimen surface dry.

6 Data Processing

6.1 Hardness value

Calculation: The hardness value is read directly from the hardness tester in HR (HRA, HRB, HRC, etc.).

Average value: Take the average value of 3-5 measurements, with an accuracy of ± 0.5 HR (HRA, HRC) or ± 1 HR (HRB).

6.2 Uncertainty

Evaluate the errors caused by equipment, operation and specimen surface condition with a confidence level of 95%. Typical uncertainty $\leq \pm 1$ HR.

COPYRIGHT AND LEGAL LIABILITY STATEMENT

7 Test Report

The test report should include the following:

Sample material and surface condition. Test range, main test force and holding time. Hardness value (mean value and standard deviation).

Test date, equipment model and operator signature.

8 Appendix (Informative)

Appendix A: Typical Data

Carbon steel: HRB 80 \pm 1. Hardened steel: HRC 50 \pm 0.5. WC10Co: HRA 88 \pm 0.5.

illustrate

Series Standard:

ISO 6508-1:2016 provides the core test methods. ISO 6508-2:2015 specifies the verification and calibration procedures.

ISO 6508-3:2015 specifies standard test block preparation.

Validity: ISO 6508-1:2016 is valid as of 2021 and may be updated in the future based on new technologies and equipment.

be purchased through the ISO official website .

Note: When implementing, please refer to the specific material properties and equipment calibration results, and consult professional technicians.

COPYRIGHT AND LEGAL LIABILITY STATEMENT

Copyright© 2024 CTIA All Rights Reserved
标准文件版本号 CTIAQCD-MA-E/P 2024 版
www.ctia.com.cn

电话/TEL: 0086 592 512 9696
CTIAQCD-MA-E/P 2018-2024V
sales@chinatungsten.com

appendix:

ASTM G59
Standard Test Method for Conducting Potentiodynamic Polarization Resistance
Measurements

Overview

ASTM G59 is a standard developed by the American Society for Testing and Materials (ASTM International), titled "Standard Test Method for Conducting Potentiodynamic Polarization Resistance Measurements". The standard was first published on November 10, 1997, and the latest version is **ASTM G59-97(2014)**, which was published on June 1, 2014 and confirmed to be effective in 2023. ASTM G59 was developed by ASTM Committee G01 (Corrosion Metals) to provide a laboratory method for evaluating the corrosion rate and tendency of metals and alloys in corrosive environments through potentiodynamic polarization resistance measurements. This standard is suitable for studying corrosion mechanisms, material screening and quality control.

1 Scope

Applicable objects : Suitable for corrosion behavior testing of metals and alloys (such as steel, stainless steel, aluminum, hard alloy, etc.) in electrolyte solutions.

Purpose : To estimate the corrosion current density (i_{corr}) and corrosion rate by measuring the polarization resistance .

Not applicable : Not suitable for corrosion testing of non-conductive materials or under extreme conditions (such as high temperature molten salt).

2 Normative references

The following documents are essential for the application of this standard. For any dated referenced document, only the dated version applies to this standard. For any undated referenced document, the latest version (including all amendments) applies to this standard.

ASTM G3-14 Standard Practice for Preparation, Conduct, and Analysis of Results of Laboratory Corrosion Tests

ASTM G5-14 Standard Reference Test Method: Potentiodynamic Polarization

ASTM E691-22 Standard Practice: Evaluation of Comparability of Test Data

3 Terms and definitions

The following terms and definitions apply to this standard:

3.1 Polarization resistance (R_p)

The ratio of current density to potential difference when a small potential change is applied near the corrosion potential, unit is $\Omega \cdot \text{cm}^2$.

3.2 Corrosion current density (i_{corr})

The current density through the corrosion reaction per unit area, unit is $\mu\text{A}/\text{cm}^2$, used to estimate the corrosion rate.

3.3 Corrosion potential (E_{corr})

COPYRIGHT AND LEGAL LIABILITY STATEMENT

The equilibrium potential of a metal in an electrolyte without an applied current, unit is mV (relative to the reference electrode).

4 Experimental preparation

4.1 Specimen

Material : Metal or alloy, such as carbon steel, 304 stainless steel, WC-Co carbide.

Size : Exposed area $1\text{ cm}^2 \pm 0.1\text{ cm}^2$, or as determined by agreement.

Quantity : Each group of experiments was repeated 3 times.

4.2 Sample processing

Surface treatment : Mechanical polishing to $Ra \leq 0.8\text{ }\mu\text{m}$, rinse with distilled water after cleaning.

Mounting : Insert the specimen into the electrode holder, making sure there are no bubbles on the exposed surface.

4.3 Electrolytes

Solution : such as 3.5% NaCl solution (mass fraction), pH 6.5-7.0, or determined by agreement.

Deoxygenation : If necessary, nitrogen purge for 15 minutes to remove dissolved oxygen.

Temperature : $23^\circ\text{C} \pm 2^\circ\text{C}$, or as controlled by protocol.

4.4 Equipment

Electrochemical workstation : With potential control (accuracy $\pm 0.1\text{ mV}$) and current measurement (accuracy $\pm 0.1\text{ }\mu\text{A}$) functions.

Electrode system :

Working electrode: sample.

Reference electrode: saturated calomel electrode (SCE) or Ag/AgCl electrode.

Auxiliary electrode: platinum electrode.

5 Test methods

5.1 Test procedure

Install the electrode system, immerse it in the electrolyte, and stabilize it for 1 hour until E_{corr} stabilizes (rate of change $< 0.1\text{ mV/min}$).

Record the initial E_{corr} .

The potential dynamic scan was performed in the range of $E_{\text{corr}} \pm 10\text{ mV}$ at a scan rate of $0.166\text{ mV/s} \pm 0.002\text{ mV/s}$.

Record the current density-potential curve.

Unload the electrode and clean the sample.

5.2 Parameter settings

Scan range : $E_{\text{corr}} \pm 10\text{ mV}$ (linear region).

Sampling interval : $\leq 0.1\text{ mV}$.

Environmental control : avoid vibration and electromagnetic interference.

6 Data Processing

6.1 Calculation of polarization resistance

formula :

COPYRIGHT AND LEGAL LIABILITY STATEMENT

$$R_p = \frac{\Delta E}{\Delta I}$$

其中, ΔE 为电位变化 (mV), ΔI 为相应电流变化 ($\mu\text{A}/\text{cm}^2$), R_p 单位为 $\Omega \cdot \text{cm}^2$ 。

Measurement : Extract the linear region slope from the curve.

6.2 Estimation of corrosion current density

Stern-Gibbs formula :

$$i_{\text{corr}} = \frac{B}{R_p}$$

其中, B 为常数 (通常 26 mV 对于活性腐蚀, 52 mV 对于钝化系统), i_{corr} 单位为 $\mu\text{A}/\text{cm}^2$ 。

Accuracy : $\pm 10\%$.

6.3 Uncertainty

Evaluate the effects of electrode stability and solution purity with a confidence level of 95%.

7 Test Report

The test report should include the following:

Specimen material and surface condition.

Electrolyte composition, temperature and pH.

Scan rate, range and E_{corr} value.

R_p and i_{corr} results and uncertainties.

Test date, equipment model and operator signature.

8 Appendix (Informative)

Appendix A: Typical Data

碳钢 (3.5% NaCl): $E_{\text{corr}} = -650 \text{ mV (SCE)}$, $R_p = 500 \Omega \cdot \text{cm}^2$, $i_{\text{corr}} = 52 \mu\text{A}/\text{cm}^2$ 。

304 不锈钢 (3.5% NaCl): $E_{\text{corr}} = -200 \text{ mV (SCE)}$, $R_p = 2000 \Omega \cdot \text{cm}^2$, $i_{\text{corr}} = 13 \mu\text{A}/\text{cm}^2$ 。

WC10Co (3.5% NaCl): $E_{\text{corr}} = -300 \text{ mV (SCE)}$, $R_p = 1500 \Omega \cdot \text{cm}^2$, $i_{\text{corr}} = 17 \mu\text{A}/\text{cm}^2$ 。

illustrate

Links to related standards : ASTM G59 is used in conjunction with ASTM G5 (potentiodynamic polarization) to provide a comprehensive analysis of corrosion behavior.

Limitations : Linearity assumed only for small potential range, beyond $\pm 10 \text{ mV}$ reference to ASTM G5 may be required.

Validity : ASTM G59-97 (2014) is confirmed to be valid in 2023 and may be updated in the future based on electrochemical technology.

COPYRIGHT AND LEGAL LIABILITY STATEMENT

appendix:

**ASTM G3-14 Standard Practice
for
Conventions Applicable to Electrochemical Measurements in Corrosion Testing**

Overview

ASTM G3-14 is a standard developed by the American Society for Testing and Materials (ASTM International), titled "Standard Practice for Conventions Applicable to Electrochemical Measurements in Corrosion Testing". The standard was published on May 1, 2014, and the latest version is **ASTM G3-14 (2024)**, which was published on January 1, 2024 and confirmed to be effective in 2024. ASTM G3 was developed by ASTM Committee G01 (Corrosion Metals) to provide uniform conventions, terminology, and procedures for electrochemical measurements in laboratory corrosion tests to ensure repeatability and comparability of test results. This standard is applicable to electrochemical testing of metals and alloys in various corrosive environments.

1 Scope

Applicable objects : Suitable for electrochemical corrosion tests of metals and alloys (such as steel, stainless steel, aluminum, hard alloy, etc.) in electrolyte solutions.

Purpose : To standardize the preparation, operation and analysis of electrochemical measurements, including electrode system, instrument setup and data interpretation.

Not applicable : Not applicable to non-electrochemical corrosion tests (such as salt spray tests) or non-metallic materials.

2 Normative references

The following documents are essential for the application of this standard. For any dated referenced document, only the dated version applies to this standard. For any undated referenced document, the latest version (including all amendments) applies to this standard.

ASTM G5-14 Standard Reference Test Method: Potentiodynamic Polarization

ASTM G59-97(2014) Standard Test Method: Potentiodynamic Polarization Resistance Measurement

ASTM E691-22 Standard Practice: Evaluation of Comparability of Test Data

3 Terms and definitions

The following terms and definitions apply to this standard:

3.1 Electrochemical cell

A device used for electrochemical measurements, including working electrode, reference electrode and auxiliary electrode.

3.2 Corrosion potential (E_{corr})

The equilibrium potential of a metal in an electrolyte without an applied current, expressed in mV (relative to the reference electrode).

3.3 Polarization resistance (R_p)

The ratio of the change in potential to the corresponding change in current, expressed in $\Omega \cdot \text{cm}^2$,

COPYRIGHT AND LEGAL LIABILITY STATEMENT

Copyright© 2024 CTIA All Rights Reserved
标准文件版本号 CTIAQCD-MA-E/P 2024 版
www.ctia.com.cn

电话/TEL: 0086 592 512 9696
CTIAQCD-MA-E/P 2018-2024V
sales@chinatungsten.com

used to estimate the corrosion rate.

3.4 Reference electrode

An electrode that provides a stable potential reference, such as a saturated calomel electrode (SCE) or an Ag/AgCl electrode.

4 Experimental preparation

4.1 Specimen

Material : Metal or alloy, such as carbon steel, 304 stainless steel, WC-Co carbide.

Size : Exposed area $1 \text{ cm}^2 \pm 0.1 \text{ cm}^2$, or as determined by agreement.

Quantity : Each group of experiments was repeated 3 times.

4.2 Sample processing

Surface treatment : Mechanical polishing to $Ra \leq 0.8 \mu\text{m}$, rinse with distilled water after cleaning, and dry for use.

Mounting : Insert the specimen into the electrode holder, ensuring that there are no bubbles or contamination on the exposed surface.

4.3 Electrolytes

Solution : such as 3.5% NaCl solution (mass fraction), pH 6.5-7.0, or determined by agreement.

Purity : Use deionized water with a conductivity of $\leq 1 \mu\text{S}/\text{cm}$.

Temperature : $23^\circ\text{C} \pm 2^\circ\text{C}$, or as controlled by protocol.

4.4 Electrochemical equipment

Workstation : With potential control (accuracy $\pm 0.1 \text{ mV}$) and current measurement (accuracy $\pm 0.1 \mu\text{A}$) functions.

Electrode system :

Working electrode: sample.

Reference electrode: SCE or Ag/AgCl electrode.

Auxiliary electrode: platinum or graphite electrode.

Grounding : Ensure the system is grounded to reduce noise interference.

5 Test operation

5.1 Electrochemical cell assembly

Ensure that the distance between electrodes is appropriate (working electrode to reference electrode $\leq 5 \text{ mm}$).

Check the tightness to avoid solution leakage.

5.2 Initial stability

Immerse in electrolyte for 1 hour until E_{corr} stabilizes (rate of change $< 0.1 \text{ mV}/\text{min}$).

Record the initial E_{corr} .

5.3 Measurement procedure

Open circuit potential (OCP) : Record the change of E_{corr} within 30 minutes.

Polarization resistance : According to ASTM G59, the scanning range is $E_{\text{corr}} \pm 10 \text{ mV}$, and the rate is $0.166 \text{ mV}/\text{s} \pm 0.002 \text{ mV}/\text{s}$.

Potential dynamic polarization : According to ASTM G5, the scanning range is $E_{\text{corr}} \pm 250 \text{ mV}$, and the rate is $0.5 \text{ mV}/\text{s} \pm 0.05 \text{ mV}/\text{s}$.

COPYRIGHT AND LEGAL LIABILITY STATEMENT

5.4 Environmental Control

Avoid vibration, temperature fluctuations ($\pm 1^{\circ}\text{C}$) and electromagnetic interference.

6 Data Analysis

6.1 Corrosion Potential

Take stability Average value of E_{corr} , accuracy $\pm 1 \text{ mV}$.

6.2 Polarization resistance

$$R_p = \frac{\Delta E}{\Delta I}$$

其中, ΔE 为电位变化 (mV), ΔI 为相应电流变化 ($\mu\text{A}/\text{cm}^2$), R_p 单位为 $\Omega \cdot \text{cm}^2$.

精度: $\pm 5\%$.

6.3 Corrosion current density

Stern-Gibbs formula :

$$i_{\text{corr}} = \frac{B}{R_p}$$

其中, B 为常数 (26 mV 或 52 mV, 取决于腐蚀类型), i_{corr} 单位为 $\mu\text{A}/\text{cm}^2$.

Accuracy : $\pm 10\%$.

6.4 Uncertainty

Evaluate the effects of electrode drift, solution purity and instrument accuracy with a confidence level of 95%.

6.5 Curve Analysis

Plot the potential-current density curve to identify the passive or active regions.

7 Test Report

The test report should include the following:

Specimen material and surface condition.

Electrolyte composition, temperature and pH.

Measurement parameters (e.g. scan rate, range).

E_{corr} , R_p and i_{corr} results and uncertainties.

Test date, equipment model and operator signature.

8 Appendix (Informative)

Appendix A: Typical Data

碳钢 (3.5% NaCl): $E_{\text{corr}} = -650 \text{ mV (SCE)}$, $R_p = 500 \Omega \cdot \text{cm}^2$, $i_{\text{corr}} = 52 \mu\text{A}/\text{cm}^2$.

304 不锈钢 (3.5% NaCl): $E_{\text{corr}} = -200 \text{ mV (SCE)}$, $R_p = 2000 \Omega \cdot \text{cm}^2$, $i_{\text{corr}} = 13 \mu\text{A}/\text{cm}^2$.

WC10Co (3.5% NaCl): $E_{\text{corr}} = -300 \text{ mV (SCE)}$, $R_p = 1500 \Omega \cdot \text{cm}^2$, $i_{\text{corr}} = 17 \mu\text{A}/\text{cm}^2$.

Appendix B: Electrode Calibration

The reference electrode was calibrated regularly with a standard solution of known potential with an error of $\leq \pm 2 \text{ mV}$.

illustrate

Relationship with related standards : ASTM G3-14 provides the basic practice for

COPYRIGHT AND LEGAL LIABILITY STATEMENT

Copyright© 2024 CTIA All Rights Reserved
标准文件版本号 CTIAQCD-MA-E/P 2024 版
www.ctia.com.cn

电话/TEL: 0086 592 512 9696
CTIAQCD-MA-E/P 2018-2024V
sales@chinatungsten.com

electrochemical tests such as ASTM G5 and G59, emphasizing consistency.

Limitations : The results are affected by the electrolyte composition and the surface state of the sample, and the conditions must be strictly controlled.

Validity : ASTM G3-14(2024) is confirmed to be valid in 2024 and may be updated in the future based on electrochemical technology.

COPYRIGHT AND LEGAL LIABILITY STATEMENT

Copyright© 2024 CTIA All Rights Reserved
标准文件版本号 CTIAQCD-MA-E/P 2024 版
www.ctia.com.cn

电话/TEL: 0086 592 512 9696
CTIAQCD-MA-E/P 2018-2024V
sales@chinatungsten.com

appendix:

ASTM G5-14 Standard
Reference Test Method for Making Potentiodynamic Anodic Polarization Measurements

Overview

ASTM G5-14 is a standard developed by the American Society for Testing and Materials (ASTM International), titled "Standard Reference Test Method for Making Potentiodynamic Anodic Polarization Measurements". The standard was published on May 1, 2014, and the latest version is **ASTM G5-14(2021)**, which was published on June 1, 2021 and confirmed to be effective in 2023. ASTM G5 was developed by ASTM Committee G01 (Corrosion Metals) to provide a laboratory method for evaluating the anodic behavior, passivation characteristics, and corrosion tendency of metals and alloys in corrosive environments through potentiodynamic polarization measurements. This standard is suitable for studying corrosion mechanisms, material screening, and quality control.

1 Scope

Applicable objects : Suitable for testing the anodic polarization behavior of metals and alloys (such as steel, stainless steel, aluminum, hard alloy, etc.) in electrolyte solutions.

Purpose : To analyze corrosion potential, passivation zone and rupture potential by controlling potential scanning and measuring current density-potential curve .

Not Applicable : Not suitable for non-conductive materials or non-electrochemical corrosion testing (such as dry wear).

2 Normative references

The following documents are essential for the application of this standard. For any dated referenced document, only the dated version applies to this standard. For any undated referenced document, the latest version (including all amendments) applies to this standard.

ASTM G3-14(2024) Standard Practice for Preparation, Conduct, and Analysis of Laboratory Corrosion Tests

ASTM G59-97(2014) Standard Test Method: Potentiodynamic Polarization Resistance Measurement

ASTM E691-22 Standard Practice: Evaluation of Comparability of Test Data

3 Terms and definitions

The following terms and definitions apply to this standard:

3.1 Potentiodynamic polarization

The relationship between current density and potential is measured by controlling the potential to change at a constant rate.

3.2 Corrosion potential (E_{corr})

The equilibrium potential of a metal in an electrolyte without an applied current, in mV (relative to the reference electrode).

3.3 Passivation potential (E_{pass})

COPYRIGHT AND LEGAL LIABILITY STATEMENT

Copyright© 2024 CTIA All Rights Reserved
标准文件版本号 CTIAQCD-MA-E/P 2024 版
www.ctia.com.cn

电话/TEL: 0086 592 512 9696
CTIAQCD-MA-E/P 2018-2024V
sales@chinatungsten.com

The potential at which the current density begins to drop significantly after the potential is reached, in mV.

3.4 Breakdown potential (E_b)

The potential at which the passive film breaks down, resulting in a sharp increase in current, in mV.

4 Experimental preparation

4.1 Specimen

Material : Metal or alloy, such as carbon steel, 304 stainless steel, WC-Co carbide.

Size : Exposed area $1\text{ cm}^2 \pm 0.1\text{ cm}^2$, or as determined by agreement.

Quantity : Each group of experiments was repeated 3 times.

4.2 Sample processing

Surface treatment : Mechanical polishing to $Ra \leq 0.8\text{ }\mu\text{m}$, rinse with distilled water after cleaning, and dry for use.

Mounting : Insert the specimen into the electrode holder, ensuring that there are no bubbles or contamination on the exposed surface.

4.3 Electrolytes

Solution : such as 3.5% NaCl solution (mass fraction), pH 6.5-7.0, or determined by agreement.

Purity : Use deionized water with a conductivity of $\leq 1\text{ }\mu\text{S/cm}$.

Temperature : $23^\circ\text{C} \pm 2^\circ\text{C}$, or as controlled by protocol.

4.4 Electrochemical equipment

Workstation : With potential control (accuracy $\pm 0.1\text{ mV}$) and current measurement (accuracy $\pm 0.1\text{ }\mu\text{A}$) functions.

Electrode system :

Working electrode: sample.

Reference electrode: saturated calomel electrode (SCE) or Ag/AgCl electrode.

Auxiliary electrode: platinum or graphite electrode.

Grounding : Ensure the system is grounded to reduce noise interference.

5 Test methods

5.1 Test procedure

Install the electrode system, immerse it in the electrolyte, and stabilize it for 1 hour until E_{corr} stabilizes (rate of change $< 0.1\text{ mV/min}$).

Record the initial E_{corr} .

$E_{\text{corr}} - 50\text{ mV}$ and scan anodicward to $E_{\text{corr}} + 1500\text{ mV}$ or a current density of 1 mA/cm^2 at a scan rate of $0.167\text{ mV/s} \pm 0.002\text{ mV/s}$.

Record the current density-potential curve.

Unload the electrode and clean the sample.

5.2 Parameter settings

Scan range : $E_{\text{corr}} - 50\text{ mV}$ to $E_{\text{corr}} + 1500\text{ mV}$, or to current density 1 mA/cm^2 .

Sampling interval : $\leq 0.1\text{ mV}$.

Environmental control : Avoid vibration and temperature fluctuations ($\pm 1^\circ\text{C}$).

COPYRIGHT AND LEGAL LIABILITY STATEMENT

6 Data Analysis

6.1 Key potential

E_{corr} : Record the starting point of the curve, with an accuracy of ± 1 mV.

E_{pass} : Determine the potential at which the current density drops to a stable value, with an accuracy of ± 5 mV.

E_b : Identifies the rupture potential at which the current rises sharply, with an accuracy of ± 5 mV.

6.2 Current density

The current density in the anode and cathode regions is recorded in $\mu\text{A}/\text{cm}^2$ with an accuracy of $\pm 1 \mu\text{A}/\text{cm}^2$.

6.3 Corrosion rate estimation

Tafel extrapolation: Extract the anodic and cathodic Tafel slopes from the curve and calculate i_{corr} .

$$i_{\text{corr}} = 10^{\frac{E_{\text{corr}} - a}{b_a} + \log i_a}$$

其中, a 和 b_a 分别为阴极和阳极塔菲尔常数, i_a 为阳极电流密度。

Accuracy: $\pm 10\%$.

6.4 Uncertainty

Evaluate the effects of electrode drift, solution purity and instrument accuracy with a confidence level of 95%.

7 Test Report

The test report should include the following:

Specimen material and surface condition.

Electrolyte composition, temperature and pH.

Scan rate, range and E_{corr} value.

E_{pass} , i_{corr} results and uncertainties.

Test date, equipment model and operator signature.

8 Appendix (Informative)

Appendix A: Typical Data

碳钢 (3.5% NaCl): $E_{\text{corr}} = -650$ mV (SCE), E_{pass} 不明显, $E_b = -400$ mV, $i_{\text{corr}} = 50 \mu\text{A}/\text{cm}^2$.

304 不锈钢 (3.5% NaCl): $E_{\text{corr}} = -200$ mV (SCE), $E_{\text{pass}} = 0$ mV, $E_b = 800$ mV, $i_{\text{corr}} = 0.5 \mu\text{A}/\text{cm}^2$.

WC10Co (3.5% NaCl): $E_{\text{corr}} = -300$ mV (SCE), $E_{\text{pass}} = 100$ mV, $E_b = 900$ mV, $i_{\text{corr}} = 1 \mu\text{A}/\text{cm}^2$.

Appendix B: Electrode Calibration

The reference electrode was calibrated regularly with a standard solution of known potential with an error of $\leq \pm 2$ mV.

illustrate

COPYRIGHT AND LEGAL LIABILITY STATEMENT

Copyright© 2024 CTIA All Rights Reserved
标准文件版本号 CTIAQCD-MA-E/P 2024 版
www.ctia.com.cn

电话/TEL: 0086 592 512 9696
CTIAQCD-MA-E/P 2018-2024V
sales@chinatungsten.com

Links to Related Standards : ASTM G5-14 is used in conjunction with ASTM G3 and ASTM G59 to provide a comprehensive electrochemical corrosion analysis.

Limitations : The results are affected by the scan rate and electrolyte composition and need to be verified by comparison with the actual environment.

Validity : ASTM G5-14(2021) is confirmed to be valid in 2023 and may be updated in the future based on electrochemical technology.

COPYRIGHT AND LEGAL LIABILITY STATEMENT

Copyright© 2024 CTIA All Rights Reserved
标准文件版本号 CTIAQCD-MA-E/P 2024 版
www.ctia.com.cn

电话/TEL: 0086 592 512 9696
CTIAQCD-MA-E/P 2018-2024V
sales@chinatungsten.com

Table of contents

Part 3: Performance Optimization of Cemented Carbide

Chapter 8: Corrosion and high temperature resistance of cemented carbide

8.1 Mechanism of corrosion resistance of cemented carbide

8.1.1 Electrochemical Behavior of Tungsten Carbide (WC) and the Binder Phase in Cemented Carbide

8.1.2 Cemented Carbide Acidic/Salt Spray Environment

8.1.2.1 Principle and Technical Overview

8.1.2.2 Mechanism and analysis of cemented carbide in acidic/salt spray environment

8.1.2.3 Analysis of factors affecting corrosion of cemented carbide in acidic and salt spray environments

8.1.2.4 Optimization strategy for the corrosion effects of cemented carbide in acidic and salt spray environments

8.1.2.5 Engineering applications of cemented carbide in acidic and salt spray environments Tips for carbide corrosion in this section

(1) Corrosion path of cemented carbide

(2) Cemented carbide enhances surface protection

(3) Grain boundary density of cemented carbide

(4) Corrosion stress of cemented carbide

(5) Pitting on cemented carbide surface

8.2 High Temperature Properties of Cemented Carbide

8.2.1 Oxidation resistance of cemented carbide (800-1000°C)

8.2.1.1 Overview of the principles and technologies of oxidation resistance of cemented carbide

8.2.1.2 Oxidation resistance mechanism and analysis of cemented carbide

8.2.1.3 Analysis of factors affecting the oxidation resistance of cemented carbide

8.2.1.4 Strategy for optimizing oxidation resistance of cemented carbide

8.2.1.5 Engineering Application of Cemented Carbide's Oxidation Resistance

8.2.2 Thermal fatigue and creep of cemented carbide

8.2.2.1 Overview of thermal fatigue and creep principles and technologies of cemented carbide

8.2.2.2 Thermal fatigue and creep mechanism and analysis of cemented carbide

8.2.2.3 Factors affecting thermal fatigue and creep of cemented carbide and their coupling effects

8.2.2.4 Thermal fatigue and creep optimization strategies for cemented carbide

8.2.2.5 Engineering Application of Thermal Fatigue and Creep Performance Optimization of Cemented Carbide

8.3 Methods for optimizing the corrosion resistance and high temperature resistance of cemented carbide

8.3.1 Corrosion resistance advantages of Ni-based bonding phase in cemented carbide

8.3.1.1 Principle and technical overview of the corrosion resistance advantages of Ni -based

COPYRIGHT AND LEGAL LIABILITY STATEMENT

cemented carbide bonding phase

8.3.1.2 Analysis of corrosion resistance mechanism of Ni-based bonding phase in cemented carbide

8.3.1.3 Microscopic analysis and verification of corrosion resistance of Ni-based bonding phase in cemented carbide

8.3.1.4 Analysis of factors affecting corrosion resistance of Ni-based bonding phase in cemented carbide

8.3.1.5 Optimization of Ni- based binder phase preparation process

8.3.1.6 Test specification for Ni- based bonding phase of cemented carbide

8.3.1.7 Mechanical properties test of cemented carbide Ni-based bonding phase

8.3.1.9 Engineering applications of Ni-based cemented carbide binder phase

8.3.1.10 Application advantages and expansion of Ni-based cemented carbide

8.3.2 Introduction of Cr_3C_2 Additives in Cemented Carbide

8.3.2.1 Principle and technical overview of the introduction of Cr_3C_2 additives into cemented carbide

8.3.2.2 Analysis of the Anti-Oxidation and Corrosion Resistance Mechanism Introduced by Cr_3C_2 Additives in Cemented Carbide

8.3.2.3 Microscopic analysis and verification of the introduction of Cr_3C_2 additives into cemented carbide

8.3.2.4 Analysis of factors affecting the performance of cemented carbide Cr_3C_2 additives

8.3.2.5 Optimization of the preparation process of cemented carbide Cr_3C_2 additives

8.3.2.6 Cemented Carbide Cr_3C_2 Additive Engineering Case and Performance Comparison

8.3.2.7 Application expansion and limitations of Cr_3C_2 additives in cemented carbide

8.3.2.8 Optimization direction and future prospects of the introduction of Cr_3C_2 additives in cemented carbide

8.3.3 Hard alloy surface coating protection

Overview of the Principle and Technology of Cemented Carbide Surface Coating Protection

Analysis of corrosion resistance and oxidation resistance mechanism of cemented carbide surface coating

Microscopic analysis and verification of cemented carbide surface coating

Analysis of factors affecting cemented carbide surface coating

8.3.3.6 Optimization of the preparation process of cemented carbide surface coating protection

Engineering Cases and Performance Comparison of Cemented Carbide Surface Coatings

8.3.3.8 Application expansion and limitations of cemented carbide surface coatings

Optimization direction and future prospects of cemented carbide surface coating

8.3.4 Optimization of process parameters for corrosion resistance and high temperature resistance of cemented carbide

8.3.4.1 Overview of the Principles and Technologies for Optimizing Process Parameters for Cemented Carbide Corrosion and High Temperature Resistance

8.3.4.2 Analysis of corrosion resistance and performance mechanism of cemented carbide process parameter optimization

COPYRIGHT AND LEGAL LIABILITY STATEMENT

- 8.3.4.3 Microscopic analysis and verification of process parameter optimization for corrosion resistance and high temperature resistance of cemented carbide
- 8.3.4.4 Analysis of factors affecting process parameter optimization of cemented carbide corrosion resistance and high temperature resistance
- 8.3.4.5 Optimization strategy of process parameters for corrosion resistance and high temperature resistance of cemented carbide
- 8.3.4.6 Engineering Cases and Performance Comparison of Process Parameter Optimization for Cemented Carbide Corrosion Resistance and High Temperature Resistance
- 8.3.4.7 Application extension and limitations of process parameter optimization for corrosion resistance and high temperature resistance of cemented carbide
- 8.3.4.8 Optimization of process parameters for corrosion resistance and high temperature resistance of cemented carbide and future prospects
- 8.3.5. Control of cemented carbide microstructure
 - 8.3.5.1 Overview of the principles and technologies for cemented carbide microstructure control
 - 8.3.5.2 Analysis of the corrosion resistance and performance mechanism of cemented carbide microstructure regulation
 - 8.3.5.3 Microanalysis and verification of cemented carbide microstructure control
 - 8.3.5.4 Analysis of factors affecting the microstructure of cemented carbide
 - 8.3.5.5 Cemented Carbide Microstructure Control Strategy
 - 8.3.5.6 Cemented Carbide Microstructure Control Engineering Case and Performance Comparison
 - 8.3.5.7 Application Expansion and Limitations of Cemented Carbide Microstructure Control
 - 8.3.5.8 Direction and future prospects of cemented carbide microstructure control and optimization
- 8.4 Testing and evaluation of corrosion resistance and high temperature resistance of cemented carbide
 - 8.4.1 Cemented Carbide Corrosion Rate (Electrochemical Tafel Curve)
 - 8.4.1.2 Mechanism and analysis of cemented carbide corrosion rate
 - 8.4.1.3 Analysis of factors affecting the corrosion rate of cemented carbide
 - 8.4.1.4 Test method for corrosion rate of cemented carbide
 - 8.4.1.6 Application extension and limitations of cemented carbide corrosion rate
 - 8.4.1.7 Optimization direction and future prospects of cemented carbide corrosion rate
 - 8.4.2 High temperature hardness and thermal shock test of cemented carbide
 - Overview of the Principle and Technology of Cemented Carbide High Temperature Hardness and Thermal Shock Test
 - Mechanism and analysis of high temperature hardness and thermal shock test of cemented carbide
 - 8.4.2.3 Analysis of factors affecting high temperature hardness and thermal shock test of cemented carbide
 - Test methods for high temperature hardness and thermal shock test of cemented carbide

COPYRIGHT AND LEGAL LIABILITY STATEMENT

8.4.2.5 Engineering Application of Cemented Carbide High Temperature Hardness and Thermal Shock Test

Application extension and limitations of high temperature hardness and thermal shock test of cemented carbide

8.4.2.7 Optimization direction and future prospects of cemented carbide high temperature hardness and thermal shock test

References

appendix:

Comparative analysis of cemented carbide high temperature molds and high density tungsten alloy molds

Comparative analysis of cemented carbide high temperature molds and titanium zirconium molybdenum (TZM) alloy molds

Overview of Cemented Carbide Gas Turbine Components

Carbide food processing tools and food processing equipment parts

Carbide gas turbine nozzle

Hard alloy chemical pipeline valve

Carbide papermaking equipment parts

National Standard of the People's Republic of China GB/T 7997-2017

Cemented Carbide Performance Test Method

National Standard of the People's Republic of China GB/T 3851-2015

Method for determination of microstructure of cemented carbide

National Standard of the People's Republic of China GB/T 3850-2015

Method for determination of microstructure of cemented carbide National Standard of the People's Republic of China

GB/T 18376-2014

Method for impact fatigue test of cemented carbide

National Standard of the People's Republic of China GB/T 7997-2017

Method for performance test of cemented carbide

International Standard ISO 15156-1:2020

Oil, petrochemical and natural gas industries — Materials for use in H₂S-containing environments in oil and gas production

— Part 1 : General principles for selection of cracking-resistant materials

Petroleum, petrochemical and natural gas industries — Materials for use in H₂S-containing environments in oil and gas production — Part 1: General principles for selection of cracking-resistant materials

International Standard ISO 15156-2:2020

Petroleum, petrochemical and natural gas industries

— Materials for use in H₂S-containing environments in oil and gas production

— Part 2: Cracking-resistant carbon and low alloy steels, and the use of cast irons

Petroleum, petrochemical and natural gas industries — Materials for use in H₂S-containing environments in oil and gas production

COPYRIGHT AND LEGAL LIABILITY STATEMENT

Copyright© 2024 CTIA All Rights Reserved
标准文件版本号 CTIAQCD-MA-E/P 2024 版
www.ctia.com.cn

电话/TEL: 0086 592 512 9696
CTIAQCD-MA-E/P 2018-2024V
sales@chinatungsten.com

— Part 2: Use of carbon and low alloy steels and cast irons resistant to cracking

International Standard ISO 15156-3:2020

Petroleum, petrochemical and natural gas industries

— Materials for use in H₂S-containing environments in oil and gas production

— Part 3: Cracking-resistant CRAs (corrosion-resistant alloys) and other alloys
Petroleum, petrochemical and natural gas industries — Materials for use in environments containing H₂S in oil and gas production

— Part 3: Corrosion-resistant alloys (CRAs) and other alloys resistant to cracking

Carbide high temperature mold

CTIA GROUP Carbide Paper Cutter

ISO 9227:2017 Corrosion test Salt spray test in artificial atmosphere

National Standard of the People's Republic of China GB/T 18376-2014

Test methods for corrosion resistance and wear resistance of cemented carbide

International Standard ISO 4287:1997

Geometrical Product Specifications - Surface texture: Profile method - Terms, definitions and surface texture parameters

Geometrical Product Specifications (GPS)

— Surface texture: Profile method

— Terms, definitions and surface texture parameters

International Standard ISO 3274:1996

Geometrical Product Specifications — Surface texture: Profilometry — Nominal characteristics of contact instruments

Geometrical Product Specifications (GPS)

— Surface texture: Profile method

— Nominal characteristics of contact (stylus) instruments

ISO 4288:1996

Geometrical Product Specifications — Surface texture: Profile method — Rules and procedures for the evaluation of surface texture

— Surface texture: Profile method

— Rules and procedures for the assessment of surface texture

National Standard of the People's Republic of China GB/T 12444-2006

Test methods for sliding friction and wear of metallic materials

National Standard of the People's Republic of China GB/T 16545-2008

Test methods for salt spray corrosion of metallic materials

National Standard of the People's Republic of China GB/T 3850-2015

General guidelines for corrosion tests of metals and alloys

International Standard ISO 8044:2015

Corrosion of metals and alloys — Basic terms and definitions

International Standards ISO 9223:2012

COPYRIGHT AND LEGAL LIABILITY STATEMENT

Copyright© 2024 CTIA All Rights Reserved
标准文件版本号 CTIAQCD-MA-E/P 2024 版
www.ctia.com.cn

电话/TEL: 0086 592 512 9696
CTIAQCD-MA-E/P 2018-2024V
sales@chinatungsten.com

Corrosion of metals and alloys — Corrosivity of atmospheres — Classification

GB/T 38512015 National Standard of the People's Republic of China

Method for determination of microstructure of cemented carbide

National Standard of the People's Republic of China

GB/T 7997-2017 Cemented carbide performance test method

International standard ISO 6508

Metallic materials — Rockwell hardness test

Metallic materials — Rockwell hardness test

International Standard ISO 6508-3:2015

Metallic materials — Rockwell hardness test — Part 3: Calibration of reference blocks

International Standard ISO 6508-1:2016

Metallic materials — Rockwell hardness test — Part 1: Test method

ASTM G59

Standard Test Method for Conducting Potentiodynamic Polarization Resistance Measurements

Standard test method for determination of potentiodynamic polarization resistance

ASTM G3-14 Standard Practice

for

Conventions Applicable to Electrochemical Measurements in Corrosion Testing

ASTM G5-14 Standard

Reference Test Method for Making Potentiodynamic Anodic Polarization Measurements

COPYRIGHT AND LEGAL LIABILITY STATEMENT

Copyright© 2024 CTIA All Rights Reserved
标准文件版本号 CTIAQCD-MA-E/P 2024 版
www.ctia.com.cn

电话/TEL: 0086 592 512 9696
CTIAQCD-MA-E/P 2018-2024V
sales@chinatungsten.com

CTIA GROUP LTD

30 Years of Cemented Carbide Customization Experts

Core Advantages

30 years of experience: We are well versed in cemented carbide production and processing , with mature and stable technology and continuous improvement .

Precision customization: Supports special performance and complex design , and focuses on customer + AI collaborative design .

Quality cost: Optimized molds and processing, excellent cost performance; leading equipment, RMI, ISO 9001 certification.

Serving Customers

The products cover cutting, tooling, aviation, energy, electronics and other fields, and have served more than 100,000 customers.

Service Commitment

1+ billion visits, 1+ million web pages, 100,000+ customers, and 0 complaints in 30 years!

Contact Us

Email : sales@chinatungsten.com

Tel : +86 592 5129696

Official website : www.ctia.com.cn

WeChat : Follow "China Tungsten Online"



COPYRIGHT AND LEGAL LIABILITY STATEMENT

Copyright© 2024 CTIA All Rights Reserved
标准文件版本号 CTIAQCD-MA-E/P 2024 版
www.ctia.com.cn

电话/TEL: 0086 592 512 9696
CTIAQCD-MA-E/P 2018-2024V
sales@chinatungsten.com